The synthesis and characterisation of analogues of the antimicrobial peptide iturin A_2

by

Marina Rautenbach
M.Sc. (Biochemistry)

December 1998

Dissertation approved for the degree
Doctor of Philosophy (Biochemistry)
in the
Faculty of Science
at the
University of Stellenbosch

Supervisor: Prof. J.-H. S. Hofmeyr
Co-supervisor: Prof. P. Swart
Department of Biochemistry
University of Stellenbosch

Declaration

By submitting this thesis electronically, I declare that the entirety of the work contained therein is my own, original work, that I am the sole author thereof (save to the extent explicitly otherwise stated), that reproduction and publication thereof by Stellenbosch University will not infringe any third party rights and that I have not previously in its entirety or in part submitted it for obtaining any qualification.

December 1998

Summary

Iturin A, an antifungal lipopeptide, is produced by *Bacillus subtilis*. This cyclic peptide consists of seven D- and L-α-amino acid residues (L-Asn_2-D-Tyr_3-D-Asn_4-L-Gln_5-L-Pro_6-D-Asn_7-L-Ser_8) and a β-amino fatty acid residue. Eight analogues of iturin A_2 were synthesised and purified by high performance chromatography (HPLC). Electrospray ionisation mass spectrometry (ESI-MS), amino acid analysis and HPLC confirmed high chemical purity of the synthetic products. The influence of primary structure on conformation, hydrophobicity, interaction with alkali metal ions and bioactivity was investigated using the purified peptides.

Two low energy *in vacuo* structures of a linear iturin A_2 analogue (8-Beta), one with a distorted W-backbone structure and one with a twisted S-backbone structure, were predicted with HyperChem®4.5. Nuclear magnetic resonance spectrometry confirmed the existence of two slow interconverting conformations, possibly a W↔S equilibrium. The predicted S-structure of 8-Beta includes two turns that approximate β-turns. In natural iturin A, the same two peptide moieties, β-aminotetradecanoyl-L-Asn_2-D-Tyr_3-D-Asn_4 and L-Gln_5-L-Pro_6-D-Asn_7-L-Ser_8, each adopt a type II β-turn conformation. ESI-MS fragmentation patterns of sodiated 8-Beta indicated that the sodium interacts with the majority of the amide bond oxygens in the predicted turns. The linear peptides associated with either one or two alkali metal ions, while the cyclic analogues associated only with one ion. The alkali metal ion selectivity sequence of all the lipopeptides was $Na^+ > K^+ > Rb^+$, indicating a size limitation in interaction cavities. Iturin A possibly has a direct interaction with alkali metal ions and it is proposed that these ions are chelated by the carbonyl oxygens in either one of the two β-turns of natural iturin A.

It was found that the more hydrophobic the iturin A_2 analogue, the better it interacted with lipid membranes and octadecanoylsilane matrices (HPLC retention), except if it had a high tendency to aggregate in solution. Aggregation in the membrane is part of iturin A's mechanism of action. It is proposed that solution-phase aggregates are not the active form of iturin A as the lipopeptide preparations, which self-aggregated in solution, lost their antibacterial activity. Circular dichroism (CD) spectra of the peptides in liposomes revealed the possibility of type II β-turns in all the octalipopeptides. There is, however, a marked difference between the overall cyclic and linear structures in membranes, although diastereomers, differing in configuration of β-aminotetradecanoic acid (β-NC_{14}) residue, had

similar structures. The possibility of self-assembly of synthetic iturin A_2 in antiparallel β-sheets was also indicated by CD.

Haemolytic activity of the iturin A_2 analogues depended on cyclisation, inclusion of L-Asn_2 and β-NC_{14} configuration. This activity is possibly stereoselective as synthetic iturin A_2 and its linear analogue were the most haemolytic. Growth inhibition of *Micrococcus luteus* mainly depended on hydrophobic interaction and not on cyclisation or configuration of the β-NC_{14} residue, therefore this activity differs in mechanism of action from that of haemolysis. Lysis of *M. luteus* protoplasts, however, decreased with decrease in peptide length: 8-Beta>7-Beta>6-Beta. The activity against *Botrytis cinerea* depended mainly on cyclisation. The hydrophobic hub, formed by the invariant Tyr residue and the β-NC_{14} residue, is a possible key to antifungal activity. This hub is absent in the predicted S-structure of 8-Beta and may be influenced in cyclic 8-Beta and shorter analogues by the configuration of the β-NC_{14} residue, resulting in good overall bioactivity of only the synthetic iturin A_2.

Opsomming

Iturin A, ’n antifungiese lipopeptied, word deur *Bacillus subtilis* geproduseer. Hierdie sikliese peptied bestaan uit sewe D- en L-α-aminosuurresidue (L-Asn_2-D-Tyr_3-D-Asn_4-L-Gln_5-L-Pro_6-D-Asn_7-L-Ser_8) en ’n β-aminovetsuurresidu. Agt analoë van iturin A_2 is gesintetiseer en m.b.v. hoë doeltreffendheid chromatografie (HPLC) gesuiwer. Die hoë chemiese suiwerheid van die sintetiese produkte is deur elektrosproei-ionisasie massaspektrometrie (ESI-MS), aminosuuranalise en HPLC bevestig. Die gesuiwerde peptiede is gebruik om die invloed van primêre struktuur op konformasie, hidrofobisiteit, interaksie met alkalimetaal-ione en bioaktiwiteit te ondersoek.

Twee lae-energie *in vacuo* strukture van die lineêre iturin A_2 analoog (8-Beta), een met ‘n verwronge W-ruggraatstruktuur en een met ’n gedraaide S-ruggraatstruktuur, is deur HyperChem®4.5 voorspel. Kernmagnetiese resonansspektrometrie het die bestaan van twee interomskakelende konformasies bevestig, moontlik ’n W↔S ewewig. Die voorspelde S-struktuur van 8-Beta bevat twee draaie wat neig na β-draaie. Dieselfde twee peptiedeenhede, β-aminotetradekanoiël-L-Asn_2-D-Tyr_3-D-Asn_4 en L-Gln_5-L-Pro_6-D-Asn_7-L-Ser_8, neem elk ’n tipe II β-draai konformasie in die natuurlike iturin A aan. ESI-MS fragmentasiepatrone van die 8-Beta natruimaddukte het aangedui dat die natriumione met die meeste van die amiedbinding-suurstowwe in die voorspelde draaie interaksie het. Die lineêre peptiede het met een of twee alkalimetaal-ione geassosieer, terwyl die sikliese analoë slegs met een ioon geassosieer het. Al die lipopeptiede se alkalimetaal-ioon selektiwiteitsvolgorde was $Na^+ > K^+ > Rb^+$, wat aandui dat daar ’n grootte limiet is in die interaksieholtes. Iturin A het moontlik ’n direkte interaksie met alkalimetaal-ione en dit word voorgestel dat hierdie ione deur die karbonielsuurstowwe in enige een van die twee β-draaie van natuurlike iturin A gechelateer word.

Daar is gevind dat hoe meer hidrofobies die iturin A_2 analoog is, hoe beter is die interaksie daarvan met lipiedmembrane en oktadekanoïelsilaanmatrikse (HPLC retensie), behalwe as dit ’n groot tendens het om in oplossing te aggregeer. Aggregasie in die membraan is deel van iturin A se meganisme van aksie. Daar word voorgestel dat die aggregate in oplossing nie die aktiewe vorm van iturin A is nie, omdat die lipopeptiedpreparate wat in oplossing selfaggregeer antibakteriële aktiwiteit verloor. Sirkulêre dichroïsme (CD) spektra van die

peptiede in liposome het die moontlikheid van tipe II β-draaie in al die oktalipopeptiede uitgewys. Alhoewel daar merkbare verskille tussen die totale sikliese en lineêre strukture in die membrane voorgekom het, was die diastereomere, wat verskil t.o.v. konfigurasie van β-aminotetradekanoësuurresidu (β-NC_{14}), se strukture baie dieselfde. Die moontlikheid van selfverpakking van sintetiese iturin A_2 in antiparallele β-plate is ook deur CD aangedui.

Hemolitiese aktiwiteit van die iturin A_2 analoë het afgehang van siklisering, die insluiting van L-Asn_2 en die β-NC_{14}-konfigurasie. Hemolise is moontlik stereoselektief want sintetiese iturin A_2 en sy lineêre analoog was die aktiefste. Groei-inhibisie van *Micrococcus luteus* het hoofsaaklik afgehang van hidrofobiese interaksie en nie van siklisering of die konfigurasie van die β-NC_{14}-residu nie, dus verskil hierdie aktiwiteit in meganisme van aksie van diè van hemolise. Die lise van *M. luteus* protoplaste daarenteen neem af met verkorting van peptiedketting: 8-Beta>7-Beta>6-Beta. Die aktiwiteit teen *Botrytis cinerea* het hoofsaaklik afgehang van siklisering. Die hidrofobiese eenheid, gevorm deur die invariante Tyr-residu en die β-NC_{14}-residu, is ’n moontlike sleutel tot die antifungiese aktiwiteit. Hierdie eenheid is afwesig in die voorspelde S-struktuur van 8-Beta en mag ook in die sikliese 8-Beta en korter analoë beïnvloed word deur die konfigurasie van die β-NC_{14}-residu, wat lei tot goeie algemene bioaktiwiteit van slegs die sintetiese iturin A_2.

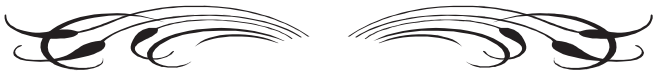

Met liefde opgedra aan my ouers

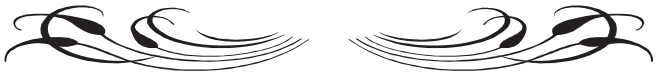

Acknowledgements

I would like to express my thanks and gratitude to the following persons:

- Prof. Jannie Hofmeyr, my supervisor and head of the department of Biochemistry, University of Stellenbosch, for his critical evaluation that constantly motivated me and excellent guidance in the preparation of this manuscript;

- Prof. Pieter Swart, my co-supervisor, for his assistance with the high performance liquid chromatography, his guidance in the mass spectrometry work and his encouragement during my Ph.D. studies;

- Dr. Tinus van der Merwe, for the huge body of the electrospray mass spectrometry work, helpful discussions and guidance in interpretation of the results;

- Prof. Kirsten van der Merwe for the initial funding of this project and his dedication in establishing the electrospray mass spectrometry facility in the department of Biochemistry;

- Prof. D. Ferreira form department of Chemistry, University of the Free State, for the use of their circular dichroism facility and Dr. L. Fourie form department of Chemistry, University of Potchefstroom, for the fast atom bombardment mass spectrometry on the first peptide synthesis products in this study;

- Prof. G. Holz from the department of Plant Pathology, University of Stellenbosch for the antifungal studies on some of the peptides and the donation of the *Botrytis cinerea* spores, Dr. B. Janse from the department of Microbiology, University of Stellenbosch for the donation of freezer stock cultures of *Micrococcus luteus* and Dr. R. Levitt for the donation of gramicidin S and the HCl salt of N^{β}-t-butyloxycarbonyl-β-aminotetradecanoic acid;

- personnel from the department of Chemistry, University of Stellenbosch for their assistance in this project—Ms. V. Truter for the electron impact ionisation mass spectrometry; Mr. H. Spies for the nuclear magnetic resonance spectrometry and interpretation of the results; Prof. W. Engelbrecht for the use of the Hyperchem®4.5 molecular modelling program; Dr. P. Verhoeven for his advice on molecular modelling

and Ms. Mare-Loe Prinsloo for synthesis of the enantiomerically pure N^{β}-t-butyloxycarbonyl-β-D-aminotetradecanoic acid;

- Ms. Charlene Stötter for her proof-reading, preparation of some of the figures in this manuscript and general assistance during the last year;

- my two M.Sc. students, Ms. Gertrude Lourens and Mr. Etienne du Toit, my part-time research assistants and all my Honours students over the years, that worked hard with me to establish the Peptide Synthesis Laboratory and related techniques;

- my colleagues and co-workers in the department of Biochemistry, who endured my running from my office to my laboratory and back, for all the helpful discussions and encouragement;

- my many friends, who remained my friends in spite of my pre-occupation with my work and research;

- and last but definitely not least, I would like thank my parents, Mr. Ben Rautenbach and Ms. Maureen Rautenbach and for their love, their absolute belief in my abilities and moral support throughout my years of academic studies. *Baie dankie Ma en Pa!*

Table of Contents

List of Abbreviations and Acronyms

2D	two-dimensional
3D	three-dimensional
4D	four-dimensional
AMU	atomic mass units
Asn	asparagine
Asp	aspartic acid
B. cinerea	*Botrytis cinerea*
β-NC_{14}	β-aminotetradecanoic acid
B. subtilis	*Bacillus subtilis*
BOC-ON	2(BOC-oxyimino)-2-phenylacetonitrile
BOP	benzotriazol-1-yl-oxy-tris dimethylaminophosphonium hexafluorophosphate
CD	circular dichroism
CE	capillary electrophoresis
CID	collision induced dissociation/decomposition
CMC	critical micellular concentration
COSY	correlation spectroscopy
CSP	chiral stationary phases
CV	cone voltage
Da	dalton
DCC	dicyclohexylcarbodiimide
DCM	dichloromethane
DCU	dicyclohexylurea
Dhbt	3,4-dihydro-4-oxo-1,2,3-benzotriazin-3-yl
DIPCIDI	diisopropylcarbodiimide
DIPEA	N, N'-diisopropylethyl amine
DMF	N, N'-dimethylformamide
DMPC	dimyristoyl-L-α-phosphatidylcholine
DOPA	3,4-dihydroxyphenylalanine
DPPC	dipalmitoyl-L-α-phosphatidylcholine
EDTA	ethylenediaminetetraacetic acid
EI	electron impact ionisation

ESI	electrospray ionisation
FAB	fast atom bombardment
FDNB	1-fluoro-2,4-dinitrobenzene
Fmoc	N^9-fluorenylmethyloxycarbonyl
G	glycine
GC	gas chromatography
Gln	glutamine
Glu	glutamic acid
HC_{50}	peptide concentration leading to 50 % haemolysis
HEPES	2-[4-(2-hydroxyethyl-1-perazinyl]-ethane sulphonic acid
HF	hydrofluoric acid
HOBt	1-hydroxybenzotriazol
HPLC	high performance liquid chromatography
i	immonium ion
I_{50}	MS collision energy that induces a 50% decrease in molecular ion signal
IR	infrared
k’	HPLC capacity factor
LC	liquid chromatography
m	m-ion, molecular ion of a peptide minus one of the side chains
[M]	molecular ion
M	molar
MALDI	matrix-assisted laser desorption/ionisation
mbh	4, 4’-dimethoxybenzhydryl
MRM	multiple reaction monitoring
MS	mass spectrometry
M. luteus	*Micrococcus luteus*
m/z	mass over charge ratio
N	asparagime
NMR	nuclear magnetic resonance
NOESY	nuclear Overhauser effect spectroscopy
ODS	octadecanoylsilane
ORD	optical rotary dispersion
P	proline
PBS	phosphate buffered saline

PC	phosphatidylcholine
PE	phosphatidylethanolamine
Pfp	pentafluorophenyl
PITC	phenylisothiocyanate
ppm	parts per million
Pro	proline
PTC	phenylthiocyanate
PyBOP®	benzotriazol-1-yl-oxy-tris-pyrrolidinophosphonium hexafluorophosphate
Q	glutamine
RP-HPLC	reverse phase high performance liquid chromatography
R_t	retention time of analyte in column chromatography
R_f	distance that analyte moved relative to solvent front
S	serine
S. cerevisiae	*Saccharomyces cerevisiae*
SEM	standard error of the mean
Ser	serine
SIR	single ion recording
SPE	solid phase extraction
tBoc	N^{α}-t-butyloxycarbonyl
tBu	t-butyl ester
TEA	triethylamine
TFA	trifluoroacetic acid
THF	tetrahydrofuran
TLC	thin layer chromatography
Tris-HCl	2-amino-2-(hydroxymethyl)-1,3-propandiol-hydrochloride
Tyr	tyrosine
UV	ultraviolet
Y	tyrosine

Preface

About 50 years ago in the Belgium Congo a scientist collected a soil sample. This sample harboured a treasure-trove of microscopic organisms. One such treasure was a new strain of *Bacillus subtilis*, which produced cyclic lipopeptides that inhibit fungal growth. These compounds were called iturins; many of them were isolated and characterised during the following years, and some were even tested in clinical trails, patented and used as biofungicides. This long history of research included structure-function studies which lead to a partial elucidation of their mechanism of action, particularly that of iturin A. All but one of these studies used natural iturins, leaving open a whole spectrum of possibilities for using synthetic analogues of iturin A for structure-function studies.

This thesis describes how some of these possibilities were exploited by synthesising analogues of iturin A_2 and characterising them in terms of their chemical and biological nature. First, a short overview of the history of iturins is given in Chapter 1. The following five chapters describe the experimental results obtained in this study. To ease future publication, each of these chapters were written with an article format in mind and form, to a degree, independent units. Although some repetition is unavoidable, it has been kept to a minimum. In the final chapter the results of this study are related to iturin A's mechanism of action.

In short, the aim of this Ph.D. project was to propose a more detailed mechanism of action of iturin A. To achieve this, the following objectives were set:

- the synthesis, purification and chemical characterisation of eight iturin A_2 analogues (Chapters 2 and 3);
- structural investigation of octalipopeptide analogues of iturin A_2, using nuclear magnetic resonance, circular dichroism and computer-assisted modelling (Chapter 4);
- investigation, using electrospray ionisation mass spectrometry, of the influence of structure and chirality on the ability of the iturin A analogues to associate with alkali metal ions (Chapter 5);
- investigation of the influence of structure and chirality of the iturin A_2 analogues on hydrophobicity and biological activity (Chapter 6).

Before any of these objectives could be met, a peptide synthesis facility and techniques necessary for the purification and analysis of peptides had to be established. In this we were so successful that our facility currently has the ability to synthesise high purity peptides on a regular basis for research purposes and commercial use. A number of new techniques, especially those related to the investigation of biological activity, were also developed. This project helped to lay the foundation for three other current projects, all around the central theme of antimicrobial peptides.

Chapter 1

The iturins: Cyclic antimicrobial peptides produced by Bacillus subtilis

1.1 Introduction

In a world laden with bacteria, fungi and parasites, many strategies of defence have evolved among the living organisms in the fight for survival. One of the weapons in this repertoire of host defence mechanisms is a group of peptides with antimicrobial activity. Although most of these peptides share functional similarities, such as interacting in some way with a target cell membrane, wide structural diversity exists among these peptides. The antimicrobial peptides consist of between 5 and 50 residues and are either cyclic, linear or contain disulphide bonds. Many of these peptides, contain only the natural L-amino acids, while others contain highly modified and non-amino acid residues. Among this chemical diversity these peptides share one important feature namely, an amphipathic character enabling them to interact with both non-polar lipids and the aqueous environment.

Many microorganisms produce antimicrobial peptides, as the excretion of an antibiotic obviously provides a competitive advantage to the producing microorganism. Some of these organisms have been very successful in the fight for survival, such as the archaic soil bacterium *Bacillus subtilis* that has been around for millennia. *B. subtilis* produces, depending on environmental pressures, many different cyclic peptides with antimicrobial activity, and especially, broad spectrum antifungal activity. These cyclic peptides include mycobacillin [1], subsporins [2], fungistatin [3], bacilysin [4], fengimycin [4], surfactin [5] and a group of peptides collectively known as the iturins [6-24]. The iturins will be discussed in the rest of this chapter with specific emphasis on iturin A, the focus of this thesis.

1.2 The iturins–an overview

One of the iturins, iturin A, was the active compound in some of the first antibiotic preparations from *B. subtilis.* In 1946 Johnson and Burdon [9] isolated eumycin from *B. subtilis*, which was active against pathogenic fungi. In 1950, Raubitschek and Dostrovsky [10] described an antibiotic, also isolated from *B. subtilis* cultures, that was active against dermatophytes. In 1952 Babad *et al*. [11] reported the isolation of bacillomycin R and in 1954 Shibasaki and Terui [12] isolated bacillomycin B. In 1957 Delcambe and Devignat [13] described the properties of an antibiotic preparation from the cultures from a strain of *B. subtilis* isolated by Devignat in the Belgian Congo (presently the Democratic Republic of Congo). They called their preparation "iturine", after the iturinic acid (β-amino fatty acid) found in the preparation. This preparation consisted of three compounds, A, B and C of which iturin A was the sole active agent [14]. In 1976 it was shown that eumycin, Raubitschek's antibiotic, bacillomycin B and bacillomycin R were identical to iturin A [15]. To date eight peptide families in the iturin group have been isolated and characterised (Table 1.1) [6-24].

1.2.1 Structures

The iturins have many structural features in common, such as a constant LDDLLDL chiral sequence of seven α-amino acids, a β-D-amino fatty acid residue and a cyclic structure closed by a lactam ring at the β-D-amino acid. All the iturins, except iturin C and bacillomycin F, contain an invariable tetrapeptide moiety, namely β-amino fatty acyl-L-Asn_2-D-Tyr_3-D-Asn_4 (Table 1.1).

The three-dimensional structures of only two iturins, mycobacillin and iturin A, have been elucidated using nuclear magnetic resonance (NMR) spectroscopy and computer assisted molecular modelling [25, 26]. Although the only difference in primary structure between iturin A and mycosubtilin is the inversion of the D-Asn-L-Ser sequence to D-Ser-L-Asn in mycosubtilin, a striking difference in three-dimensional structure was found.

Iturin A's three-dimensional structure was originally proposed by Garbay-Jaureguiberry *et al.* [27] and refined by Marion *et al.* [25] (Fig. 1.1). The cyclic peptide structure of iturin A is stabilised by two type II β-turns in the two tetrapeptide units: β-amino fatty acyl-Asn_2-D-Tyr_3-D-Asn_4 (turn A) and L-Gln_5-L-Pro_6-D-Asn_7-L-Ser_8 (turn B). Turns A and B are linked by a

third turn, consisting of L-Asn_2-D-Tyr_3-D-Asn_4-L-Gln_5 (turn C), that could be classified as a type I' or III' β-turn or the beginning of a 3_{10}-helix. The hydrogen bonds are somewhat distorted in the turns, with the carboxyl oxygen of L-Gln_5 acting as the hydrogen acceptor for the amino group of L-Ser_8 and the amino group of the β-amino fatty acid, and the peptide bond amino group of L-Gln_5 interacting with the carboxyl oxygen of L-Asn_2. The peptide backbone of iturin A appears somewhat rigid with the polar side chains having a larger degree of freedom allowing interaction with the aqueous environment [25]. Also refer to Chapter 4 for more information on iturin A's structure.

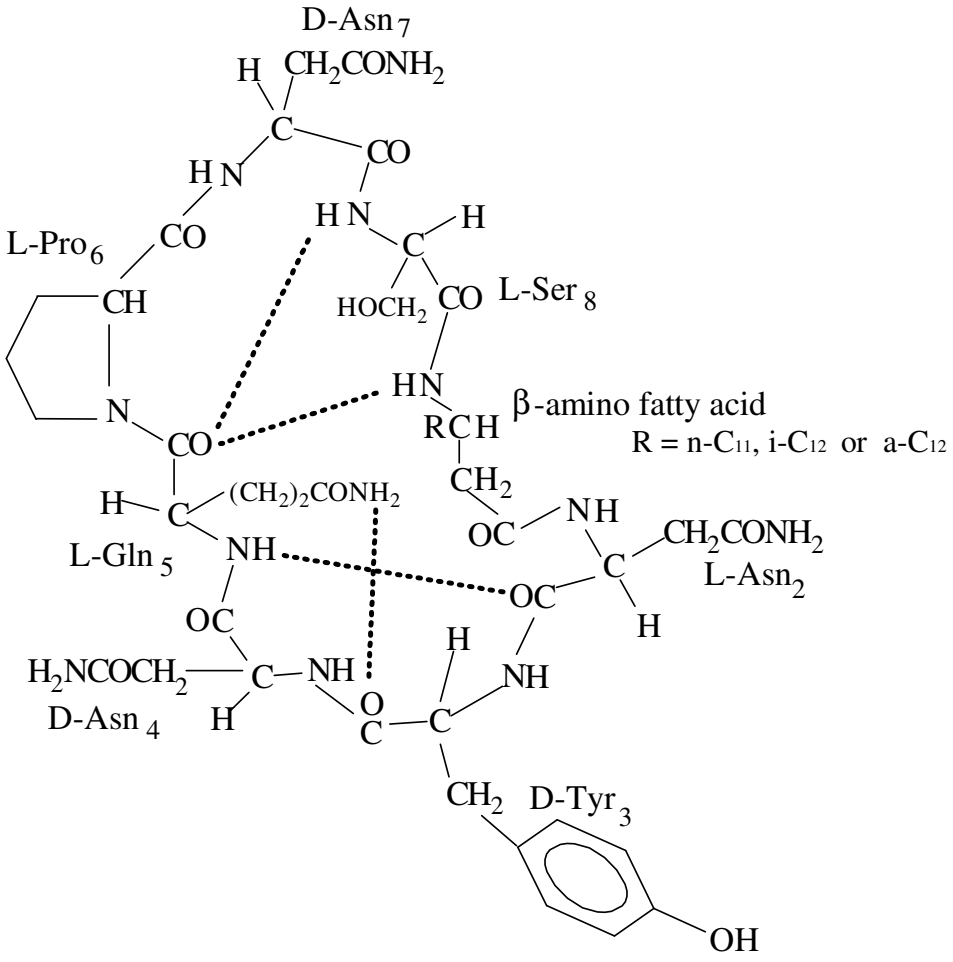

Figure 1.1 The structure of iturin A. The dashed lines represent hydrogen bonds that stabilise the structure [25].

The structure of mycosubtilin contains a rigid C_7-bend (γ-turn) involving L-Gln_5-L-Pro_6-D-Ser_7-L-Asn_8 [26]. This bend allows the carboxyl group of D-Ser_7 to form a hydrogen bond with its own hydroxyl group. In contrast, the region around the D-Tyr_3 residue was found to be more flexible. The L-Gln_5 side chain is exposed to the solvent [26] in contrast to its hidden

position in iturin A [25]. This difference in structure demonstrates the crucial role of sequence in conformation, and as we shall see, also in activity (discussed in section 1.2.4).

Table 1.1 The primary structures of the eight different iturin A families. The shaded areas show the α-amino acid residues that are identical to that of iturin A (major β-amino acids = >30% of total content, *n = normal; i = iso; a = ante-iso*)

	Major β-amino fatty acids	**α-amino acid position** N ⟶ ⟶ C							
Iturin family	position 1	2	3	4	5	6	7	8	**Refs.**
Iturin A	*n*-C_{14}, *i*-C_{15}, *a*-C_{15}	L-Asn	D-Tyr	D-Asn	L-Gln	L-Pro	D-Asn	L-Ser	6, 14, 16-18
Iturin A_L	*n*-C_{16},*i*-C_{16},	L-Asn	D-Tyr	D-Asn	L-Gln	L-Pro	D-Asn	L-Ser	6, 19
Iturin C	*n*-C_{14}, *i*-C_{15}, *a*-C_{15}	L-Asp	D-Tyr	D-Asn	L-Gln	L-Pro	D-Asn	L-Ser	6, 20
Mycosubtilin	*i*-C_{16}, *a*-C_{17}	L-Asn	D-Tyr	D-Asn	L-Gln	L-Pro	D-Ser	L-Asn	6, 21
Bacillomycin F	*i*-C_{16}, *i*-C_{17}, *a*-C_{17}	L-Asn	D-Tyr	D-Asn	L-Gln	L-Pro	D-Asn	L-Thr	6, 22
Bacillomycin D	*n*-C_{14}, *i*-C_{15}, *a*-C_{15}	L-Asn	D-Tyr	D-Asn	L-Pro	L-Gln	D-Ser	L-Thr	6, 23
Bacillomycin L	*n*-C_{14}, *i*-C_{15}, *a*-C_{15}	L-Asp	D-Tyr	D-Asn	L-Ser	L-Gln	D-Ser	L-Thr	6, 24
Bacillopeptin/ Bacillomycin L_c	*n*-C_{14},*a*-C_{15} *i*-C_{15}, *i*-C_{16}	L-Asn	D-Tyr	D-Asn	L-Ser	L-Glu	D-Ser	L-Thr	7, 8

1.2.2 Biosynthesis

Many antibiotic peptides, including the iturins, contain non-protein constituents such as D-amino acids, β-amino acids, modified amino acids and unusual residues. The biosynthesis of most of these peptides is non-ribosomal and they are the metabolic end products of an enzymatic system that uses a thiotemplate multienzymic mechanism [28]. In this biosynthetic pathway the constituent residues are activated by ATP to form amino acyl-AMP (ATP/pyrophosphate exchange) on the enzymatic template. The amino acyl group is then coupled to specific template thiols; modifications, such as epimerisation occur at this stage. A phoshopanthetheine swinging arm in the multienzyme structure directs the elongation steps (including possible cyclisation or terminal modification reactions). None of the iturin synthetases have been fully characterised, except for two subunits of the iturin A synthetase. For the iturin A synthetase it was shown that subunit *Its* only activated L-Ser and the subunit *ITagp* activated L-Asn, D-Asn, L-Gln and L-Pro [29]. The precise mechanism and structure of the iturin A multienzyme system is still unknown. The excretion mechanism and storage of the iturins also have not been elucidated.

The synthesis of antibiotics in the *Bacillus* species is regulated by mechanisms shared with starvation induced activities such as sporulation [30]. The production of bacillomycin L by *B. subtilis* NCIB 8872 takes place during the stationary phase and a direct correlation between sporulation and antibiotic production has been found [31]. Another factor is temperature—for *B. subtilis* RB14, a duel producer of iturin A and surfactin, the optimal temperature for the production of iturin A was found to be 25^{o}C, while 37^{o}C gave the best yield of surfactin [32]. The carbon and nitrogen sources in the culture medium also have a strong influence on antibiotic production. For a bacillomycin F producer, *B. subtilis* I164, isoleucine was found to be a good carbon source for the biosynthesis of the branched (*anteiso* C_{17}) β-amino fatty acid, and also enhanced bacillomycin F production [33]. In an iturin A producer, however, leucine was the better option for normal (*n*-C_{16}) and branched (*iso, anteiso* C_{15}) β-amino fatty acid biosynthesis and iturin A production [34]. The *B. subtilis* strains can consequently be divided into two groups, the first containing the producers of mycosubtilin and bacillomycin F, which synthesise high levels of the longer branched β-amino acids, and the second containing the producers of bacillomycin D, bacillomycin L and iturin A which synthesise predominantly unbranched β-amino acids [35]. For the biosynthesis of the peptidic part in iturin A,

asparagine was found to be the best precursor [36, 37] and for the overall production of iturin A, mannitol is also a good general carbon source [37]. Culture conditions consequently have a large influence on the production of the iturins.

1.2.3 Bioactivity and antimicrobial specificity

Iturin A and the rest of the iturin family have a wide spectrum of antifungal activities and are regarded as strongly antifungal [6]. The original iturin A isolates were shown to be effective against a number of dermatophytes, plant pathogens and yeasts [9-16]. Phae *et al.* [38] showed that purified peptide fractions of the iturin A producer *B. subtilis* NB22 inhibited phytopathogenic fungi. These fungi included *Fusarium oxysporum* (wilt), *Botrytis cinerea* (grey mould) and *Rhizoctonia solani* (sheath blight of rice). Some antibacterial activity against *Xanthomonas oryzae* and *Pseudomonas lachrymans* was also observed in the purified fractions [39]. Antibacterial activity of all the iturins is generally restricted to activity against gram-positive bacteria such as *Micrococcus luteus* [6, 39-42]. The iturins are also active against *Saccharomyces cerevisiae* [43-46]. They possess lytic activity and are able to lyse protoplasts from *M. luteus* [39-41], spheroplasts from *S. cerevisiae* [43] and erythrocytes [47, 48]. The plasma membrane seems to be the primary target of the iturins and their specificity must be linked to one or more components in the cell membrane.

1.2.4 Structure-function relationship

The inclusion of the lipid moiety, with a C_{14} to C_{17} aliphatic chain in the polar peptide ring, ensures the amphipathic nature of the iturins. Amphipathic properties promote the interaction of any antibiotic peptide with the plasma membrane. Amphipathic compounds, or amphiphiles, aggregate spontaneously to form micelles in an aqueous medium and they can act as surfactants, lowering the surface tension of aqueous solutions by forming monolayers at the air/water interface. The critical micellular concentration (CMC) of iturin A decreases with an increase in aliphatic chain length [49]. This decrease corresponds with an increase in antifungal activity [50]. The hydrophobic moiety was found to be absolutely critical for iturin activity. The removal of the aliphatic chain, by replacing the β-amino fatty acid with a β-alanine in iturin A, leads to total loss of bioactivity [51].

The differences between the sequences of the peptide moiety contributed to the partial elucidation of its role in the mechanism of action. That a carboxyl group, in the vicinity of the β-amino fatty acid, eradicates the activity of iturin A, is exemplified by the natural inactive analogue, iturin C. This iturin analogue has an L-Asp residue in position 2, at the C-terminal side of the β-amino fatty acid [20, 47]. Two α-amino residues, D-Tyr_3 and L-Asn_4, on the C-terminal side of the β-amino fatty acid, are conserved in all the iturins (Table 1.1) [6]. The O-methylation or O-acetylation of the D-Tyr_3 residue in iturin A, mycosubtilin and bacillomycin L [46], eradicates all activity against *S. cerevisiae.* The haemolytic activity of the iturin A derivative with the O-methylated Tyr (MeTyr-iturin A)[52] is also lost, probably due to modification of its interaction with membranes. MeTyr-iturin A aggregates at a ten times lower concentration than iturin A and tended to form stable monolayers [53, 54]. Modification in the region flanking the N-terminal side of the β-amino fatty acid seems to be a natural evolution in the peptide sequence (Table 1.1). The O-acetylation of the L-Ser residue in iturin A and mycosubtilin did not alter the activity to the same extent [46]. Mycosubtilin, with a D-Ser_7-L-Asn_8 sequence (inverted from that of iturin A) flaking the N-terminal side of the β-amino fatty acid, were more active against *S. cerevisiae* than iturin A [46]. The tetrapeptide moiety, β-amino fatty acyl-L-Asx_2-D-Tyr_3-D-Asn_4, (Asx = Asp or Asn) may have a conserved role in the mechanism of action of the iturins.

1.2.5 Mechanism of action

The iturin cytotoxic action causes an initial K^+ release from the target cell, followed by the leakage of cellular contents (including proteins and nucleic acids) and release of vesicles (containing membrane lipids and iturins) [55, 56]. The steps in this mechanism of action, and that of most antimicrobial peptides, can be described as follows: (a) recognition of target cell, (b) interaction with, or transport over plasma membrane, (c) formation of active complexes and (d) disruption/inhibition of cellular function causing the death of the cell.

The recognition of membrane components such as lipids or a chiral receptor determines target cell specificity. In fungal membranes, the interaction of iturin A with different membrane lipids possibly forms part of its recognition mechanism. Iturin A's action against *S. cerevisiae* is inhibited by cholesterol, ergosterol (a sterol in fungal membranes), oleic acid, *cis*-vaccenic acid, phosphatidylcholine (PC), phosphatidic acid and petroselinic acid [45]. The lytic action

of the iturins on erythrocytes is probably dependent on the PC and cholesterol in the outside layer of their membranes [57]. It is possible that the iturins recognise cholesterol or ergosterol and PC in its eukaryotic target cell membranes. The preference of iturin A for specific membrane lipids is probably part of the immunity of the *B. subtilis* producer against iturin A lysis. *B. subtilis* contains phosphatidylethanolamine and lysophosphatidylglycerol in the outer membrane leaflet, but no PC or membrane sterols [58].

It has been suggested that iturin A first penetrates the lipid layer and, after lateral diffusion self-associates to form aggregated structures of unknown size and conformation [6, 54, 58]. The invariant Tyr plays a significant role in membrane interaction and in aggregation [54, 58, 59]. The aggregates in dimiristoylphosphatidylcholine (DMPC) membranes consist of only iturin A molecules, while that of mycosubtilin consists of a mycosubtilin-DMPC (1:2) complex [58]. MeTyr-iturin A also forms a 1:2 complex with DMPC, but in contrast to mycosubtilin this complex is miscible with the lipid film [58]. Mycosubtilin interacts better with cholesterol than iturin A and here a complex stoichiometry of 1:2 for mycosubtilin-cholesterol and 1:1 for iturin-cholesterol is found [58]. Iturin A has weaker interaction with ergosterol, forming a 2:3 iturin A-ergosterol complex [58]. Mycosubtilin's superior interaction with lipids may be an explanation for its higher activity [46]. The immiscibility of these complexes with the lipid bilayer lead to the formation of clusters, possibly the active complexes that function as ion-pores [59-62].

It has also been suggested that iturin A interacts with membrane proteins. For example, iturin A activates phospholipases in membrane vesicles of *S. cerevisiae* [63]. This activation can be direct and stereoselective or indirect by exposure of the phospholipid substrates to the action of the enzyme. Other interactions may also take place such as the recently observed synergistic interaction between the co-produced cyclic lipopeptide, surfactin, and iturin A [32, 64].

The influence of iturins on cellular function depends mainly on disruption of the osmotic balance in the cell and the membrane potential. Iturin A causes a slow increase in membrane conductance—an action independent of the membrane potential [6]. This is the result of the formation of ion-conducting pores by iturin A [59-62], but their precise composition and structure has not been elucidated [1]. Membranes doped with iturin A or mycosubtilin are slightly anion selective [59, 60, 62]. It has been suggested the binding of cations in the pores

will lead to anion selective pores [6]. This is indeed possible, as the CMC values (2-8x10^{-5} M) of the iturins is not affected by the presence of 0.1 M electrolytes, whereas the formation of monolayers (as deduced from surface tension data) is reduced by 50% by the presence of chloride salts [65]. Because of iturin A and mycosubtilin's ability to bind cations [65] they may also act as ionophores [6]. This disruption of the osmotic balance and membrane potential by the ion-pores, and possible transport by iturin ionophores, plus the possible destructive action of the activated phospholipases on the plasma membrane, finally leads to cell death.

1.2.6 Pharmaceutical and agricultural use of iturins

It is well known that a group of "super" microorganisms have emerged because of the overuse of antibiotics and fungicides in medicine and agriculture [66, 67]. The search is therefore on for alternative agents. Because of a wide spectrum of activity, the iturins are promising candidates as the antifungal agents in seed, vegetable and food preservation and as antifungal antibiotics in medicine.

The use of the iturins as antibiotics is hampered by various factors such as high production costs, proteolytic susceptibility, toxicity and delivery of the peptide to its target. The difficulty, and high cost, of synthesis and purification of the cyclic iturin analogues, makes this methodology unsuitable for large scale production. On a more positive side, iturins are less susceptible to proteolytic degradation, because of their cyclic nature and the inclusion of three D-amino acids and the β-amino acid in their structures. This means lower dosages which counteracts the high production costs. As many fungal infections in mammals are topical, iturins can be applied topically. As early as 1958 crude iturin A was submitted for clinical trials as treatment for dermatomycoses in animals and man and it was shown to have excellent potential because of its low toxicity, wide antifungal spectrum and low allergenic effect [68]. One of the iturins, bacillomycin F, has been patented for application in medicine and agriculture [69]. It may be worthwhile to investigate some of the iturins again as antifungal agents in the treatment of fungal infections in humans and animals in the light of the immense increase in resistant fungi in the last decade [66]. There is already a renewed interest in iturin A after the observation that this peptide works synergistically with a co-produced peptide surfactin [32, 62]. Surfactin is similar to iturin A, but acts as a powerful biosurfactant [70].

The removal of many synthetic fungicides from the market has created a demand for new, environmentally safe, fungicides. Because of their low mammalian toxicity, iturins has enormous potential as fungicides in agriculture. Many iturin producer organisms have been identified [71] and used on several occasions as bio-fungicides. *B. subtilis* RB14, a producer the antibiotics iturin A and surfactin, inhibited the damping-off of tomato seedlings caused by *Rhizoctonia solani* [72]. *Bacillus subtilis* B-3, an iturin A producer, was shown to control brown fruit rot (*Monilinia fructicola*) of stone fruits [73] and also a spectrum of other phytopathogenic fungi [74]. In one field study it was found that 50 to 100 ppm of purified iturin A significantly reduced the total mycoflora on stored feed grains such as corn, peanuts and cottonseed [75].

The pharmacological and agricultural use of iturins is hampered by high production costs, which is presently preventing their application as environmental friendly fungicides and new antibiotics. The financial problem may be overcome by the improved biological production and isolation of the peptides. The antibiotic resistance crisis will undoubtedly increase the future use of antibiotic peptides in food, agricultural and pharmaceutical, especially because of their “green” character.

This study of the iturins was initiated with the intention to find a short active iturin A analogue that could be readily synthesised at low cost. As discussed in this chapter, the mechanism of action of iturin A is not fully elucidated and the influence of primary structure on activity must first be understood before such an iturin A analogue can be designed. The next five chapters in this thesis are dedicated to the characterisation of selected synthetic iturin A_2 analogues and the search for “just one more piece in the iturin A puzzle”.

1.3 References

1. Majumbar S. K., Bose S. K. (1958) *Nature* **181**, 134-135;
   Majumbar S. K., Bose S. K. (1960) *Arch. Biochem. Biophys.* **90**, 154-158

2. Ebata M., Miyazaki K., Takahasri Y. (1969) *J. Antibiotics* **22**, 467-472

3. Hobby G. L., Regna P. P., Dougherty N., Stieg W. E. (1949) *J. Clin. Invest.* **28**, 927-933

4. Isogai A., Takayama S., Murakoshi S., Suzuki A. (1982) *Tetrahedron Lett.* **23**, 3065-3068

5. Kakinuma A., Sugino H., Isono M., Tamura G., Arima K. (1969) *Agric. Biol. Chem*. **33**, 973-967

6. Maget-Dana R., Peypoux F. (1994) *Toxicology*, **87**, 151-174

7. Kajimura Y., Sugiyama M., Kaneda M. (1995) *J. Antibiotics*, **48**, 1095-1103

8. Eshita S. M., Roberto N. H., Beale J. M., Mamiya B. M., Workman R. F. (1995) *J. Antibiotics* **48**, 1240-1247

9. Johnson E. A., Burdon K. L. (1946) *J. Bacteriol*. **51**, 591

10. Raubitschek F., Dostrovsky (1950) *Dermatologica* **100**, 45-49

11. Babad J., Turner-Graff R., Pinsky A., Sharon N. (1952) *Nature* **170**, 618-619

12. Shibasaki I., Terui G. (1954) *Nature* **174**, 1190-1194

13. Delcambe L., Devignat R. (1957) *Acad. R. Sci. Coloniales*. **6**, 1-78

14. Peypoux F., Guinand M., Michel G., Delcambe L., Das B. C., Varenne P., Lederer E. (1973) *Tetrahedron* **29**, 3455-3459

15. Besson F., Peypoux F., Michel G., Delcambe L. (1976) *J. Antibiotics* **26**, 1043-1049

16. Delcambe L. (1965) *Bull. Soc. Chim. Belges*. **74**, 315-328

17. Peypoux F., Guinand M., Michel G., Delcambe L., Das B. C., Lederer E. (1978) *Biochemistry* **17**, 3992-3996

18. Nagai U., Besson F., Peypoux F. (1979) *Tetrahedron Lett*. **25**, 2359-2360

19. Winkelmann G., Allgaier H., Lupp R., Jung G. (1983) *J. Antibiotics* **36**, 1451-1457

20. Peypoux F., Besson F., Michel G., Delcambe L., Das B. C. (1978) *Tetrahedron* **34**, 1147-1152

21. Walton R. B., Woodruff H. B. (1949) *J. Clin. Invest*. **28**, 924-926;
Peypoux F., Michel G., Delcambe L. (1976) *Can. J. Biochem.* 63, 391-398 ;
Peypoux F., Pommier M. T., Marion D., Ptak M., Das B. C., Michel G. (1986) *J. Antibiotics* **36**, 636-641

22. Mhammedi A., Peypoux F., Besson F., Michel G. (1982) *J. Antibiotics* **35**, 306-311;
Peypoux F., Marion D., Maget-Dana R., Ptak M., Das B. C., Michel G. (1985) *Eur. J. Biochem.* **153**, 335-340

23. Peypoux F., Besson F., Michel G. (1980) *J. Antibiotics* **33**, 1146-1149;
Peypoux F., Besson F., Michel G., Delcambe L. (1981) *Eur. J. Biochem.* **118**, 232-327

24. Peypoux F., Pommier M.-T., Das B. P., Besson F., Delcambe L., Michel G. (1984) *J. Antibiotics* **37**, 1600-1604

25. Marion D., Genest M., Caille A., Peypoux F., Michel G., Ptak M. (1986) *Biopolymers* **25**, 153-170

26. Genest M., Marion D., Caille A., Ptak M. (1987) *Eur. J. Biochem*. **169**, 389-398

27. Garbay-Jaureguiberry C., Roques B. P., Delcambe L., Peypoux F., Michel G. (1978) *FEBS Lett*. **93**, 151-156

28. Kleinkauf H., Von Döhren H. (1990) *Eur. J. Biochem*. **192**, 1-15

29. Feignier C., Besson F., Michel G. (1996) *FEMS Microbiol. Lett*. **136**, 117-122

30. Marahiel M. A., Nakano M. M., Zuber P. (1993) *Mol. Microbiol*. **7**, 631-636

31. Chevanet F., Besson F., Michel G. (1986) *Can. J. Microbiol*. **32**, 254-258

32. Ohno A., Ano T., Shoda M. (1995) *J. Ferment. Bioeng*. **80**, 517-519

33. Besson F., Hourdou M. L. (1987) *J. Antibiotics* **40**, 221-223

34. Hourdou M. L., Besson F., Michel G. (1988) *Lipids* **24**, 940-944

35. Hourdou M. L., Besson F., Tenoux I., Michel G. (1988) *J. Antibiotics* **41**, 207-211

36. Besson F., Hourdou M. L., Michel G. (1990) *Biochim. Biophys. Acta* **1063**, 101-106

37. Besson F., Cevanet C., Michel G. (1990) *J. General Microbiol.* **133**, 767-772

38. Phae C. G., Shoda M., Kubota H. (1990) *J. Ferment. Bioeng*. **69**, 1-7

39. Peypoux F., Besson F., Michel G., Delcambe L. (1979) *J. Antibiotics* **32**, 136-140

40. Besson F., Peypoux F., Michel G. (1979) *Biochim. Biophys. Acta*. **552**, 558-562

41. Besson F., Peypoux F., Michel G. (1978) *FEBS Lett.* **90**, 36-40

42. Besson F., Peypoux F., Michel G., Delcambe L. (1978) *Biochem. Biophys. Res. Commun.* **81**, 297-304

43. Besson F., Peypoux F., Quentin M. J., Michel G. (1984) *J. Antibiotics* **37**, 172-177

44. Besson F., Michel G. (1989) *Microbios* **59**, 113-121

45. Latoud C., Peypoux F., Michel G. (1987) *J. Antibiotics* **40**, 1588-1595

46. Latoud C., Peypoux F., Michel G. (1979) *J. Antibiotics* **32**, 828-833

47. Quentin M. J., Besson F., Peypoux F., Michel G. (1982) *Biochim. Biophys. Acta*. **684**, 207-211

48. Latoud C., Peypoux F., Michel G., Genet R., Morgat J. L. (1986) *Biochim. Biophys. Acta.* **856**, 526-535

49. Thimon L., Peypoux F., Maget-Dana R., Michel G. (1992) *J. Am. Oil. Chem. Soc.* **62**, 92-93

50. Bland J. M., Lax A., Klich M. (1995) In: Proceedings of the Plant Growth Regulation Society of America (Ed. Green D. W.) Plant Growth Regulation Society of America, pp. 102-107
Bland J. M., Lax A., Klich M. In: Peptides 1992: Proceedings of the Twenty-Second European Peptide Symposium (Eds. Schneider C. H., Erberle A. N.) ESCOM, Leiden, IL, pp. 332-333

51. Bland J. M., Lax A., Klich M. In: Peptides 1990: Proceedings of the Twenty-First European Peptide Symposium (Eds. Giralt E., Andreu D.) ESCOM, Leiden, IL, pp. 426-427

52. Besson F., Peypoux F., Michel G., Delcambe L. (1979) *J. Antibiotics* **32**, 828-833

53. Harnois I., Maget-Dana R., Ptak M. (1989) *Biochimie* **71**, 111-116

54. Harnois I., Maget-Dana R., Ptak M. (1988) *J. Colloid. Interface Sci.* **123**, 85-91

55. Thimon. L., Peypoux F., Wallach J., Michel G. (1995) *FEMS Microbiol. Lett*. **128**, 101-106

56. Thimon. L., Peypoux F., Exbrayat J. M., Michel G. (1994) *Cytobios* **79**, 69-83

57. Op den Kamp J. A. F. (1979) *Ann. Rev. Biochem*. **48**, 47-71

58. Maget-Dana R., Harnois I., Ptak M. (1989) *Biochim. Biophys. Acta* **981**, 309-314

59. Maget-Dana R., Ptak M., Peypoux F., Michel G. (1987) *Biochim. Biophys. Acta* **898**, 1-5

60. Maget-Dana R., Ptak M., Peypoux F., Michel G. (1985) *Biochim. Biophys. Acta* **815**, 405-409

61. Maget-Dana R., Heitz F., Ptak M., Peypoux F., Guinand M. (1985) *Biochem. Biophys. Res. Commun*. **129**, 965-971

62. Maget-Dana R., Ptak M. (1990) *Biochim. Biophys. Acta* **1023**, 34-40

63. Latoud C., Peypoux F., Michel G. (1988) *J. Antibiotics* **41**, 1699-1700

64. Maget-Dana R., Thimon L., Peypoux F., Ptak M. (1992) *Biochimie* **74**, 1047-1051;
Thimon L., Peypoux F., Maget-Dana R., Roux B., Michel G. (1992) *Biotechnol. Appl. Biochem*. **16**, 144-151;
Razafindralambo H., Popineau Y., Deleu M., Hbid C., Jacques P., Thonart P., Paquot M. (1997) *Langmuir* **13**, 6026-6031

65. Maget-Dana R., Thimon L., Peypoux F., Ptak M. (1992) *J. Colloid. Interface Sci.* **149**, 174-183

66. Neu H. C. (1992) *Science* **257**, 1064-1072;
Amábile-Cuevas C. F., Cárdenas-García M., Ludgar M. (1995) *Am. Scientist* 83, 320-329;
Levy S. B. (1998) *Scientific American*, 32-39

67. DeMuri G. P., Hostetter M. K. (1995) *Pediatric Clinics of North America*, 42, 665-685

68. Blocquiaux S., Delcambe L. (1956) *Arch. Belg. Derm. Symp*. **12**, 224-227
Clairbois J. P., Delcambe L. (1958) *Arch. Belg. Derm. Symp*. **14**, 63-82

69. Yavordious D., Michel G., Peypoux F., Besson F. (1983) French Patent no. 81 13118 (July 3)

70. Razafindralambo H., Paquot M., Baniel A., Popineau Y., Hbid C., Jacques P., Thonart P., (1996) *JAOCS* **73**, 149-151

71. Besson F., Peypoux F., Michel G., Delcambe L. (1978) *J. Antibiotics* **31**, 284-288

72. Asaka O., Shoda M. (1996) *App. Environ. Microbiol*. **62**, 4081-4085

73. Pusey P. L., Wison C. L. (1984) *Plant Disease* **68**, 753-756

74. Pusey P. L. (1989) *Pestic. Sci*. **27**, 133-140

75. Klich M. A, Arthur K. S., Lax A. R., Bland J. M. (1994) *Mycopathologia* **127**, 123-127

Chapter 2

Synthesis and purification of iturin A_2 and analogues

2.1 Introduction

Synthetic peptides have been used in the study of structure-function relationships of a number of antibiotic peptides such as gramicidin S [1], melittin and melittin hybrids [2], magainin and magainin analogues [3]. This approach also contributed to the development of a new generation of antibiotic peptide analogues of, for example magainin [3], with potential pharmaceutical applications. Studies using synthetic model peptides with antimicrobial activity have been very successful in identifying highly active non-toxic peptides [4]. In contrast, studies on iturin A have mostly used the natural products isolated from *Bacillus subtilis* [5]; the mechanism of action of iturin A has only been partially elucidated (as discussed in Chapter 1). An opportunity therefore existed for investigation of the structure-function relationship of this antimicrobial lipopeptide using synthetic analogues.

Chemical peptide synthesis has been extensively reviewed in the literature [6-11]; only a brief overview will be given in this section. The chemical synthesis of any given peptide involves a number of steps, including the activation of groups participating in the peptide bond to facilitate formation, and protection of other chemically active groups to limit side reactions. Challenged by the formidable task of peptide synthesis, organic chemists developed various different synthesis techniques over the last century. These techniques can be divided into two principal categories: solution phase and solid phase peptide synthesis. The latter has proved to be the most successful, eliminating many of the laborious isolation and purification steps necessary in solution phase synthesis. Solid phase peptide synthesis was pioneered by R.B. Merrifield in 1959, who subsequently won the Nobel prize for Chemistry in 1984 in recognition of the impact of this approach. Two of Merrifield's early achievements were the first solid phase synthesis of a biologically active peptide, bradykinin in 1964 [12], and the first active enzyme, ribonuclease A, in 1969 [13].

Solid phase peptide synthesis entails the following:

- covalent attachment or anchoring of the first amino acid to a functionalised insoluble polymeric support;
- elongation of the peptide chain by stepwise addition of activated amino acid derivatives (suitably and reversibly protected);
- removal of excess reagents and by-products by filtration;
- and, the release of the assembled crude peptide from the support followed by purification and characterisation.

In all current solid phase methods peptide chain elongation proceeds from the C-terminal towards the N-terminal. Synthesis in the C→N direction lends itself to better chemical control than the N→C direction, where the activation of the acyl-amino acids results in optically impure peptides because of racemisation [7]. Peptide bond formation in the C→N direction requires the activation of the α-carboxyl group (to facilitate bond formation) and reversible protection of the α-amino group of the incoming amino acid (to limit polymerisation). Usually, the protection schemes used in the synthesis methods are two-dimensional in that they provide "permanent" protection for the functional amino acid side-chains and "temporary" protection for the α-amino group during synthesis, as will become clear in the following discussion.

The Merrifield peptide synthesis protocol uses functionalised cross-linked polystyrene as solid phase and a protection scheme based on graduated acidolysis. The "temporary" protection of the α-amino group is provided by the N^{α}-tertiary-butyloxycarbonyl (tBoc) group, which is removed with trifluoroacetic acid (TFA) [7, 12-14]. The "permanent" side-chain protection is conferred by ether, ester and urethane derivatives based on benzyl alcohol with electron-withdrawing halogens for greater acid stability. Other side-chain protection schemes are based on ether and ester derivatives of cyclopentyl and cyclohexyl alcohol. These "permanent" groups are removed when the anchoring linkages are cleaved with hydrofluoric acid (HF) in the presence of carbonium ions such as anisole [7]. The Merrifield protection scheme is summarised in Fig. 2.1.

Although many peptides of high purity have been, and are still being produced, the Merrifield protocol is associated with several problems caused by the successive harsh acid treatments needed to remove the α-amino tBoc-group, and by the HF treatment for the final release of the assembled peptide. These problems include premature loss of the peptide from solid phase, trifluoroacetylation, and destructive side reactions during the HF exposure [7, 11]. Laborious neutralisation and capping steps and the need for special apparatus for the hazardous HF treatments also encouraged researchers to look for alternative protection schemes.

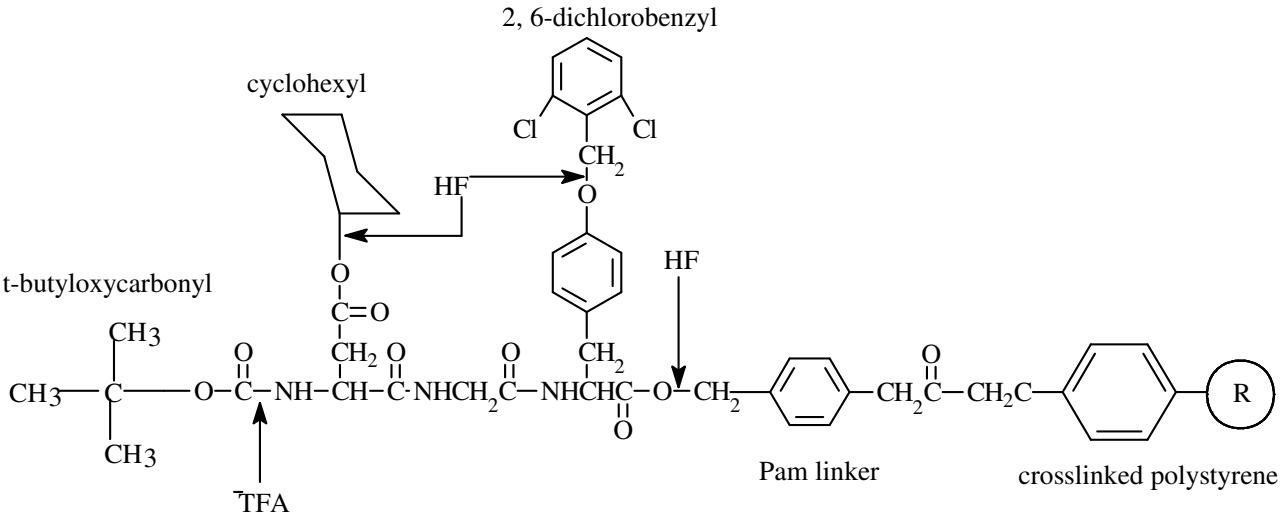

Figure 2.1 A two-dimensional protection scheme for solid phase synthesis of the standard Merrifield protocol based on graduated acidolysis [11].

An alternative synthesis protocol, developed by Atherton, Sheppard and Dryland (reviewed in 6, 9, 10), employs a protection scheme in which the acid-labile tBoc-amino protective group was replaced with a base-labile N^9-fluorenylmethyloxycarbonyl (Fmoc) group requiring only mild removal conditions [15, 16]. This base-labile Fmoc-group, developed by Capino and Han [17], can be rapidly removed by a β-elimination mechanism brought about by secondary amines such as piperidine, which also scavenges the dibenzofulvene intermediate and thereby prevents back-addition to the peptide chain [7, 15, 17]. This replaced the harsh acid treatments of the tBoc procedure with a mild basic treatment and reduces the extent of destructive side reactions. The "permanent" side-chain protection is provided by tertiary butanol-based ether, ester and urethane derivatives, which are cleaved under relatively moderate conditions by TFA with concomitant release of the peptide acid from the solid phase [7, 18]. An additional feature of the Atherton, Sheppard, Dryland synthesis protocol is the use of a rigid solid phase consisting of functionalised dimethylacrylamide polymerised within Kieselguhr (marketed as

Pepsyn K or NovaSyn®K) which allows continuous solvent flow synthesis [9, 19, 20]. The protection scheme based on the Fmoc-chemistry is summarised in Fig. 2.2.

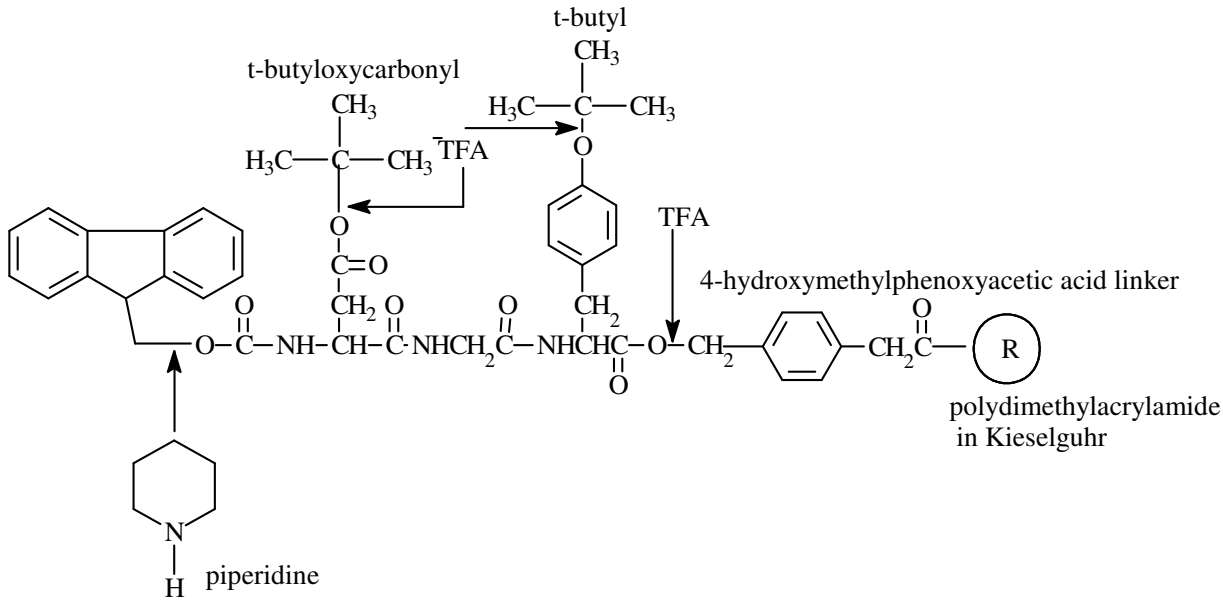

Figure 2.2 A two-dimensional protection scheme for solid phase synthesis by the Fmoc-polyamide protocol based on mild base treatment to remove the N-terminal protection and mild acid treatment to release the free peptide [11].

Considering the whole scheme of reactions in peptide synthesis, the most important reaction is obviously the formation of the peptide bond. The coupling of the incoming amino derivative to the peptide chain does not occur spontaneously; it must be facilitated by some form of activation. A number of activation methods are suitable for peptide synthesis. Only three of the most widely used methods will subsequently be discussed.

- The α-carboxyl group of an amino acid can be activated by formation of an active anhydride. Carbodiimides, such as dicyclohexylcarbodiimide (DCC) and diisopropylcarbodiimide (DIPCIDI), are frequently used in this type of *in situ* activation of amino acids. Side reactions, such as racemisation of amino acids and dehydration of the acid amide side-chains of asparagine and glutamine residues during the coupling, can be eliminated by the use of 1-hydroxybenzotriazole (HOBt), a so-called “trapping agent” [7, 10, 21]. In Fig. 2.3 the coupling reactions with DCC as activation agent are summarised.

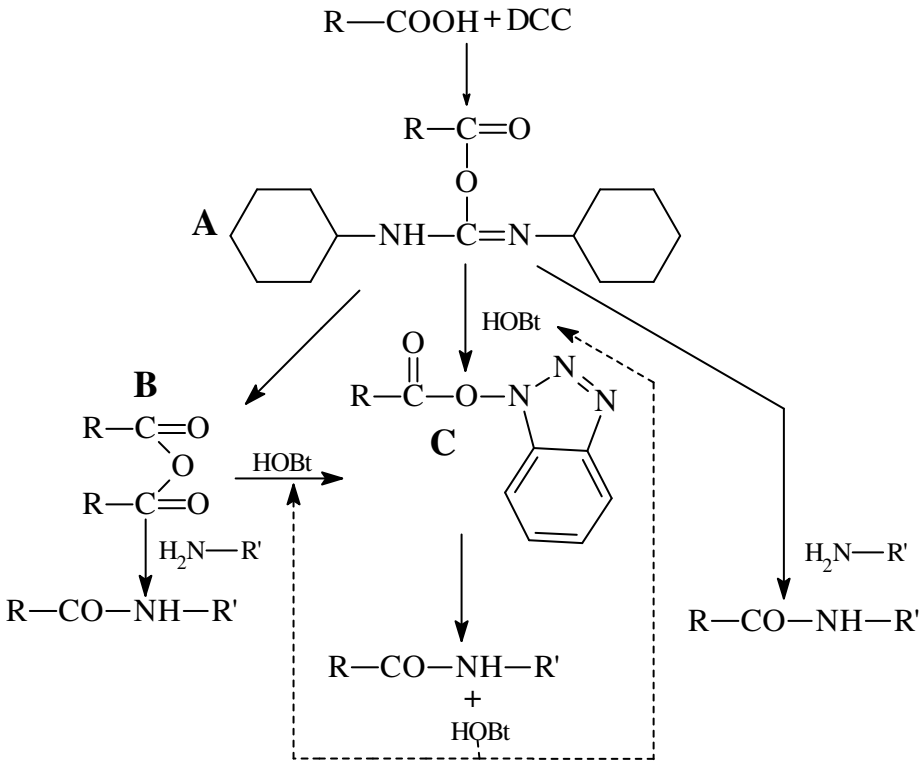

Figure 2.3 The activation of amino acids with DCC and HOBt to yield a dicyclohexylcarbodiimide-activated amino acid (A), a symmetrical anhydride of the amino acid (B) or a oxybenzotriazolyl ester of the amino acid (C). [7]

- Active esters amino acid esters of p-nitrophenyl [9], 3,4-dihydro-4-oxo-1,2,3-benzotriazin-3-yl (Dhbt) [9, 10, 22-24], and pentafluorophenyl (Pfp) [9, 10, 16, 19, 25, 26] are generally used with HOBt as acylation catalyst (Fig. 2.4). The latter two esters are generally suitable for peptide synthesis when used in polar aprotic solvents such as dimethylformamide (DMF). Most of the active esters are commercially available, consequently avoiding the laborious preparation of activated amino acids (e.g. symmetrical anhydrides). A reaction scheme, illustrating the use of active esters, is given in Fig. 2.4.

- A third type of *in situ* activation of amino acids employs benzotriazol-1-yl-oxy-tris-dimethylaminophosphonium hexafluorophosphate (BOP) [27, 28] and its lesser toxic analogue, benzotriazol-1-yl-oxy-tris-pyrrolidinophosphonium hexafluorophosphate (PyBOP®) [29, 30], both of which proved to be promising and relatively low cost reagents (Fig. 2.5). These reagents react with the N^{α}-protected amino acids in the presence of a base to form highly active oxybenzotriazolyl esters [7, 30]. These reagents also eliminate

the laborious symmetrical anhydride preparation and are cheap alternatives for the expensive active esters.

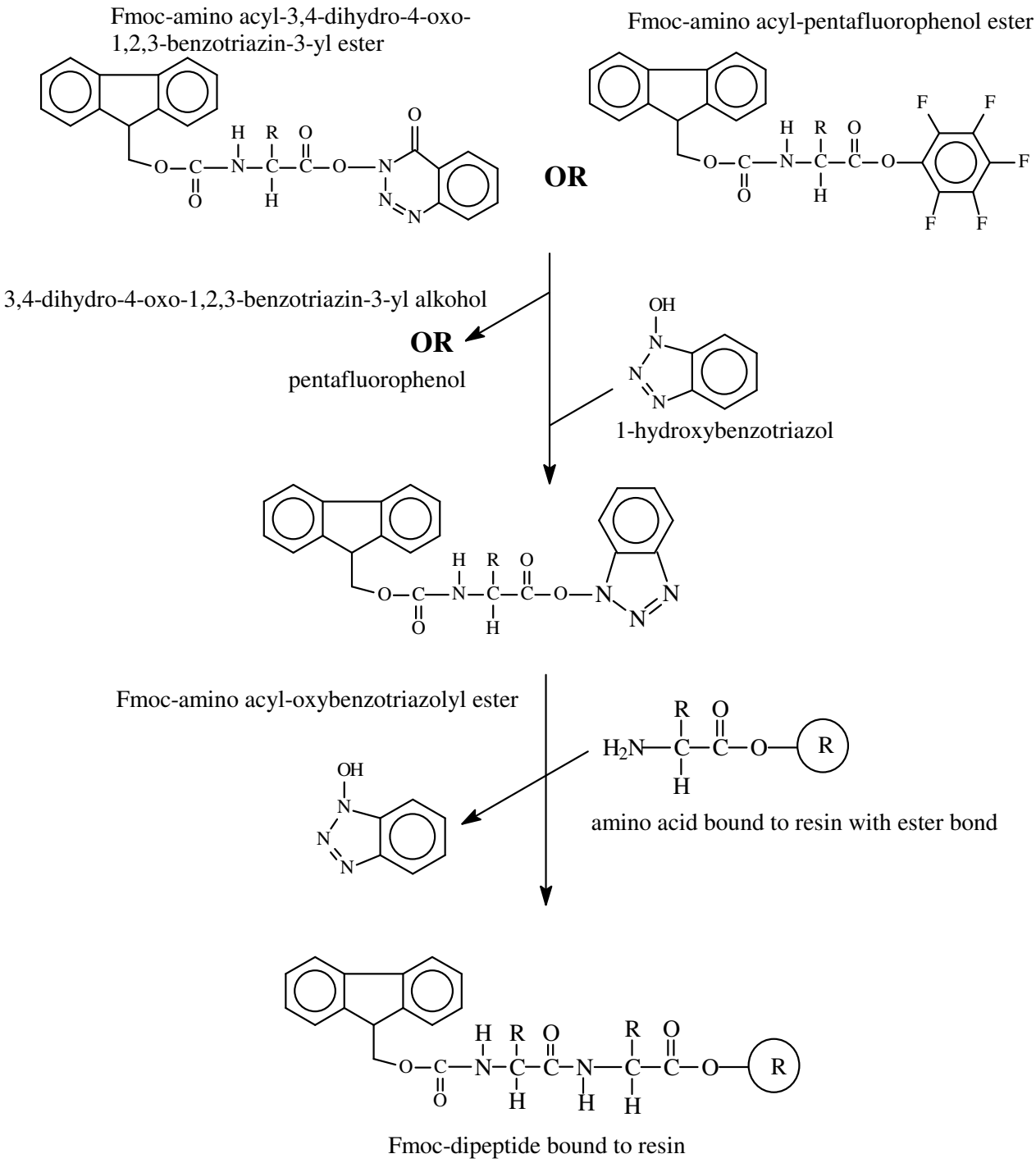

Figure 2.4 Reactions in peptide bond formation facilitated by using Fmoc-amino acyl-OPfp or Fmoc-amino acyl-ODhbt with HOBt as catalyst [adapted from 6].

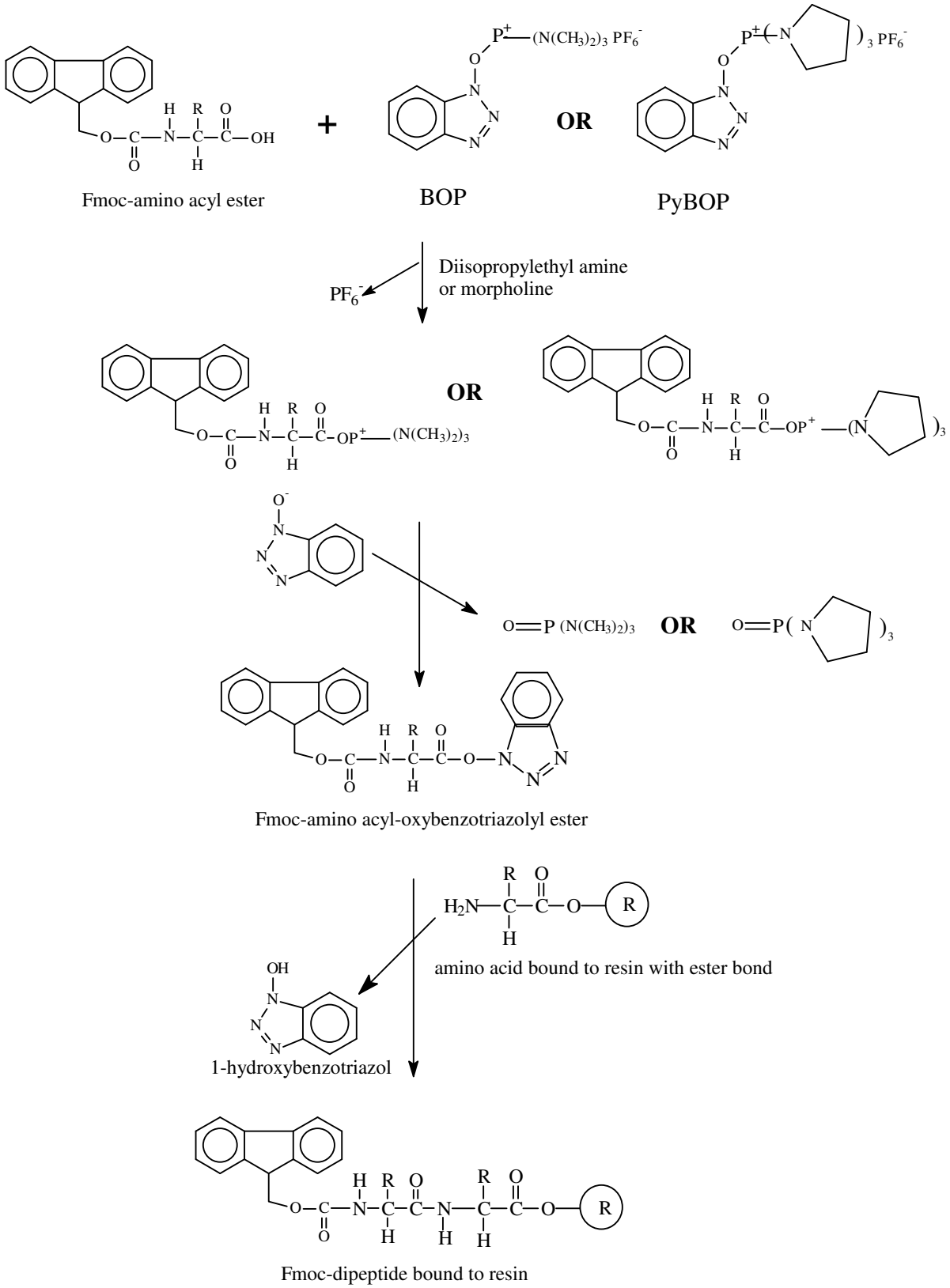

Figure 2.5 Reactions in peptide bond formation facilitated by using benzotriazol-1-yl-oxy-tris-dimethylaminophosphonium hexafluorophosphate (BOP) [27, 28] or its lesser toxic analogue benzotriazol-1-yl-oxy-tris-pyrrolidinophosphonium hexafluorophosphate (PyBOP®) [29, 30].

The establishment of an easily maintained peptide synthesis facility, preferably mechanised and automated, was a prerequisite for this investigation of iturin A. The peptide synthesis protocol of Atherton, Sheppard and Dryland, also called the Fmoc-polyamide peptide synthesis method, was chosen because of its milder chemical approach and previous experience with this method [6]. The simplicity and elegance of the Fmoc-polyamide chemistry allows the use of only one solvent throughout synthesis and has the added convenience that the Fmoc-group allows UV-monitoring of coupling reactions. Small scale syntheses in this study were conducted in a continuous flow system, while larger scale syntheses were done with a shake flask method (refer to section 2.3.3 for more detail).

When commercially available, the Pfp and Dbht active esters of the Fmoc-amino acids were used; otherwise the Fmoc-amino acids were activated using either DCC or the PyBOP® reagent. The efficiency of the coupling reactions was monitored by destructive procedures such as amino acid analysis, a simple ninhydrin test (Kaiser test [31]) or a Fmoc test [10]. The Kaiser test was used for monitoring the disappearance of amino groups during coupling and the appearance of amino groups after deblocking. Amino acid side-chain protection was provided by t-butyl ester (tBu), and in some cases by ether and urethane derivatives. These groups are cleaved under relatively moderate acidic conditions (95% TFA) used for releasing the peptide acid from the acid-labile linkage on the resin.

Eight different iturin A_2 analogues were synthesised (the subscript 2 in the name refers to the β-aminotetradecanoic acid residue in these iturin A analogues). One, two or all three of the amino acid residues in the conserved iturin sequence (L-Asn_2-D-Tyr_3-D-Asn_4), were omitted in the shorter peptides (Table 2.1). Two factors limited the range of synthetic analogues: (i) the financial expense of anchoring any one of the D-amino acids to the resin (first amino acid or C-terminal), and (ii) the β-aminotetradecanoic acid (β-NC_{14}) in the sequence. Because the synthesis of the Fmoc-derivative of the β-NC_{14} was greatly impaired by solubility factors, the tBoc derivative was prepared, even though this derivative is not compatible with the Fmoc-chemistry. This restricted the incorporation of the β-NC_{14} residue at the N-terminal in the final synthesis step (Table 2.1). The insolubility and pronounced amphipathic character of the peptide products restricted final purification to high performance liquid chromatography (HPLC). Chemical purity of products was evaluated with amino acid analysis, thin layer chromatography (TLC), fast atom bombardment mass spectrometry (FAB-MS) and electrospray ionisation mass spectrometry (ESI-MS).

Table 2.1 Primary structures of the iturin A_2 analogues synthesised in this study.

Iturin A_2 analogue	**Peptide primary structure**	**M_r**
5-Beta	β-NC_{14}—L-Gln—L-Pro—D-Asn—L-Ser	670.82
6-Beta	β-NC_{14}—D-Asn—L-Gln—L-Pro—D-Asn—L-Ser	783.92
7-Beta	β-NC_{14}—D-Tyr—D-Asn—L-Gln—L-Pro—D-Asn—L-Ser	947.10
8-Beta (linear Iturin A_2)	β-NC_{14}—L-Asn—D-Tyr—D-Asn—L-Gln—L-Pro—D-Asn—L-Ser	1061.20
cyclic 7-Beta	β-NC_{14}—D-Tyr—D-Asn—L-Gln—L-Pro—D-Asn—L-Ser	929.09
cyclic 8-Beta (Iturin A_2)	β-NC_{14}—L-Asn—D-Tyr—D-Asn—L-Gln—L-Pro—D-Asn—L-Ser	1043.20
YNQPNS	D-Tyr—D-Asn—L-Gln—L-Pro—D-Asn—L-Ser	721.72
NYNQPNS	L-Asn—D-Tyr—D-Asn—L-Gln—L-Pro—D-Asn—L-Ser	835.83

2.2 Materials

2.2.1 General reagents and solvents

N, N'-dimethylformamide (DMF; 99.5%), potassium hydroxide (KOH), sodium carbonate (anhydrous) and self-indicating silica gel were from Saarchem (Krugersdorp, South Africa). Trifluoroacetic acid (TFA; >98% and 99.5%), glacial acetic acid, chloroform (>99%), dichloromethane (DCM; 99.5%), diethyl ether (99.5%), petroleum ether (boiling point 40–60°C), ethanol (99.8%), butan-1-ol (99.5%), pyridine (99.5%), hexane (99.8 %), citric acid-1-hydrate (99.5%), potassium cyanide (KCN), *di*-phosphorous-pentoxide, 2',7'-dichlorofluorescein, ninhydrin, molecular sieve (0.3 nm pore size), aluminium oxide 90 and Kieselgel 60-F_{254} thin layer plates were from Merck (Darmstadt, Germany). Piperidine (98%), ethyl acetate (99.8%) and 2-methylbutan-2-ol (t-amyl alcohol; 98%) were from BDH

Chemicals (Poole, UK). TFA (>98%) and piperidine (98%) were also purchased from Sigma Chemical Co. (St. Louis, USA). Fluka Chemicals (Buchs, Switzerland) supplied 1-fluoro-2,4-dinitrobenzene (FDNB). High purity dry nitrogen gas was from Afrox, South Africa.

2.2.2 Derivatives, catalysts and resins for peptide synthesis

Fmoc-L-Ser(tBu)-Pepsyn KA-resin (0.09 meq/g), Fmoc-L-Asn-OPfp, Fmoc-L-Asn(mbh)-OH, Fmoc-D-Asn-OPfp, Fmoc-L-Gln-OPfp, Fmoc-L-Pro-OPfp, Fmoc-L-Pro-OH, Fmoc-L-Ser(tBu)-OPfp, Fmoc-L-Ser(tBu)-OH and Fmoc-D-Tyr(tBu)-OPfp were from Milligen-Millipore (Milford, USA). Fmoc-D-Asn-OH and Fmoc-L-Ser(tBu)-OH and pentafluorophenol were from Sigma Chemical Co. (St. Louis, USA). Fmoc-D-Tyr(tBu)-OH and benzotriazol-1-yl-oxy-tris-pyrrolidinophosphonium hexafluorophosphate (PyBOP®) were from Calbiochem-Novabiochem Co. (La Jolla, USA). N, N'-dicyclohexylcarbodiimide (DCC) was from Merck (Darmstadt, Germany). Fluka Chemicals (Buchs, Switzerland) supplied 1-hydroxy-benzotriazole (HOBt), N, N'-diisopropylethyl amine (DIPEA) and 2-(BOC-oxyimino)-2-phenylacetonitrile (BOC-ON). The HCl salt of β-aminotetradecanoic acid (β-NC_{14}.HCl) was donated by Dr. R. Levitt, formerly from Fine Chemicals, South Africa.

2.2.3 Reagents and solvents for amino acid analysis and chromatography

TFA (99.5%), constant boiling hydrochloric acid (HCl, 30%), sodium acetate (99.5%) and phenol (99.5%) were from Merck (Darmstadt, Germany). Phenylisothiocyanate (PITC) and amino acid standards were from Pierce Chemicals (Rockford, USA). Ethylenediaminetetraacetic acid tetrasodium salt dihydrate (EDTA, >98%) was from Fluka Chemicals (Buchs, Switserland). Methanol (HPLC-grade, UV cut-off 205 nm) and acetonitrile (HPLC-grade, UV cut-off 190 nm) were from Romil LTD (Cambridge, UK). Pico-Tag® sample diluent, Nova-Pak analytical HPLC columns, 0.45 mikron HV membrane filters were from Waters-Millipore (Milford, USA). Polygosil (C_{18}, 60 Å, irregular particles) packing material, used to prepare the semi-preparative HPLC column, was from Macherey-Nagel (Düren, Germany). High quality triethylamine (TEA) was from Aldrich Chemical Co. (Gillingham, UK). Sephadex LH20 was from Pharmacia (Uppsala, Sweden). Analytical grade water was prepared by filtering glass distilled water through a Millipore Milli Q® water purification system.

2.2.4 Drying and storage of reagents and products

Fmoc-amino acids, peptide synthesis resins, β-NC_{14}.HCl, tBoc-β-NC_{14}, BOC-ON and HOBt were stored at 4°C in desiccators with silica gel as drying agent. The FDNB was stored at 10°C and PyBOP® at −20°C, both with silica gel (with indicator) as drying agent. Before use, amino acid derivatives, resin, PyBOP® and HOBt were dried overnight under high vacuum, with

di-phosphorous-pentoxide as drying agent. The DMF was stored over molecular sieve (0.3 nm) at room temperature. PITC and amino acid standards were stored at −20°C and TEA (high quality for amino acid analysis) at 10°C, all under N_2-atmosphere. Lyophilised peptides were stored under vacuum at room temperature in a desiccator with silica gel as drying agent. All other reagents were stored at room temperature.

Great care was also taken to avoid detergent contamination of glassware, as such contamination of peptide preparation could influence the structure-function studies. Detergent contamination could easily be detected with ESI-MS as most laboratory detergents contain highly charged compounds. The glassware, returned from the regular wash, was rinsed three times with distilled water, three times with 60% ethanol and then washed three times with analytical grade water. It was placed in a oven to dry at temperatures ranging between 110°C and 140°C. Bottles for amino acid derivatives and purified peptide were also prepared in the same way and then pyrolised at 565 - 570°C for two hours.

2.3 Methods

2.3.1 Preparation of solvents

2.3.1.1 Distillation and testing of N, N'-dimethylformamide [adapted from 6]

DMF is the principal solvent used in the Fmoc-polyamide peptide synthesis method. Impure DMF contains contaminants such as secondary amines and H_2O, causing to the loss of the Fmoc and active ester groups respectively. DMF also reacts with water to form dimethylamine and formic acid: $\mathbf{(CH_3)_2NCOH + H_2O \rightarrow (CH_3)_2NH + HCOOH}$

To avoid side reactions with the amines, water and other impurities it was imperative to use freshly distilled, high purity DMF in the Fmoc-polyamide peptide synthesis procedure. DMF

was shaken up with 10-20 g/L dry potassium hydroxide pellets or 0.3 nm molecular sieve to remove residual water. Other impurities such as volatile secondary amines were removed by fractional distillation under reduced pressure (high vacuum pump, 5-10 mm Hg) and a dry nitrogen bleed. As DMF has a boiling point of 153^{o}C at atmospheric pressure, it was necessary to distil DMF under vacuum to avoid possible decomposition at high temperatures. The first 10% of the distillate was discarded and the constant boiling fraction (45^{o}C at 10 mm Hg) was collected. The distilled DMF was stored in dark bottles at room temperature over 0.3 nm molecular sieve. If it passed the Sanger test (see below), the freshly distilled DMF was used within seven days, otherwise it was re-distilled.

2.3.1.2 Sanger's test for amines

It was necessary to test for amines in DMF, because the Fmoc-group is very labile in the presence of secondary amines. Sanger's test for amines [32] was carried out by mixing equal volumes of 1-fluoro-2,4-dinitrobenzene (1.0 mg/mL FDNB in 95% ethanol) and DMF and leaving it at room temperature for 30 minutes. The absorbance of the reaction mixture was determined at 381 nm and 0.5 mg/mL FDNB in 95% ethanol was used as blank. The blank's absorbance was normally in the region of 0.2 absorbance units, while suitably pure DMF had an absorbance at 38l nm of not more than 0.07 units higher than the blank.

To ensure the removal of all traces of piperidine (used in the deblocking steps, refer to section 2.3.3.3) during the peptide synthesis protocol, the Sanger test was performed on DMF samples from final washing steps. The samples were in most cases incubated for 2-3 minutes and compared to a blank solution.

2.3.1.3 Distillation of piperidine and pyridine

Piperidine used in peptide synthesis must also be of a high purity, for the same reasons as the DMF. Piperidine was purified by distillation over dry potassium hydroxide (10 to 20 g/L) and a dry nitrogen bleed at atmospheric pressure. The first 10% of the distillate was discarded and the constant boiling fraction (105^{o}C) was collected. The distilled piperidine was stored in dark bottles [33]. Pyridine used in the Kaiser test was prepared in the same manner.

2.3.2 Preparation of amino acid derivatives

2.3.2.1 Synthesis of N^{β}-t-butyloxycarbonyl-β-aminotetradecanoic acid [adapted from 34]
The HCl salt of β-aminotetradecanoic acid (1.05 g, 3.75 mmole) was suspended in 5 mL freshly distilled DMF. TEA (2 mL) was added to the suspension while stirring at 50°C over an oil-bath. An 1.2 fold excess (1.16 g; 4.6 mmole) of 2-tertiary-butyloxycarbonyl-oxyimino-2-phenylacetonitrile (BOC-ON) was dissolved in 1.5 mL DMF and added drop-wise to the stirring suspension. The resulting yellow suspension was stirred for 2 hours at 50°C until the solution became clear. (In some cases it was necessary to add additional amounts of 100 µL 10% BOC-ON in DMF.) The reaction mixture was evaporated to an oil under high vacuum at 45°C. The residual oil was dissolved in 25 mL diethyl ether (filtered though activated aluminium oxide to remove residual peroxides) and extracted twice with 5 mL saturated aqueous citric acid (59.2% m/m at 20°C) to remove residual BOC-ON. The aqueous fractions were combined and extracted twice with 5 mL diethyl ether. The combined diethyl ether fraction was washed twice with 25 mL water and dried with anhydrous sodium sulphate. The diethyl ether was evaporated under vacuum and residual oil dissolved in 5 volumes (10 mL) heated acetonitrile (40°C). It was allowed to cool in an ice-bath and left overnight at 4°C. The resulting white crystalline material was filtered, washed with chilled acetonitrile and dried overnight under vacuum at room temperature. The product showed a negative Kaiser test and the yield was 91%. The melting point was 56–58°C.

TLC was performed on aluminium backed Kieselguhr 60-F_{254} TLC-plates developed in chloroform:methanol:acetic acid (85:10:5) [6, 8]. Plates were carefully air-dried and first visualised under UV-light (254 nm). The dried plates were sprayed with 0.025% of 2',7'-dichlorofluorescein in 95% ethanol, developed for 5 minutes at 110°C and visualised under UV-light. The plates were then sprayed with 0.2% ninhydrin in 95% ethanol and developed at 110°C for 10 minutes to detect residual amino groups. A single spot (R_f of 0.66) for the product was detected with the 2',7'-dichlorofluorescein reagent and there was no visible contamination from BOC-ON or β-NC_{14}.

Electron impact ionisation mass spectrometry analyses of the product yielded results corresponding to that obtained by Levitt [34] and confirmed the integrity of the product.

2.3.2.2 Preparation of the Fmoc-amino acid derivatives

Most of the Fmoc-amino acid derivatives were readily available commercially, but at a considerable expense. The syntheses of most Fmoc-amino acids have been described in literature [9, 35, 36] and *de novo* synthesis was sometimes a way to reduce excessive costs associated with peptide synthesis. Kaiser tests (which must be negative), melting point determinations (which must be within 5°C literature value [10, 36]) and TLC on each of the amino acids derivatives used in synthesis were done to ensure product quality. Kaiser positive samples of Fmoc-amino acids without acid-labile side-chain protection were suspended in 1% acetic acid (or 0.1% acetic acid if it contained acid-labile side-chain protection) and the precipitate collected by filtration. The precipitate was then washed with water, ice-cold methanol, ethyl acetate and diethyl ether and subsequently dried under vacuum. This procedure normally gave Kaiser-negative samples. If the derivative remained outside quality control limits it was recrystallised from hexane/ethyl acetate. The Pfp esters were recrystallised from hexane and/or washed with ice-cold ethyl acetate and n-hexane.

The pre-activation of Fmoc-Asn-OH and Fmoc-Gln-OH to form their pentafluorophenyl esters was necessary. Other activation procedures, such as with PyBOP® and DCC, lead to the dehydration of their side-chains to form aspartimides and glutamimides [10]. As an alternative, the addition of HOBt to Fmoc-Asn-OH or Fmoc-Gln-OH, before addition of PyBOP® and DIPEA, limits the dehydration of the acid amide side-chain [a].

A method described by Atherton *et al.* [25] for the synthesis of Fmoc-L-Leu-OPfp was adapted for the synthesis of Fmoc-D-Asn-OPfp. Fmoc-D-Asn-OH (3.54 g; 10 mmole) and pentafluorophenol (2.02 g; 11 mmole) was suspended in 17 mL dioxan and cooled in an ice-bath. DCC (2.27 g; 11 mmole) in 8 mL dioxan was added drop-wise to the stirring slurry. The stirring solution was left to react for 75 minutes in the ice-bath. The white creamy slurry was further diluted with 27 mL dioxan and stirred for another 23 hours at room temperature. The reaction mixture was filtered to remove the white dicyclohexylurea (DCU) precipitate. The precipitate was washed with two times 10 mL dioxan and the combined filtrate was evaporated under vacuum. The pentafluorophenyl ester crystallised when n-hexane was added. The slightly yellow crystals were washed with ice-cold ethyl acetate and methanol and then dried under vacuum (68% yield). The melting point of the product was 156°C-160°C, which

[a] The protection of the side-chain with e.g. 4, 4'-dimethoxybenzhydryl-group (mbh) is recommended [10], when using PyBOP® or DCC.

agreed with that of commercial Fmoc-L-Asn-OPfp. The product was further evaluated by TLC (refer to section 2.3.2.1) which showed a UV detectable spot ($R_f = 0.7$) corresponding to that of the commercial Fmoc-L-Asn-OPfp. Both the commercial and the synthesised product contained a small amount of Fmoc-L-Asn-OH. The product was further tested by a small scale coupling to 10 mg of the solid phase resin (Pepsyn KA with L-Ser(OtBu) as the first amino acid; see 2.3.3.2). After 60 minutes coupling an Fmoc-test (see 2.3.3.5) confirmed completion of acylation of the resin, and by implication the integrity of the activated amino acid.

2.3.2.3 Preparation of symmetrical anhydrides of amino acid derivatives

The reactive anhydrides were prepared immediately before their use in the elongation step in peptide synthesis [6, 20]. Eight times molar excess of the protected amino acid was dissolved in a small volume (<4 mL/mmole) of dichloromethane (DCM) by stirring in a closed vessel. A few drops of DMF were added to improve solubility. Four times molar excess of crystalline DCC dissolved in minimum DCM (<2 mL/mmole) was added to the amino acid solution, and stirred for 15 minutes at room temperature in the closed vessel. The progression of the reaction was indicated by the formation of the insoluble by-product DCU. The white DCU precipitate was removed from the reaction mixture by filtration on a sintered glass filter, before drying by rotary evaporation. The symmetrical anhydrides were dissolved in minimum DMF (1–2 mL) shortly before use.

2.3.3 Synthesis of the linear peptides

The peptides were synthesised at room temperature using the Fmoc-polyamide protocol on either a self-assembled manual peptide synthesiser (Fig. 2.6) for small scale synthesis or using a shake flask bench procedure for larger scale synthesis (Fig. 2.7). The first synthesis of 8-Beta was done separately using the continuous flow method in the Econopep MRII Synthesiser (Fig. 2.6). The synthesis of 7-Beta, 6-Beta and 5-Beta, up to the tetrapeptide unit L-Gln-L-Pro-D-Asn-L-Ser, was done with the shake flask method on the same batch of resin The resin batch was split in two and the β-amino acid residue was coupled to one batch to produce 5-Beta. D-Asn was coupled to the other tetrapeptide containing batch and the resin batch was split again. One batch was used for the synthesis of 6-Beta and the other for 7-Beta. In the third and fourth synthesis 8-Beta, 7-Beta and 6-Beta were synthesised using our shake flask method (Fig. 2.7), each time starting with one batch of Pepsyn KA resin. Small

quantities of the peptides YNQPNS and NYNQPNS were also synthesised and purified (refer to Chapter 3 for more detail).

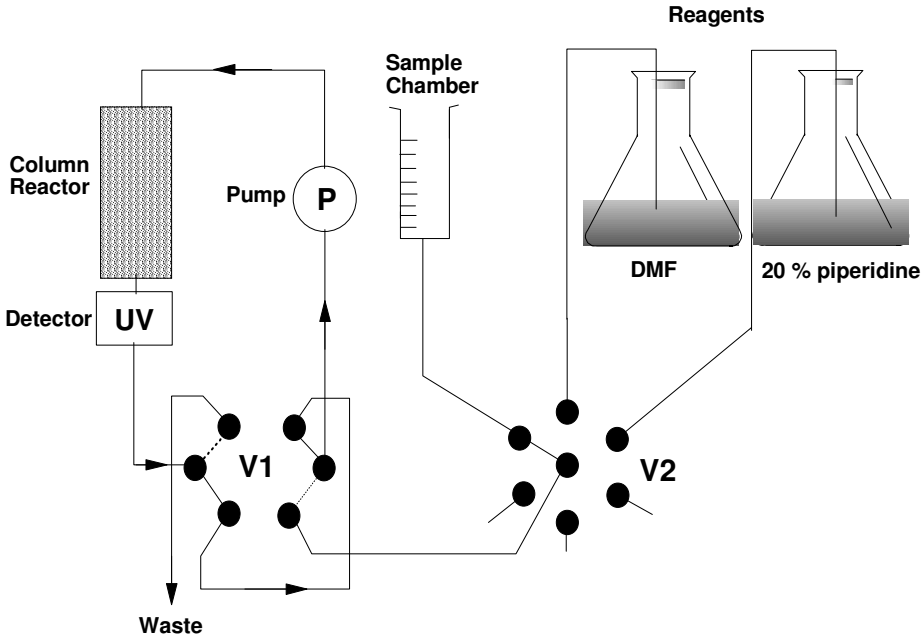

Figure 2.6 "Econopep MRII Synthesiser": A schematic representation of a manually controlled peptide synthesiser. V1 and V2 are selector valves.

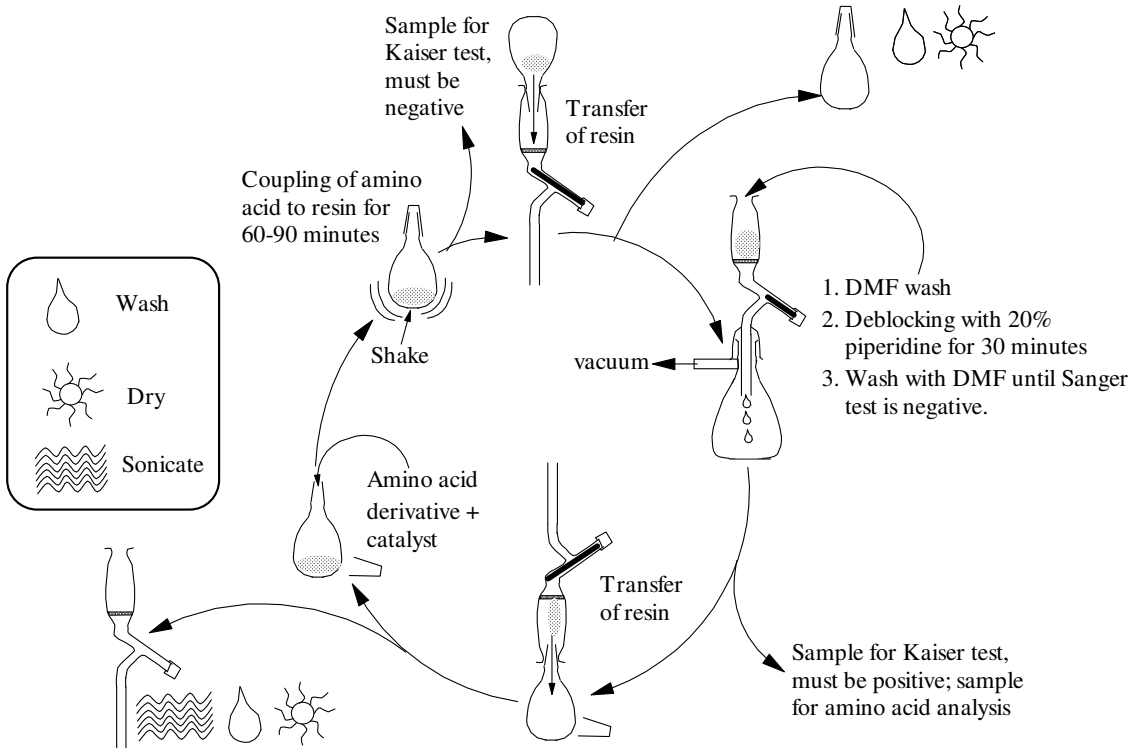

Figure 2.7 Apparatus set-up and methodology used in the shake-flask procedure.

The protocol for a complete cycle of operations including washing, coupling, deblocking and sampling steps for the continuous flow and bench Fmoc-polyamide solid phase peptide synthesis is set out in Table 2.2.

Table 2.2 Operations for one cycle of the peptide synthesis procedure

Synthesis step	Time	Volume	Monitoring	Comment
1. Swelling of resin	20 min.	4 bed volumes		bed volume = 5 mL/gram resin
1. Anchoring of first amino acid using activated Fmoc-amino acid to resin	2 hours	< ½ bed volume	Fmoc-test	Refer to sections 2.3.3.1 and 2.3.3.5
1. DMF wash		6 X 3 bed volumes	Absorbance at 290 or 310 nm	Absorbance must be baseline or zero
1. Resin sample A			i. Kaiser test (2.3.3.4) (ii. Amino acid analysis; 2.3.6.3)	i. If test not negative, extent or repeat coupling step in elongation. ii. Amino acid analysis is used in monitoring anchoring step
1. Removal of Fmoc group (deblocking) with 20% piperidine in DMF	30 min.	3 bed volumes	Absorbance at 290 or 310 nm or Fmoc test	Refer to sections 2.3.3.3 and 2.3.3.5
1. DMF wash		10 X 3 bed volumes		
1. DMF wash sample		0.5 mL	Sanger test	Wash until test is negative (refer to 2.3.1.2)
1. Resin sample B			i. Kaiser test ii. Amino acid analysis	i. If test is not positive, repeat deblocking ii. Post synthesis evaluation
1. Coupling of next amino acid using activated Fmoc-amino acid	60 min.	< ½ bed volume		Refer to 2.3.3.2 Repeat steps 3 and 9 if necessary
1. Repeat steps 3 to 8				
1. Repeat steps 9 and 10 for α-amino acids in sequence				
1. Coupling of activated tBoc derivative of β-NC_{14} residue				Refer to 2.3.3.2 and 2.3.2.3
1. Repeat steps 3 and 4				
1. Washing and drying of resin				Refer to 2.3.3.6
1. Liberation of peptide acid from resin				Refer to 2.3.3.6

2.3.3.1 Coupling of the first amino acid

Commercially available Pepsyn KA-resin (capacity of 0.09 milli-equivalent per gram of dry resin), with Fmoc-L-Ser(tBu) acid already attached, was used in all the syntheses. For each synthesis the resin was swollen for 20 minutes in high purity DMF (20 mL/g). Resin samples, taken to evaluate the resins, were treated with 20% piperidine for the Fmoc test (see section 2.3.3.5) or washed with ether and dried for amino acid analysis and the Kaiser test.

2.3.3.2 Elongation of the peptide chain

For the elongation steps the required reagent quantities were calculated from the resin capacity (0.09 milli-equivalent per gram of dry resin). A three times molar excess of the subsequent active Fmoc-amino acids and HOBt as catalyst were used in the elongation of the peptide chain. The pentafluorophenyl esters of Fmoc-L-Pro, Fmoc-L-Asn, Fmoc-L-Gln, Fmoc-D-Asn and Fmoc-D-Tyr(OtBu) were used in the relevant coupling reactions. The tBoc derivative of the β-aminotetradecanoic was coupled after activation by the symmetrical anhydride method (described under section 2.3.2.3) or activation by the PyBOP® reagent. Fmoc-D-Tyr(OtBu)-OH, Fmoc-L-Asn(mbh)-OH and Fmoc-L-Pro-OH were coupled using the PyBOP® reagent. The PyBOP® reagent was used as follows: a three fold molar excess of both the protected amino acid and HOBt, each in minimum DMF (0.5-1.0 mL), were mixed thoroughly with the resin, followed by the addition of three fold molar excess PyBOP® mixed with a six fold molar excess N, N'-diisopropylethyl amine (DIPEA) in minimum DMF (0.5-1 mL) [30]. In the shake flask method the total volume of DMF was limited to <5 mL/gram of resin. The reaction time of the coupling steps varied from 60 to 90 minutes. The coupling time depended on the completeness of acylation as determined with the Kaiser test (section 2.3.3.4) or the Fmoc test (section 2.3.3.5).

2.3.3.3 Removal of Fmoc-group from the attached amino acid

After the coupling step was completed (as determined by two consecutive negative Kaiser tests; refer to section 2.3.3.4), the resin was washed thoroughly to remove any trace of active amino acid derivative and catalyst. Piperidine (20% in DMF) was added to the resin and the deblocking reaction was allowed to proceed for 30 minutes. The absorbance of the piperidine mixture was measured at 290 nm (refer to 2.3.3.5) or the deblocking step was continuously monitored at 310 nm in order to follow the liberation of the Fmoc group. The piperidine was removed and the resin washed with DMF until the DMF-wash tested negative with the Sanger

test (refer to 2.3.1.2). For a successful synthesis it was imperative that all the piperidine be removed from the resin and glassware in contact with the reaction mixture.

2.3.3.4 Kaiser test for free primary amino groups

The Kaiser test [31] is specific for primary amino groups and was conducted on resin samples to monitor the completeness of the acylation reaction or removal of the Fmoc-group. Three solutions are required: (a) 500 mg ninhydrin in 10 ml 95% ethanol, (b) 40 g phenol in 10 ml 95% ethanol, and (c) 2 ml 0.001 M KCN solution diluted to 100 ml with distilled pyridine. (The test was adapted by using only half the recommended phenol.)

Four drops of each of these solutions were mixed with an ether-washed and dried resin sample taken during peptide synthesis; the mixture was heated for 5 to 10 minutes on a 80^{o}C water bath. The presence of remaining free amino groups caused the resin beads to turn a characteristic deep blue colour. Otherwise, the reaction solution and resin particles remained yellow. Two (or more) samples were taken during synthesis, one during the coupling step (sample A at 60 minutes), which should be negative, and one after the piperidine deblocking step (sample B), which should be positive before the synthesis can be continued. If the test did not confirm completion of the reaction, that particular step was repeated or the reaction time extended. Some of the N-terminal amino acids gave anomalous bead colours and not the intense blue of the free amino acid when reacting with the ninhydrin, e.g. proline gave a brown colour and serine, asparagine and glutamine a green-orange colour.

Quality control of Fmoc-amino acid derivatives was also done by dissolving 5.0 mg derivative in 100 µL DMF and adding 100 µL of each of the Kaiser test solutions. Colours were evaluated after 5 minutes incubation in a 80^{o}C water bath by comparison with standardised colour results on a colour chart.

2.3.3.5 The Fmoc-test

To evaluate the coupling of an Fmoc amino acid, and especially the coupling of the first amino acid, the characteristic UV absorbance of the liberated Fmoc-fulvene group was exploited [10, 17]. For the Fmoc-test a small amount of resin (typically 10 mg) was removed after the coupling reaction, washed with ether, dried under vacuum and analytically weighed. An accurate volume of 20% piperidine in DMF (200 µL/µmole expected Fmoc-groups) was added to the dried resin and then the deblocking reaction was allowed to proceed for 30 minutes. The absorbance of the deblocking mixture, diluted 10 or 20 times with DMF, was

measured at

290 nm. The coupling efficiency was the calculated from the following relationship:

% Coupling efficiency of step = (dilution x **A_{290}-0.9975) / 0.2848**

Light path = 1.0 cm; resin capacity = typically 0.09 mmoles/1000 mg

2.3.3.6 Removal of the completed peptides from the resin

After the final coupling reaction of the tBoc-β-NC_{14} residue and DMF wash, the resin was washed on a sintered glass filter with t-amyl alcohol, acetic acid, t-amyl alcohol and finally with peroxide free diethyl ether and then dried under vacuum [6, 9, 10]. The peptides were cleaved from the resin with 95% TFA and 5% H_2O or 5% phenol as scavenger [b]. The peptide resin was treated for three to six hours with four bed volumes 95% TFA and 5% scavenger. After cleavage, the resin was removed by filtration and washed with 50% TFA and water. The resin was then washed with t-amyl alcohol, acetic acid, t-amyl alcohol and ether, dried and analysed for amino acids to evaluate the extent of peptide cleavage. The filtrate containing the peptide was dried under high vacuum on a Buchi Rotavapor at 40°C, resuspended in 50% acetonitrile and lyophilised. Because of the lipopeptides insolubility in most solvents, an organic solvent/water extraction was not used as initial purification step.

Small amounts of peptide without the β-amino acid residue, YNQPNS and NYNQPNS, were also prepared using the above protocol and resin samples taken before the final coupling step in 7-Beta and 8-Beta syntheses.

2.3.4 Cyclisation of the peptides

2.3.4.1 Cyclisation using DCC

Several attempts to cyclise 8-Beta, using DCC, proved to be marginally successful and therefore only one protocol is described here. A small quantity of crude 8-Beta (5 μmol) was dissolved in 1 mL freshly distilled DMF, after which 20 mL DCM was added. DCC and HOBt (2 mmole each) were dissolved in 50 mL DMF. The peptide solution was added slowly (over about 30 minutes) to the DCC/HOBt solution while stirring and left to react for 3 days. The

[b] Removal conditions generally include scavengers, which are used to remove reactive by-products such as carbonium-ions that may cause unwanted side reactions with the released peptide [7, 9, 10].

reaction mixture was extracted once with 100 mL 50% acetic acid. The acetic acid fraction was lyophilised and the residue dissolved in 50% acetonitrile for further HPLC purification .

2.3.4.2 Cyclisation using PyBOP®

Method A: A small quantity (15 µmole) of 8-Beta or 7-Beta was dissolved in 3 mL freshly distilled DMF, after which 15 mL DCM was added. PyBOP®, HOBt (30 µmole each) and DIPEA (60 µmole) in 0.5 mL DMF was added slowly to the peptide mixture while stirring. The mixture was left to react for 5 days at room temperature. The reaction mixture was dried under vacuum and a N_2 stream and dissolved in 3 mL 50% acetonitrile for HPLC purification.

Method B: The test method was adapted in an attempt to limit polymerisation and improve yields. Firstly the peptide solution (15 µmole in 3 mL DMF) was diluted 10 times with DCM and titrated with DMF to keep the solution clear. The resultant mixture was subsequently cooled to 0^oC. PyBOP®, HOBt (30 µmole each) and DIPEA (60 µmole) in 0.5 mL DMF was added slowly to the cooled peptide mixture while stirring, and left to react for 5 days at room temperature. The reaction mixture was dried under a N_2-stream and dissolved in 3 mL 50% acetonitrile for HPLC purification.

2.3.5 Purification of the lipopeptides

2.3.5.1 Hydrophobic interaction chromatography

Sephadex LH20 chromatography was used in a trial purification of the crude linear peptides. The solubility of the peptides was very poor (<1 mg/mL) in either methanol, ethanol, acetonitrile or water alone. Solubility improved in mixtures of water and organic solvent. A small quantity of lyophilised crude peptide (4 mg) was consequently dissolved in 600 µL of a 50% methanol/water mixture. The absorption at 230 and 260 nm was determined and the solution was applied to a column (50 mm X 10 mm). Peptides were eluted using a 50% water/methanol mixture at a flow rate of 20 mL/hour. Column eluates were monitored at 230 nm and 260 nm. The major absorbing fractions were collected and lyophilised.

2.3.5.2 High performance liquid chromatography

Semi-preparative HPLC was preferred to purify the crude peptides, because of low yields obtained by Sephadex LH20 chromatography. Samples (5 mg/mL) were dissolved in 50 % acetonitrile in water and centrifuged for 5 minutes at 1000 g to remove undissolved particulate

and subjected to purification on a semi-preparative C_{18} Polygosil HPLC column (irregular particle size, 60 Å pore size, 250 mm x 10 mm). The chromatography system consisted of two Waters 510 pumps, MAXIMA software control system, Waters Model 440 detector and a WISP 712 sample processor. A linear gradient, at a flow rate of 3 mL/min, was created using eluant A (0.1% TFA in water) and eluant B (90% acetonitrile and 10% A) [30] (Table 2.3). The separation was monitored at 254 nm with a Waters Model 440 UV-detector. Peptide fractions were collected, lyophilised and analysed further.

Certain cyclic peptides were purified on a C_{18} Nova-Pak HPLC column (5 µm particle size, 60 Å pore size, 150 mm x 3.9 mm). Racemic mixtures of 8-Beta, originating from the introduction of a racemic mixture of β-aminotetradecanoic acid, were further purified on an analytical C_8 Nova-Pak HPLC column (5 µm particle size, 60 Å pore size, 150 mm x 4 mm). A linear gradient was created using the same eluants A and B as for the preparative HPLC purification. The gradient program, specifically developed for these amphipathic lipopeptides, used in both separation procedures is described in Table 2.3.

Table 2.3 Gradient programs used in the chromatography of the lipopeptides

Time (min)	**Flow preparative HPLC (mL/min)**	**Flow analytical HPLC (mL/min)**	**% A**	**% B**	**MAXIMA curve type**
0	3.0	1.0	70	30	
1	3.0	1.0	70	30	linear (6)/curve (5)
13	3.0	1.0	0	100	linear (6)/curve (5)
14	3.0	1.0	0	100	linear (6)
20	3.0	1.0	70	30	linear (6)
25	3.0	1.0	70	30	

2.3.6 Analysis of the purified peptides

2.3.6.1 Thin layer chromatography

Peptides were analysed with TLC on aluminium backed Kieselguhr 60-F254 TLC-plates developed in butan-1-ol:pyridine:acetic acid:water (90:80:60:72) [8]. TLC was also done on the hydrolysates of the lipopeptides in a petroleum ether:diethyl ether:acetic acid (90:10:1) solvent system. Visualisation was done as described for the TLC under section 2.3.2.1.

2.3.6.2 Analytical high performance liquid chromatography

Reverse phase HPLC was used to assess the purity of the synthetic peptides. A C_{18} Nova-Pak HPLC column, or C_8 Nova-Pak HPLC column, was used with the system described under section 2.3.5.2. The chromatography was monitored at 254 nm. Linear and non-linear gradients were created using eluant A (0.1% TFA in water) and eluant B (90% acetonitrile and 10% A). Elution program 1 was identical to the one shown in Table 2.3 with a flow-rate of 1.0 mL/minute and the MAXIMA linear gradient no. 6. In elution program 2, a non-linear gradient (gradient 5 in MAXIMA control) was run from 1 to 13 minutes.

2.3.6.3 Amino acid analysis

Amino acid analyses were done using a pre-column derivatisation with phenylisothiocyanate (PITC), according to the Pico-Tag® method [37, 38]. Vacuum-dried samples (peptide synthesis resin samples, crude peptide and purified peptide preparations) were analysed for amino acid composition after 24 hour gaseous phase hydrolysis at 110°C or after a shortened hydrolysis (150°C, 1 hour). Gaseous phase hydrolysis was done under a nitrogen atmosphere using 6 N HCl containing 1% phenol. After hydrolysis the acid was removed from the samples under high vacuum. In the next step, the so-called "re-drying" step, 10 µL methanol:water:TEA (1:2:1) was added to each sample to ensure the optimal pH for derivatisation. The samples were thoroughly vacuum-dried before derivatisation with 20 µL methanol:TEA:water:PITC (7:1:1:1). The derivatisation proceeded for 20 minutes at room temperature. Samples were again vacuum-dried, dissolved in an appropriate amount (50-300 µL) of Pico-Tag® diluent and filtered through HV 0.45 µm Millipore membrane filters.

Chromatography was done at 44°C on the Waters HPLC system described under 2.3.5.2 using a Nova-Pak C_{18} HPLC column (150 mm x 3.9 mm). The derivatised amino acids were separated with a binary non-linear gradient using eluant A (0.14 M sodium acetate, 10 mM

EDTA and 0.5 mL TEA per litre water, titrated to pH 6.40 with acetic acid mixed with 6% acetonitrile) and eluant B (60% acetonitrile containing 10mM EDTA) (Table 2.4). A Pierce standard amino acid mixture (hydrolysis standard) was used to calibrate the analyses.

Table 2.4 The gradient program used in the chromatography of the PTC amino acids [adapted from 38]

Time (min)	Flow (mL/min)	% A	% B	MAXIMA curve type
0.00	1.0	98.5	1.5	
10.0	1.0	50	50	5
10.5	1.0	0	100	6
12.2	1.0	0	100	6
12.7	1.5	0	100	6
13.2	1.5	98.5	1.5	6
20.7	1.5	98.5	1.5	6
21.0	1.0	98.5	1.5	6

2.3.6.4 Mass spectrometry

Electrospray ionisation mass spectrometry (ESI-MS) was performed using a Micromass Quattro triple quadrupole mass spectrometer fitted with an electrospray ionisation source. The carrier solvent was 50% acetonitrile in water, delivered at a flow rate of 20 µL/minute during each analysis. Ten µL of the sample solution (2 ng peptide in 50% acetonitrile/water containing 0.05% TFA) was introduced into the ESI-MS using a Rheodyne injector valve. A capillary voltage of 3.5 kV was applied, with the source temperature set at 80^{o}C. The cone voltage was set at 70 V with the skimmer lens offset at 5 V. Data acquisition was in the positive mode, scanning the first analyser (MS_1), through m/z = 300–1500 or 1200 at a scan rate of 100 atomic mass units/second (m/z is defined as the molecular mass to charge ratio). Representative scans were produced by combining the scans across the elution peak and subtracting the background.

The FAB-MS was done at the Chemistry Department, University of Potchefstroom by Dr. L. Fourie.

2.4 Results and Discussion

2.4.1 Peptide preparation

2.4.1.1 Synthesis of the peptides

The successful solid phase peptide synthesis of the amphiphatic iturin A_2 analogues demonstrated the applicability of the Fmoc-polyamide peptide synthesis protocol. During each of the syntheses, negative Kaiser test for amino groups after the coupling steps showed that each of the couplings were complete. Positive Kaiser tests, after the removal of the Fmoc groups, confirmed successful coupling and deblocking steps. The amino acid analysis on the resin samples confirmed that each of the resin bound peptides had the correct amino acid composition and that the sequential integrity of the peptides was maintained (Table 2.5). The amino acid analysis of the TFA-treated resins showed that the peptide release step was successful in each case (results not shown).The amino acids, Asn and Gln, are deaminated during the hydrolysis procedure and therefore Asp and Glu are detected during the amino acid analysis. The Pro-values, obtained in the amino acid analysis, were slightly higher than expected as a result of the unresolved separation of the phenylthiocyanate (PTC) derivative of Pro and PTC-NH_2 during chromatography. The Ser- and Tyr-values were slightly lower than expected because of the oxidative degradation of these hydroxyl-containing derivatives during hydrolysis. The PTC derivative of the β-NC_{14} eluted very late during the amino acid analysis chromatography and could not be resolved from contaminating components and was therefore not determined.

The chiral integrity of the residues was not determined, but the use of HOBt as catalyst and so-called trapping agent ensures a greater than 99.6% “trapping” of each residue in its original configuration during coupling [7, 10, 21]. There was, however, uncertainty about the chiral nature of the N^{β}-tBoc-aminotetradecanoic acid derivative used during the syntheses. Liquid chromatography electrospray mass spectrometry (LC-ESI-MS) and chiral chromatography of the N^{β}-tBoc-aminotetradecanoic acid was used to investigate this derivative and its lipopeptide products (reported in Chapter 3).

Table 2.5 Summary of amino acid composition of resin samples taken during one of the syntheses of 5-Beta, 6-Beta, 7-Beta and 8-Beta. Values are the ratio between picomole residue and picomole Ser. The values of Ser and Tyr were adjusted by 17% and 13% respectively for oxidative loss that occurred during hydrolysis. (nd = not determined)

C-terminal ——— Coupling sequence ⟶

Peptide	Residue coupled ↘	L-Ser	D-Asn	L-Pro	L-Gln	D-Asn	D-Tyr	L-Asn	**average**
All	L-Ser	1	1	1	1	1	1	1	**1 (1)**
All		D-Asn	0.96	1.08	0.79	-	-	-	**0.94 (1)**
All			L-Pro	1.15	1.02	nd	1.04	1.37	**1.15 (1)**
All				L-Gln	1.02	nd	1.03	1.03	**1.03 (1)**
8-Beta; 7-Beta; 6-Beta					D-Asn	nd	1.87	-	**1.87 (2)**
8-Beta 7-Beta						D-Tyr	0.88	0.95	**0.92 (1)**
8-Beta							L-Asn	3.07	**3.07 (3)**

2.4.1.2 Purification of peptides

The purity of the crude peptides, as determined by ESI-MS, was already high with very little or no contaminating peptide material (results not shown). It was, however important to ensure even higher purity of the peptides for use in the structure-activity studies, as impurities can considerably influence bioactivity results.

Sephadex LH20 chromatography was used in a trial purification of linear 7-Beta and 8-Beta (Fig. 2.8). The low yields from this procedure (<50%) were probably due to the use of plastic tubing in the chromatography set-up. The highly lipophilic peptides tended to adsorb to the hydrophobic plastic surfaces. The use of methanol in the procedure also posed problems. The lipopeptides, only partially soluble in this solvent, could form methyl esters between methanol

and their carboxyl terminals. This procedure was therefore abandoned for the purification by semi-preparative HPLC.

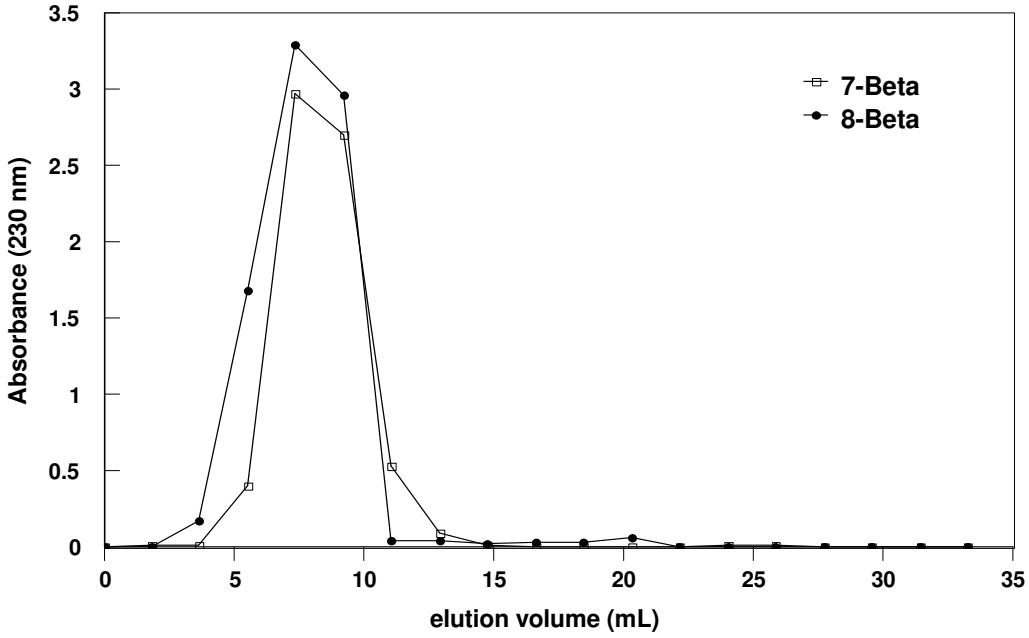

Figure 2.8 Sephadex LH20 chromatography of 4 mg each of crude 7-Beta (--) and 8-Beta (–). The eluant was 50% methanol in water at a flow rate of 20 mL/hour and the bed volume of the column was 4 mL.

The four different linear peptides (combined products of the different syntheses) were subsequently purified using HPLC. In the early stages of the development of purification procedures we were unaware that the lipopeptides, especially the shorter analogues, tended to aggregate at high concentrations and with time (refer to Chapter 6 for more detail); the ESI-MS facility was also not available for fast analysis of fractions. Some losses therefore occurred because of the aggregation and adherence to plastic as well as membranes used in the preparation of the HPLC samples.

The HPLC gradient program was successful in the purification of 8-Beta and 7-Beta. With a linear gradient program using a flow rate of 3 mL/min as depicted in Table 2.3, two peptide fractions were collected, named 7-Beta I and 7-Beta II, corresponding to 7-Beta (evaluated by TLC, amino acid analysis and ESI-MS; refer to Chapter 3 for more detail) (Fig. 2.9 A). Two peak fractions corresponding to 8-Beta (evaluated by TLC, amino acid analysis and ESI-MS; also refer to Chapter 3 for more detail), named 8-Beta I and 8-Beta II, were also collected (Fig. 2.9 B). Other fractions, with significant UV absorbance, did not contain any peptide material and were probably residual phenol and side-chain deprotection products. Yields of the

purified 7-Beta and 8-Beta were satisfactory, although higher yields were expected (Table 2.6).

Table 2.6 A summary of the yields obtained for the synthesis and purification of the iturin A_2 analogues. Yields were determined on the dry mass of each peptide.

Peptide	**% Crude yield**	**% Average coupling efficiency**	**% Yield from preparative HPLC**
5-Beta	90	98	24
6-Beta	99	99.8	44
7-Beta I,II	94	99	62
8-Beta I,II	87	98	73
cyclic 7-Beta I,II	-	-	47 (Method B)
cyclic 8-Beta I,II	-	-	20 (DCC method) 42 (Method A) 47 (Method B)

The purification of 5-Beta and 6-Beta was complicated by a number of factors. First, these two peptides do not contain any aromatic UV absorbing residues and consequently the sensitivity of detection at 254 nm was low. Therefore, instead of 5 mg/mL, a much higher peptide concentration (8-10 mg/mL) had to be used. Second, 5-Beta and 6-Beta are strongly hydrophobic, with only 4 or 5 slightly polar residues coupled to the highly lipophilic β-NC_{14} residue. These peptides readily formed micellular aggregates of different sizes and polarity in aqueous solutions. Their hydrophobic nature complicated HPLC purification because the formation of aggregates made separations unpredictable (results not shown). Some 5-Beta and 6-Beta were, however, purified by this means, but yields were low at 24% and 44% respectively (refer toTable 2.6). ESI-MS analysis of fractions collected during the chromatography of 5-Beta and 6-Beta indicated that fractions throughout the gradient, especially the very early eluting fractions, contained peptide material (results not shown).

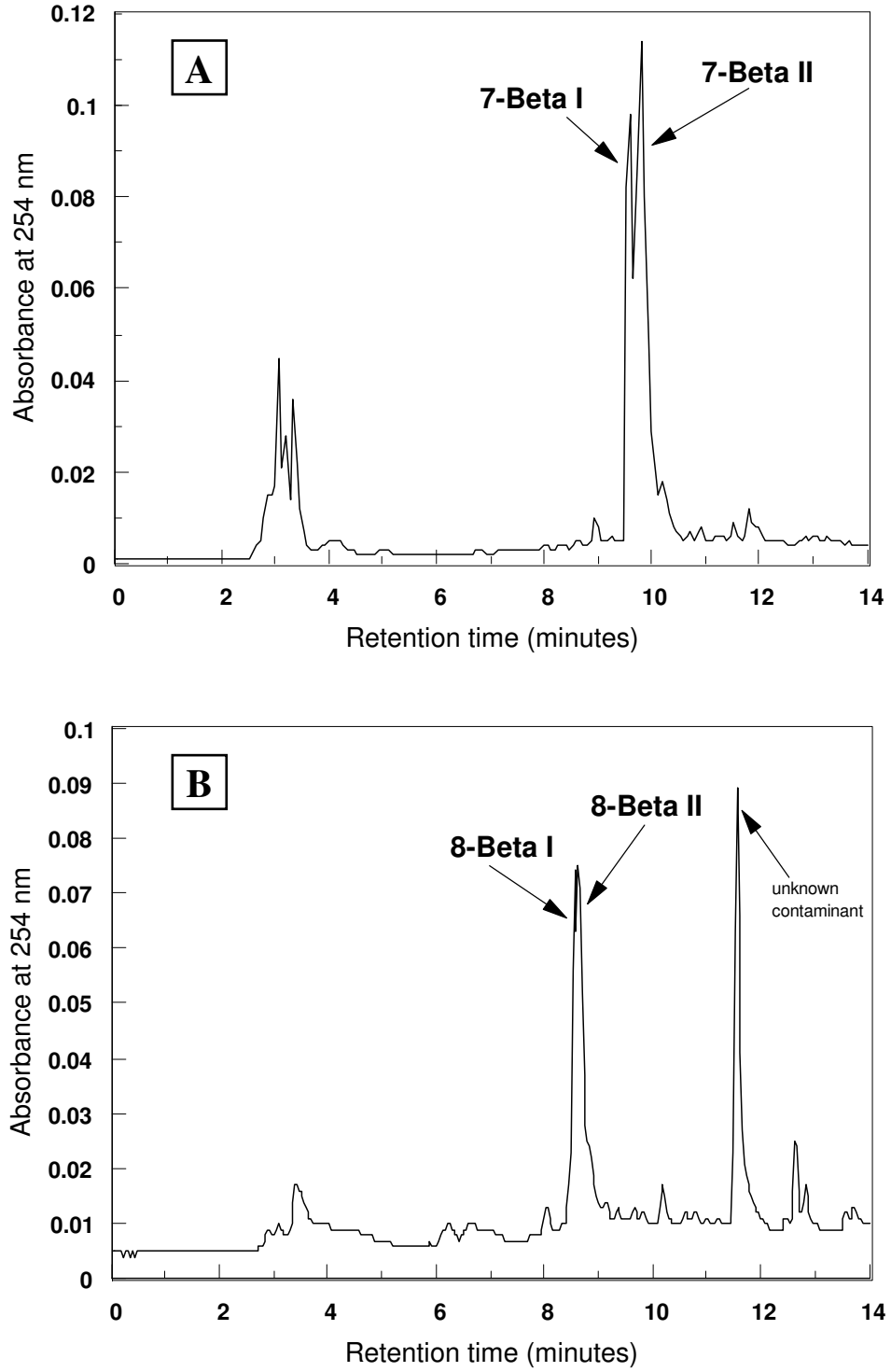

Figure 2.9 HPLC chromatograms of the crude linear lipopeptides (**A**:7-Beta and **B**: 8-Beta) using a 250 mm X 8 mm C_{18} Polygosil column. The linear gradient was developed over 13 minutes with 0.1% TFA in water as solvent A and acetonitrile plus 10% A as solvent B at a flow rate of 3 mL/min. Fractions that contained the specific peptide (as evaluated by ESI-MS) are each indicated on the chromatograms.

The N→C peptide cyclisation procedures with the PyBOP® reagent proved to be more successful than any of the DCC procedures. The highest yield of cyclic 8-Beta from a DCC procedure, using purified peptide as starting material, was only 20%. FAB-MS analysis showed that this preparation contained only the cyclic peptide (results not shown). The main solvent used in these procedures was DMF which, because of its ability to participate in hydrogen bonds, is a good chaotrophic solvent. However, although the peptides and reagents dissolved very well in DMF, the peptides were possibly in an extended conformation with non-optimal positioning of the N- and C-terminals. As natural iturin A has intra-peptide backbone hydrogen bonds the non-polar dichloromethane was used to facilitate the formation of hydrogen bonds and ensure close proximity of the N and C terminals. Combined with the highly effective PyBOP® as activation agent, the two peptides 7-Beta and 8-Beta were successfully cyclised using the crude peptide mixtures as starting material.

ESI-MS showed that the PyBOP® cyclisation mixture contained only cyclic peptide after five days (Fig. 2.10). By eliminating the linear peptide contamination of the cyclic peptide preparation, the problem of overlapping HPLC retention times of linear and cyclic peptides was overcome (refer to Figs.2.13, 2.15 in the following section). At this time it was not clear which of the two cyclic 8-Beta fractions contained synthetic iturin A_2. Cyclisation improved the HPLC resolution of the two peptide fractions (named cyclic 7-Beta I & II and cyclic 8-Beta I & II) and each of the peptides in the cyclisation mixtures could be purified with relative ease (Fig. 2.11 A and B).

The purified yields of cyclic 8-Beta and 7-Beta, using the PyBOP® method B, were respectively 33% and 30% both corresponding to a 47% yield from purified peptide preparations (refer to Table 2.6). A marginal improvement of 5% in yield of cyclic 8-Beta was obtained by improving the solubility and increasing the peptide dilution factor. Bland reported in 1996 the synthesis of iturin A_2 [39] with a purified product yield of 46% for the cyclic peptide. In this synthesis, the cyclisation step involved the use of a linear lipopeptide analogue identical to 8-Beta, but with the side-chain groups still protected which accounted for the higher yields obtained. The yields could probably be improved by also using a protected precursor, a lower reaction temperature to limit polymerisation and a different means of activation (PyBOP® has limited stability [10]).

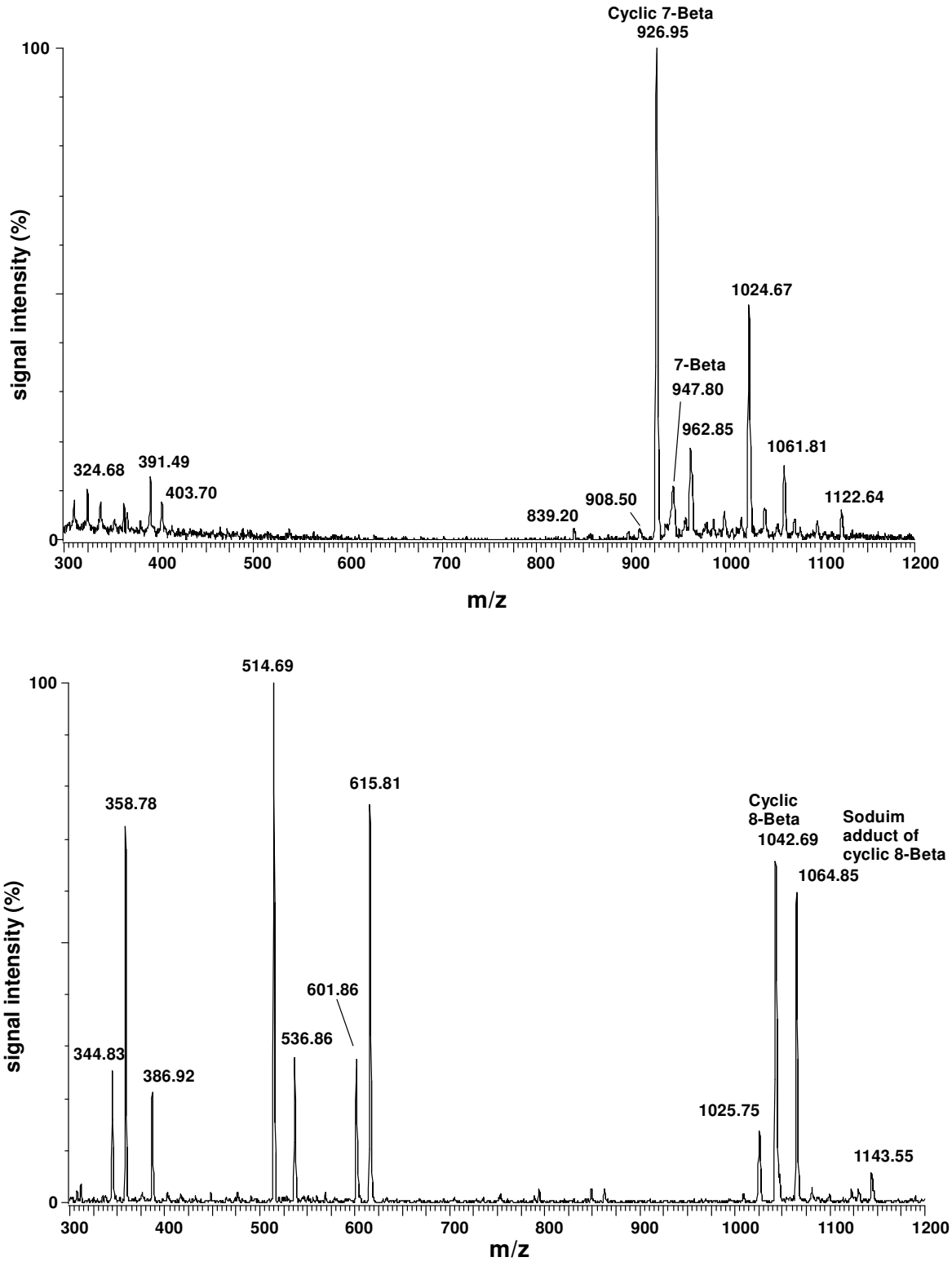

Figure 2.10 ESI-MS analysis of A cyclisation mixtures of 7-Beta and 8-Beta. The reaction mixture was dried and the residue dissolved in 50% acetonirtile in water containing 0.5% NH_3. Analyses conditions were as described under 2.3.6.4.

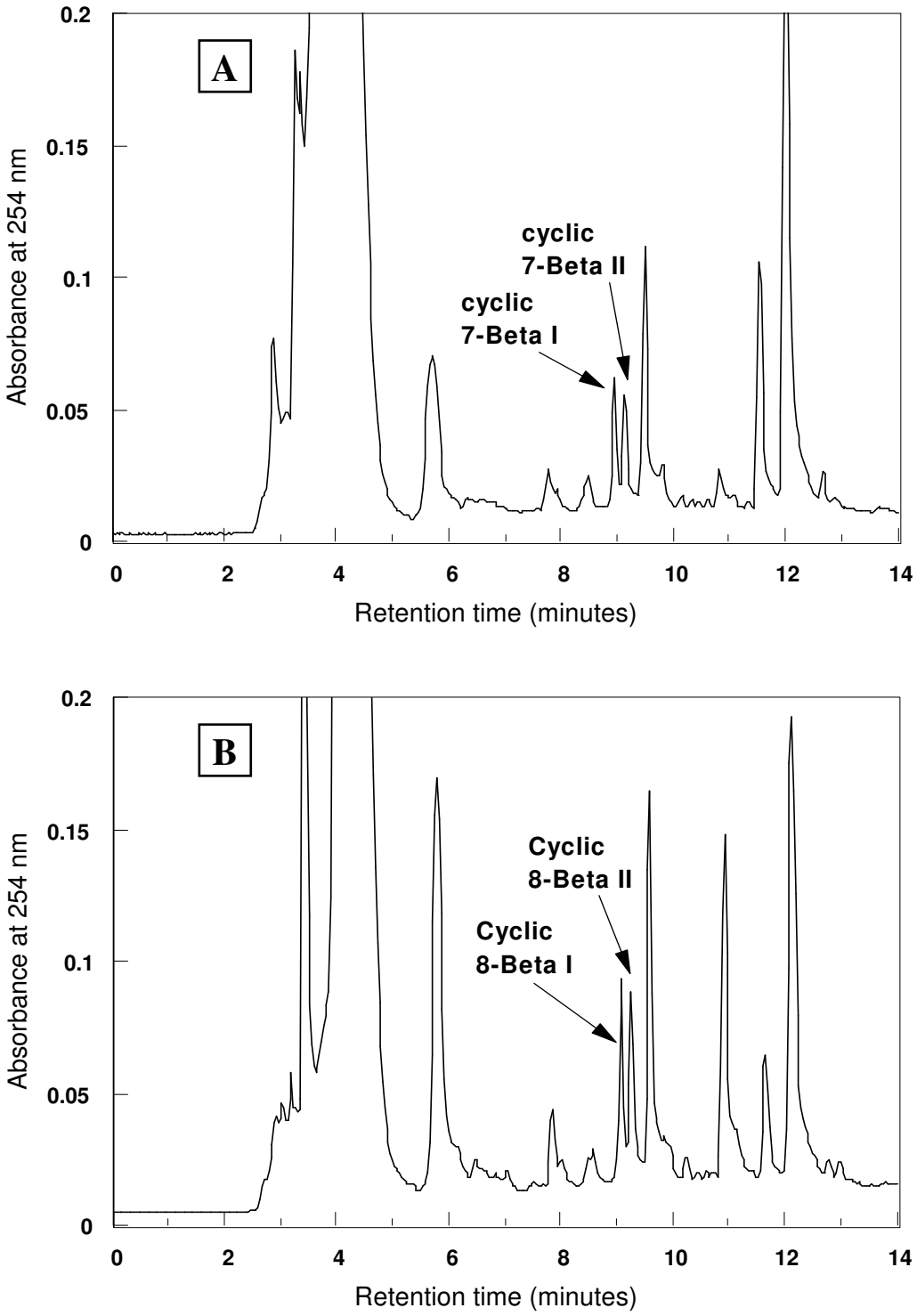

Figure 2.11 HPLC chromatograms of the crude cyclic lipopeptide reaction mixture (**A**: cyclic 7-Beta and **B**: cyclic 8-Beta as synthesised using Method B) using a 250 mm X
8 mm C_{18} Polygosil column. The linear gradient was developed over 13 minutes with 0.1% TFA in water as solvent A and acetonitrile plus 10% A as solvent B at a flow rate of 3 mL/min. Fractions that contained the specific peptide (as evaluated by ESI-MS) are each indicated on the chromatograms.

2.4.2 Analysis of purified peptides

2.4.2.1 Analytical TLC and HPLC of the purified lipopeptides

To assess the semi-preparative purification of the peptides, analytical TLC and HPLC were employed. TLC on the different linear lipopeptides revealed only one ninhydrin-detectable spot per linear peptide. The R_f values of all the linear lipopeptides were 0.81, an indication of the dominating influence of the β-NC_{14} moiety on the hydrophobicity of these peptides; the two peptides without the fatty acid, namely NYNQPNS and YNQPNS, had R_f values of 0.65 and 0.54 respectively. TLC of the linear lipopeptide hydrolysates showed that each of these peptides contained the β-aminotetradecanoic acid residue.

During the semi-preparative HPLC of the lipopeptide preparations of 7-Beta, 8-Beta and their cyclic analogues it was observed that each contained two peptide fractions with identical molecular masses (as shown with ESI-MS) and amino acid compositions, but differing in their HPLC properties. The elucidation of this phenomena was accomplished using ESI-MS and it was concluded that the introduction of a D/L racemic mixture of the β-NC_{14} into the peptides, lead to two isomeric peptides in each (refer to Chapter 3 for details).

Analytical HPLC of the purified 7-Beta I and 7-Beta II confirmed their purity, with only a small amount of the contaminating diastereomer in each (Fig 2.12). The preparation of 7-Beta I was particularly pure with only minor contamination of 7-Beta II. Purification of the two diastereomers of 8-Beta was exceptionally difficult, because of the low resolution between the two diastereomers. Different gradient profiles (linear and non-linear), with either analytical C_{18} or C_8 HPLC columns, did not improve the resolution (results not shown). A chiral based separation could have been an alternative, but the high cost of chiral columns precluded its use at this stage of purification. The purification of 8-Beta I and II were, however, successful as evaluated by C_{18} HPLC (Fig. 2.13) and C_8 HPLC (results not shown). All these linear preparations were therefore highly enriched with one diastereomer, but not chiraly homogeneous. Improved resolution between the cyclic diastereomers enabled the isolation of peptides with high chiral purity, especially cyclic 7-Beta I and cyclic 8-Beta I. The other diastereomers, cyclic 7-Beta II and cyclic 8-Beta II, had only minor contamination of their diastereomers (Figs. 2.14 and 2.15). A peak fraction with R_t of 8.13 in the cyclic 7-Beta II preparation was probably an aggregate of this diastereomer (Fig 2.14), as no peptide

contamination was detected by ESI-MS (Fig. 2.19). The analytical HPLC analyses of YNQPNS and NYNQPNS are discussed in Chapter 3.

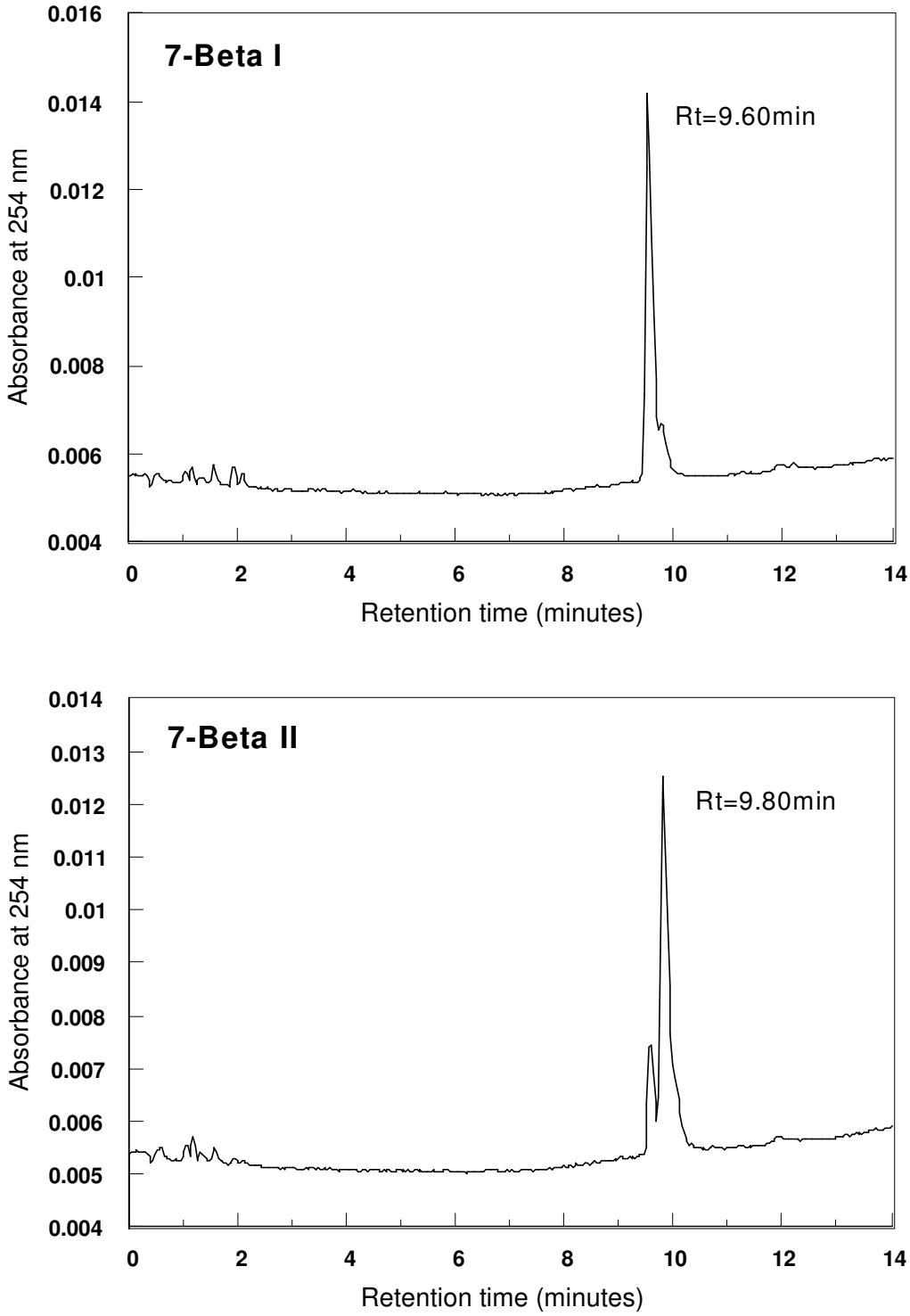

Figure 2.12 HPLC chromatograms of the purified 7-Beta I and 7-Beta II using a 150 X 3.9 mm C_{18} Nova-pak column. The linear gradient was developed over 13 minutes with 0.1% TFA in water as solvent A and acetonitrile plus10% A as solvent B. Approximately 4 µg peptide was injected per HPLC analysis.

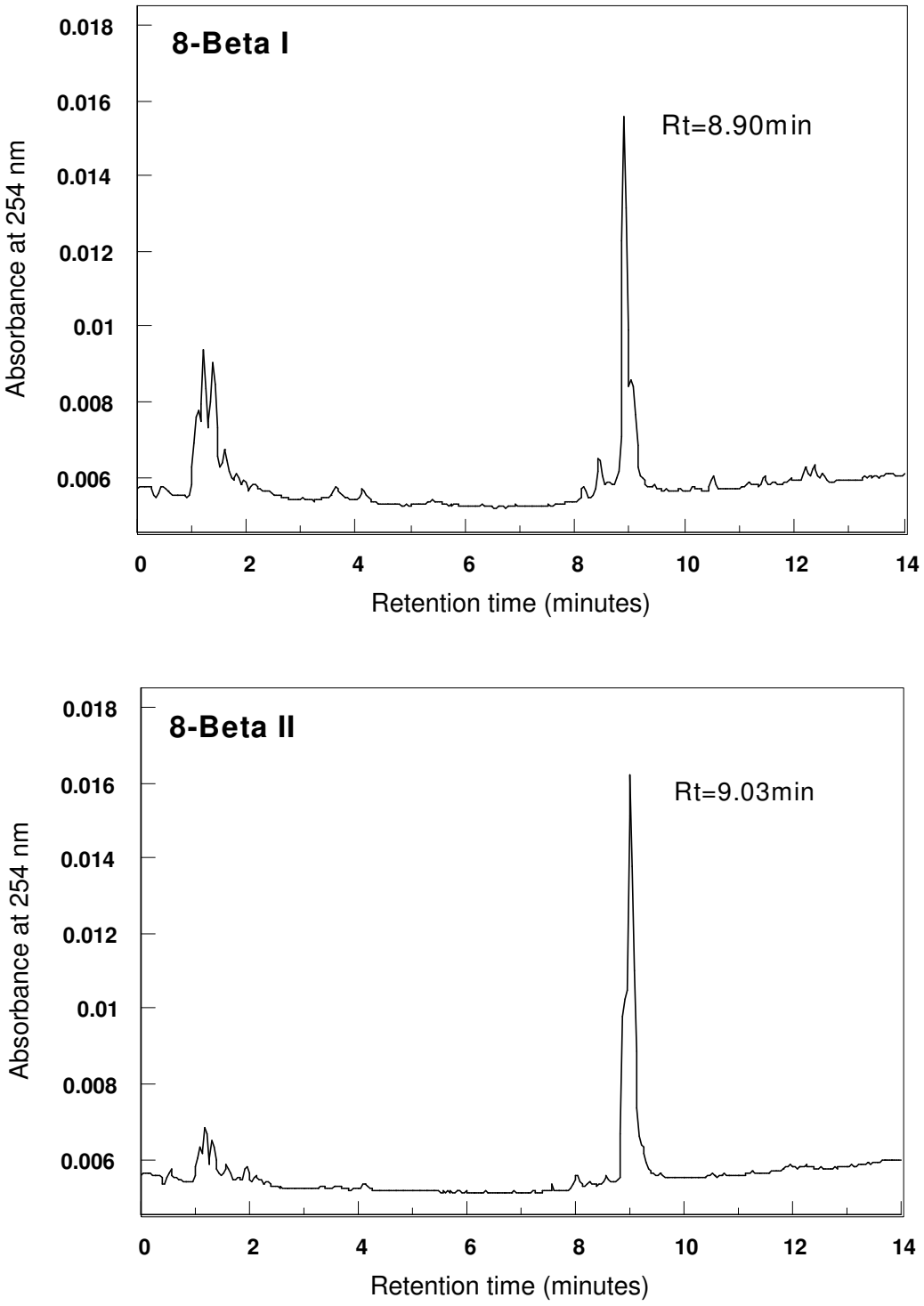

Figure 2.13 HPLC chromatograms of the purified 8-Beta I and 8-Beta II using a 150 X 3.9 mm C_{18} Nova-pak column. The linear gradient was developed over 13 minutes with 0.1% TFA in water as solvent A and acetonitrile plus 10% A as solvent B. Approximately 4 µg peptide was injected per HPLC analysis.

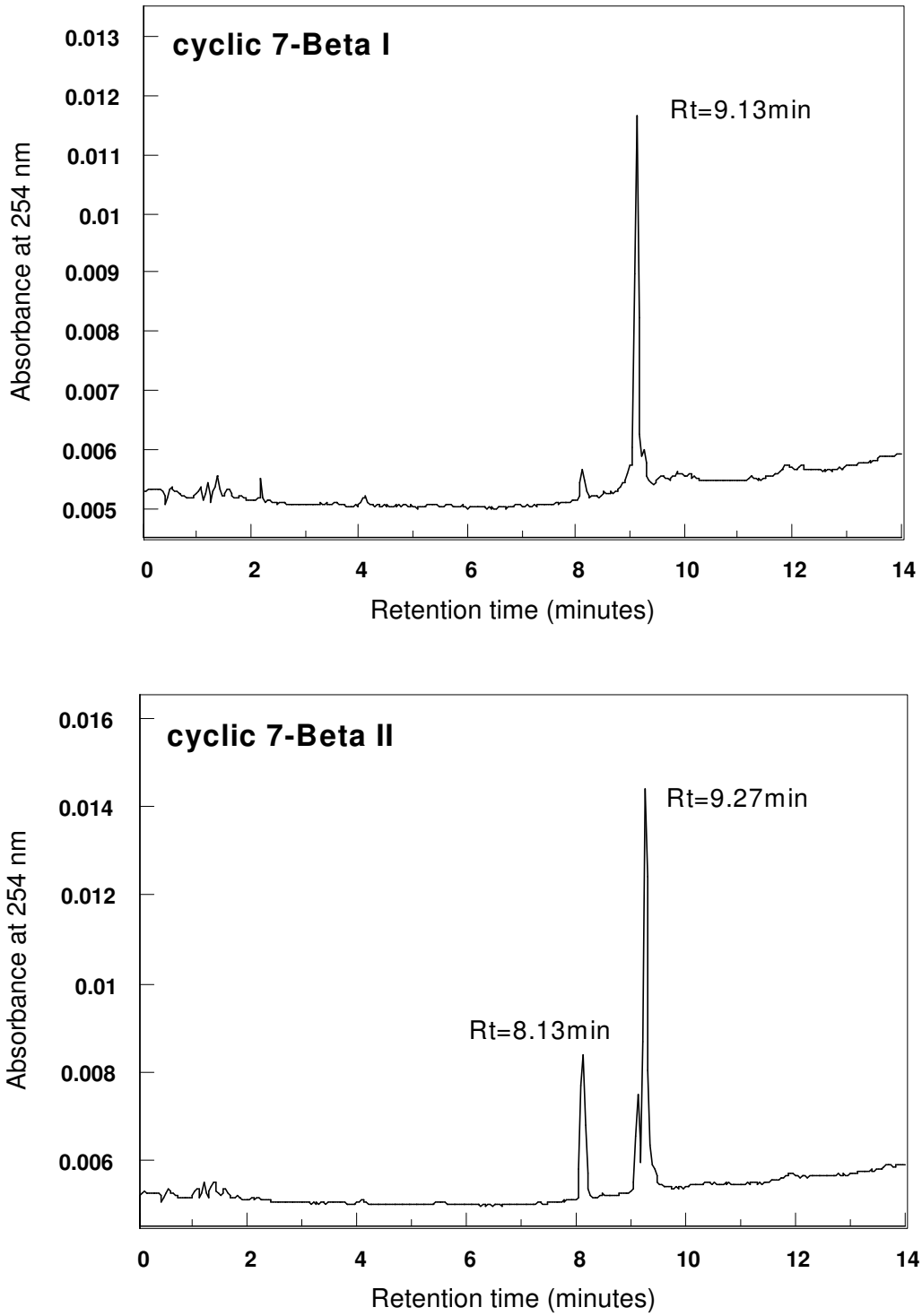

Figure 2.14 HPLC chromatograms of the purified linear and cyclic lipopeptides using a 150 X 3.9 mm C_{18} Nova-pak column. The linear gradient was developed over 13 minutes with 0.1% TFA in water as solvent A and acetonitrile plus 10% A as solvent B. Approximately 4 µg peptide was injected per HPLC analysis.

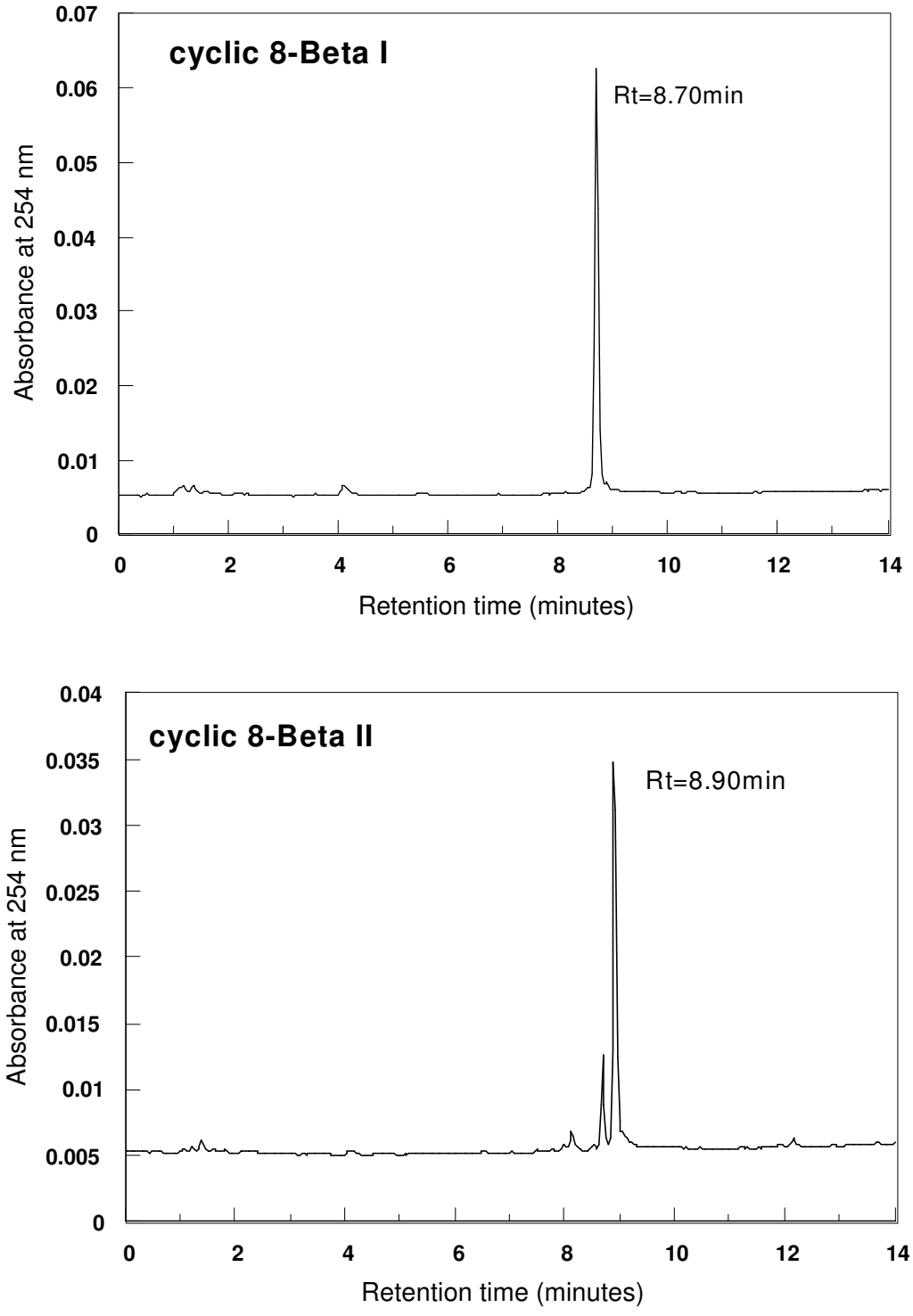

Figure 2.15 HPLC chromatograms of the purified linear and cyclic lipopeptides using a 150 X 3.9 mm C_{18} Nova-pak column. The linear gradient was developed over 13 minutes with 0.1% TFA in water as solvent A and acetonitrile plus 10% A as solvent B. Approximately 4 µg peptide was injected per HPLC analysis.

2.4.2.2 Electrospray mass spectrometry of the purified lipopeptides

Only a brief overview of the ESI-MS results will be given as an in depth study of the iturin A_2 analogues with ESI-MS are discussed in detail in Chapter 5. The correct *m/z* (molecular mass/charge ratio) was found for each of the purified linear peptides (Figs. 2.16-2.20, also refer to Table 2.1). One of the peptides, 5-Beta, fragmented extensively under the ESI-MS conditions used in the analysis (Fig. 2.16). The correct *m/z* of 5-Beta (670), was however observed as was it's Na and K cationised species. The two major fragments (product ions) corresponded to the sequences PNS (y''_3 with *m/z* 317) and β-NC_{14}-Q (b_2 with *m/z* 354), confirming the peptide sequence. The correct *m/z* of 784 was found for 6-Beta and also the two product ions PNS (y''_3 with *m/z* 317) and β-NC_{14}-NQ (b_3 with *m/z* 468), confirming its sequence (Fig. 2.16). Although the two shorter lipopeptides consisted of diastereomeric mixtures, they were chemically pure.

Increased stability under the ESI-MS conditions was observed for all of the longer lipopeptides. The spectra of 7-Beta I and 7-Beta II were near identical in terms of molecular ions, Na and K cationised species and limited fragmentation (Fig. 2.17). For both these diastereomers the correct *m/z* of 974, low intensity product ions, such as y''_3 (*m/z* 317) corresponding to PNS were detected. The same was true for 8-Beta I and 8-Beta II, also with identical spectra (Fig. 2.18). For these peptides the correct *m/z* of 1061 for the molecular ion was found, with the y''_3 (*m/z* 317) and b_5 (*m/z* 744; sequence β-NC_{14}NYNQ) as major product ions. The mass spectra of these longer linear lipopeptides confirmed their purity, and identical chemical nature and sequence of their diastereomers.

The ESI-MS analysis of the cyclic peptides confirmed of the cyclic nature of cyclic 7-Beta I and II and cyclic 8-Beta I and II, with the *m/z* of each cyclic peptide differing by 18 Da (M_r of H_2O) from that of their linear analogues (Figs. 2.19, 2.20, also refer to Table 2.1). Fragmentation of the cyclic peptides was limited to only the dehydrated product ions; these peptides are exceptionally stable under ESI-MS conditions. According to the ESI-MS analysis these preparations did not contain any linear peptide contamination, confirming successful cyclisation and purification of each cyclic diastereomer.

The ESI-MS of YNQPNS and NYNQPNS are reported on in Chapter 3. Refer to Chapter 5 for more detail on ESI-MS and fragmentation of peptides under ESI-MS conditions.

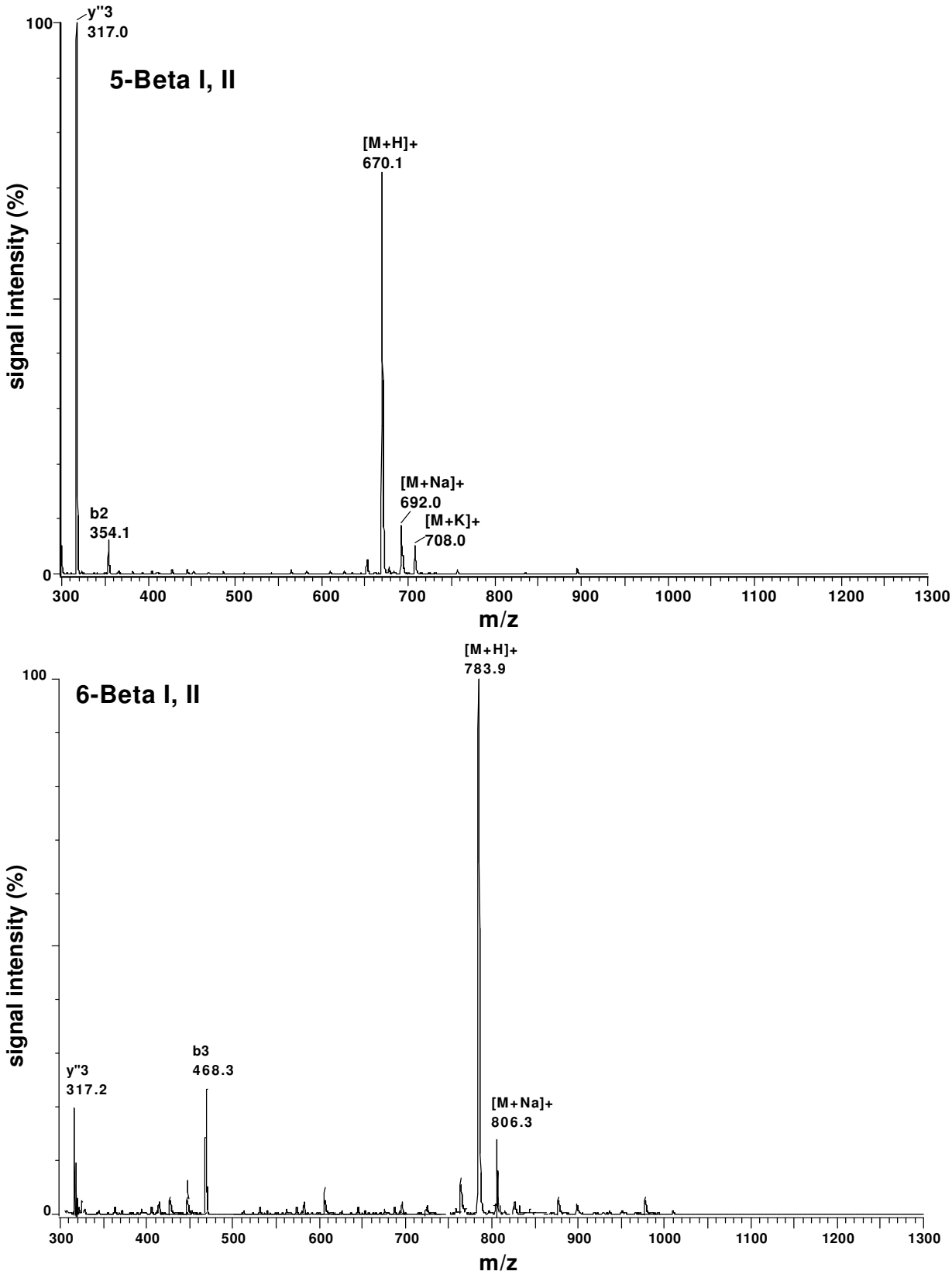

Figure 2.16 Positive mode ESI-MS spectra of the purified linear 5-Beta and 6-Beta. Analyses were done as described under section 2.3.6.4.

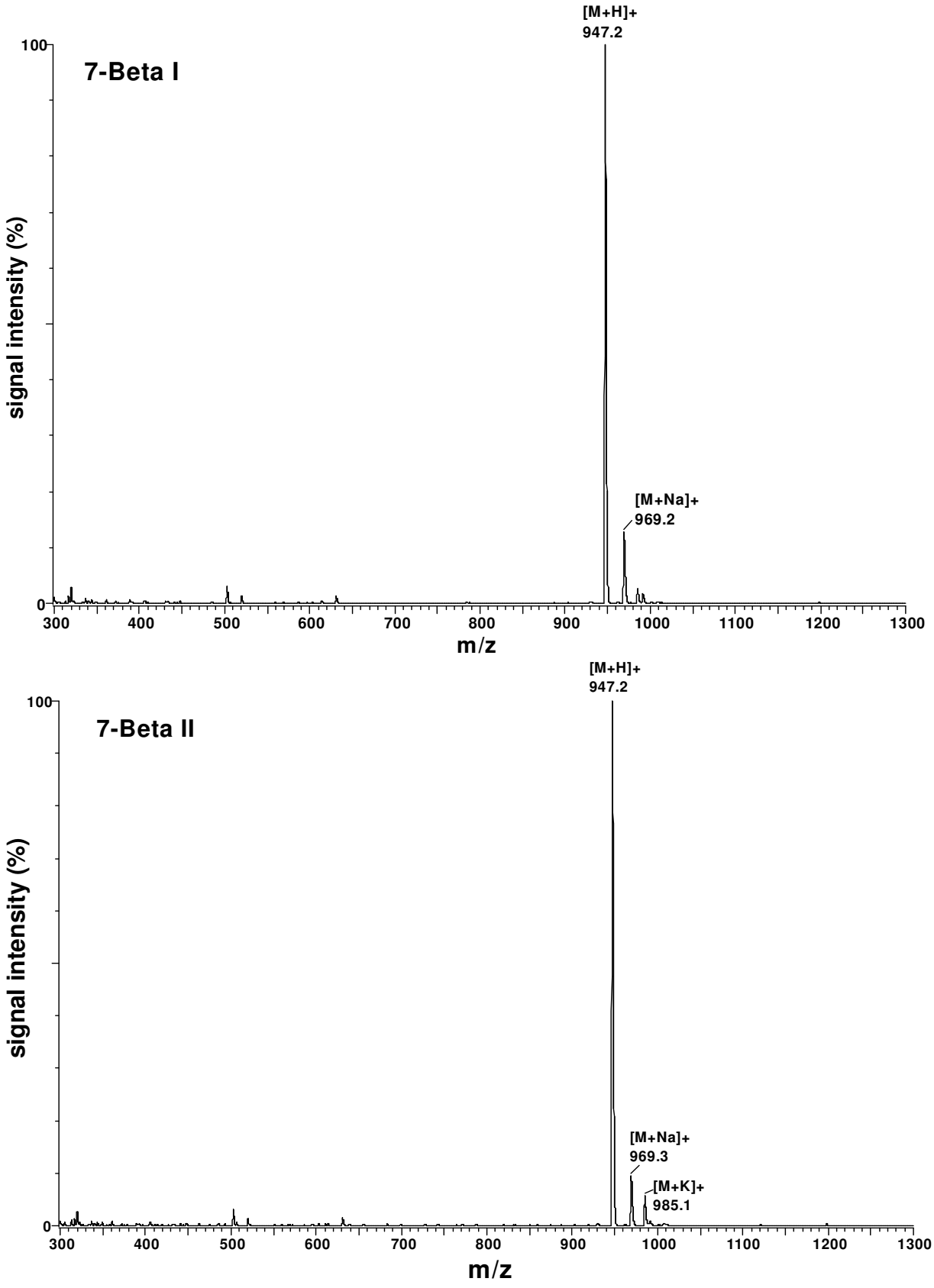

Figure 2.17 Positive mode ESI-MS spectra of the purified linear 7-Beta I and II. Analyses were done as described under section 2.3.6.4.

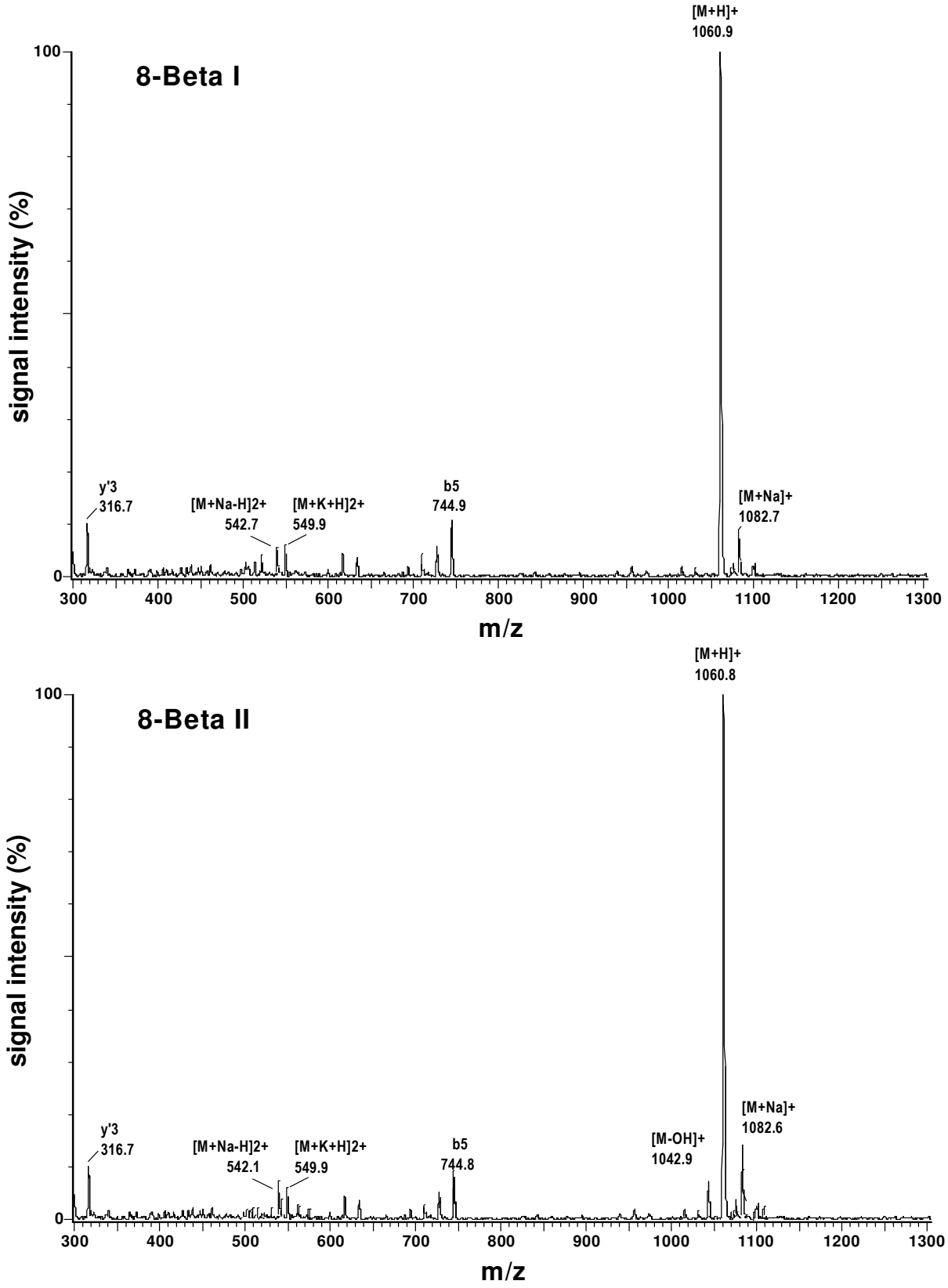

Figure 2.18 Positive mode ESI-MS spectra of the purified linear 8-Beta I and II. Analyses were done as described under section 2.3.6.4.

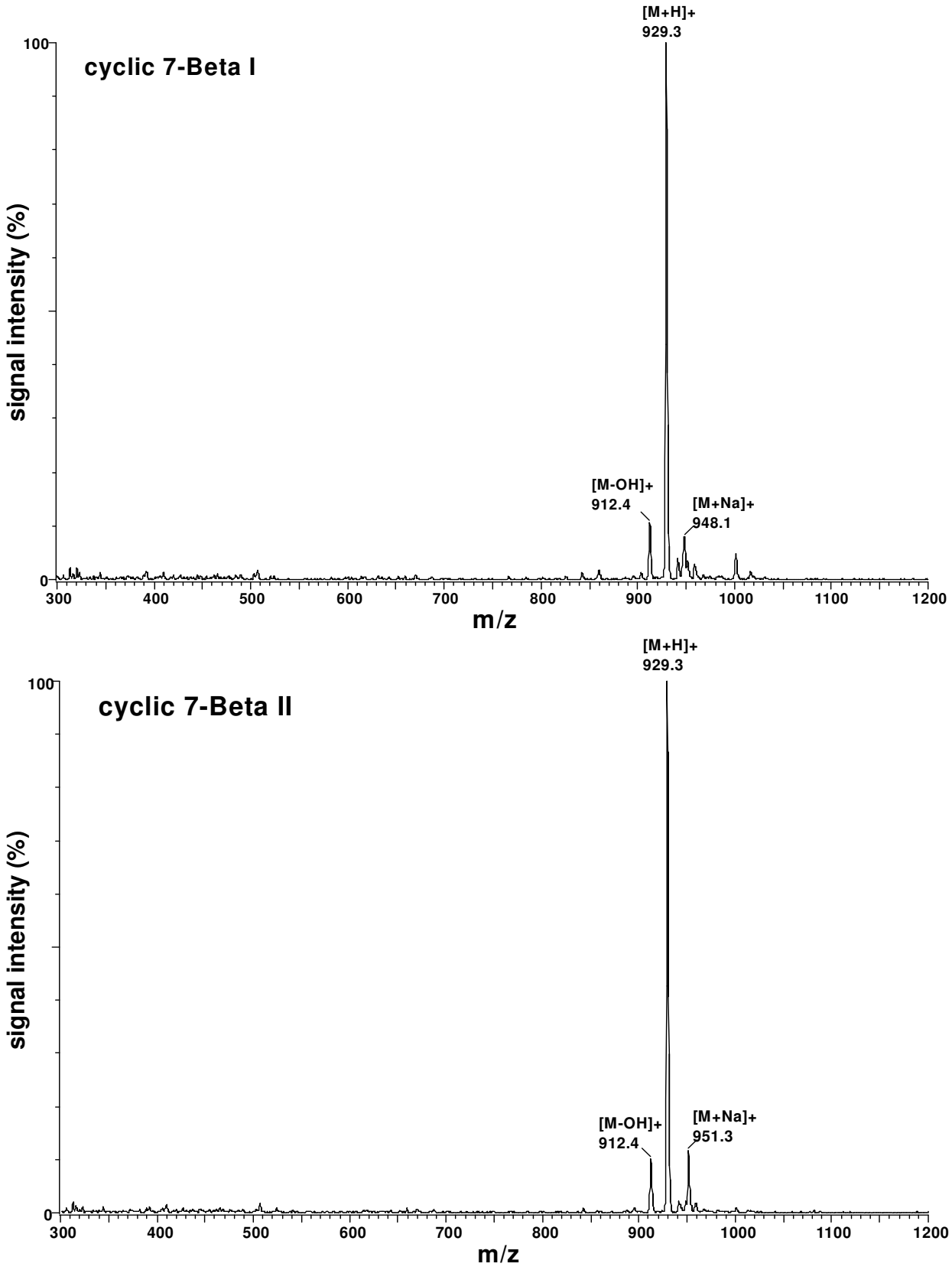

Figure 2.19 Positive mode ESI-MS spectra of the purified cyclic 7-Beta I and II. Analyses were done as described under section 2.3.6.4.

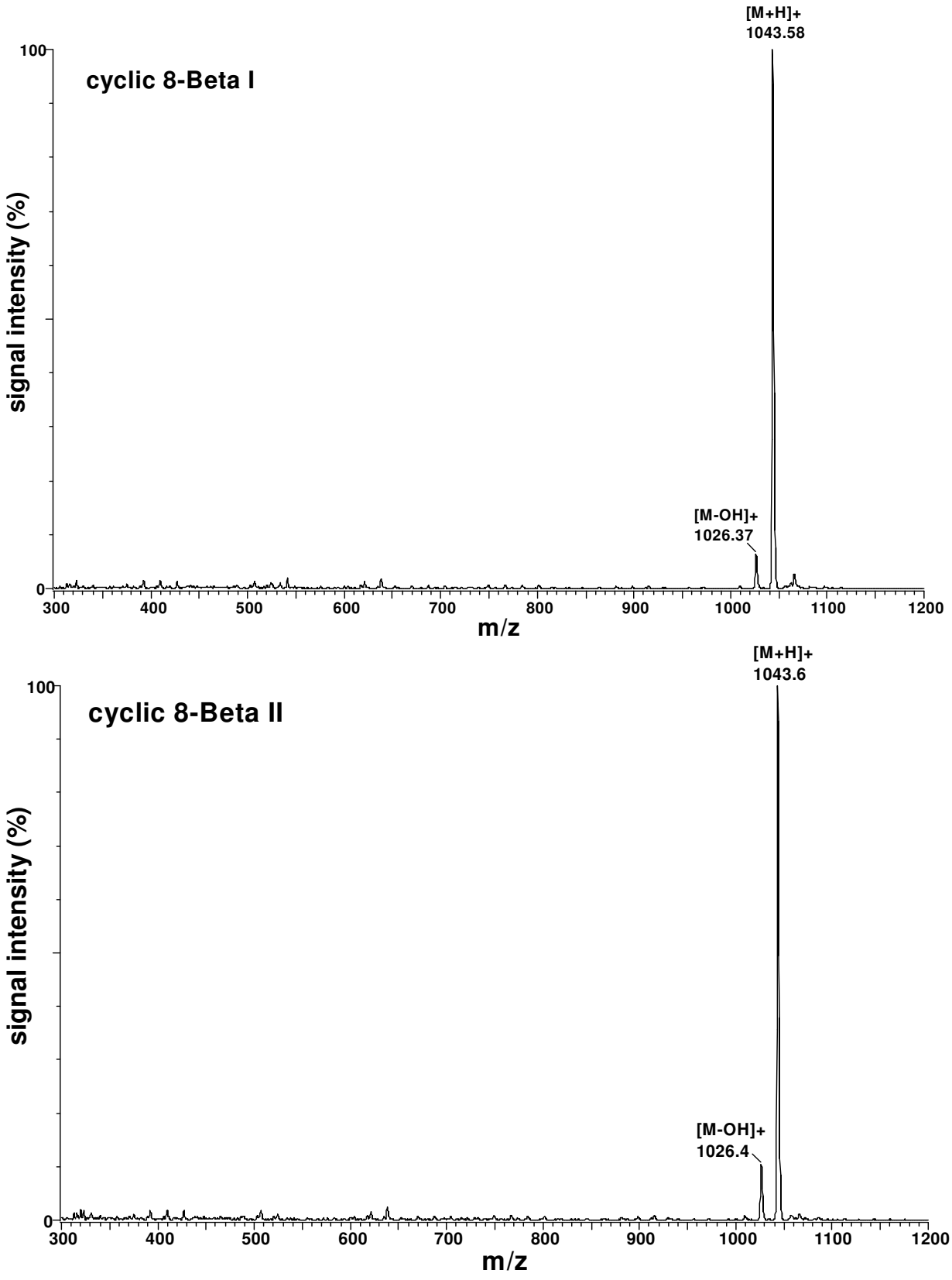

Figure 2.20 Positive mode ESI-MS spectra of the cyclic 8-Beta I and II. Analyses were done as described under section 2.3.6.4.

2.4.2.3 Amino acid analysis of purified peptides

The powerful analytical techniques utilised in the analysis of the synthetic peptides, such as HPLC and ESI-MS, already confirmed the chemical purity of each of the peptides. Nevertheless, this study would have been incomplete without the traditional amino acid analysis (Table 2.7).

Table 2.7 Amino acid composition of the different HPLC purified peptides. (# hydrolysis at 110°C for 18 hours, values of Ser and Tyr were adjusted by 10% and 3% respectively; $ hydrolysis at 150°C for 1 hour, values of Ser and Tyr were adjusted by 17% and 13% respectively for oxidative loss that occurred during hydrolysis; Asx = Asn or Asp and Glx = Gln or Glu. Duplicate analyses were done for each peptide.)

	Amino acid composition					
Peptide	**β-NC_{14}**	**Asx**	**Tyr**	**Glx**	**Pro**	**Ser**
YNQPNS #	-	1.97 (2)	0.69 (1)	1.00 (1)	1.20 (1)	0.91 (1)
NYNQPNS #	-	3.00 (3)	0.72 (1)	1.00 (1)	1.20 (1)	0.89 (1)
5-Beta $	(1)	1.11 (1)	-	1.00 (1)	1.05 (1)	0.88 (1)
6-Beta $	(1)	2.17 (2)	-	1.00 (1)	1.02 (1)	0.86 (1)
7-Beta I $	(1)	2.20 (2)	0.86 (1)	1.00 (1)	1.02 (1)	1.00 (1)
7-Beta II $	(1)	2.25 (2)	0.95 (1)	1.00 (1)	1.03 (1)	0.93 (1)
cyclic 7-Beta I $	(1)	2.30 (2)	0.83 (1)	1.11 (1)	1.12 (1)	0.81(1)
cyclic 7-Beta II $	(1)	2.16 (2)	0.92 (1)	0.91 (1)	1.05 (1)	0.84 (1)
8-Beta I $	(1)	3.12 (3)	0.88 (1)	1.03 (1)	1.01 (1)	0.87 (1)
8-Beta II $	(1)	2.99 (3)	0.96 (1)	1.15 (1)	1.23 (1)	0.80 (1)
cyclic 8-Beta I $	(1)	3.05 (3)	0.93 (1)	1.06 (1)	1.32 (1)	0.60 (1)
cyclic 8-Beta II $	(1)	3.04 (3)	0.90 (1)	1.18 (1)	1.04 (1)	0.65 (1)

The amino acid analyses of the peptide hydrolysates (Table 2.7) confirmed the results from the ESI-MS study, but were more useful in the determination of analytical concentrations of the peptide solutions used in HPLC, ESI-MS and biological activity discussed in the following chapters. Each of the peptides analysed had the correct α-amino acid composition (the β-aminotetradecanoic acid was not analysed). The values for Ser and Tyr were lower than expected for some of the peptides due to oxidative degradation during hydrolysis. Another factor contributing to the low values of Ser and Tyr, especially in the cyclic peptides, may be shielding of peptide bonds with respect to hydrolysis. The Pro-value was too high in many of the analyses because of interference by PTC-NH_2. In all the analyses only the deamination products of Gln and Asn, namely Glu and Asp were detected.

2.5 Conclusions

Both continuous flow and shake flask solid phase peptide synthesis, and amino acid analysis techniques were successfully established in this laboratory. It made possible the synthesis of high purity peptides on a regular basis for both commercial and research purposes. Amino acid analysis, analytical HPLC and ESI-MS unambiguously confirmed that the correct lipopeptides had been synthesised in this study. Lipopeptides of high purity were obtained, although synthesis of iturin A_2 and some of its cyclic analogues proved to be chemically challenging. An N→C cyclisation is in it's very nature a difficult synthesis step, further complicated by ring size and the pronounced amphipathic nature of iturin A_2 and some of its analogues.

The synthetic lipopeptides also tended to self-aggregate, especially the shorter peptides, and adhere to hydrophobic surfaces, which lead to losses because of handling, and diminished biological activity in aggregated peptide samples (discussed in Chapter 6). Natural iturin A is a membrane active peptide, and hypotheses have been put forward that the formation of aggregates in the membrane is part of its mechanism of action [40]. The polar character of the lipopeptides also affected their purification, as we observed a tendency of these lipopeptides to associate with Na^+ and K^+, especially in samples that have been repetitively lyophilised (residual Na^+ and K^+ in water and on glass concentrates in the sample). It has been suggested that the affinity of natural iturin for alkali metal ions is part of its mechanism of action [40]. An ESI-MS study on the interaction between alkali metal ions and the iturin A_2 analogues will be discussed in detail in Chapter 5. Other complications arose because iturin A_2 also contains,

apart from the α-amino acids, a β-NC_{14} in the absolute R-configuration (D-enantiomer). An enantiomerically pure β-D-aminotetradecanoic acid was first synthesised in 1995 by Bland [41], only the racemic D/L mixture of β-NC_{14} was available at the time of our synthesis. Consequently two diastereomers of the different lipopeptides were synthesised during each synthesis. Even though the insolubility of the iturin A_2 analogues in most solvents limited the purification possibilities, eight of these diastereomers from the longer lipopeptides could be purified with C_{18}-HPLC. These diastereomers probably have different conformations, which influence their hydrophobicity and interaction with the C_{18} stationary phase. The effect of these differences on structure and biological activity will be discussed in Chapters 4 and 6. The determination of the absolute configuration of the β-NC_{14} in eight of these peptide diastereomers will be addressed in the next chapter.

2.6 References

1. Waki M., Izumiya N. (1967) *Bull. Chem. Soc. Jpn*. **40**, 1687-1692;
Tamaki M., Arai A., Akabori S., Muramatsu I. (1987) *Bull. Chem. Soc. Jpn*. **60**, 2101-2104;
Tamaki M., Arai A., Akabori S., Muramatsu I. (1988) *Bull. Chem. Soc. Jpn*. **61**, 3925-3929;
Tamaki M., Arai A., Akabori S., Muramatsu I. (1995) *Int. J. Peptide Protein Res*. **45**, 299-302;
Tamaki M., Akabori S., Muramatsu I. (1996) *Int. J. Peptide Protein Res*. **47**, 369-375

2. Pérez-Pay E., Houghten R. A., Blondelle S. E. (1994) *Biochem. J*. **229**, 587-591;
Blondelle S. E., Houghten R. A. (1991) *Biochemistry* **30**, 4671-4678;
Blondelle S. E., Houghten R. A. (1991) *Peptide Res*. **4**, 12-18;
Shin S. Y, Lee M. K., Kim K., L Hahm K.-S. (1997) *Peptide Res*. **50**, 279-285

3. Zasloff M., Martin B., Chen H.-C. (1988) *Proc. Natl. Acad. Sci.* USA **85**, 910-913;
Chen H.-C., Brown J. H., Morell J. L., Huang C. M. (1988) *FEBS Lett*. **236**, 462-466;
Bessalle R., Haas H., Gorea A., Shalit I., Fridkin M. (1992) *Antimicrob. Agents Chemotherapy* **36**, 313-317;
Wade D., Boman I. A., Wahlin B., Drain C. M., Andreu D., Boman H. G., Merrifield R. B. (1990) *Proc. Natl. Acad. Sci. USA* **87**, 4761-4765;
Lazarollanos N., Hammer N., Maloy W. L., Blazyk J. (1997) *FASEB J*. **11**, 3397

4. Lee S., Mihara H., Aoyagai H., Kato T., Izumiya N. Yamasaki N. (1986) *Biochem. Biophys. Acta* **862**, 211-219;
Blondelle S. E., Houghten R. A., (1992) *Biochemistry* **31**, 12688-12694;
Bessalle R., Gorea A., Shalit I., Metzger J. W., Dass C., Desiderio D. M., Fridkin M. (1993) *J. Med. Chem*. **36**, 1203-1209;
Blondelle S. E., Takahashi E., Houghten R. A., Pérez-Pay E. (1996) *Biochem. J*. **313**, 141-147

5. Delcambe L. (1965) *Bull. Soc. Chim. Belg*. **74**, 315-319;
Peypoux F., Guinand G., Michel G., Delcambe L., Das B. C., Lederer E. (1978) *Biochemistry* **17**, 3992-3996;
Maget-Dana R., Ptak M., Peypoux F., Michel G. (1985) *Biochim. Biophys. Acta* **815**, 405-409

6. Rautenbach M. (1989) The synthesis and characterisation of antigenic peptide determinants, M.Sc-Thesis (Biochemistry), University of Pretoria, pp. 11-25, 28-33, 80-82

7. Bodansky M. (1984) Principles of peptide synthesis (Eds. Hafner K., Rees C. W., Trost B. M., Lehn J., Von Ragné Schleyer P., Zahradnik R.) Springer Verlag, Berlin

8. Bodansky M., Bodansky A. (1984) The practice of peptide synthesis (Eds. Hafner K., Rees C. W., Trost B. M., Lehn J., Von Ragné Schleyer P., Zahradnik R.), Springer Verlag, Berlin

9. Atherton E., Sheppard R. C. (1989) Solid phase synthesis: A practical approach, In: The practical approach series (Series Eds., Rickwood D., Hames B. D.), IRL Press, Oxford University Press, Oxford

10. Gloor A. P., Hoare S. M., Lawless K., Steinauer R. A., White P., Yong C. W. (1994/1995) NovaBiochem 94/95 Catalogue and Peptide synthesis handbook, pp. S1-S42

11. Barany G., Kneib-Cordonier N., Muller D. G. (1987) *Int. J. Peptide Prot. Res*. **30**, 705-739

12. Merrifield R. B. (1964) *Biochemistry* **3**, 1385-1390

13. Gutte B., Merrifield R. B. (1969) *J. Am. Chem. Soc*. **91**, 501-502

14. Merrifield R. B. (1965) *Science* **150**, 178-185

15. Atherton E., Fox H., Harkiss D., Logan C. J., Sheppard R. C., Williams B. J. (1978) *J. Chem. Soc. Chem. Commun.* 537-539

16. Atherton E., Sheppard R. C. (1985) *J. Chem. Soc. Chem. Commun*, 165-166

17. Carpino L. A., Han G. Y. (1972) *J. Org. Chem*. **37**, 3404-3406

18. Sheppard R. C., Williams B. J. (1982) *Int. J. Peptide Prot. Res*. **20**, 451-454

19. Dryland A., Sheppard R. C. (1988) *Tetrahedron* **44**, 859-876

20. Dryland A., Sheppard R. C. (1986) *J. Chem. Soc. Trans. I*, 125-137

21. Kemp D. S. (1979) Racemisation in peptide synthesis, In: The peptides: Analysis, synthesis, biology (Eds. Gross E., Meienhofer J.) Academic Press, New York, pp.1-10

22. Cameron L., Holder J. L., Meldal M., Sheppard R. C. (1987*) J. Chem. Soc. Chem. Commun.* 270-272

23. Atherton E., Holder J. L., Meldal M., Sheppard R. C., Valerio R. M. (1988) *J. Chem. Soc. Chem. Perkin Trans. I*, 2887-2894

24. Cameron L., Holder J. L., Meldal M., Sheppard R. C. (1988*) J. Chem. Soc. Chem. Perkin Trans. I*, 270-272

25. Atherton E., Dryland A., Goddard P., Cameron L., Richards J. D., Sheppard R. C. (1985) The peptides: Structure and function, In: Proceedings of the Ninth International Peptide Symposium (Eds. Deber D. C., Hruby V. J., Kopple K. D.) Pierce Chem. Co. Rockford, Illinois, vol. 119, pp. 249-252

26. Atherton E., Cameron L., Sheppard R. C. (1988) *Tetrahedron* **44**, 843-857

27. Castro B., Dormey J.-R., Elvin G., Selve C. (1975) *Tetrahedron Lett*. 1219-1222

28. Fourier A., Danho W., Felix A. M. (1989) *Int. J. Peptide Prot. Res.* **33**, 133-139

29. Costa J., Le-Nguyen D., Castro B. (1990) *Tetrahedron Lett*. **31**, 205-208

30. Hϕeg-Jensen T., Jakobsen M. H., Olsen C. D., Holm A. (1991) *Tetrahedron Lett*. **32**, 7617-7620

31. Kaiser E., Colescott R. L., Bossinger C. D., Cook P. I. (1970) *Anal. Biochem*. **34**, 595-598

32. Stewart J. M., Young J. D. (1984) Solid phase synthesis, 2nd edition, Pierce Chem. Co. Rockford, Illinois, pp. 69-70

33. Gait M. J. (Ed) (1984) Oligonucleotide synthesis, In: Practical Approach Series (Series Eds. Rickwood D., Hames B. D.) IRL Press, Washington D. C., p. 99

34. Levitt R. R. (1986) The synthesis of a novel octapeptidolipid antibiotic, Ph.D. Thesis (Biochemistry), University of Stellenbosch, pp. 28-31

35. Chang C., Waki M., Ahmad M., Meienhofer J., Lundell E. O., Haung J. D. (1980) *Int. J. Peptide Prot. Res.* **15**, 59-66

36. Fields G. B., Noble R. L. (1990) *Int. J. Peptide Prot. Res.* **35**, 161-214

37. Bidlingmeyer B. A., Cohen S. A., Tarvin T. L. (1984) *J. Chrom.* **336**, 93-104

38. Cohen S. A., Meys M., Tarvin T. L. The Pico-Tag® Method: A manual of advanced techniques for amino acid analysis, distributed by Waters®, Millipore

39. Bland J. M. (1996) *J. Org. Chem*. **61**, 5663-5664

40. Maget-Dana R., Peypoux F. (1994) *Toxicology* **87**, 151-174

41. Bland J. M. (1995) *Synt. Commun*. **25**, 467-477

Chapter 3

Determination of the configuration of the β-aminotetradecanoic acid in the iturin A_2 analogues

3.1 Introduction

Chirality (from the Greek word *cheir* for hand) in chemistry describes the non-superimposability of mirror images of otherwise identical chemical compounds. These mirror image compounds are also known as stereoisomers or more specifically as enantiomers (from the Greek word *enantio* meaning opposite). Enantiomers are identical in all chemical aspects, except for their opposing rotation of polarised light or so-called optical activity. An equimolar mixture of enantiomers of a specific compound, also called a racemic mixture, is optically inactive.

Although Van't Hoff has the distinction of being the founder of stereochemistry [1] in 1874, Louis Pasteur, in 1858, used the chiral selectivity of nature to become the very first scientist to resolve a racemate [2]. He observed that only the *dextro* form of ammonium tartate, which rotates polarised light to the right, is fermented by *Penicillium glaucum*. Pasteur had already separated the enantiomorphous crystals of ammonium tartate by hand and determined their optical activity in 1848. The original D/L nomenclature is based on the optical rotation of glyceraldehyde with the enantiomer rotating light to the left (*laevo*) being L-glyceraldehyde and to the right (*dextro*) being D-glyceraldehyde (Fig 3.1).

The true orientation of the atoms or groups of enantiomers in space i.e. their absolute configuration is very important in the study of biologically active compounds (as will be discussed later), although most of the fundamental research of chiral compounds was done without this knowledge. It is not always possible to equate the rotation of light to the absolute configuration of some other compounds for example, the L-enantiomer of DOPA (3,4-dihydroxy phenylalanine) rotates plane polarised light to the right. A second assignment was thus incorporated in the nomenclature to show the rotation of light of the enantiomer namely (−) for rotation of light to the left and (+) for rotation to the right. L-glyceraldehyde was thus

denoted as L-(−)-glyceraldehyde. Assignment of the D- and L- configuration is still generally used in the nomenclature of sugars and amino acids (Fig. 3.1). This system relates compounds configurationally to the structure of glyceraldehyde and is limited because it is only applicable to compounds having asymmetric carbon atoms. Cahn, Ingold and Prelog [3] developed the R/S nomenclature (S stands for *sinister* and R for *rectus*) which can be used to assign absolute configuration directly to any chiral compound by the sequential arrangement of ligands associated with an element of chirality. With this system L-glyceraldehyde is denoted as (*S*)-glyceraldehyde (Fig. 3.1).

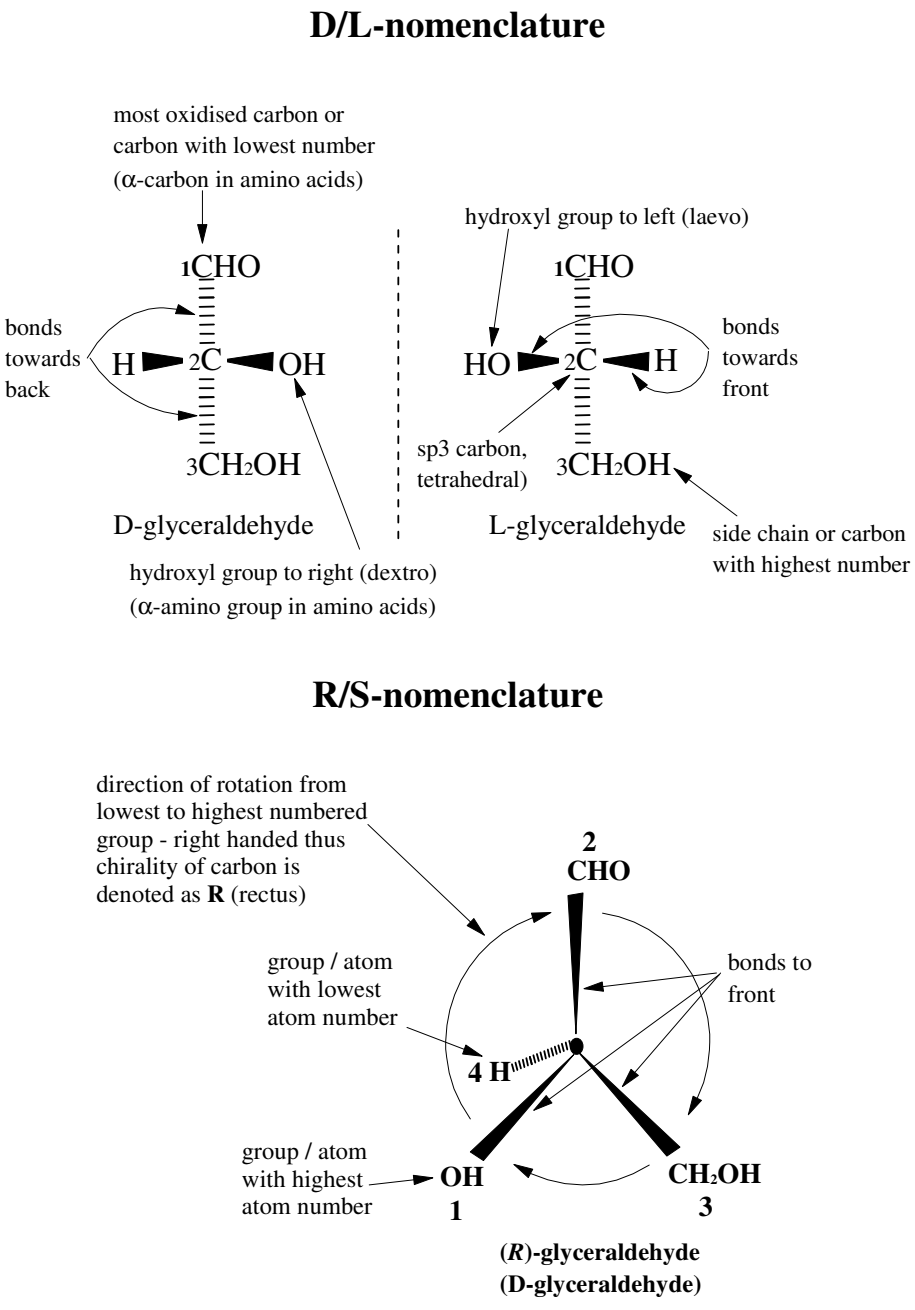

Figure 3.1 An illustration of the each of the nomenclature systems with glyceraldehyde as example.

In our synthetic approach, used to study the structure-function relationship of iturin A, an enantiomeric mixture of the β-aminotetradecanoic acid (β-NC_{14}) residue was introduced into all the iturin A_2 analogues during synthesis. The natural cyclic lipopeptide, iturin A, consists of seven α-amino acid residues and a β-amino fatty acid residue in the absolute R-configuration (D-enantiomer) [4, 5]. The elucidation of the absolute configuration of the β-NC_{14} residue in the different iturin A_2 analogues proved challenging and several different techniques were considered during this study. A summary of available techniques will be given as background. The methods generally used in stereoisomer investigations can be divided into four categories: methods involving (i) calorimetry, (ii) stereospecific enzymatic catalysis, (iii) spectrometry (polarimetry, nuclear magnetic resonance (NMR) and isotopic dilution) and (iv) chromatography (chiral gas chromatography (GC) and chiral high performance liquid chromatography (HPLC)).

A calorimetric method, such as differential scanning calorimetry, is based on the energy absorbed by a sample as a function of temperature and related to a reference of known enantiomeric composition. Data such as melting point, enthalpy of fusion and termination of fusion temperature are used to construct a melting point diagram from which enantiomeric composition can be determined [1]. This method can only be used if the material is in solid form and a reference sample of known composition is available. As with many of the techniques under discussion, differential scanning calorimetry is also limited to determination of composition and not absolute configuration, that is if standard enantiomer of known configuration is not available.

Stereospecific enzymatic catalysis, however, can be used to determine composition and absolute configuration, although general application is limited by the availability of specific enzymes. Most enzymes are highly stereospecific and can discriminate completely between enantiomers. Many enzymes are commercially available for the determination of enantiomeric purity of amino acid and peptide preparations. For example both D- and L-enantiospecific amino acid oxidases are available, but only L-enantiospecific proteases and amino acid decarboxylases. The presence of the β-amino acid and the D-amino acids in the iturin A_2 analogues prevented the use of an enzymatic method.

Before the advent of NMR and chiral chromatography, the measurement of the ability of chiral compounds to rotate the plane of polarisation of plane polarised light was the only means to distinguish between enantiomers. Plane polarised light, with its vibrational plane

limited to one direction, is composed of two perpendicular vectors (magnetic and electric). The right and left circularly polarised vectors of light will be propagated at different velocities when passing through a medium containing optically active compounds. The plane of polarisation will be rotated as a result of vector addition and measured in polarimetry as optical rotation, symbolised by α. If there is no association between enantiomers, enantiomeric purity can be determined, because it is linearly related to optical purity. The accuracy of determination can be improved if the isotopic dilution method is used [1]. The unknown enantiomeric mixture is mixed with a radioactively labelled racemate of the same compound. It is recrystallised and again analysed by polarimetry and either mass spectrometry or liquid scintillation counting to determine the optical purity and isotope content from which the original optical purity can be calculated.

In techniques such as optical rotary dispersion (ORD) and circular dichroism (CD) the optical activity is plotted as a function of wavelength. ORD and CD are closely related phenomena in the same way as absorption and refractive index. With CD, measurement of molecular ellipticity ($[\theta]$) is taken as the difference of absorption of left and right polarised light. With ORD, the difference of the refractive indices for left and right polarised light is measured and denoted as molecular rotation ($[\phi]$) [6, 7]. The sensitivity of ORD and CD improves if an aromatic group is part of the compound's structure, especially if it is near to the chiral atom [7]. If an absorption band of the compound falls in the spectral range investigated, the band will lead to one or more peaks or troughs. These curve extrema are denoted as either a positive or negative Cotton effect and could be correlated with the curve extrema of a structurally related compound of known stereochemistry. Thus, as with polarimetry, ORD and CD determination of absolute configuration is indirect and depends on the availability of a reference standard. Refer to Chapter 4 for more information on CD and ORD.

Spectrometric methods, such as NMR, do not directly distinguish between enantiomers in spectra. Enantiomers must first be transformed into a diastereomeric state with a suitable chiral reagent. Prikle [8] introduced chiral solvents to induce a chemical shift difference between enantiomers. If enantioselective interaction with chiral solvent takes place, the chiral solvent induces a difference in chemical shift leading to peak separation or peak-splitting, which can be used to determine enantiomeric composition. With most of the chiral solvents the effect is often too small for practical use, but this problem can be overcome by using highly effective lanthanide shift reagents (complexes containing Eu^{3+} or Pr^{3+}) [9]. These paramagnetic complexes interact with electron donating groups (such as hydroxyl, carbonyl

and carboxyl and amino groups) resulting in a marked downfield shift of nuclei near to loci of interaction, consequently improving resolution. The absence of a high purity reference standard, however, limits chiral NMR to determination of enantiomeric composition.

It is obvious that the accuracy with which optical purity can be determined improves when enantiomers are already separated. Chromatographic methods such as gas chromatography (GC) and liquid chromatography (LC) are therefore feasible alternatives in the determination of optical purity and absolute configuration of an enantiomer. The success of these chromatographic methods (GC or LC) depends on the type of chiral separation. Optical purity can be determined indirectly with chiral derivatisation and separation on conventional GC or LC columns. Direct determination is done by separation of enantiomers on chiral stationary phases (CSP) in GC and LC or using chiral solvents with conventional LC columns.

Chiral derivatisation produces diastereomers that can be separated by conventional GC or LC, because of their different chemical and physical properties. In GC it is often necessary to derivatise the analyte to ensure volatility; if derivatisation leads to diastereomeric analytes, determination of enantiomeric composition is possible. In LC much of the early work on chiral derivatisation was done on amino acids, because early stereochemical analysis was on peptide synthesis products. It was found that LC separation of diastereomeric dipeptides was easily accomplished and that activated amino acids are useful derivatisation agents [1]. We decided against using chiral derivatisation for determining the enantiomeric composition of β-NC_{14}, because of several drawbacks in the quantitative analysis. Firstly, contamination of the derivatisation agent may lead to formation of enantiomers that are difficult to separate; secondly racemisation or epimerisation may take place; and thirdly, the derivatisation reaction may be incomplete. More comprehensive information on chiral derivatisation and separation can be obtained from [1] and [10].

Direct optical resolution by chiral chromatography is clearly preferable to above pre-column chiral derivatisation. Chiral chromatography can be accomplished by using a chiral column with an achiral mobile phase (GC and LC) or an achiral column with chiral solvent (only LC). Optical resolution is obtained by reversible diastereomeric association between chiral selector and solute enantiomers. This non-covalent interaction is mostly steric in which dipole-dipole, charge transfer, hydrogen bonding, electrostatic, and hydrophobic interaction are very important. Achiral stationary phases are converted to liquid chiral stationary phase in LC, if the chiral constituent in chiral solvent adsorbs on the stationary phase. If the interaction

between the chiral mobile phase constituents and the analytes are more favourable, non-covalent diastereomeric complexes are generated. In most cases separation of enantiomers is accomplished by both interaction with the liquid chiral stationary phase and formation of mobile phase non-covalent diastereomeric complexes. Some experience with this type of chromatography, using a C_{18} stationary phase and N',N-dimethyl-L-phenylalanine in copper acetate as chiral mobile phase, was gained in the analysis of enantiomeric purity of residues in a synthetic 23 residue peptide [11]. Although highly repeatable results were obtained, this separation method was found to be somewhat unpredictable because of its absolute dependence on equilibration in coating the achiral stationary phase, or the prerequisite of formation of stable diastereomeric complexes. An alternative, not limited to LC, is the use of permanent chiral stationary phases (CSP). Most of the early work on CSPs was done in the field of chiral GC. Chiral stationary phases were functionalised with an amino acid such as L-Pro (due to the limited racemisation of this residue) and have been successfully applied in chiral GC and LC. The LC mode, however, also exploits the ability of amino acids to form chelates with metal such as copper as in the previous example (Fig. 3.2 C, Table 3.1). The difference in dissociation constants of the diastereomeric complexes with the metal ions can then be used to obtain chiral resolution.

Chiral recognition in other types of CSP's depends on various types of interaction between the chiral selector and the chiral compounds. Dalgliesh [1] proposed a three-point interaction model to explain the chiral separation of some aromatic amino acids by paper chromatography. He proposed that hydrogen bonds are formed between the hydroxyl groups of the cellulose and the carboxyl and amino groups of the amino acid, while the third point of interaction was due to the aromatic ring substituents (Fig. 3.2 A, Table 3.1). Three-point interaction was also proposed by Prikle and Finn [12] for enantioselection by the charge-transfer or so-called Brush chiral selectors (Fig. 3.2 A, Table 3.1). This type of enantioselection requires at least the interaction of π-electron systems. Additional polar interaction (hydrogen bonding or dipole interactions) leads to very efficient LC chiral selectors (Fig. 3.2 A, Table 3.1). An important feature of these selectors is their reciprocity—enantioselectivity is independent of which chiral partner is immobilised.

Another type of chiral selection depends on the chiral inclusion or insertion of the enantiomer in a so-called chiral cavity. Crown ethers and polymers such as starch, cellulose derivatives, polyacrylamides and cyclodextrins have been widely used as inclusion or insertion chiral selectors (Fig. 3.2 B) [13]. The chiral cavity can either be hydrophilic (as in chiral GC and

LC) or hydrophobic (only in chiral LC) to respectively include hydrophilic and hydrophobic analytes (Fig 3.2 B; Table 3.1.). Reversed-phase LC in combination with hydrophobic interaction, with steric effects from substituents in the chiral selector, is thought to lead to enantioselection by some of the chiral cavity selectors [13].

The potential for chiral selectivity is obvious from the selective nature of protein-ligand interaction. Despite this potential only albumin and α_1-acid glycoprotein [1], and recently cellobiohydrolase I [19], have been used as LC chiral selectors, with the best results obtained when these proteins were immobilised on silica (Fig. 3.2 D, Table 3.1) [1]. Because of the complex nature of the proteins, the mechanism of chiral selection is unknown. It is, however, influenced by pH, ionic strength and organic modifier.

The principle of complex chiral selection, using various modes of interaction, has been exploited in the LC chiral selectors developed by Armstrong *et al.* [15, 16] in 1994. They used silica-bonded macrocyclic peptide antibiotics, teicoplanin and vancomycin, as chiral selectors in HPLC (marketed as Chirobiotic^{TM} columns) (Table 3.1).

Table 3.1 Classification of chiral stationary phases

Type	**Chiral selector**	**Interaction**	**Enantioselection**	**Ref.**
Brush (Prikle)	various small chiral selectors e.g. amino acid derivatives; nitroaromatics	H-bonding; dipole stacking; charge transfer (π–π interaction)	Dalgliesh or Prikle type of chiral selective interaction (Fig 3.2 A)	1, 12
Chiral cavities	crown ethers and polymers e.g. cellulose derivatives polyacrylamides cyclodextrins	inclusion/insertion complexes	hydrophobic interaction and steric interference (Fig. 3.2 B)	1, 13
Metal co-ordination	amino acid-metal complexes	diastereomeric metal complexes	diastereomeric ligand exchange (Fig 3.2 C)	1, 14
Protein	ligand specific protein e.g. bovine serum albumin, orosomucoid	selective ligand binding	stereospecific ligand binding (Fig 3.2 D)	1
Antibiotic	amphoteric glycopeptide e.g. teicoplanin (Fig 3.3); vancomycin	combination of chiral cavity and brush type interaction	various enantioselective mechanisms (Fig 3.3)	15-17

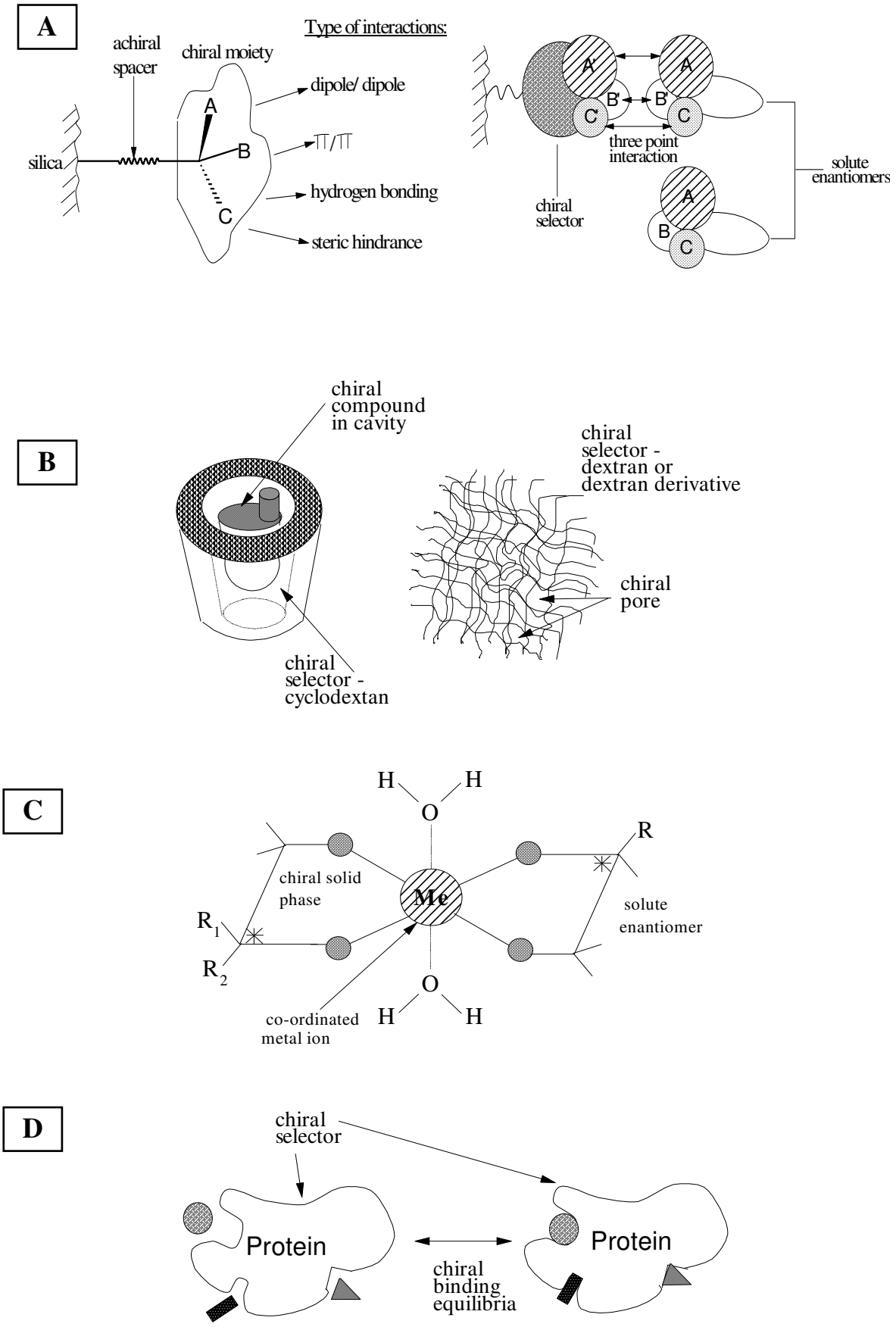

Figure 3.2 Enantioselective mechanisms: Brush chiral selection as described by Prikle and Dalgliesh's three point interaction model (A); chiral cavities (inclusion and insertion) (B); chiral metal co-ordination complexes (C); and, protein as chiral selector (D). [1,18]

Teicoplanin (Fig 3.3) and vancomycin contain multiple chiral centres, which include chiral cavities, π-electron systems, hydrogen donor and acceptor sites and several other polar interaction sites. These columns have been shown to be highly selective for several neutral molecules, amides, acids, esters and cyclic amines and possess many of the separation characteristics of protein-based CPS's [17]. The Chirobiotic™ columns, especially the teicoplanin type, are also very versatile in both reversed phase and normal phase solvents. This is of great importance for this study where the insolubility of the non-polar β-NC_{14} limited the choice of type of chiral LC. Chiral GC was not readily available although it would have been a more feasible alternative, because of the availability of chiral columns developed for the separation of aliphatic enantiomers. The use of reverse phase solvents also made the combination of chiral chromatography with electrospray mass spectrometry possible. It was therefore decided to use the teicoplanin chiral selector (Chirobiotic™ T) linked to ESI-MS to elucidate the absolute configuration of the β-NC_{14} residue in the iturin A_2 analogues.

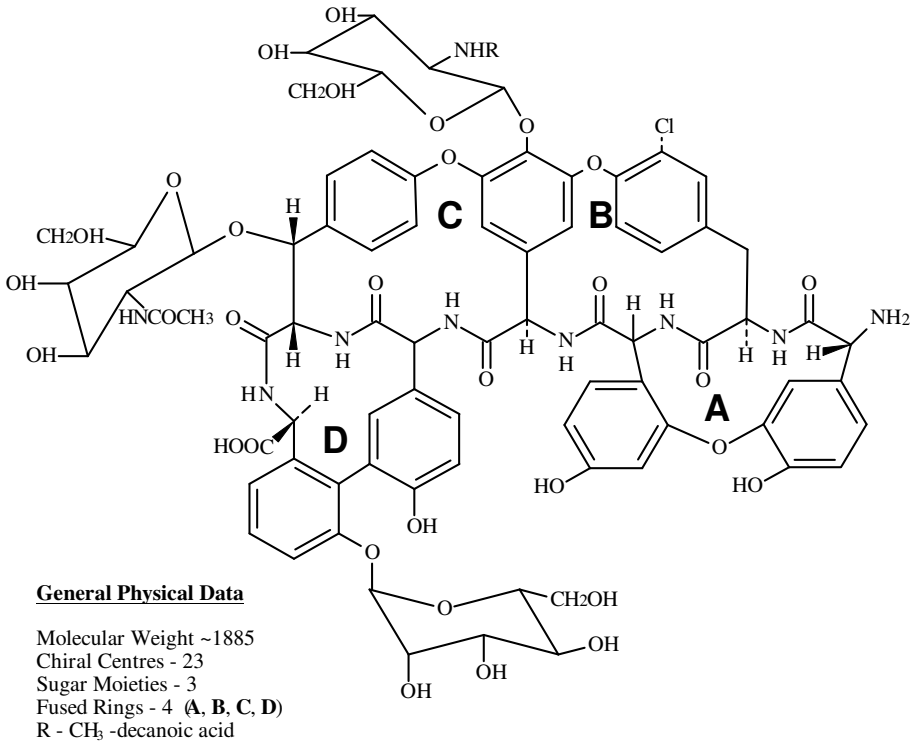

Figure 3.3 Macrocyclic peptide antibiotics teicoplanin as silica-bound chiral selector in HPLC (marketed as Chirobiotic™ T column) [17].

If the retention time of one of the enantiomers is known, it is possible to determine absolute configuration with chiral chromatography. If it is assumed that an enantiomer and a related reference standard are separated by the same chiral mechanism, absolute configuration can also be determined, but with some uncertainty—the compound's absolute configuration is

deduced solely from the enantioselectivity mechanism of the chromatographic method. In the case of complex interactions, and sometimes more complex compounds, this latter technique alone is not reliable, and data must be supported by independent techniques such as NMR or CD.

In this study of the function-structure relationship of iturin A, it was important that the synthetic products be of high chemical purity. The adaptability of electrospray ionisation mass spectrometry (ESI-MS) to HPLC and chiral LC was used to verify the optical purity of the synthetic peptide preparations. A reference standard of the D-enantiomer of β-NC_{14} was available, therefore the absolute configuration of the β-NC_{14} residue, introduced in each peptide, could be elucidated by using chiral LC linked to ESI-MS.

3.2 Materials

The four linear lipopeptides (7-Beta I, II and 8-Beta I, II), their cyclic analogues (cyclic 7-Beta I, II and cyclic 8-Beta I, II) and the two peptides without the β-NC_{14} (NYNQPNS and YNQPNS) were synthesised using the Fmoc-polyamide peptide synthesis protocol and purified using semi-preparative HPLC (described in Chapter 2). The HCl salt of racemic β-aminotetradecanoic acid (β-NC_{14}.HCl) was donated by Dr. R. Levitt, previously from Fine Chemicals, South Africa. The t-butyloxycarbonyl derivative from racemic β-NC_{14}.HCl was synthesised as described in Chapter 2 under 2.3.2.1. The enantiomerically pure t-butyloxycarbonyl derivative of β-D-aminotetradecanoic acid ((R)-(+)-tBoc-iturinic acid) was synthesised by the department of Chemistry, University of Stellenbosch, according to the method of Bland [20]. D-phenylalanine was from Aldrich Chemical Co. (Gillingham, UK). L-phenylalanine, trifluoroacetic acid (TFA, 99.5%), constant boiling hydrochloric acid (HCl) (30%), phenol (99.5%) and absolute ethanol (99.8%) were from Merck (Darmstadt, Germany). Nitrogen gas (N_2) and liquid nitrogen were from Afrox, South Africa. Acetonitrile (HPLC-grade, UV cut-off 190 nm) and methanol (HPLC-grade, UV cut-off 205 nm) were from Romil LTD (Cambridge, UK). Nova-Pak C_{18} analytical HPLC columns (150 x 3.9 mm, 60 Å, 5 micron particle size), 0.45 micron HV membrane filters were from Millipore-Waters (Milford, USA). Polygosil C_{18} packing material, Inertsil microbore C_4 and C_8 HPLC columns (150 x 2 mm, 60 Å, 5 µ particle size) were from Macherey-Nagel (Düren, Germany) and Chirobiotic T™ chiral HPLC column (150 x 4.6 mm) from Advanced Separation Technologies Inc. (Whippany, USA). Analytical grade water was prepared by filtering glass distilled water through a Millipore Milli Q® water purification system.

3.3 Methods

3.3.1 High performance liquid chromatography

Reverse phase high performance liquid chromatography, using a C_{18} Nova-Pak HPLC column with the system described under section 2.3.6.2, was used to evaluate the lipopeptides. The chromatography was monitored at 254 nm. Linear gradients were created using eluant A (0.1% TFA in water) and eluant B (90% acetonitrile and 10% A). (Refer to Chapter 2, section 2.3.5.2 for more detail.)

Isocratic liquid chromatography ESI-MS (LC-ESI-MS) was performed using an inline Inertsil C_8 microbore (150 x 2 mm) HPLC column for the lipopeptides and Inertsil C_4 microbore (150 x 2 mm) HPLC column for the N^{β}-t-butyloxycarbonyl-β-aminotetradecanoic acid preparation. Isocratic chromatography was done with 50% acetonitrile in water at a flow rate of 70 µL/min using a Pharmacia LKB 2249 gradient pump for solvent delivery.

3.3.2 Chiral liquid chromatography

Chiral LC-ESI-MS of the β-NC_{14} was done on an enantiomeric mixture and a chiraly pure preparation of the β-D-aminotetradecanoic acid. The preparation of the t-butyloxycarbonyl (tBoc) derivative of β-NC_{14} was treated with TFA (10 mg/100 µL) for 30 minutes to remove the tBoc group and liberate β-NC_{14}. The TFA was removed using a nitrogen stream followed by further drying under high vacuum and the residual material dissolved in 10 mL 50% acetonitrile for chiral LC-ESI-MS analysis. Chiral liquid chromatography (chiral LC) was performed using a Chirobiotic T^{TM} column (150 x 4.6 mm) inline with ESI-MS described hereafter under 3.3.3. Isocratic conditions, with either 30%, 40%, 50% methanol or 30% ethanol in water at a flow rate of 500 µL/min using a Pharmacia LKB 2249 gradient pump for solvent delivery, were used in chromatography of β-NC_{14}. A stream-split was used allowing 60 µL/min to enter the electrospray ionisation chamber. Chromatography of standard D/L-Phe was accomplished with 40% methanol in water as eluant. The column was regenerated with 20-50 bed volumes isopropanol followed by 20-50 bed volumes 50% acetonitrile to remove retained β-NC_{14} and other components.

The chiral identity of the β-NC_{14} residue in each of the purified lipopeptide preparations was determined by analysing the peptide hydrolysates. A small amount (0.2 to 1 mg) of each of the peptides was hydrolysed according to the protocol outlined in Chapter 2 section 2.3.6.3. The shortened hydrolysis procedure (150°C, 1 hour) was performed if possible immediately before ESI-MS analysis. Gaseous phase hydrolysis was, as before, accomplished under a nitrogen atmosphere using 6 N HCl containing 1% phenol. After hydrolysis the acid was removed from the samples under high vacuum and the residual material dissolved in 100 µL 50% acetonitrile/water for chiral LC-ESI-MS analysis. The samples were then diluted 10 times with the 40% methanol/water and 10 µL was analysed per run. Because room temperature storage leads to deamination of the β-NC_{14}, samples were either directly analysed or stored at −80°C until analysis. Isocratic conditions, with 30% ethanol in water at a flow rate of 500 µL/min., were used in chromatography of the peptide hydrolysates.

3.3.3 Electrospray mass spectrometry

ESI-MS, using a Micromass triple quadrupole electrospray mass spectrometer fitted with an electrospray source, and LC-ESI-MS was employed to investigate the synthetic components. The 50% acetonitrile in water carrier solvent was delivered at a flow rate of 20 µL/minute during each analysis. Ten µL of the sample solution (2 ng peptide in 50% acetonitrile/water containing 0.05% TFA) was introduced into the ESI-MS using a Rheodyne injector valve. A capillary voltage of 3.5 kV was applied, with the source temperature at 80°C. The cone voltage was 70 V and the skimmer lens offset 5 V. Data acquisition was in the positive mode, scanning the first analyser (MS_1), through m/z = 300–1300 or 1500 at a scan rate of 100 atomic mass units/second. Representative scans were produced by combining the scans across the elution peak and subtracting the background. Product ions were detected in MS_1 after cone voltage decomposition between 70 and 100 V or in MS_2 after decomposition at collision energy between 10 eV and 40 eV with cone voltage at 70 V and the argon pressure in the collision cell at $(2.5 \pm 0.3) \times 10^{-3}$ millibar.

LC-ESI-MS and chiral LC-ESI-MS were performed using an inline column (described under 3.3.1 and 3.3.2). The rest of the conditions and settings for both types of chromatography were as above. Single ion recording (SIR) at 243.5, the M_r of β-NC_{14}, was used to visualise the chiral chromatography of β-NC_{14}.

3.4 Results and discussion

During the purification of the four longer linear lipopeptides (discussed in Chapter 2) two fractions corresponding to each lipopeptide were collected (Figs.3.4 A, 3.5 A). These peptide fractions were identical in terms of the TLC behaviour, amino acid composition and mass spectra.

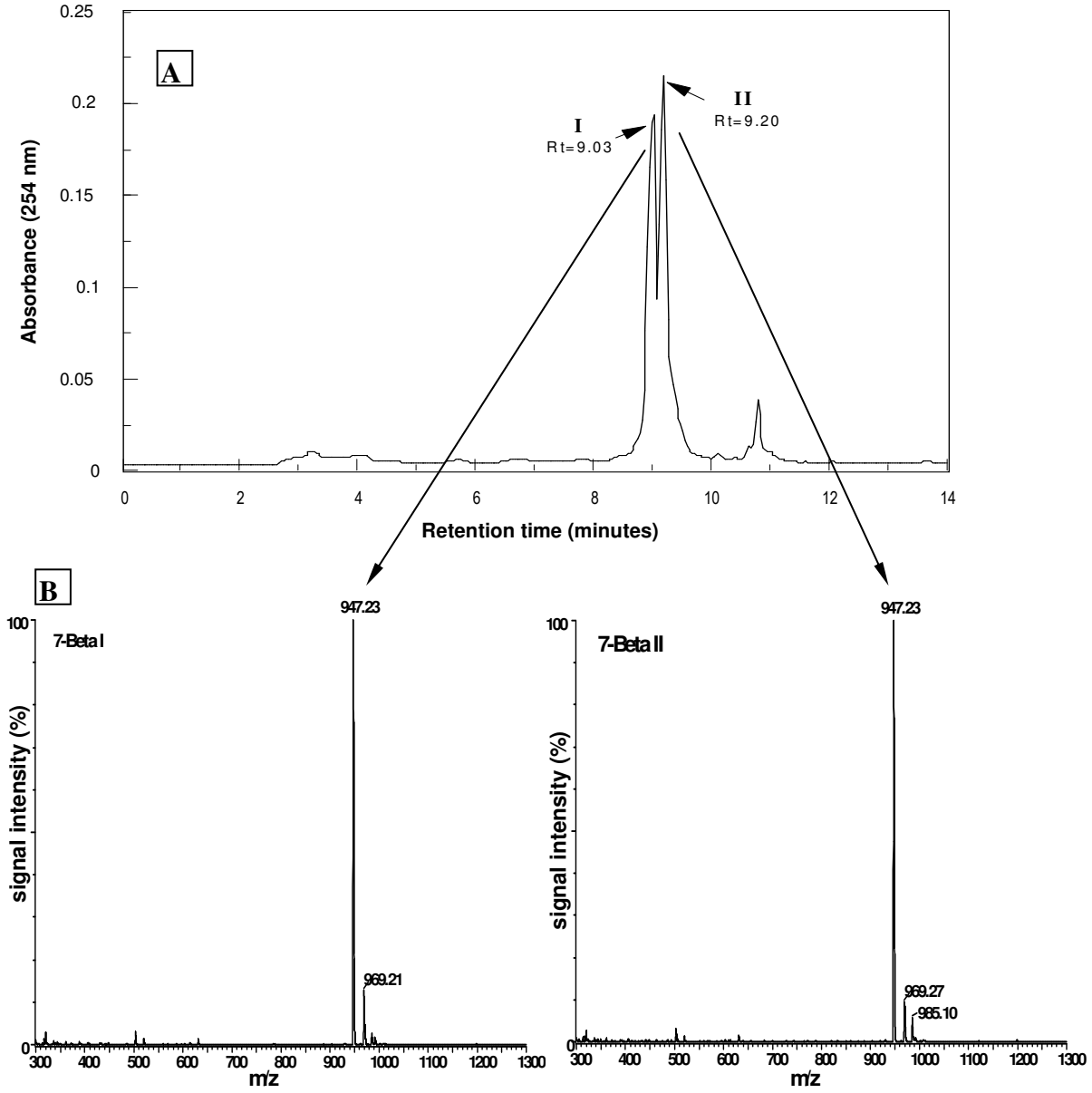

Figure 3.4 **A.** Preparative HPLC profile of the peptide preparation of 7-Beta obtained on a C_{18} Polygosil column (250 x 10 mm). The gradient was developed over 13 minutes from 30% A (0.1% TFA in water) to 100% B (90% acetonitrile, 10% A) using a flow rate of 3.0 mL/min. **B.** The ESI-MS spectra of the two partially resolved components (7-Beta I and II) of 7-Beta.

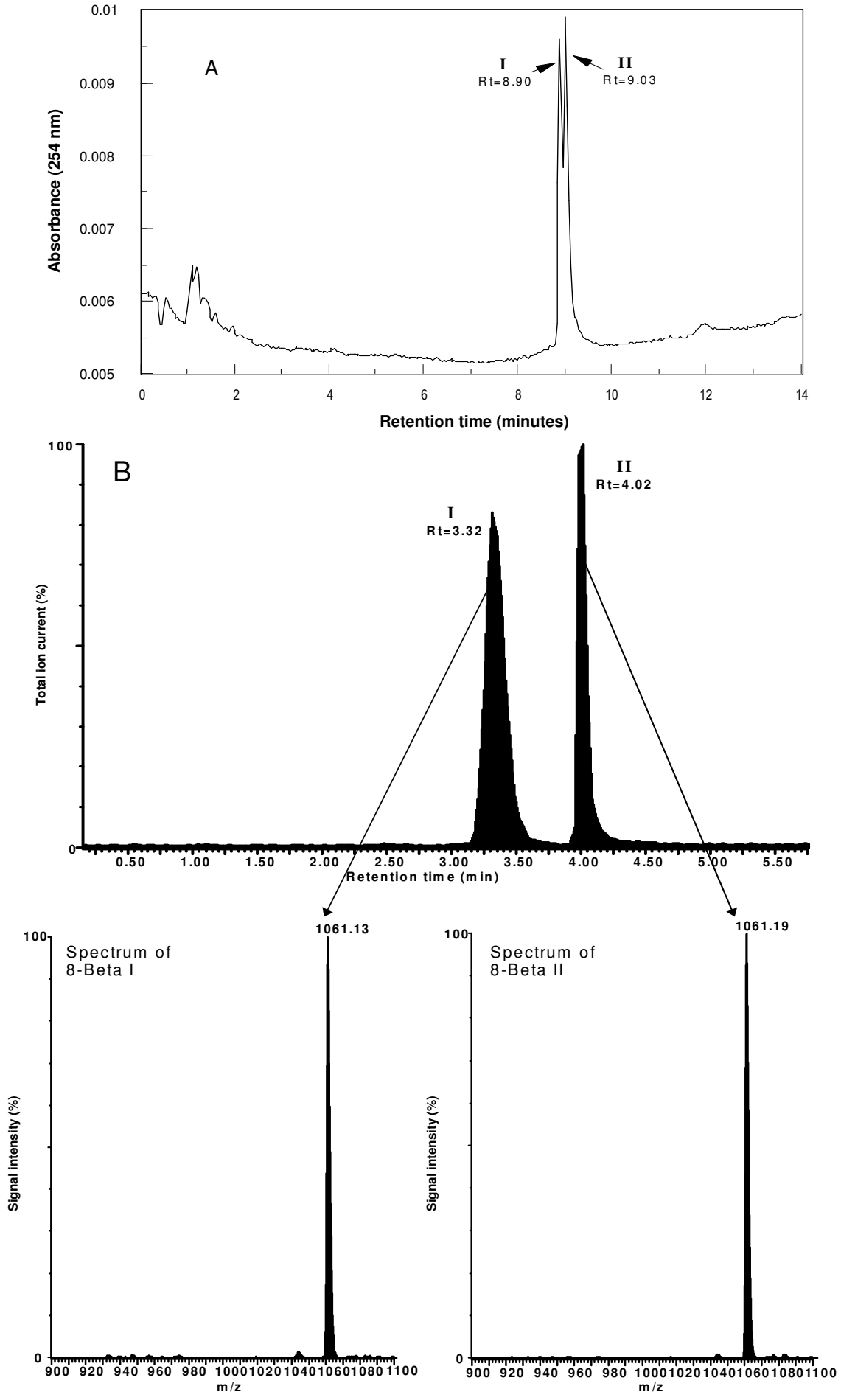

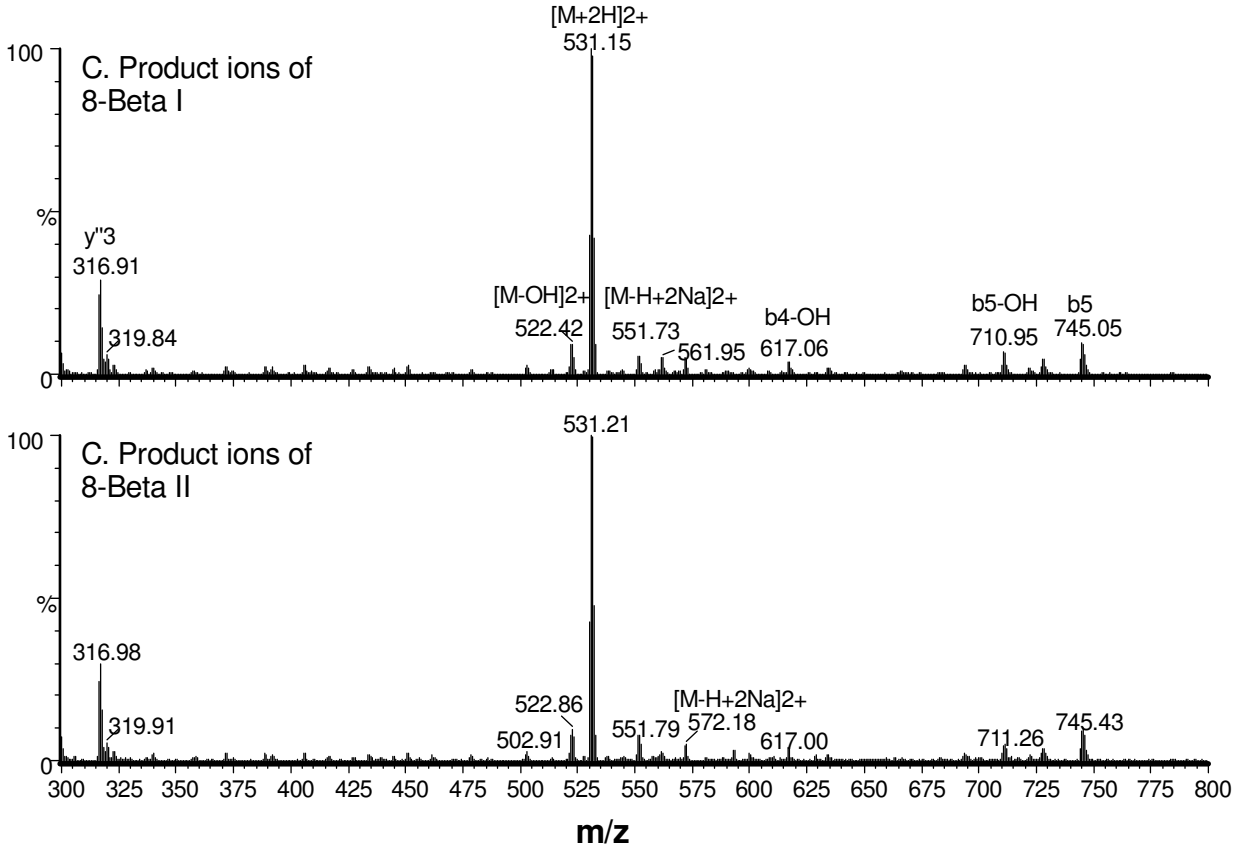

Figure 3.5 Analytical HPLC profiles of the peptide preparation of 8-Beta on a C_{18} Nova-Pak column (150 x 3.9 mm). The gradient was developed over 13 minutes from 30% A (0.1% TFA in water) to 100% B (90% acetonitrile, 10% A) using a flow rate of 1.0 mL/min. **B.** The LC-ESI-MS profile (total ion count, TIC) of the 8-Beta peptide preparation and mass spectra of the two resolved components. Chromatography was done on an inline Inertsil C_8 column (150 x 2.0 mm) with 50% acetonitrile in water as mobile phase and a flow rate of 70 µL/min. **C**. Cone voltage-induced product ions of the two resolved components, 8-Beta I and 8-Beta II.

The two HPLC purified fractions of the linear 7-Beta preparation were analysed by ESI-MS and it was found that the spectra of these two fractions were identical (Fig. 3.4 B). The HPLC behaviour (Fig 3.4 A) of these two compounds could not be explained by differences in peptide sequence, as their amino acid composition is also identical (see Chapter 2). The two components in the 8-Beta preparation differed very little in their HPLC behaviour (Fig 3.5 A) and it was thus difficult to prepare a homogenous peptide. LC-ESI-MS analyses with its high resolving power again revealed two components of the 8-Beta preparation with identical molecular ions (Fig. 3.5 B). Fragmentation by cone voltage-induced dissociation produced identical fragments from both components, indicating identical amino acid sequences (Fig. 3.5 C).

Analytical HPLC and ESI-MS of the purified hexapeptide (YNQPNS) and purified heptapeptide (NYNQPNS) confirmed the purity of the peptide moieties of 7-Beta and 8-Beta (Fig. 3.6).

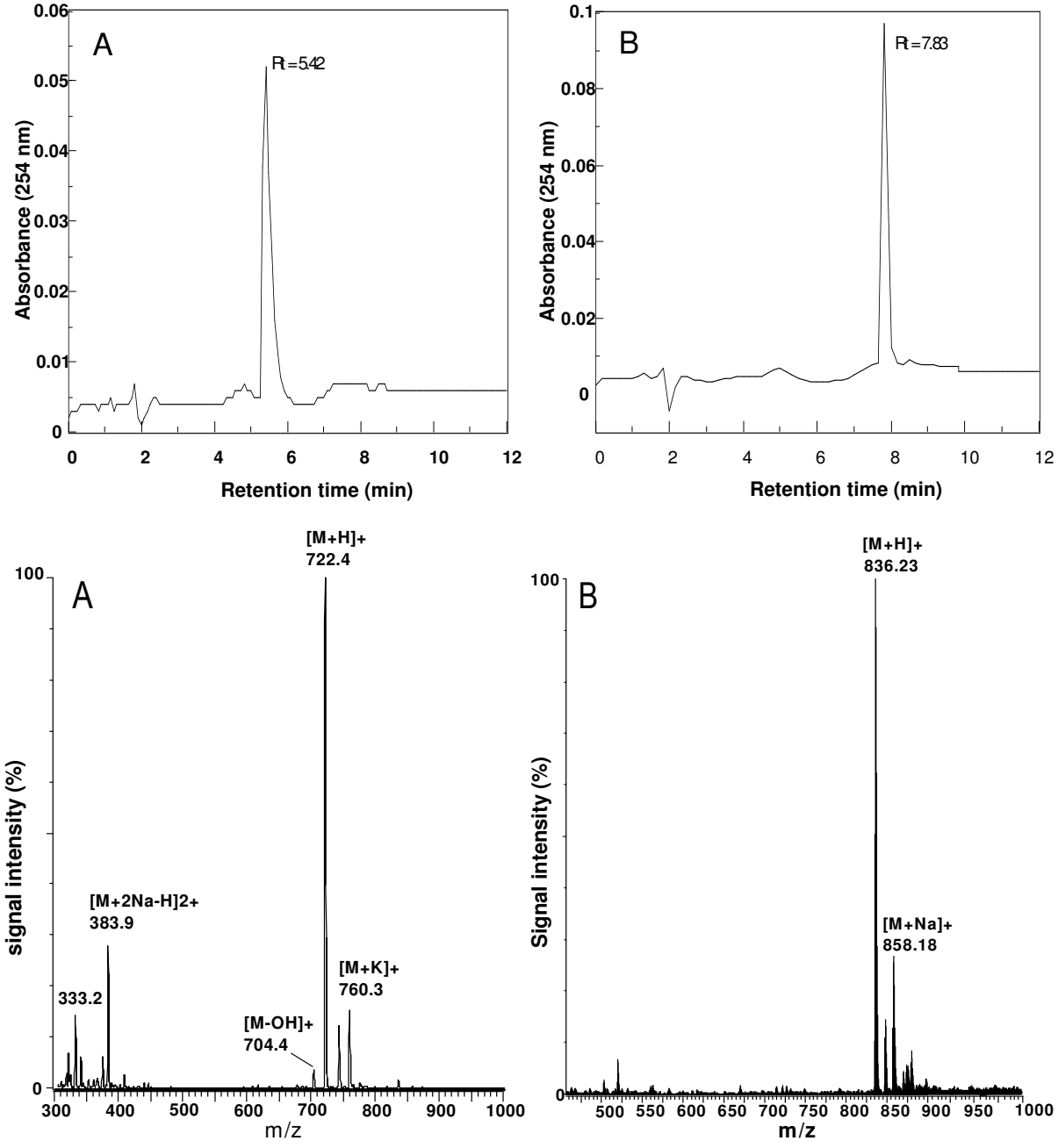

Figure 3.6 Analytical HPLC profiles and the ESI-MS-spectra of YNQPNS hexapeptide (**A**), and NYNQPNS heptapeptide (**B**). Chromatography was done on a C_{18} Nova-Pak column (150 x 3.9 mm). The gradient was developed over 15 minutes from 95% A (0.1% TFA in water) to 100% B (90% acetonitrile, 10% A); flow rate 1.0 mL/min.

The fact that the second HPLC peak appeared only after coupling the β-amino fatty acid to the peptide indicated that the introduction of this residue was the cause of the appearance of two compounds, which could be either enantiomers or conformers. The synthesis method limits

racemisation of the amino acids during coupling to a maximum of 0.4% [21]. The two peptides observed in each preparation were probably the consequence of the introduction of a racemic mixture of the N-terminal β-NC_{14} residue. Most of the peptide synthesis work was completed before Bland [20] in 1995 successfully synthesised enantiomerically pure β-D-amino-tetradecanoic acid. A product synthesised with the protocol of Levitt [22], which produced a racemic mixture of β-NC_{14}, was incorporated into the iturin A_2 analogues. LC-ESI-MS of the t-butyloxycarbonyl derivative of β-NC_{14}, used in the syntheses, revealed two components, with identical molecular ions, confirming that the preparation was a racemic mixture (Fig. 3.7).

Repeated crystallisation of the N^{β}-t-butyloxycarbonyl-β-aminotetradecanoic acid from acetonitrile resulted in an enriched preparation of one of the isomers. The isomeric composition of the enriched preparation could not be accurately determined using normal reverse phase LC-ESI-MS (Fig. 3.7) because of insufficient resolution. The percentage enriched isomer was determined by chiral chromatography linked to ESI-MS as 60% of the total (Fig. 3.8).

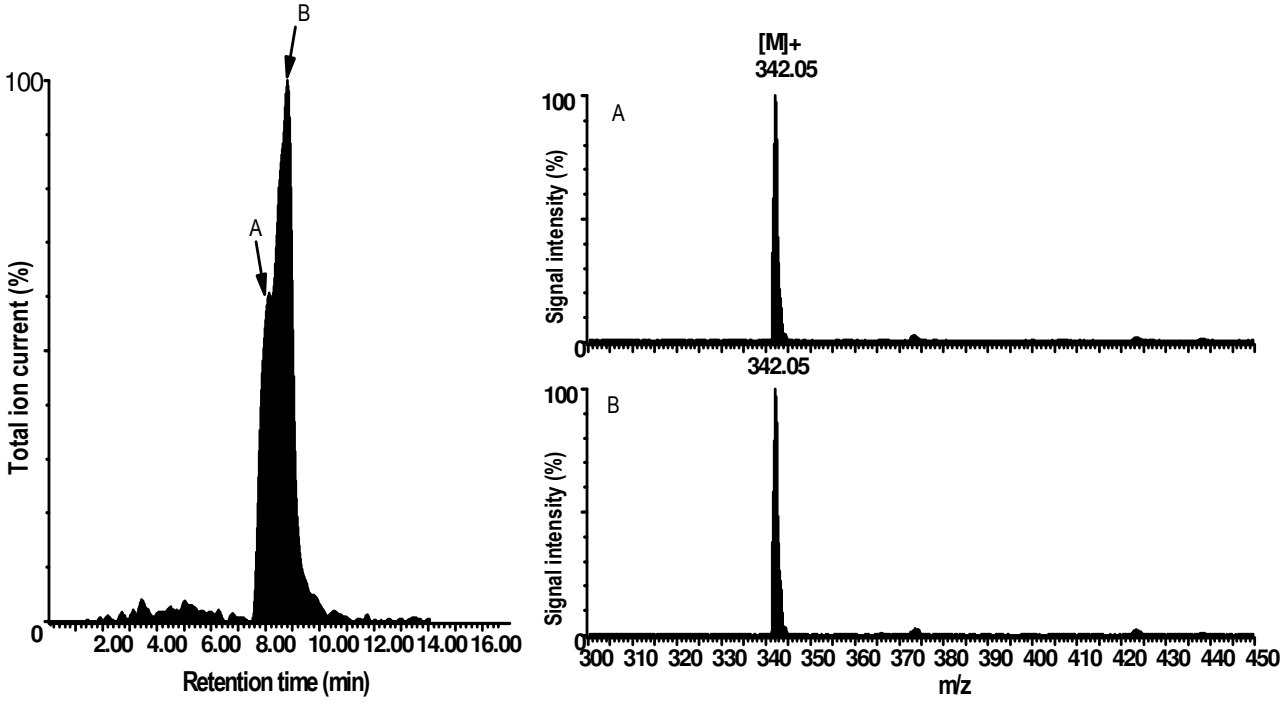

Figure 3.7 LC-ESI-MS profile (TIC) of the enriched preparation of N^{β}-t-butyloxycarbonyl-β-aminotetradecanoic acid and mass spectra of the two components. Chromatography was done on an inline Inertsil C_4 microbore column (150 x 2.0 mm) with 50% acetonitrile in water as mobile phase and a flow rate of 70 μL/min.

The results, obtained during the development of a chiral separation method for β-NC_{14} using different isocratic conditions (30%, 40% and 50% methanol in water), are depicted in Fig. 3.8. It was not possible to obtain baseline separation with any of the methanol mixtures or if the methanol was substituted with ethanol. Addition of 0.1% TEA/acetate in 30% methanol resulted in total depression of the ESMS signal (results not shown). Other solvent mixtures such as 40 to 50% acetonitrile in water, sometimes containing a small percentage of isopropanol, did not resolve the enantiomers. The best separation (sufficient resolution with a short elution time) between the two enantiomers was obtained by using the general α-amino acid isocratic LC conditions (40% methanol in water) (Fig. 3.8 B)[17].

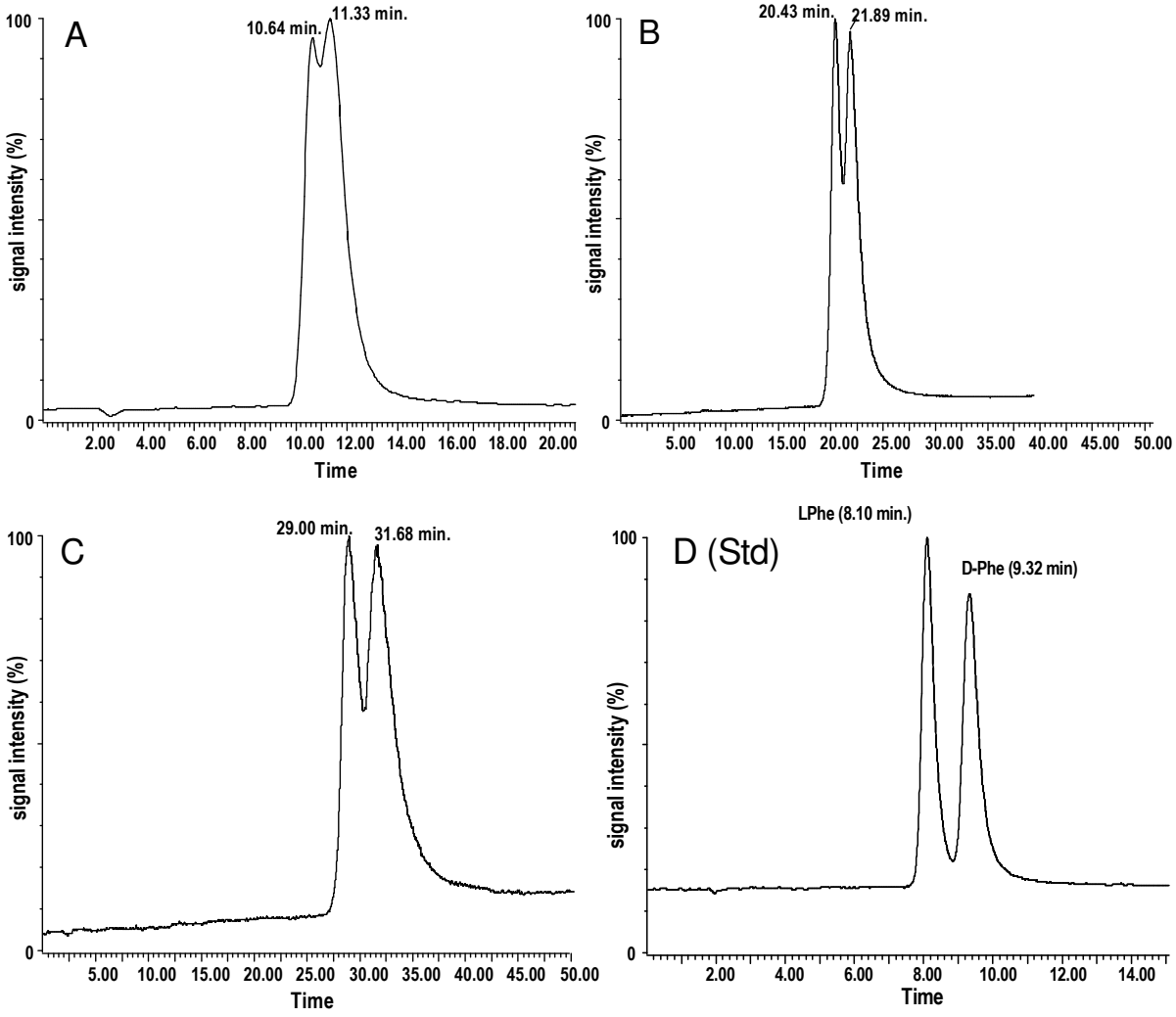

Figure 3.8 Chiral LC-ESI-MS profiles of the enriched N^{β}-t-butyloxycarbonyl-β-aminotetradecanoic acid preparation after treatment with TFA to liberate β-NC_{14}. Chromatography was done on an inline Chirobiotic T^{TM} column (150 x 5.0 mm) with mobile phases (**A**) 50% methanol in water; (**B**) 40% methanol in water, and (**C**) 30% methanol in water. The flow rate was 0.5 mL/min and single ion recording (SIR) at 243.5, the M_r of β-NC_{14}, was used to visualise the chromatography. (**D**) Chromatography of standard D-Phe and L-Phe with 40% methanol in water as eluant and SIR at 165.2, the M_r of Phe.

The absolute configuration of components in the N^{β}-t-butyloxycarbonyl-β-aminotetradecanoic acid preparation, after treatment with TFA to liberate β-NC_{14}, could not be deduced from only chiral chromatography without using the pure enantiomer with known chirality as a reference standard (Fig. 3.8). It was, however, observed during the chiral separation of L-Phe and D-Phe that the L-enantiomer eluted first and the D-enantiomer second on the Chirobiotic T™ column (Fig. 3.8). These results were in accordance with the elution profiles observed for all of the 20 α-amino acids on the teicoplanin type chiral selector as shown by Armstrong *et al.* [15, 16].

Cyclisation of the 7-Beta and 8-Beta lipopeptide preparations produced the cyclic 7-Beta and cyclic 8-Beta diastereomers (refer to Chapter 2). To ascertain the absolute configuration of the β-NC_{14} residue in each of the eight lipopeptide preparations, the β-NC_{14} in each of the peptide hydrolysates was identified by chiral chromatography (chiral LC-ESI-MS) (Figs. 3.9, 3.10, Table 3.2). During the first analysis of the peptide hydrolysates, using 40% methanol in water as eluant, extensive peak retention drift occurred from elution at about 20 minutes to elution after more than an hour (Fig. 3.9). This drift coincided with the total loss of resolution. This method probably failed because of column coating by β-NC_{14}, effectively converting the chiral stationary phase to a reverse phase. The column was washed with different organic solvents and revived to such an extent that base line separation of L- and D-Phe (Fig. 3.8 D) was again obtained. The separation of the enantiomers of β-NC_{14} was, however, not regained. Because of the enormous expense of chiral LC columns it was not possible to replace the item. An alternative chromatographic technique such as chiral GC, which would have been a better option, was not available to us. Alternative solvents were again investigated and some resolution, with less drift in retention volume, was obtained between the β-NC_{14} enantiomers using 30% ethanol in water as mobile phase (Fig. 3.10). This resolution was not adequate for chiral purity assessment, but sufficient for identification of the major enantiomer in each preparation (Fig. 3.10).

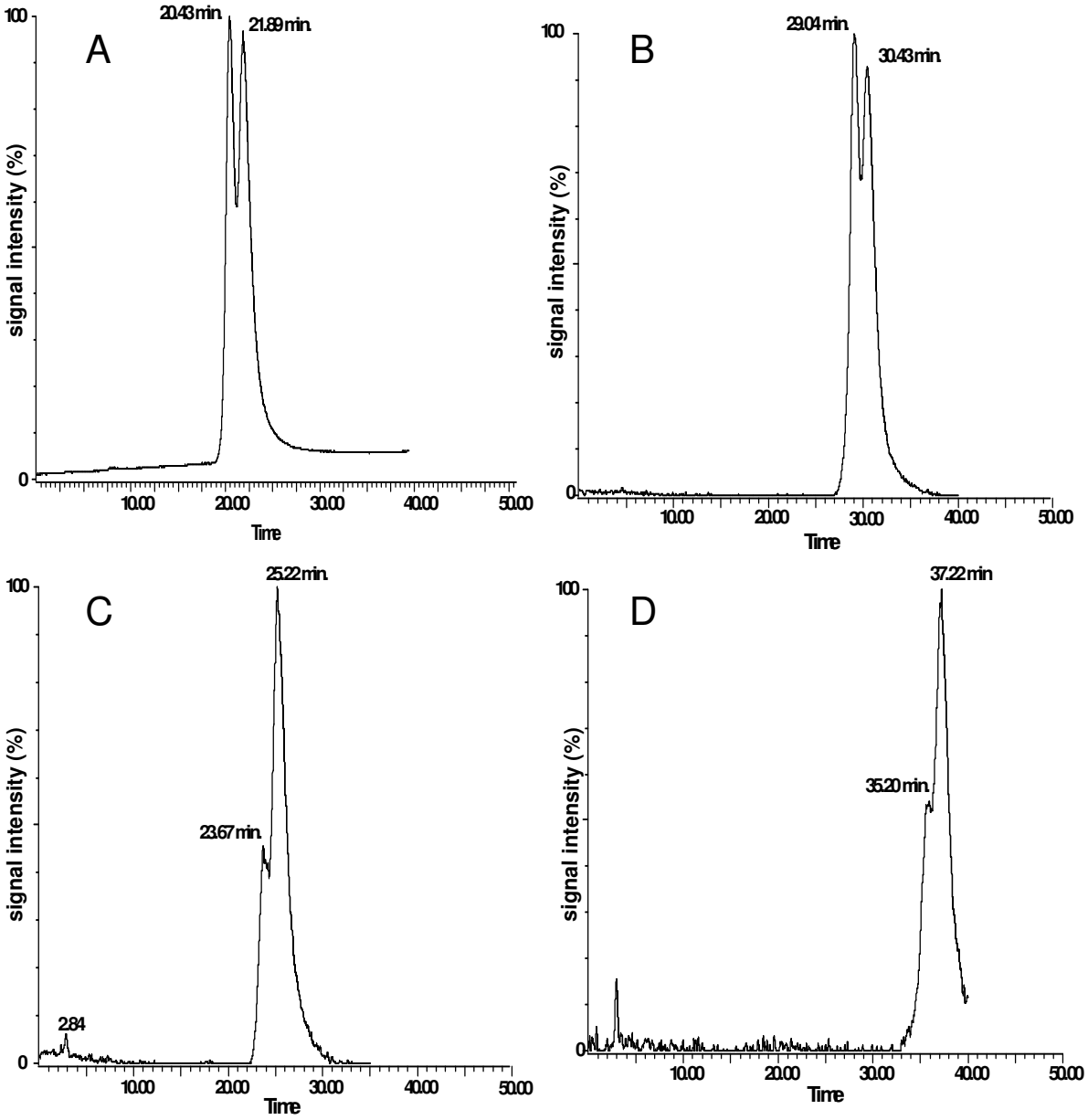

Figure 3.9 Example chiral LC-ESI-MS profiles of β-NC_{14} (A, B) and a hydrolysate of 8-Beta II (C, D) illustrating the retention time drift experienced with 40% methanol in water as eluant. Chromatography was accomplished by using a Chirobiotic T^{TM} column (150 x 5.0 mm) with flow rate of 500 µL/min. Chromatography was visualised using SIR of β-NC_{14} (*m/z* 243.5).

If the β-NC_{14} chiral separation took place *via* the same mechanism as with the α-amino acids it could be hypothesised that the L-enantiomer is the first eluting component and the D-enantiomer the second eluting component, although this could only be verified with the use of a β-NC_{14} reference standard of known chirality. Biological activity in the cyclic 8-Beta II preparation was, however, similar to that of natural iturin A [5] (refer to Chapter 6). If cyclic 8-Beta II is the synthetic iturin A_2 analogue it must contain the D-enantiomer of β-NC_{14}; therefore we cannot deduce that the elution order of the enantiomers of β-NC_{14} is the same as

that of α-amino acids. It was therefore necessary to synthesise a pure enantiomer of β-NC_{14}. A t-butyloxycarbonyl derivative of β-D-aminotetradecanoic acid was synthesised according to Bland [20], with some adaptations, and used as the reference standard (Fig. 3.10 B).

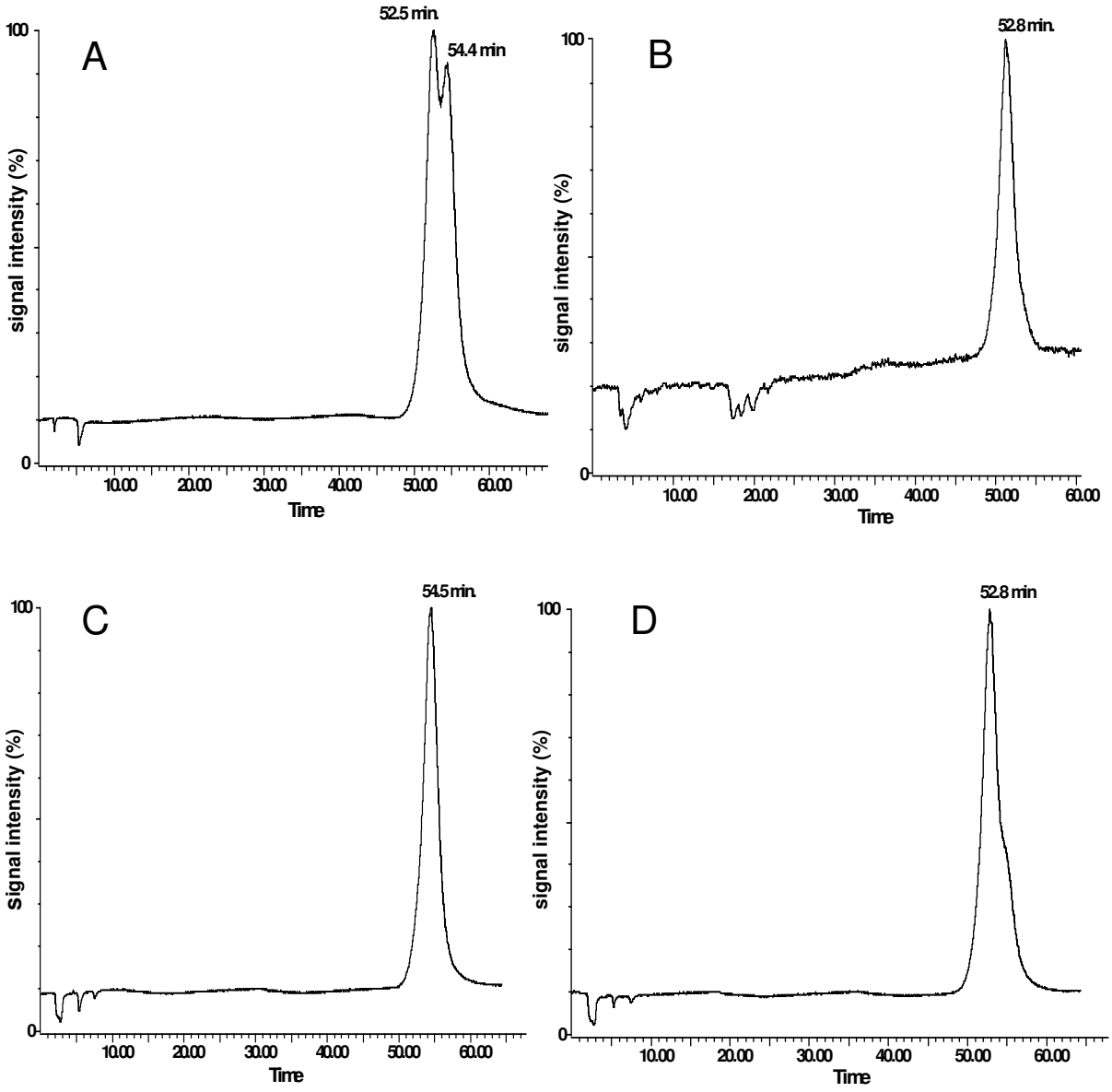

Figure 3.10 Example chiral LC-ESI-MS profiles of (A) the β-NC_{14} preparation used in syntheses; (B) enantiomerically pure β-D-NC_{14} , and hydrolysates of (C) cyclic 8-Beta I and (D) cyclic 8-Beta II. Chromatography was done one an inline Chirobiotic T ^{TM} column (150 x 5.0 mm) with 30% ethanol in water as mobile phase and a flow rate of 500 µL/min. Chromatography was visualised using SIR of β-NC_{14} (*m/z* 243.5).

We were able to obtain separation of the eight HPLC purified lipopeptides using analytical HPLC (refer to Chapter 2, section 2.4.2.1), facilitating the determination of the chiral purity of the peptide samples (Table 3.2).

Table 3.2 A summary of the data (duplicate analyses) obtained from analytical RP-HPLC, chiral-LC-ESI-MS and CD for β-NC_{14} and the 8 purified lipopeptide isomers (# refer to Chapter 2, section 2.4.2.1; retention times were corrected for * +5% and $^{\$}$ –3% drift).

Peptide	**RP-HPLC R_t (min.) of peptide #**	**Chiral LC R_t (min.) of β-NC_{14}**	**Absolute configuration of β-NC_{14}**	**Chiral purity (%)**	**Revised name of peptide**
Std β-D,L-NC_{14}	–	52.5; 54.4	D, L	–	–
Std β-D-NC_{14}	–	52.8$^{\$}$	D	–	–
7-Beta I	9.60	54.9	L	89	7-Beta I (L)
7-Beta II	9.80	52.3	D	84	7-Beta II (D)
8-Beta I	8.90	52.8*	D	79	8-Beta I (D) (linear iturin A_2)
8-Beta II	9.03	55.1*	L	83	8-Beta II (L)
cyclic 7-Beta I	9.13	52.5*	D	100	cyclic 7-Beta I (D)
cyclic 7-Beta II	9.27	55.7	L	82	cyclic 7-Beta II (L)
cyclic 8-Beta I	8.70	54.5	L	100	cyclic 8-Beta I (L)
cyclic 8-Beta II	8.90	52.8	D	84	cyclic 8-Beta II (D) (iturin A_2)

The difference in HPLC retention of the peptide diastereomers is the result of the chiral difference between the incorporated β-NC_{14} residues. The chiral purity of all the HPLC purified peptides was greater than 80%, except 8-Beta I (D) at 79%. Two of the cyclic peptides were virtually 100% pure in terms of HPLC and enantiomeric purity.

3.5 Conclusions

The peptides synthesised in this study were found to be isomeric mixtures with the mixed chiral centre located at the β-carbon of the β-NC_{14} residue. The racemic nature of the synthetic lipopeptides complicated purification and decreased yields. The HPLC behaviour of the peptides was influenced by the β-NC_{14} residue, as the conformation of the diastereomers in solution is probably different, resulting in different hydrophobicities. Purification of the diastereomers to greater than 80% chiral purity in all but one preparation was accomplished. The inclusion of the racemic β-amino fatty acid in the peptides, however, introduced a new structural aspect in this investigation.

Chiral and reverse phase LC-ESI-MS proved powerful tools to resolve chiral composition (optical purity) of the lipopeptides in this study. Using standard β-D-NC_{14}, the absolute configuration of the β-NC_{14} residue in each peptide preparation was determined. This is the first time that the combination of chiral LC, using a Chirobiotic T^{TM} column, and ESI-MS was successfully used to elucidate the composition and chiral identity of a β-amino acid residue. This method may prove useful for future investigation of chirality in peptides.

The influence of deviation from the constant cyclic DLDDLLDL chiral sequence of iturin A on its structure, as studied with NMR, CD and molecular modelling of the four octalipopeptides, will be discussed in Chapter 4. In Chapter 5 the influence of chirality and peptide structure on the association of the lipopeptide with alkali metal ions will be reported. The importance of stereoselectivity on the bioactivity of the lipopeptides will be addressed in Chapter 6.

3.6 References

1. Allenmark S. G. (1988) Chromatographic enantioseparation: methods and applications, John Wiley & Sons, New York

2. Pasteur L. (1850) *Ann. Chim Phys.* **28**, 56

3. Cahn R. S., Ingold C. K., Prelog V. (1956) *Experientia* **12**, 81-124

4. Nagai U., Besson F., Peypoux F. (1979) *Tetrahedron Lett*. **25**, 2359-2360

5. Maget-Dana R., Peypoux F. (1994) *Toxicology* **87**, 151-174

6. Urry D. W. (1985) Modern physical methods in Biochemistry (Eds. Neuberger A., Van Deenen L. L. M.), Elsevier, New York, pp. 275-346

7. Freifelder D. (1982) Physical Biochemistry: Applications to biochemistry and molecular biology Second Edition, W. H. Freeman and Company, New York, pp. 573-595

8. Prikle W.H. (1966) *J. Am. Chem. Soc*. **88**, 1837

9. Whitesides G. M., Lewis D. W. (1970) *J. Am. Chem. Soc*. **92**, 6979-6980

10. Souter R. W. (1985) Chromatographic Separation of Stereoisomers, John Wiley & Sons, New York

11. Rautenbach M., Visser L. (1990) Innovations and Perspectives in solid phase synthesis (Editor R. Epton), SPCC (UK) Ltd. Birmingham, England, pp. 547-550

12. Prikle W. H., Finn J. (1981) *J. Org. Chem.* **46**, 2935-2938

13. Armstrong D. W. (1984) *J. Liq. Chrom*. **7**, 253-376

14. Rogozhin S. V., Davankov V. A. (1971) *Chem. Commun.*, 490

15. Armstrong D. W., Tang Y., Chem S., Zhou Y., Bagwill C., Chen J. R. (1994) *Anal. Chem*. **66**, 1473-1484

16. Armstrong D. W., Liu Y., Ekborg-Ott. K. H. (1995) *Chirality* **7**, 474-497

17. Chirobiotic Handbook: A guide to use macrocyclic antibiotic bonded phases for chiral LC separations (1996) Advanced Separation Technologies Inc. (Astec), USA

18. Chirex: Guidebook to chiral HPLC–column selection and method development techniques, distributed by Phenomenex ®

19. Marle I., Jönsson S., Isaksson R., Petterson C. (1993) *J. Chrom*. **648**, 333-347

20. Bland J. M. (1995) *Synt. Commun*. **25**, 467-477

21. Kemp D. S. (1979) Racemisation in peptide synthesis, In: The peptides: Analysis, synthesis, biology (Eds. Gross E., Meienhofer J.) Academic Press, New York, pp.1-10

22. Levitt R. R. (1986) The synthesis of a novel octapeptidolipid antibiotic, Ph.D. Thesis (Biochemistry), University of Stellenbosch, Stellenbosch, pp.14-34

Chapter 4

A structural study of the octalipopeptide analogues of iturin A_2

4.1 Introduction

An range of physical methods, that make use of some part of the electromagnetic spectrum (Fig. 4.1), is available for the structural analysis of simple molecules. The highly complicated structures of peptides and proteins challenged the physical chemistry field to such an extent that many of these methods evolved to accommodate even the most complicated structure. This challenge also extended into the realm of computer science: molecular modelling programs for the prediction of molecular structure were developed and are still evolving along with the accumulation of physical data, such as covalent bond distances and angles, group planarity, van der Waals radii and other inter atom distances in chemical groups. A short summary of some of the main techniques for the study of molecular structure, such as nuclear magnetic resonance, spectroscopic methods based on the chromatophoric properties of molecules, and the ultimate method for three-dimensional (3D) structure determination namely, X-ray crystallography, will be given in this chapter.

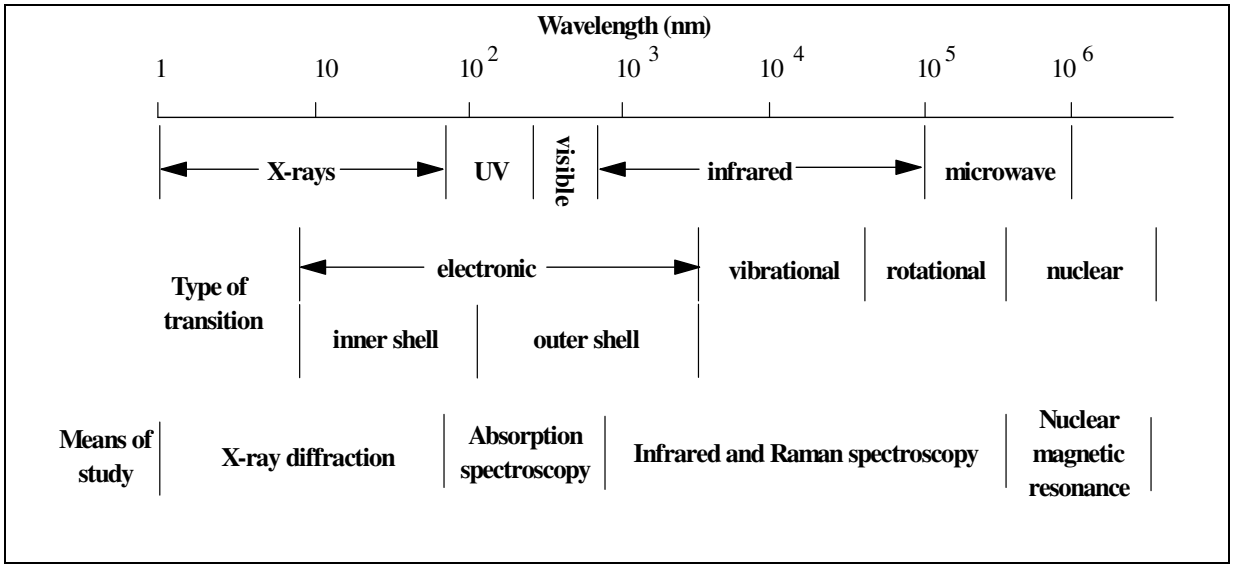

Figure 4.1 The relevant part of the electromagnetic spectrum in structure determination with spectroscopic methods [adapted from 1].

The determination of the 3D structures of small proteins and peptides became possible with the development of two-dimensional (2D) nuclear magnetic resonance (NMR) spectroscopy and more recently 3D and 4D techniques. NMR is the result of the absorption and re-emission of radio-frequency radiation by atomic nuclei, when placed in a strong magnetic field, and depends on the charge and spin of nuclei. NMR spectroscopy can also give the position of individual hydrogen atoms, which is beyond the scope of X-ray crystallography. Because of the differences between the resonance frequency of isotopes in a given magnetic field, only one isotope is studied directly in an NMR experiment. NMR studies in biochemistry utilised nuclei with spin number (I) of ½, namely ^{1}H, ^{13}C, ^{15}N, ^{19}F and ^{31}P. In a stationary magnetic field only one energy transition is possible for a nucleus with I = ½ and the transition is the result of absorption of electromagnetic radiation with a specific frequency (v). The shielding of nuclei from the external magnetic field by their electrons differ in different chemical groups. These atoms will therefore resonate at different frequencies or will have different chemical shifts (symbolised by δ in parts per million; ppm), which will facilitate identification. The resonance intensity of a chemical group is directly proportional to its quantity. NMR spectra often contain multiplets of two or more clustered spectral lines, exceeding the number of chemically different nuclei. The splitting of resonance lines into multiplets is not due to chemical shift, but the result of electron-coupled interactions between spins of covalent bonded nuclei (spin-spin coupling). The molecular structure and stereochemistry, including electron distributions and bond angles, can be correlated to the observed coupling constants. Two dimensional correlation spectroscopy (2D-COSY) provides connectivity between spins through, for example, scalar coupling. The interproton distances through space are determined by the nuclear Overhauser effect spectroscopy (NOESY). Refer to [1-3] for more information on NMR spectrometry.

An NMR study in 1978 of iturin A dissolved in pyridine was the first attempt to elucidate the 3D structure of iturin A [4]. It was proposed that the characteristic constant LDDLLDL chiral sequence of the seven α-amino acid residues and the β-D-amino fatty acid (iturinic acid) in the peptide ring included two hydrogen-bonded β-turns. Garbay-Jaureguiberry *et al.* [4] proposed that one turn, a type II β-turn, is formed by L-Gln_5-L-Pro_6-D-Asn_7-L-Ser_8 and the second, a type I' β-turn, by Asn_2-D-Tyr_3-D-Asn_4-L-Gln_5. This structure of iturin A in pyridine was refined by Marion *et al.* [5] using NMR combined with molecular modelling (Fig. 4.2). The two tetrapeptide units, β-amino fatty acyl-Asn_2-D-Tyr_3-D-Asn_4 (turn A) and L-Gln_5-L-Pro_6-D-Asn_7-L-Ser_8 (turn B), were classified as type II β-turns with distorted hydrogen bonds.

A third turn is formed by Asn_2-D-Tyr_3-D-Asn_4-L-Gln_5 (turn C), as originally proposed [4], and could be classified as a type I' or III' β-turn or the beginning of a 3_{10}-helix. The existence of these β-turns in the iturin A structure may be of importance in the interaction of the peptide with the monovalent cations, Na^+ and K^+. Our investigation into interaction with Na^+ and K^+ is reported in Chapter 5.

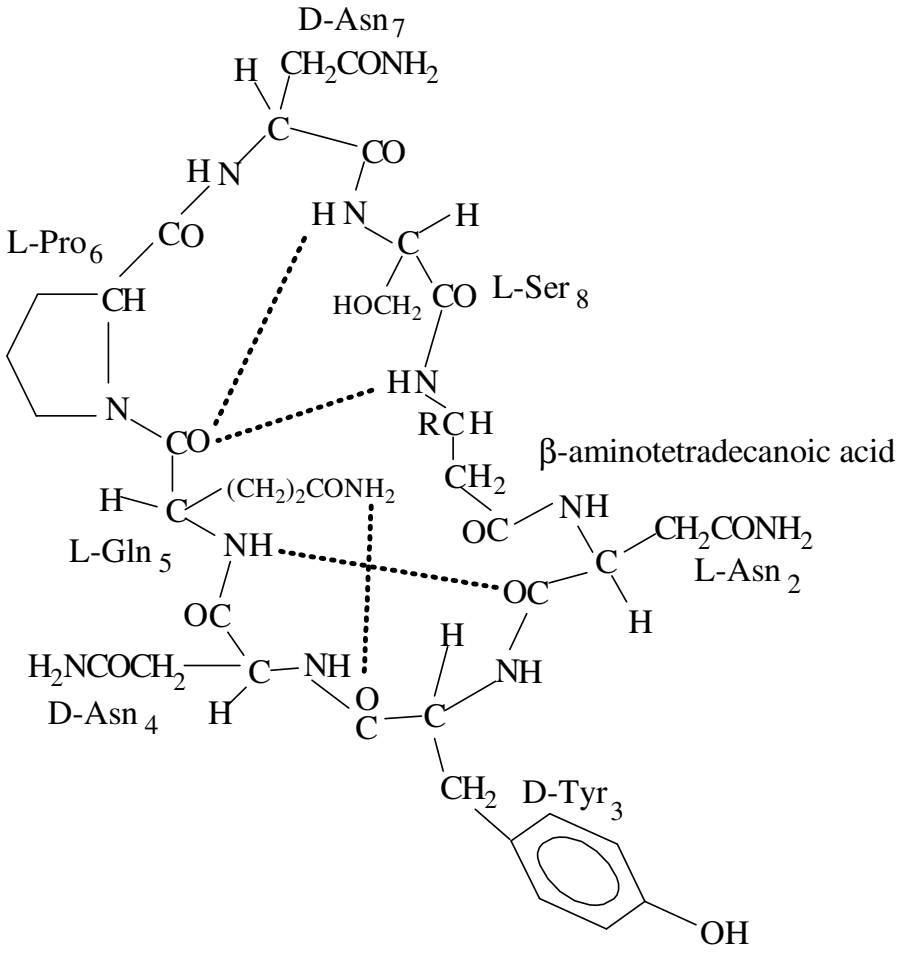

Figure 4.2 The structure of iturin A_2. This drawing is an adaptation from the structure deduced by Marion *et al*. [5] from nuclear magnetic resonance spectrometry data and molecular modelling of natural iturin A. The dashed lines represent hydrogen bonds that stabilise the structure.

The physical phenomena on which light spectroscopic methods are based, namely absorption, refraction, circular dichroism (CD) optical rotary dispersion (ORD), are closely related, because of their dependence on the properties of light. Light may be described as an oscillating electric vector that is affected by the electric dipole moment of an absorbing unit (chromophore) and *vice versa* [6] (Fig 4.3). Light is circularly polarised if the electric vectors of two electromagnetic waves are 0.25 λ out of phase. The resulting molecular ellipticity ([θ]; the difference in absorbance of left and right circularly polarised light) is measured with CD

and molecular rotation ([ϕ]; the difference in refractive index of left and right circularly polarised light) with ORD (Fig. 4.3; also refer to Chapter 3).

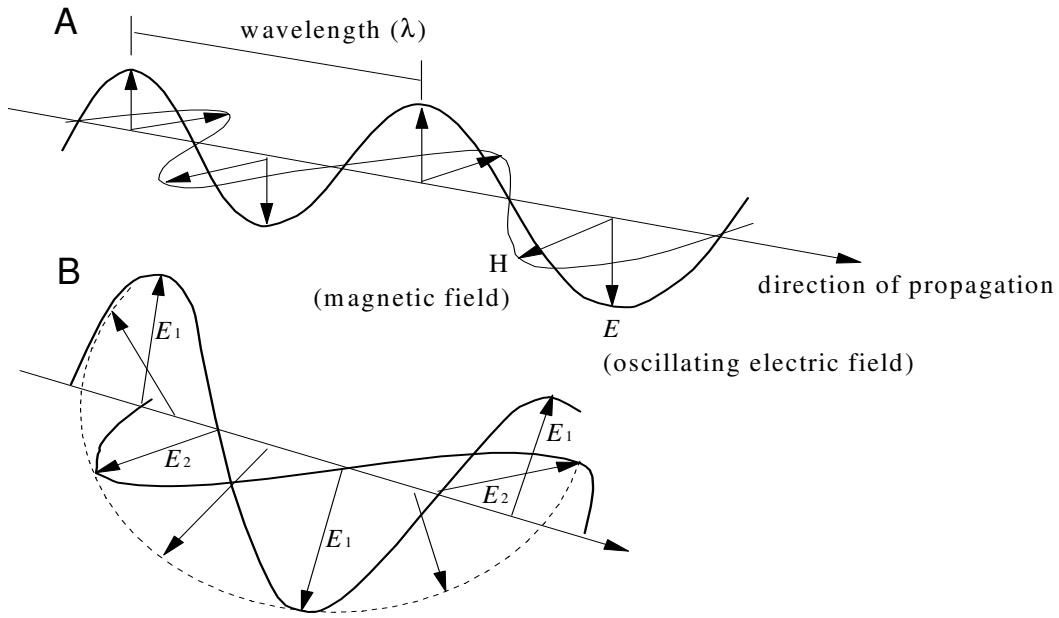

Figure 4.3 **A.** Propagation of an electromagnetic wave. The thick line follows the path of the *E*-vector and the thin line that of the H-vector. These vectors are perpendicular and mutually perpendicular to the direction of propagation.
B. Generation of circularly polarised light. If the *E*-vectors of two electromagnetic waves are 0.25 λ out of phase, circularly polarised light is generated [adapted from 1].

Beer's Law states that the absorbance of a solution is directly proportional to the concentration of the chromatophores. This law is no longer valid if the chromatophores aggregate or are within one large molecule such as a peptide or a protein. The absorption band of the chromatophore can undergo a blue shift to shorter wavelengths, a red shift to longer wavelengths, split into two bands, increase in intensity (hyperchromism) or decrease in intensity (hypochromism) [6]. These changes can be related to the conformation and interactions of the polymer. The major absorbing units, generally exploited in the spectrophotometry of protein and peptides, are the amide bonds (peptide bonds) and the aromatic side-chain groups of Tyr, Trp and Phe. These chromatophores and their interaction in the protein structure can be analysed by CD and ORD to elucidate the secondary conformation of a solvated protein. ORD and CD curves of model polypeptides with a single conformation were used to construct "standard" curves for α-helical-, β-sheet-, β-turn- and random coil conformation (Fig. 4.4) [1]. It is assumed that no other conformation exists and the percentage of secondary structure is predicted from the "standard" curves [1]. These predictions are fairly accurate, but not exact.

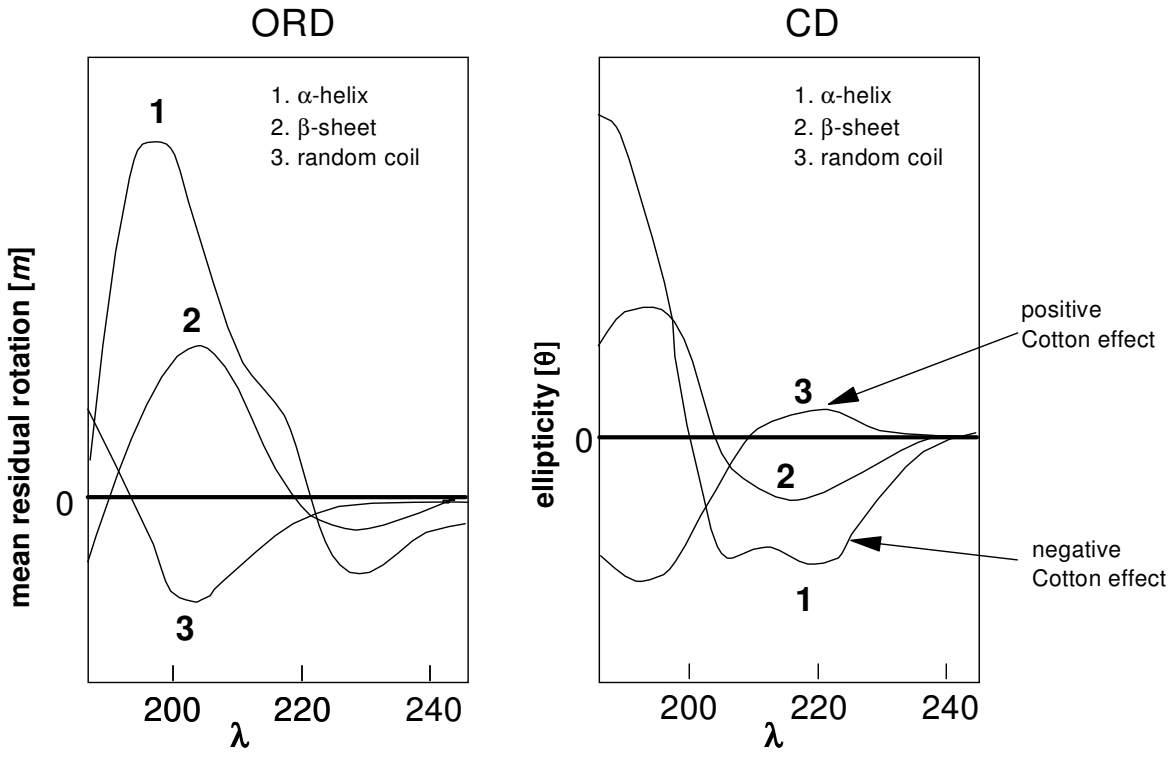

Figure 4.4 A comparison between ORD and CD spectra of a protein [adapted from 1].

The secondary structures of antimicrobial peptides in synthetic membranes (liposomes) such as melittin [7], selected melittin analogues [8], and gramicidin S analogues [9] have been determined with CD. The design and analysis of model membrane active peptides also depended extensively on CD [10]. Only one study by Besson *et al*. [11] on iturin A, using CD, has been reported to date. The CD spectra of iturin A were recorded in tetrahydrofuran (THF) and water and indicated that iturin A conformation in water was vastly different from that in a hydrophobic environment (as simulated with THF). The existence a type II β-turn conformation in THF was again indicated.

Infrared (IR) spectroscopy utilises the absorption of light in the infrared region (10^3-10^5 nm), which causes transitions between vibrational levels of a molecule. IR spectra are consequently generated by the vibrational motions of functional groups, motions such as bond stretching and bond bending. IR absorption spectra are plotted against wave numbers ($1/\lambda$) or frequency (ν). The amide I band, characteristic of the peptide bond, is of enormous value in the study of protein and peptide structure. Its absorption frequency depends on environment of the bond such as in an α-helix ($1/\lambda$ =1650 cm^{-1}), β-sheet ($1/\lambda$ =1632; 1685 cm^{-1}) or random coil ($1/\lambda$ =1658 cm^{-1})[1]. The relative proportion of the amino acids in any of the three conformations can be determined from the intensity of the absorption of the bands. IR-spectroscopy can also be used to investigate hydrogen bonding in a macromolecule. An infrared study of iturin A

confirmed the existence of hydrogen bonded type II β-turns in the peptide ring, with a characteristic amide component band in the range of 1638-1646 cm^{-1} [11]. It was also concluded from the IR study that different solvents induced significant conformational changes in iturin A.

Raman spectroscopy is related to IR-spectroscopy as it also monitors the vibrational motions of atoms. It does, however, not have the disadvantage of the strong interference of water in the IR spectrum that makes the analysis in aqueous solution virtually impossible [1]. The Raman spectrum is generated when the wavelength of a small fraction of the incident monochromatic light increases (frequency decreases) because of vibrational transitions. Raman scattering has a very low probability and therefore produces low line intensity. Highly concentrated samples must be used and this may lead to aggregation, which may complicate the interpretation of the spectra. With improved laser technology and the powerful computerised data analyses this technique is gaining ground in the investigation of macromolecules such as proteins and peptides in membrane environments. For more information refer to [13].

Technological and theoretical advances in macromolecular X-ray crystallography, since the first X-ray photograph of a protein crystal was obtained by Bernal and Crowfoot [12] in 1934, made possible the elucidation of well over 200 protein crystal structures. The structural detail provided by X-ray crystallography allows atomic models to be built for larger molecules than those handled by NMR spectroscopy. In X-ray crystallography a crystal of a molecule is exposed to a collimated beam of monochromatic X-rays and the resultant diffraction pattern is recorded on photographic film. The X-rays, with wavelengths of the same order as covalent bond lengths (∼1.5), are scattered by the electrons that surround atoms. The position and intensities of diffraction maxima (dark spots on the film) allow the construction of an electron density map that is used to form a 3D image of the crystal. For more information refer to [14].

We synthesised diastereomers of iturin A_2 analogues by incorporating an enantiomeric mixture of the β-aminotetradecanoic acid (β-NC_{14}) residue during synthesis (refer to Chapters 2 and 3). The absolute configuration of the β-NC_{14} residue in each of the lipopeptides was determined with chiral liquid chromatography linked to electrospray ionisation mass spectrometry (refer to Chapter 3). The diastereomers differed in HPLC retention, suggesting that their hydrophobicity and therefore structures in solution must be different. The deviation from the constant DLDDLLDL chiral sequence of the iturin A_2 analogues at the chiral centre at the β-carbon of the β-NC_{14} residue consequently has an influence on their physical

properties. This influence of the β-NC_{14} residue and cyclisation on the structures of the four purified octalipopeptides (8-Beta I (D), 8-Beta II (L), cyclic 8-Beta I (L) and cyclic 8-Beta II (D)) was investigated by employing NMR, CD and molecular modelling.

Limited quantities of purified octalipopeptides (cyclic and linear peptides) precluded a full investigation with NMR, but it was possible to do ^{13}C NMR and ^{1}H NMR on a mixture of 8-Beta I (D) and II (L). CD was used for determining the influence of a lipidic environment on the structure of each of the four octalipopeptides. The structures of the octalipopeptides, especially backbone structures, were predicted using a personal computer based molecular modelling program HyperChem®4.5 [15]. The predicted structures were compared with the iturin A structure proposed by Marion *et al*. [5] and with structural data from our NMR and CD studies.

4.2 Materials

The two linear octalipopeptides (8-Beta I (D) and II (L)) and their cyclic analogues (cyclic 8-Beta I (L) and cyclic 8-Beta II (D)) were synthesised using the Fmoc-polyamide peptide synthesis protocol and purified using semi-preparative HPLC (described in Chapter 2).

HEPES (2-[4-(2-hydroxyethyl-1-perazinyl]-ethane sulphonic acid), dimyristoyl-L-α-phosphatidylcholine (DMPC) were from Sigma Chemical Co. (St. Louis, USA). Acetonitrile (HPLC-grade, UV cut-off 190 nm) was from Romil LTD (Cambridge, UK). Chloroform (99%), NaCl and Triton X100 were from Merck (Darmstadt, Germany). Nitrogen gas was supplied by Afrox, South Africa. Analytical grade water was prepared by filtering glass distilled water through a Millipore Milli Q® water purification system.

4.3 Methods

4.3.1 Structural investigation using spectroscopy

4.3.1.1 Nuclear magnetic resonance spectrometry

NMR spectra were recorded at 25±0.1°C with a Varian VXR 300 pulsed FT NMR spectrometer operating at 299.1 MHz and at 75.42 MHz for the observation of ^{1}H and ^{13}C respectively. A diastereomeric mixture of 8-Beta (1 mg) was dissolved in 650 µL 50% CD_3CN in D_2O (neutral pH) as this lipopeptide is soluble in very few solvents. ^{1}H spectra were calibrated by using the residual proton multiplet of CD_3CN at 1.91 ppm as a secondary

reference. ^{13}C spectra were calibrated using the CD_3CN multiplet at 1.28 ppm as secondary reference. To enhance the sensitivity for the protonated carbons, a pulse angle of 60 degrees and a repetition time of 0.41 seconds were used. In the ^{1}H experiments 45 degree pulses were used with a repetition time of 4.1 seconds.

4.3.1.2 Circular dichroism

Stock solutions (5 mg/mL) of the octalipopeptides were prepared in 50% acetonitrile/water. A 20 µL aliquot of these solutions was diluted to 6 mL with 20 mM HEPES containing 150 mM NaCl (pH 7.4) to give a final concentration of 1.5 µM. A second 20 µL aliquot was mixed with 500 µL of a 2.5 mg/mL dimyristoyl-L-α-phosphatidylcholine liposome preparation and then diluted to 6 mL. The peptide to lipid ratio was 1.5:25 in the final preparation. CD spectra were measured, from 260 to 180 nm, with 0.1 nm intervals over 1200 seconds (50 nm/min.) and a 4 second response time in a cuvette with a 20 mm path length in a Jasco 720 spectropolarimeter. The CD spectra of the buffer and buffer-liposome mixture (where appropriate) were subtracted from that of the sample.

4.3.1.3 Preparation of DMPC-vesicles

Small unilamellar vesicles were prepared by dissolving 10 mg dimyristoyl-L-α-phosphatidylcholine (DMPC) in 2 mL chloroform in a detergent-free glass test tube. The chloroform was evaporated either under a stream of N_2 or under vacuum (rotary evaporator) to leave a thin film of lipid on the glass. The lipid was resuspended in 4 mL 20 mM HEPES, pH 7.4 containing 150 mM NaCl, and flushed with N_2. The lipid-buffer mixture was sonicated (2 mL per tube) in a sonic bath, half filled with 0.1% (v/v) Triton X100, until the solution was translucent. Because the transition temperature of DMPC is 24°C, liposomes were prepared at 35-37°C. The duration of sonication was 60±10 minutes. (Refer to Chapter 6 for more detail.)

4.3.2 Molecular modelling using HyperChem ®4.5

In vacuo structure modelling of the octalipopeptide structures was done with the HyperChem®4.5 from HyperCube® [15]. Structural geometry was optimised with the Polak-Ribiere (conjugate gradient) general algorithm for molecular mechanics with non-varying dielectric constant and convergence limits of the RMS[a] gradient for the molecular system set

[a] The RMS gradient is the rate of change (first derivative) of energy of a molecular system as a function of atomic positions. A gradient of zero indicates a conformation with minimum energy (a local of global minimum or a

as 0.0001 kcal/ mole. The method used for chemical calculations, also known as a molecular mechanics force field, was AMBER 90[b].

Geometric optimisation started with the model build function of HyperChem®4.5. The β-NC_{14} residue was substituted with a β-NC_5 residue (indicated with a star *) to simplify the structure modelling experiments. No constraints were placed on the structure, but structures that did not settle into a stable backbone conformation were rejected if the molecular orbital energy did not decrease in subsequent experiments. Optimised structures were further refined by geometry optimisation after a molecular dynamic experiment performed over 0.3 ps with starting temperature of 100 K and final temperature 300, 400 or 500 K. If the three molecular dynamic experiments, followed by geometry optimisation, gave identical energy minima and similar structures, it was accepted that a local or global minimum had been reached. These low energy structures were also tested with other molecular mechanics force fields such as BIO+ and OPLS (both developed for proteins) followed by a geometry optimisation with AMBER 90. These structures were accepted to be "final" after again being subjected to molecular dynamic experiments as described above, their backbone conformation remained the same.

4.4 Results and discussion

4.4.1 Structural investigation using spectroscopy

4.4.1.1 Nuclear magnetic resonance spectroscopy

^{13}C and ^{1}H NMR of the diastereomeric mixture of 8-Beta was originally done to assess the purity of one of the 8-Beta synthesis products after HPLC purification. NMR confirmed the purity, but at the same time revealed interesting aspects concerning the conformation of 8-Beta in that the spectra revealed "two" tyrosine chemical shift patterns (Table 4.1). This preparation contained only the diastereomeric mixture of 8-Beta as confirmed with HPLC, amino acid analysis, HPLC and ESI-MS (refer to Chapters 2 and 3). Assignments of ^{13}C NMR chemical shift values (δ) observed for 8-Beta correlated well with amino acid δ-values in

---

transition state). The absolute quantity of the calculated molecular orbital energy has no physical implication, except as an indicator of progress in optimisation during modelling experiments.

[b] AMBER 90 force field was developed specifically for proteins and nucleic acids and provide representation for individual atoms and united atoms (groups).

literature (Table 4.1) [16]. The shaded column in Table 4.1 shows the assignments for D-Tyr_3, with δ of the β-carbon as 37.52 and 37.40 and that of C^5/C^9 as 131.34 as 131.30. The δ-value assignment of the α- and β-carbons of the Asn residues also revealed four chemical shift values, instead of the expected three (Table 4.1).

The observation of two separate sets of signals (characteristic for a para-disubstituted aromatic ring and assigned to the aromatic protons of tyrosine) in the aromatic region of the ^{1}H spectrum suggested a slow conversion between two conformations of the peptide. In each conformation the tyrosine aromatic protons experience a different chemical environment, giving rise to two sets of chemical shifts (Fig 4.5). Harnois *et al*. [17] observed, using time-resolved fluorescence of the Tyr residue of iturin A, that a slow exchange between two Tyr-rotamers (χ^1 = -60° and +180°) takes place in water. This may also happen to the Tyr-residue in 8-Beta. This structural aspect will be addressed using molecular modelling later in this chapter.

Table 4.1 ^{13}C chemical shift (δ) assignment of the amino acid carbons in the 8-Beta preparation as analysed in 50% acetonitrile (T=25±0.1°C) compared to that of literature values [16] (the latter is shown in brackets).

	L-Asn_2 D-Asn_4 D-Asn_7	**D-Tyr_3**	**L-Gln_5**	**L-Pro_6**	**L-Ser_8**	**β-NC_{14}**
C^{α}	51.72, 51.46 51.15, 51.07 (52.4)	56.25 (57.3)	56.25 (55.4)	63.39 (62.4)	56.25 (56.4, 57.4)	49.7
C^{β}	37.24, 37.15, 37.05, 36.54 (35.7)	37.52; 37.40 (37.5)	27.13 (27.4)	31.49 (30.3)	63.08 (62.3, 61.3)	not detected
C^{γ}	–	not detected (138)	33.02 (32.1)	25.62 (25.0)	–	30.09, 29.87, 29.82, 29.70 ($C^{4\text{-}11}$)
C^{n}	–	131.34; 131.30 (C^5, C^9,130.5) 116.26; (C^6, C^8 117.5) 156.44 (C^7, 156.3)	–	48.75 (C^5, 47.4)	–	32.39 (C^{12}) 23.18 (C^{13}) 14.34 (C^{14})

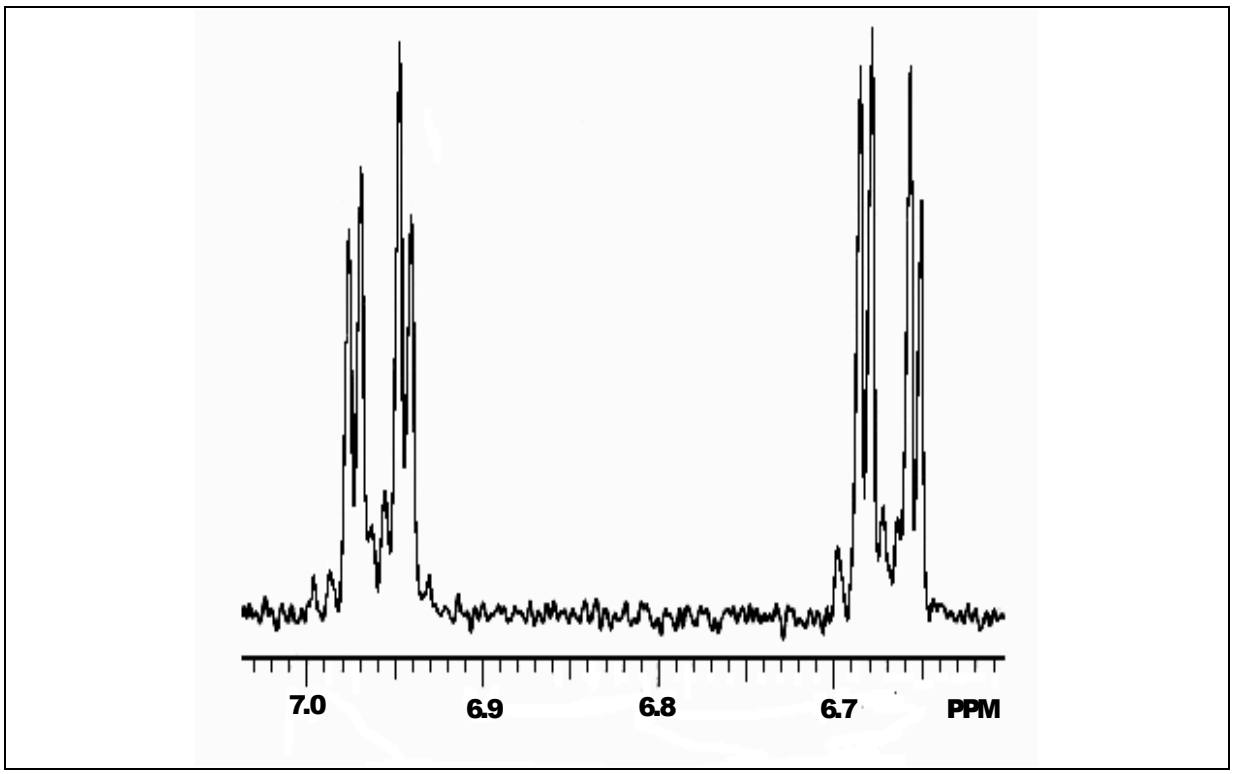

Figure 4.5 ^{1}H-NMR spectrum in the region of 6.6 to 7.4 ppm of the Tyr residue in 8-Beta at 299.1 MHz in 50 % CD_2CN in D_2O (neutral pH) at 25±0.1°C.

4.4.1.2 Circular Dichroism

Results obtained in another study (reported in Chapter 6) confirmed the association of the linear octalipopeptides with DMPC; DMPC liposomes formed a hydrophobic environment suitable for CD spectrometry experiments. The octalipopeptides in this study have the characteristic iturin LDDLLDL chiral sequence for the α-amino acid residues. The CD spectra of peptides containing D and L amino acids have not been as well studied as those of polypeptides and proteins containing just L-amino acids [18]. Nevertheless, it was possible to deduce some structural information from spectra of these peptides in buffer and in DMPC liposomes. One important result was that the CD spectra of the octalipopeptides in water and in liposomes were significantly different, indicating that solvent-induced conformational changes of each of the octalipopeptides do occur (Figs. 4.6, 4.7). Each of the four lipopeptides showed a negative mean ellipticity in the region between 199 and 201 nm, which is reminiscent of a random coil in protein samples in water [6, 18]. A similar result was obtained by Besson *et al*. [11] for iturin A in water with the negative Cotton effect centred around 198 nm. The principal Cotton effect for peptides and proteins occurs around 200 nm, the wavelength range in which the peptide bond absorbs [1].

The spectra of the linear 8-Beta diastereomers in buffer differed to a large extent (Fig. 4.6). 8-Beta I (D) showed a positive Cotton effect centred around 203 nm, whereas 8-Beta II (L) showed a negative Cotton effect at 201 nm indicating different backbone conformations. Association with liposomes induced in both the structures of 8-Beta I (D) and II (L) a conformation that gave a strong positive Cotton effect centred round 201 nm (Fig. 4.6). The spectra of the 8-Beta diastereomers in liposomes were remarkably similar, except for a small difference in the region centred around 190 nm, but both displayed an overall negative ellipticity in this region. Small negative effects at 216 nm and 226 nm were also observed for these diastereomers. The CD spectra of 8-Beta diastereomers in liposomes resembled that of the tetrapeptide, VPGG, which contains a type II β-turn. This peptide displayed negative Cotton effects at both 216 nm and 190 nm and a strong positive Cotton effect at 203 nm [6].

The cyclic lipopeptide pair displayed similar spectra in buffer (Fig. 4.7), except in the region of 203 nm and 207 nm, where cyclic 8-Beta II (D) showed a positive and negative Cotton effect respectively. The 203 nm maxima could be because of to a small amount of linear 8-Beta I (D) contamination in the cyclic 8-Beta II (D) preparation. A conformation leading to strong positive Cotton effects centred around 197 nm and 207 nm and a strong negative effect centred around 205 nm was introduced in the peptide structures of both cyclic 8-Beta I (L) and II (D) in liposomes (Fig 4.8). The ellipticity of cyclic 8-Beta II (D) at 207 nm was not as high as that of its diastereomer. A minimum at 209 nm was also observed for cyclic 8-Beta II (D). Spectra of both peptides in liposomes had a shoulder between 210 and 215 nm. The cyclic 8-Beta spectra resembled to some extent the type II β-turn spectrum of cyclo-$(VPGVG)_2$ with a positive ellipticity centred around 205 nm [6]. The spectra of another β-turn peptide, cyclo(D-Phe-L-Pro-ω-aminocaproyl) [19], showed a strong negative minimum at 206 nm and a shoulder at 213 nm. Further resemblance was observed to the spectra of poly L-Ser. This peptide has an antiparallel β-pleated sheet conformation and displayed negative Cotton effects at 214 nm and 222 nm and a strong positive Cotton effect at 197 nm [6].

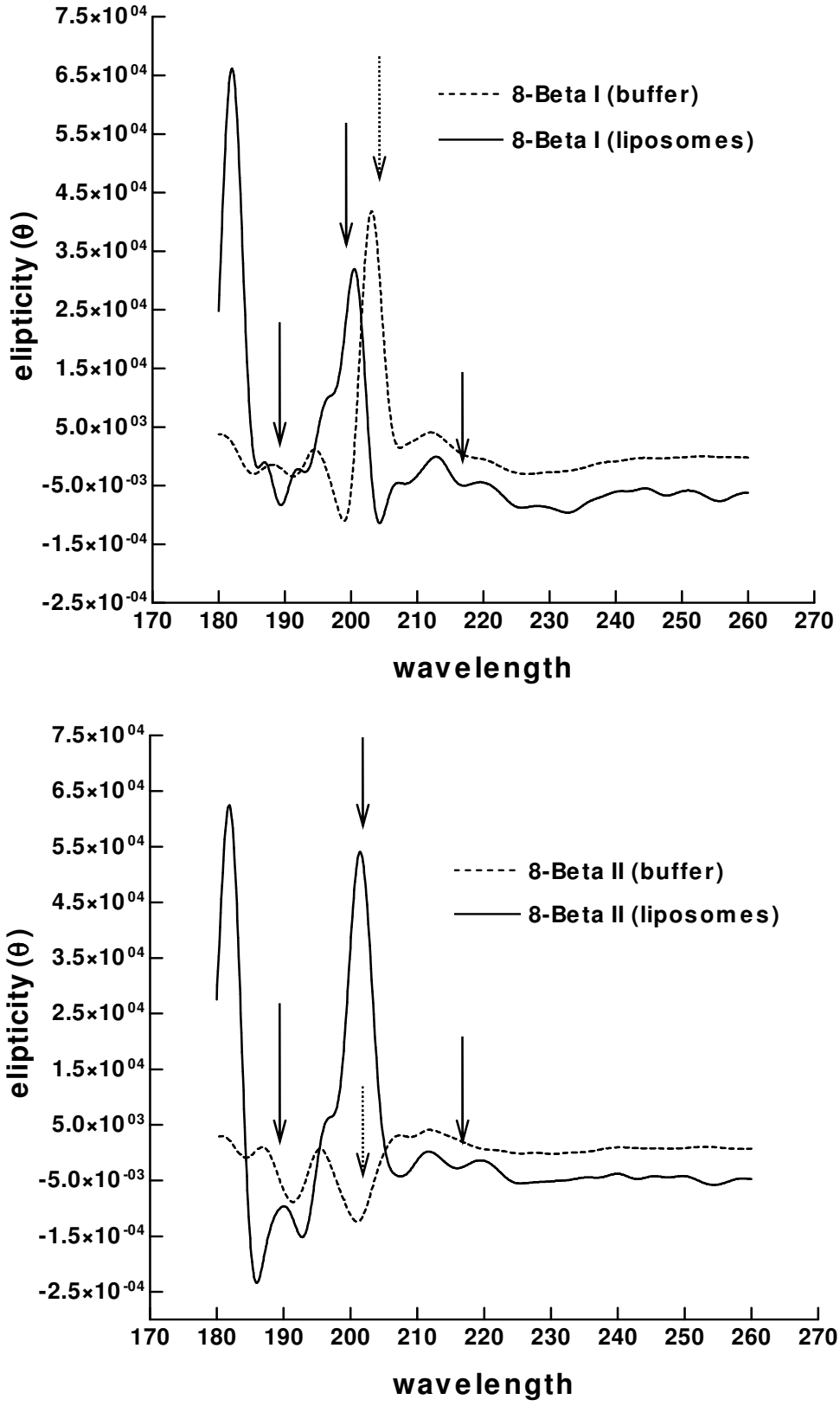

Figure 4.6 Circular dichroism spectra of the linear octalipopeptides, 8-Beta I (D) and 8-Beta II (L), in 20 mM HEPES buffer (pH 7.4) containing 0.15 M NaCl incubated with or without DMPC-liposomes. The arrows indicate the significant Cotton effects observed for the peptides in liposomes (solid line) and buffer (dashed line).

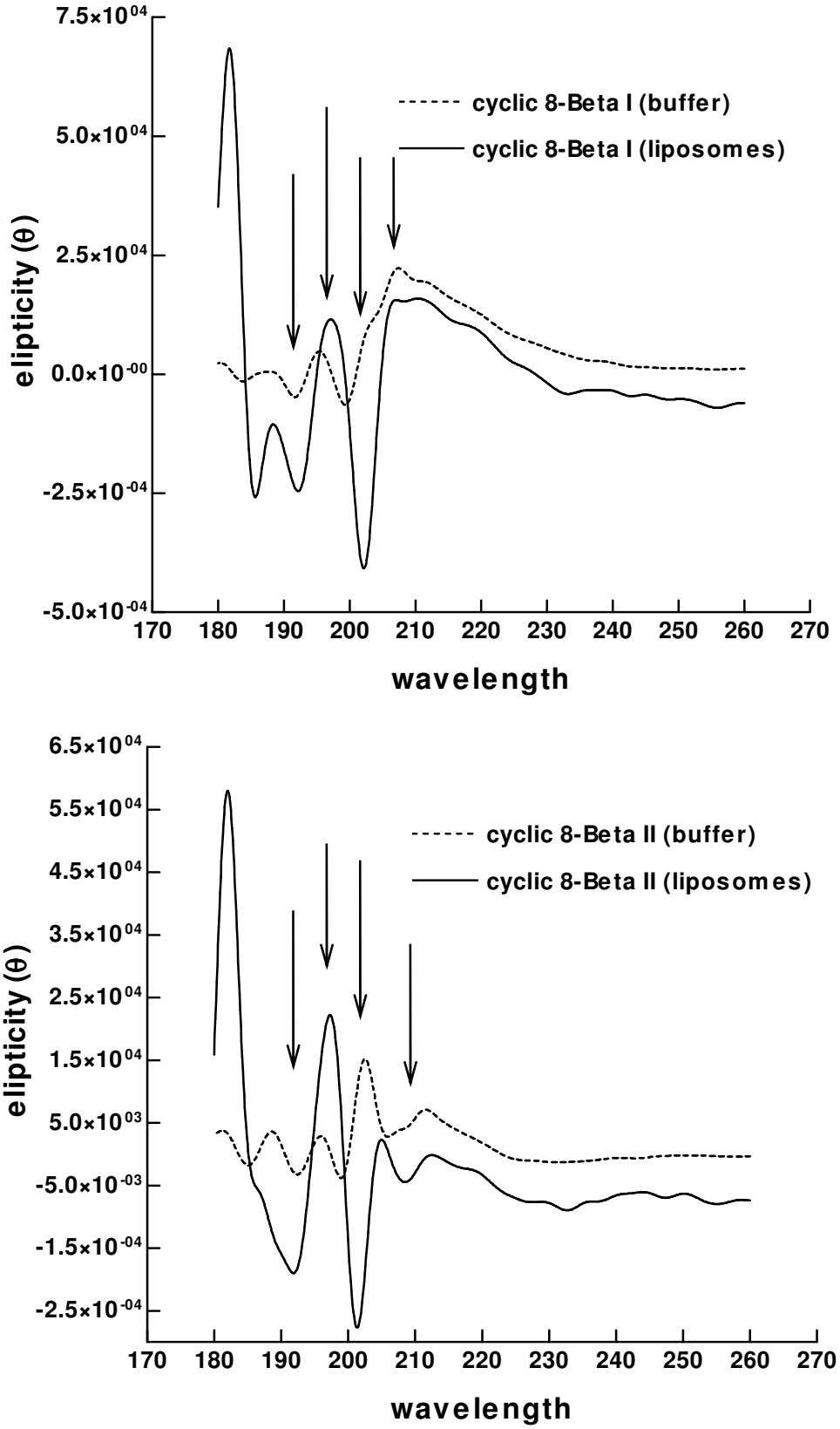

Figure 4.7 Circular dichroism spectra of the cyclic octalipopeptides, cyclic 8-Beta I (L) and II (D), in 20 mM HEPES buffer (pH 7.4) containing 0.15 M NaCl incubated with or without DMPC-liposomes. The arrows indicate the significant Cotton effects observed for the peptides in liposomes (solid line) and buffer (dashed line).

Besson *et al*. [11] found that the average CD spectrum of iturin A in tetrahydrofuran (THF) displayed positive mean ellipticity values at 190 and 210 and a negative value at 200 nm. The disagreement between these ellipticities and those of our cyclic peptides can be attributed to the differences between THF and hydrophobic membrane environment in which the two experiments were done. There was, however, a general correlation between the two spectra of the cyclic 8-Beta pair and that of iturin A. According to Besson *et al.* [11], their spectra showed similarities with that of a β-turn peptide in the region between 195 to 230 nm [20]; it is therefore possible that the cyclic 8-Beta diastereomers also contain such a turn (as discussed in above).

The spectra of the cyclic peptides in liposomes differed significantly from spectra of the linear peptides in liposomes in the 190 to 210 nm region, suggesting different backbone conformations. These differences could explain the limited bioactivity observed for the linear peptides (reported in Chapter 6). As for the linear peptides, the spectra of the cyclic 8-Beta pair in liposomes were similar, except for a small difference in the region centred around 190 nm, with cyclic 8-Beta I (L) showing a positive Cotton effect and cyclic 8-Beta II (D) a negative effect (Fig. 4.7). The relationship between the configuration of the β-NC_{14} and this observation could be of some significance. The difference in the peptide structures, observed with NMR and CD, was further investigated empirically with structure modelling.

4.4.2 Structure modelling using HyperChem®4.5

The structure modelling of the four octalipopeptides, using HyperChem®4.5 [15], suggested a probable turn conformation in each of the two tetrapeptide sequences, β-NC_5NYN and QPNS (Figs. 4.8-4.12). The predicted models therefore indicated a tendency to adopt conformations with two turns in the backbone structure.

Two types of stable backbone conformations for the linear octalipopeptides, 8-Beta*L and 8-Beta*D, called the W-structure (distorted W) and S-structure (twisted S), evolved from the soup of structures with molecular orbital energy raging between 285 and 292 kcal/ mole (Fig. 4.8). The S-type of backbone conformation was the only one observed in structure modelling including the C_{11} aliphatic chain, but it complicated the optimisation process to such an extent that it was substituted with C_2 aliphatic group (β-NC_{14} substituted with a β-NC_5). The modelled backbone conformations of the linear lipopeptide diastereomers were similar in both the S-structure (Fig. 4.9) and W-structure (Fig. 4.10). Differences were confined to the

β-carbon of β-NC_5 and backbone of the β-NC_5-L-Asn_2 dipeptide moiety. As described in section 4.4.1.2, the CD spectra of the 8-Beta diastereomers in buffer did show a large difference. The predicted conformations *in vacuo* showed no such difference, but suggested the possibility of two extreme conformations. An S ⑦ W equilibrium could be possible with hinging at D-Asn_4-L-Gln_5. The equilibrium distribution between the two forms could also be strongly influenced the longer aliphatic chain through steric interference, but this was not investigated. The predominance of different structures in each of the 8-Beta diastereomer preparations could explain the differences in CD spectra found for these diastereomers in water. NMR revealed a difference in the chemical shift patterns of the Tyr-residue in 8-Beta (refer to Table 4.1 and Fig. 4.5), which could also be explained by the slow conversion between two conformations such as the W- and S-structures.

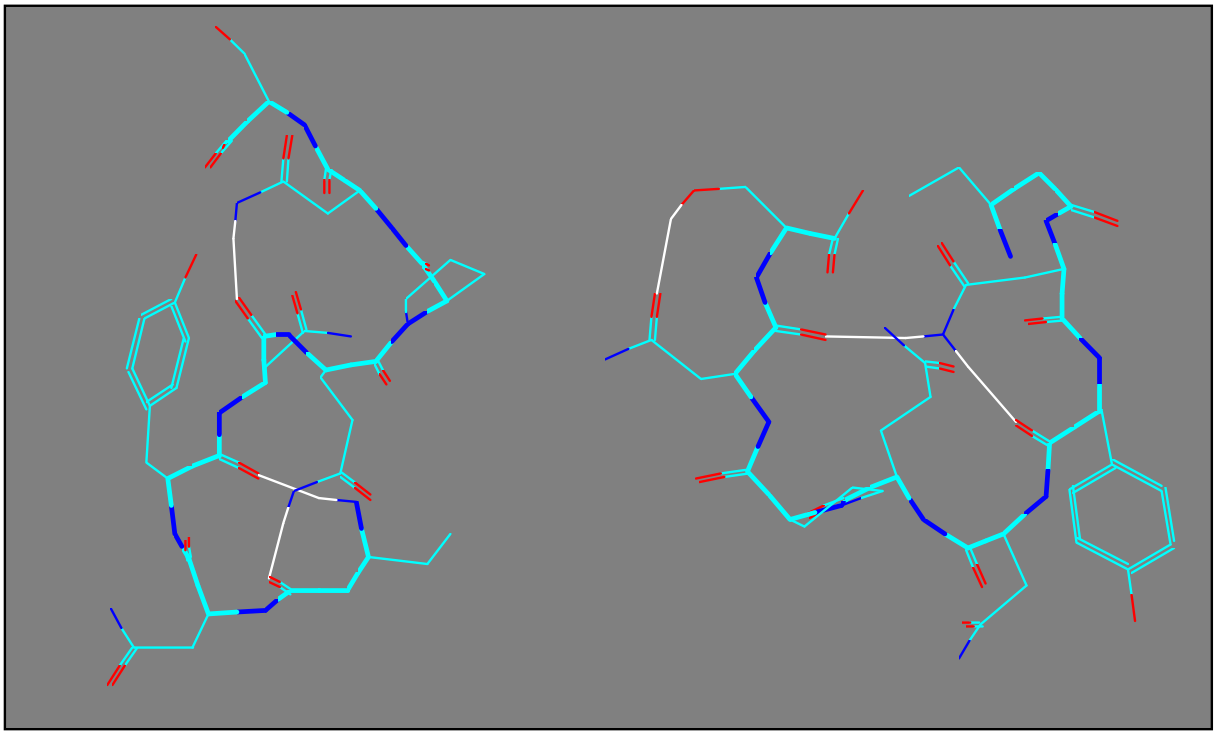

Figure 4.8 Representative low energy stick structures of 8-Beta*D, as modelled with HyperChem®4.5 [15] showing the two typical backbone conformations, the S-structure (left) and W-structure (right). (The white lines depict the hydrogen bonds, dark blue the amino groups and the red the oxygen containing groups.)

8-Beta*D
(-300.575 kcal / mole;
gradient 0.000009)

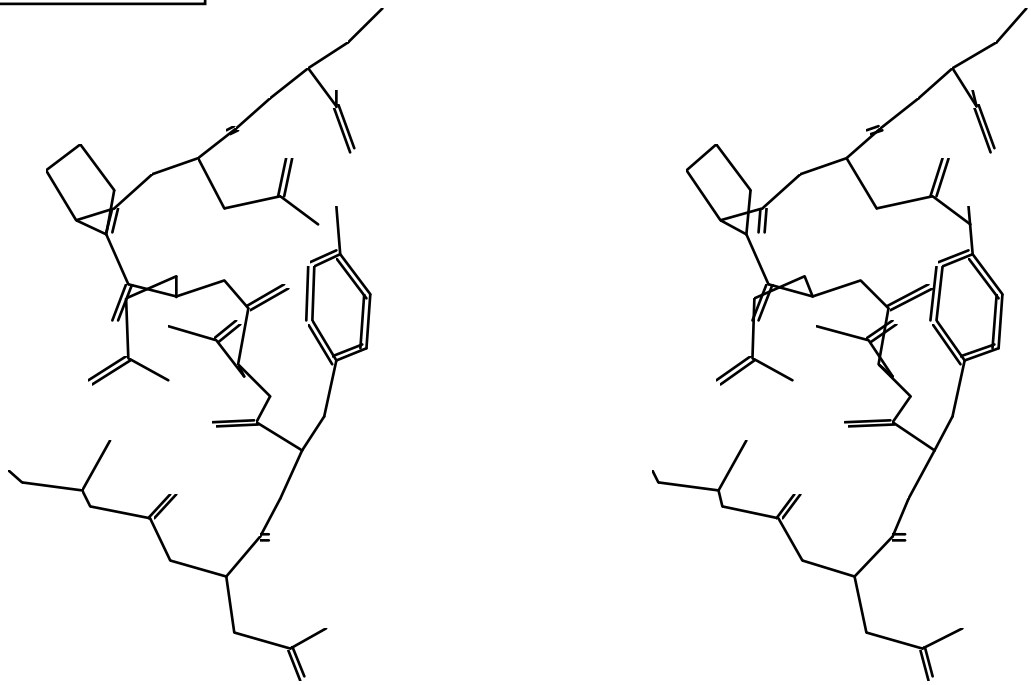

8-Beta*L
(-298.853 kcal / mole;
gradient 0.00001)

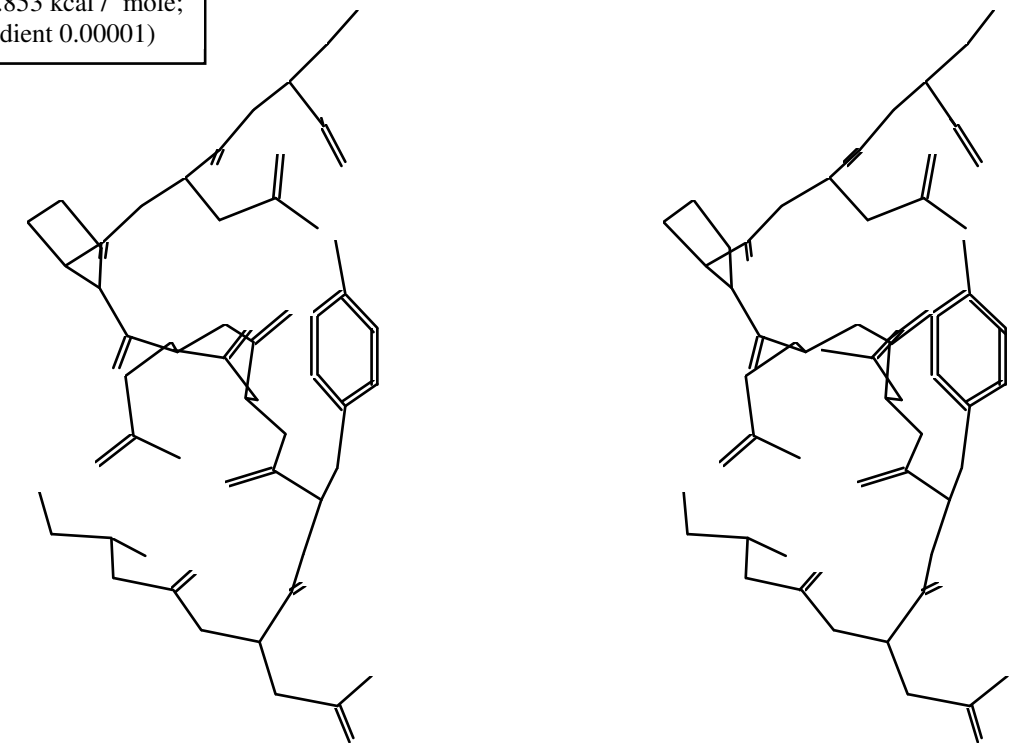

Figure 4.9 Stereotypgraphs of the "S" low energy stick structures of the two linear octalipopeptides, 8-Beta*L and 8-Beta*D as modelled with HyperChem®4.5 [15]. The minimum energy and convergence gradient of each structure are given in brackets.

8-Beta*D
(-296.492 kcal / mole;
gradient 0.000009)

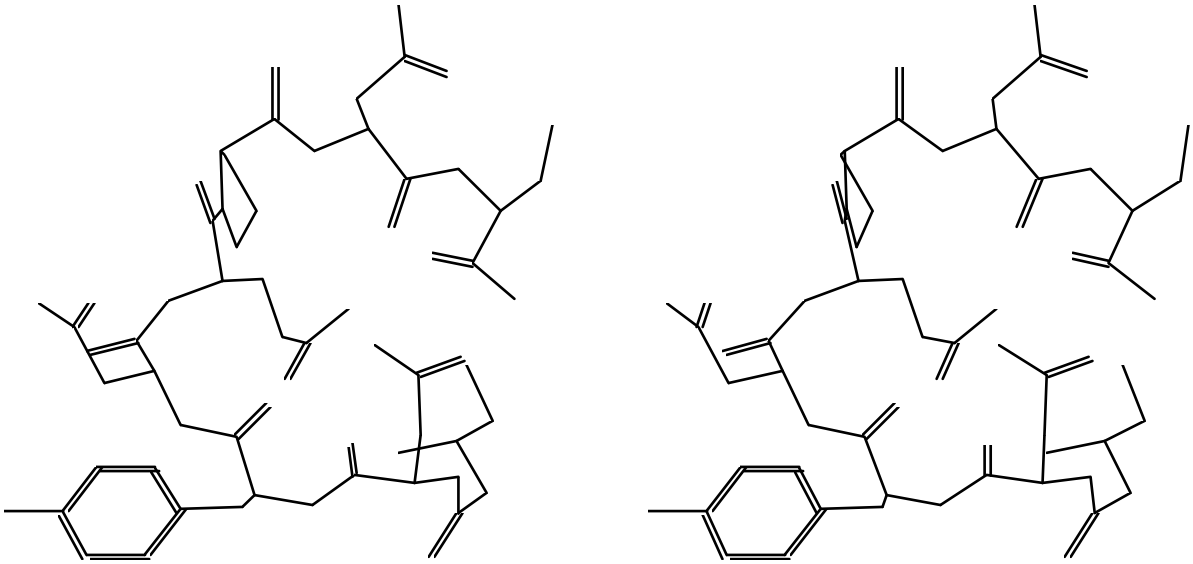

8-Beta*L
(-295.340 kcal / mole;
gradient 0.0001)

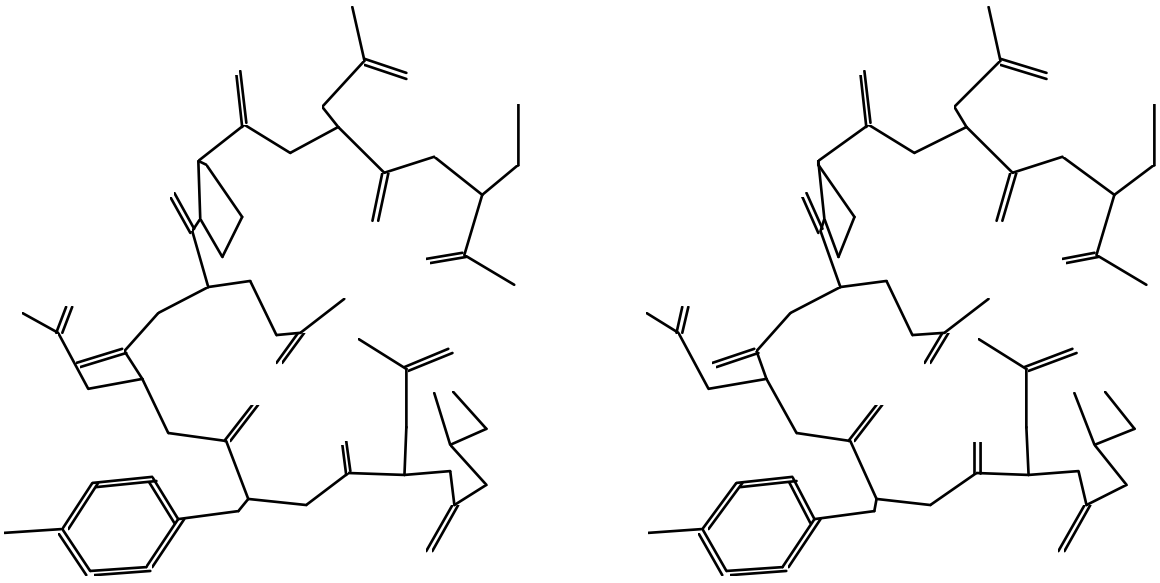

Figure 4.10 Stereotypgraphs of the "W" low energy stick structures of the two linear octalipopeptides, 8-Beta*L and 8-Beta*D as modelled with HyperChem®4.5 [15]. The minimum energy and convergence gradient of each structure are given in brackets.

In the S-structure there are two turns, β-NC$_5$NYN and QPNS, that approximate true β-turns. The correct hydrogen bond pattern, however, was not demonstrated. Hydrogen bonding in the S-structure occurs between the β-amino group of the β-NC$_5$ residue and the D-Tyr$_3$ carbonyl oxygen, and also between some of the side-chains (Fig. 4.9). The six polar side-chain groups, namely the four acid amides of the Asn residues and Gln and the two hydroxide groups of Ser and Tyr, can all participate in a hydrogen-bond network stabilising the peptide structure. Many of these groups participated in hydrogen bonding in the observed low energy structures of 8-Beta*. Freedom of movement of the amino acid side-chains was observed except for the side-chain of D-Tyr$_3$ and the naturally rigid pyrrolidine ring of L-Pro$_6$ in all the 8-Beta* structures.

The conformation of the modelled backbones of the cyclic octalipopeptides appears to be rather rigid, with the side-chains having a larger degree of freedom (Figs. 4.11, 4.12). This rigid backbone structure was found regardless of the conformation and carbon length of β-amino acyl residue (β-NC$_{14}$, β-NC$_7$ or β-NC$_5$). Backbone rigidity of the iturin A structure was also reported by Marion *et al.* [5]. The backbone NH-C$^{\alpha}$H bonds were also, as in their structure, in a trans conformation including a trans conformation for L-Pro$_5$.

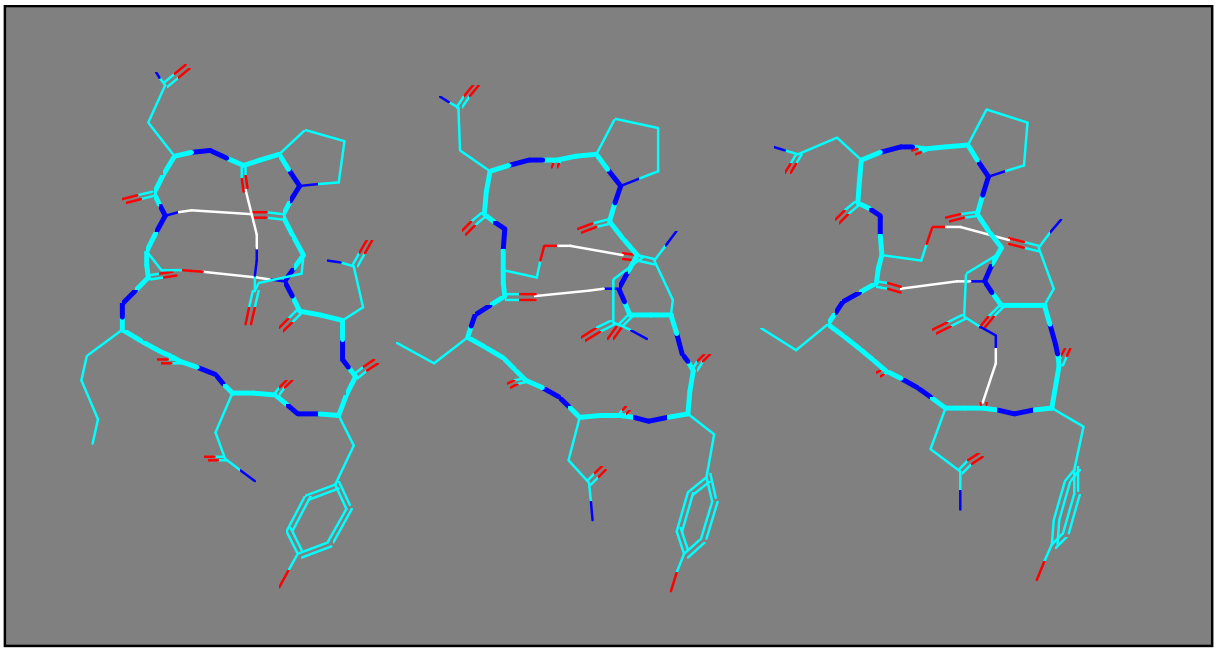

Figure 4.11 Representative low energy stick structures of cyclic 8-Beta*D, as modelled with HyperChem®4.5 [15] showing the typical backbone conformations. The left hand structure was obtained by substituting the β-D-NC$_{14}$ with a β-D-NC$_7$ residue. (The white lines depict the hydrogen bonds, dark blue the amino groups and the red the oxygen containing groups.)

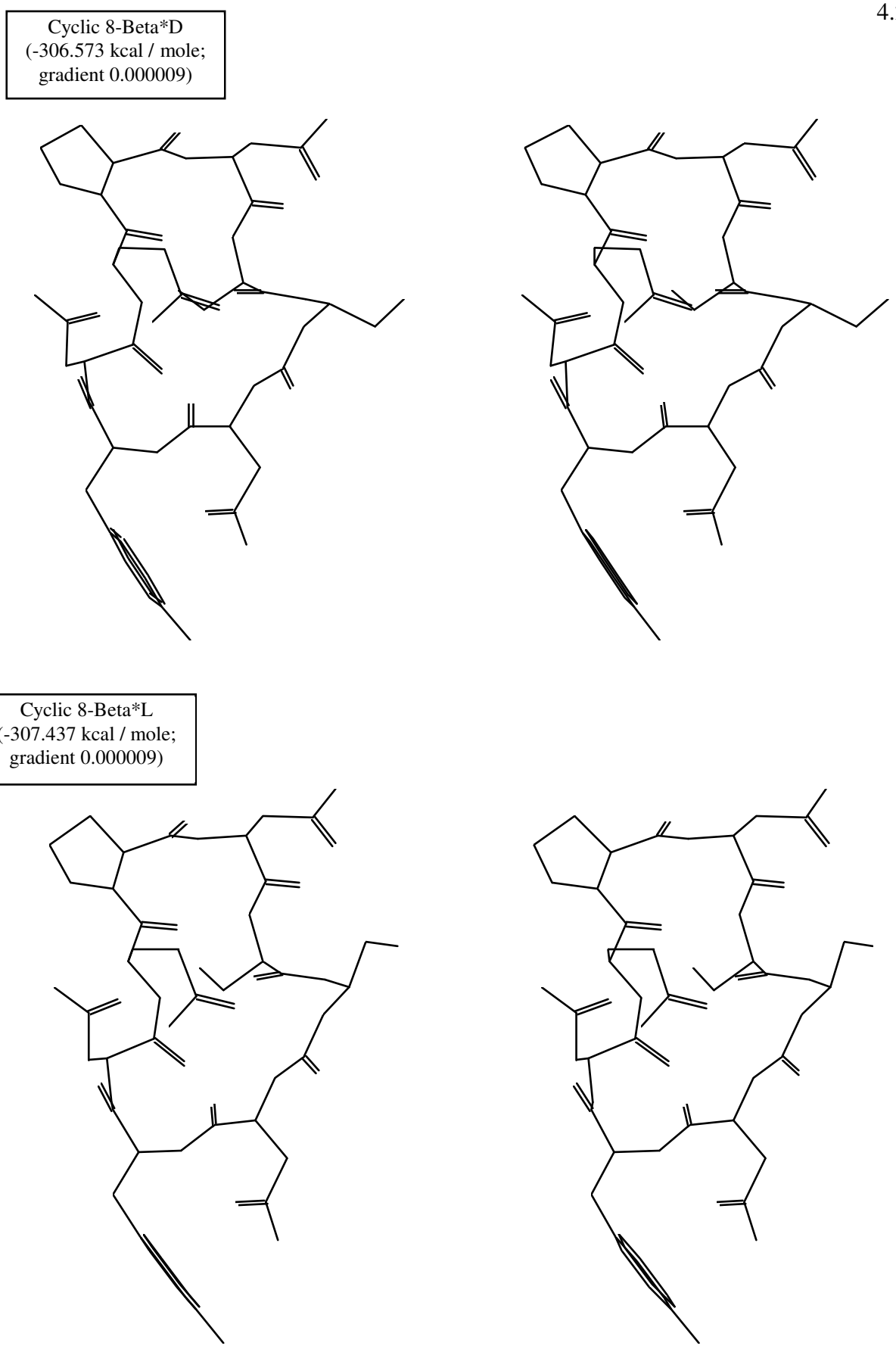

Figure 4.12 Stereotypgraphs of low energy ball-and-stick structures of the two different cyclic octalipopeptides cyclic 8-Beta L and D as modelled with HyperChem®4.5 [15]. The calculated minimum energy and convergence gradient of each structure are given in brackets.

Three turns were observed in the modelled structures: turn A in β-NC_5NYN, turn B in QPNS and turn C in NYNQ (Fig. 4.12). These turn conformations resembled the two type II β-turns and the type I' or II'-turn observed from NMR and modelling data of iturin A [5], but the predicted pattern hydrogen bonding was not correct. The side-chains protruded from the peptide ring cavity, similar to the iturin A structure [5], except for the side-chains of L-Ser_8 and L-Gln_5. Marion *et al.* [5] found that the L-Gln_5 side-chain is stabilised by a hydrogen bond between the side-chain amino group and amide carbonyl group of D-Tyr_3. In our models we, however, found that the Gln_4 side-chain amino group is hydrogen bonded with the amide carbonyl group of D-Asn_2 (refer to Figs. 4.11 and 4.12). A slight difference was observed between the relative positions of the tyrosine ring in the optimised structures of the cyclic octalipopeptide structures (Fig. 4.11). From the work of Marion *et al*. [5] it was deduced that the 60^o rotamer of the tyrosine ring is the optimum conformation in iturin A. The side-chain of Tyr in the cyclic peptide models also tended to settle into a similar position (χ_1= 49.3-52.3^o). Very little information on the three Asn side-chains is available except that those of L-Asn_2 and D-Asn_7 (and also L-Ser_8), flip-flop between extreme conformations stabilised by hydrogen bonding to the backbone [5]. The modelled structures contained a hydrogen bond between the side-chains of L-Ser_8 and D-Asn_4 and backbone hydrogen bonding between L-Ser_8 carbonyl, amino or hydroxyl group and L-Gln_5 peptide bond. The D-Asn_7 flip-flop was also observed between different models (Fig 4. 11).

The W-structure of the linear octalipopeptide somewhat resembles that of the cyclic 8-Beta* in that the L-Gln_5 side-chain and L-Asn_2 (participating in hydrogen bonds) are located in the peptide cavity with the other amino acid side-chains protruding from the peptide ring. The two turns, turn A (β-NC_5NYN) and turn B (QPNS) in the S-structure, also resemble the turns found in the cyclic structure. There is, however, a marked difference between the predicted cyclic and linear structures, but limited differences between the peptide diastereomers. These results substantiated the results obtained with NMR and CD.

4.5 Conclusions

NMR spectra of the diastereomeric mixture of 8-Beta confirmed the chemical integrity of the peptide preparation (synthesis discussed in Chapter 2). NMR results also suggested a slow conversion between two conformations in which the Tyr-residue side-chain and possibly one or more of the Asn residues are influenced. The existence of two backbone conformations was also predicted by structure modelling. CD spectra also revealed a difference between the 8-

Beta diastereomers in buffer. The CD spectra of the 8-Beta pair did not differ much in liposomes, thus a single backbone conformation, possibly a β-type II turn(s), exists if these peptides are associated with a hydrophobic environment. This backbone conformation is, however, different from that of the cyclic 8-Beta pair and iturin A [5, 11]. An induction of a secondary structure in liposomes, similar to that observed for iturin A in THF, from a possible random aqueous conformation, was observed for the cyclic 8-Beta diastereomers. This conformation of the cyclic peptides in the lipid membrane may be important in the biological activity of the peptide. There is also some resemblance between the CD spectra obtained for an antiparallel β-pleated sheet of poly L-Ser [6] and that of the cyclic 8-Beta pair. This could be an indication of ordering of the peptide aggregates, stacked to form β-sheets, in the membranes. Aggregation in the membrane is thought to be part of iturin A's mechanism of action [21].

The low energy peptide structures of the cyclic octalipopeptide (Fig. 4.8), predicted by HyperChem®4.5, corresponded to some extent to structures obtained from the NMR studies of iturin A in pyridine [5]. However, the two predicted backbone structures of linear peptide, namely the W- and S-structure, differed markedly from that of the cyclic octalipopeptides (and iturin A) and substantiated the results obtained with CD and NMR. The predicted linear octalipopeptide structure of particular interest is the so-called S-structure. Because it is difficult to relate empirically derived *in vacuo* structures with structures that exist in an aqueous environment, we can only ask whether it is possible that the so-called S-structure, with its two turns, predominates in the 8-Beta I (D) diastereomer leading to the strong positive Cotton effect observed at 203 nm. The S-structure of 8-Beta* also does not contain the "hydrophobic hub", formed by the β-NC_{14} residue and D-Tyr_3 side-chain in the cyclic iturin A molecule. If the S-structure does exist, this absence of the hydrophobic hub may help to explain the low bioactivity of the linear octalipopeptides (refer to Chapter 6). The low yields obtained during cyclisation could also be explained if the S-structure is the predominant conformation, as the W-structure would probably cyclise easier (refer to Chapter 2). The probability of β-turns in the S-structure and the position of the L-Gln_4 side-chain are also of important for the ESI-MS study of the association of this octalipopeptide with alkali metal ions (discussed in Chapter 5).

4.6 References

1. Freifelder D. (1982) Physical Biochemistry: Applications to biochemistry and molecular biology Second Edition, W. H. Freeman and Company, New York, pp. 573-652

2. Wüthrich K. (1976) NMR in biological research: Peptides and proteins, North-Holland Publishing Company, Amsterdam

3. Roberts J. K. M., Jardetzky O. (1985) Nuclear magnetic resonance spectroscopy in biochemistry, In: Modern physical methods in biochemistry, Part A (Eds. Neuberger A., Van Deenen L. L. M.) Elsevier, Amsterdam, pp. 1-68

4. Garbay-Jaureguiberry C., Roques B. P., Delcambe L., Peypoux F., Michel G. (1978) *FEBS Lett*. **93**, 151-156

5. Marion D., Genest, M., Caille A., Peypoux F., Michel G., Ptak, M. (1986) *Biopolymers* **25**, 153-170

6. Urry D. W. (1985) Absorption, circular dichroism and optical rotary dispersion of polypeptides, proteins, prosthetic groups and biomembranes, In: Modern physical methods in biochemistry, Part A (Eds. Neuberger A., Van Deenen L. L. M.) Elsevier, Amsterdam, pp. 275-346

7. Inagaki F., Shimada I., Kawaguchi K., Terasawa I., Ikura T., Go N. (1989) *Biochemistry* **18**, 55985-5991

8. Pérez-Pay E., Houghten R. A., Blondelle S. E. (1994) *Biochem. J*. **229**, 587-591

9. Ando S., Nishikawa H., Takiguchi H., Lee S., Sugihara G. (1993) *Biochim. Biophys. Acta* **1147**, 42-49

10. Mishra V. K., Palgunachari M. N. (1996) *Biochemistry* **35**, 11210-11220;
Dathe M., Schümann M., Wieprecht T., Winkler A., Beyermann M., Krause E., Matsuzaki K., Murase O., Bienert M. (1996) *Biochemistry* **35**, 12612-12622;
Kiyota T., Lee S., Sugihara G. (1996) *Biochemistry* **35**, 13196-13204

11. Besson F., Raimbault C., Hourdou M. L., Buchet R. (1996) *Spectrochimica Acta Part A* **52**, 793-803

12. Bernal J. D., Crowfoot D. C. (1934) *Nature* **133**, 794

13. Carey P. R. (1985) Raman and resonance Raman spectroscopy, In: Modern physical methods in biochemistry, Part B (Eds. Neuberger A., Van Deenen L. L. M.) Elsevier, Amsterdam, pp. 27-64

14. Johnson L. (1985) Protein chrystallography, In: Modern physical methods in biochemistry, Part A (Eds. Neuberger A., Van Deenen L. L. M.) Elsevier, Amsterdam, pp. 347-415

15. Hyperchem WWW site: http\\www.hyper.com

16. Kalinowski H.-O., Berger S., Braun S. (1988) Carbon-13 NMR Spectroscopy, John Wiley & Sons, Chichester, pp. 227-230

17. Harnois I., Genest D., Ptak M. (1988) *Biopolymers* **27**, 1403-1413

18. Wallace B.A. (1986) *Biophys. J.* **49**, 295-306

19. Lee S., Mizuno H., Nakamura H., Kodera Y., Kato T., Go N., Izumiya N. (1984) *FEBS Lett*. **174**, 310-313

20. Johnson W.C. (1990) *Proteins, Structure, Function and Genetics* **7**, 205-214

21. Maget-Dana R., Peypoux F. (1994) *Toxicology*, **87**, 151-174

Chapter 5

An electrospray ionisation mass spectrometry study of the interaction between iturin A_2 analogues and alkali metals

5.1 Introduction

Some of the interactions between metal ions and biomolecules are essential for life processes. Metal ions, such as Mg^{2+} in nucleotide complexes, have an important structural function whereas Zn^{2+} participates in the catalytic mechanism of many enzymes, for example carboxypeptidase A. As secondary messenger in cells, Ca^{2+} interacts with several proteins, whereas the redox pair Fe^{2+}/Fe^{3+} is utilised in electron transfer. The alkali metal ions, Na^+ and K^+, are very important in the osmoregulation of cells, in which Na^+/K^+-ATP-ases play a major role. Any disruption of essential ion-biomolecule interactions or new "foreign" interactions will thus have an influence on the functioning of the cell as a live unit. This has been exploited in the development of some antibiotics such as chloroquin and analogues that interrupt iron detoxification of the malarial parasite. Ionophores, such as the cyclic antibiotic dodecapeptide, valinomycin, disrupt the osmotic balance by specifically complexing with K^+ and transporting it over the cell membrane [1]. The single ion is coordinated by six carbonyl oxygens in the interior of the cyclic peptide. Valinomycin is a perfect example of a biological counterpart of the crown ethers. Crown ethers are known to complex alkali metal ions in their cyclic cavity with oxygens as the chelating atoms [2]. Gramicidin S, a cyclic decapeptide with a β-pleated sheet conformation [3] and one cyclic octalipopeptide in this study, iturin A_2, both contain two type II' β-turns [4]. The biological action of these peptides on membranes leads to the leakage of the alkali metal ions, Na^+ and K^+. Iturin A's action initially leads to a continuous increase, in contrast to a stepwise increase, of the K^+ and Na^+ permeability and ion conductivity of the target membrane, followed by the release of cellular contents [5]. Although iturin A has been under investigation for about 50 years, the precise mechanism of action of this peptide still remains unclear. Iturin A shows an affinity for alkali metal cations such as Na^+ and K^+ [6], but precipitates in the presence of divalent cations such as Mg^{2+} and Ca^{2+} [7]. It has been suggested that specific interaction between iturin A and alkali metal ions may be an important feature of its mechanism of action [6]. Other cytolytic peptides such as

the linear α-helical gramicidin A [8] also transport both Na^+ and K^+ over target cell membranes by the formation of ion channels. A myriad of antimicrobial peptides, the magainins [9], defensins [10], cecropins [11], and tachyplesin [12], all anion selective ion channel forming peptides [13], and many others [14] have been discovered and shown to be cytotoxic for a wide range of microorganisms. The activity of many of these membrane active peptides is partially or totally dependent on inducing leakage of the alkali metal ions, Na^+ and K^+, over target cell cytoplasmic membranes. The investigation of these antibiotic peptides and their interaction with alkali metal ions at an atomic level, is therefore important to elucidate their structure-function relationship and mechanism of action.

Nuclear magnetic resonance (NMR), ion selective electrodes and conductive methods have been used to assess peptide-ion complexation [15]. The use of mass spectrometry as a tool to probe gas-phase peptide-ion complexation became possible with the development of new desorption and ionisation techniques. These techniques include fast atom bombardment (FAB) [16], matrix-assisted laser desorption/ionisation (MALDI) [17] and electrospray ionisation (ESI) [18-20]. Mass spectrometry (MS) in general, with specific emphasis on ESI-MS, will be discussed briefly as background to the ESI-MS investigation of peptide-ion interaction.

A mass spectrometer (Fig 5.1) is an analytical instrument that measures the molecular mass of chemical compounds by the separating ions according to their mass-to-charge ratio (*m/z*) in a mass filter/analyser such as quadrupoles, magnetic sector, time-of-flight or ion trap. The ions are then detected by either an electron multiplier or a scintillation counter. Ions are generated in the ionisation source for example by either electron impact ionisation, fast atom bombardment, matrix assisted laser desorption/ionisation or electrospray ionisation. The ions include molecular ions ([M]) or parent ions, product ions or daughter ions and ions complexed to metal ions, water, solvent or other molecules (adducts). Samples can be introduced in several ways: using a solid probe inserted into the mass spectrometer, direct infusion without pre-analysis separation of analytes or direct infusion using gas chromatography (GC), high performance liquid chromatography (HPLC), solid phase extraction (SPE) or capillary electrophoresis (CE) linked the mass spectrometer. The last three methods are used only in electrospray ionisation mass spectrometry.

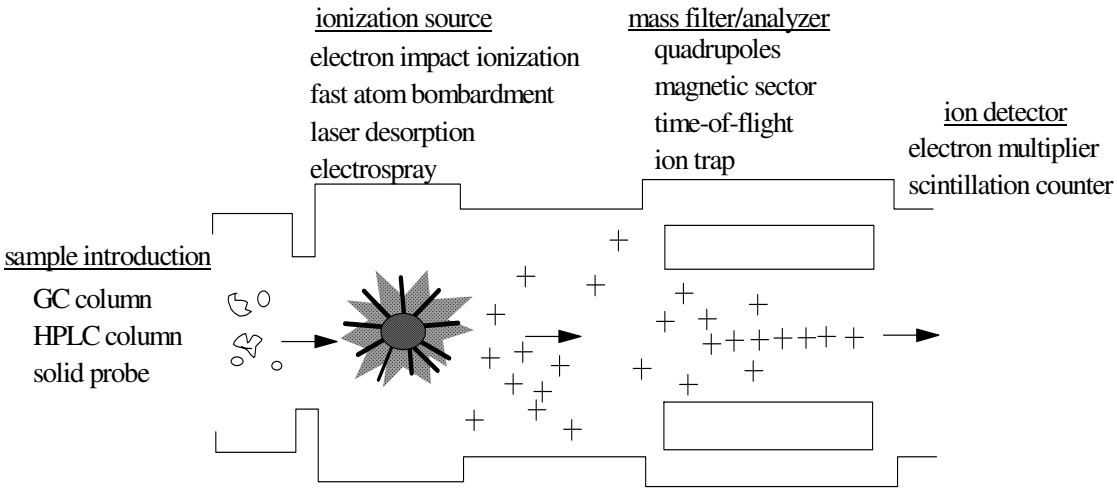

Figure 5.1 Components in mass spectrometers [adapted from 21].

Ions, the molecular products detected in mass spectrometry, are created in various ways such as through electron ejection, electron capture, transfer of a charged molecule from a condensed phase to a gas-phase, protonation, deprotonation or cationisation (Fig. 5.2).

Ion transfer

$[M]^{+}_{solution} \blacklozenge [M]^{+}_{gas}$

Electron ejection

$[M] \blacklozenge [M]^{-} + e^{-}$

Electron capture

$[M] + e^{-} \blacklozenge [M]^{-}$

Protonation/Deprotonation

$[M] + H^{+} \blacklozenge [MH]^{+}$

$[M] - H^{+} \blacklozenge [M]^{-}$

Cationisation

$[M] + Cation^{+} \blacklozenge [M \boxtimes Cation]^{+}$

$[MH]^{+} + Cation^{+} \blacklozenge [M \boxtimes Cation]^{+} + H^{+}$

Figure 5.2 Different mechanisms of ionisation in mass spectrometry [adapted from 21].

Until the 1980's electron impact ionisation (EI) was the primary ionisation mode available for mass analysis, but due to harsh ionisation conditions its use was limited to the analysis of small volatile molecules. EI commonly depends on electron ejection to give a net positive charge. Pioneers such as M. Barber, F. Hillenkamp, M. Karas, M. Dole and J. B. Fenn developed the techniques of FAB, MALDI and ESI. These new ionisation processes extended

mass spectrometry into the realm of biology by allowing the analysis of large biomolecules [21].

In FAB and MALDI, ions are liberated from analytes imbedded in a solid matrix by ion beam bombardment and laser beam respectively. Electron capture occurs in FAB and MALDI by the absorption of an electron to give a net negative charge to the analyte. Protonation and deprotonation also form ions that may be detected by FAB and MALDI. Cationisation, which occurs by the association of a small cation, such as the alkali metal cations, with a neutral complex, is also commonly observed in FAB and MALDI spectra.

In the ESI process ions are liberated from solvent droplets by desolvation, making this the mildest ionisation process currently available (Fig. 5.3). Gaseous ionised molecules are created when a fine spray of highly charged droplets are introduced into a strong electric field and the solvent is removed by heat, vacuum and dry gas. Protonation, deprotonation, cationisation and transfer of charged molecules from the aqueous phase are frequently observed in ESI.

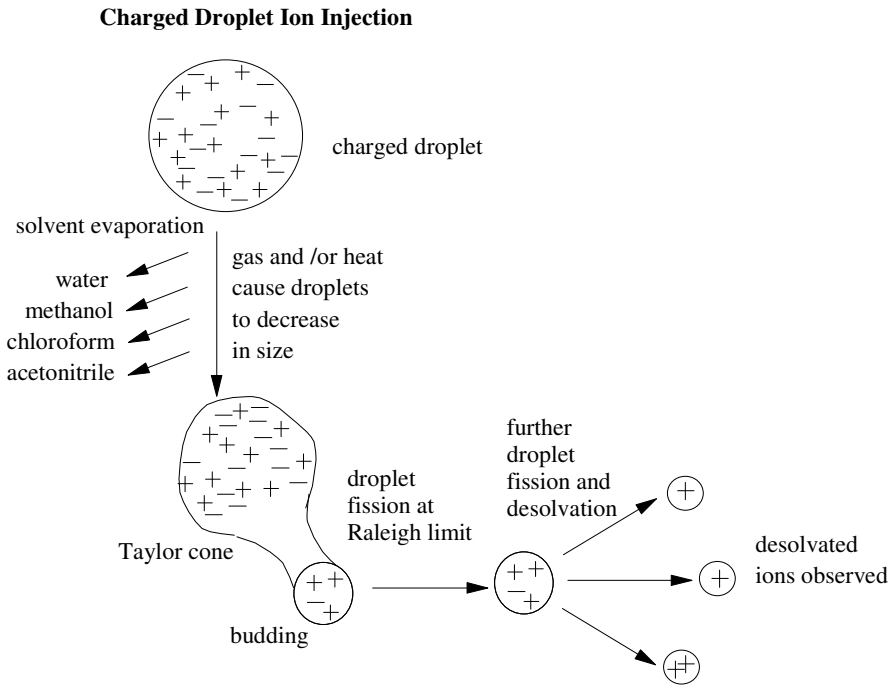

Figure 5.3 Process of electrospray ionisation [adapted from 20, 21].

The use of solvent in the ESI-MS makes it feasible to link it to liquid chromatography systems such as HPLC and SPE, therefore increasing its analytic capability. The mild electrospray ionisation, wide mass detection range (up to 200 000 Da) and femtomole sensitivity made it

possible to study large biomolecules and weak non-covalent interactions. ESI-MS spectrometry is therefore the most versatile mass analytical technique. A detailed diagram of an electrospray ionisation mass spectrometer, similar to the one used in this study, is given in Fig. 5.4. For more technical detail, specific applications and coverage of early ESI literature other reviews should be consulted [19, 20].

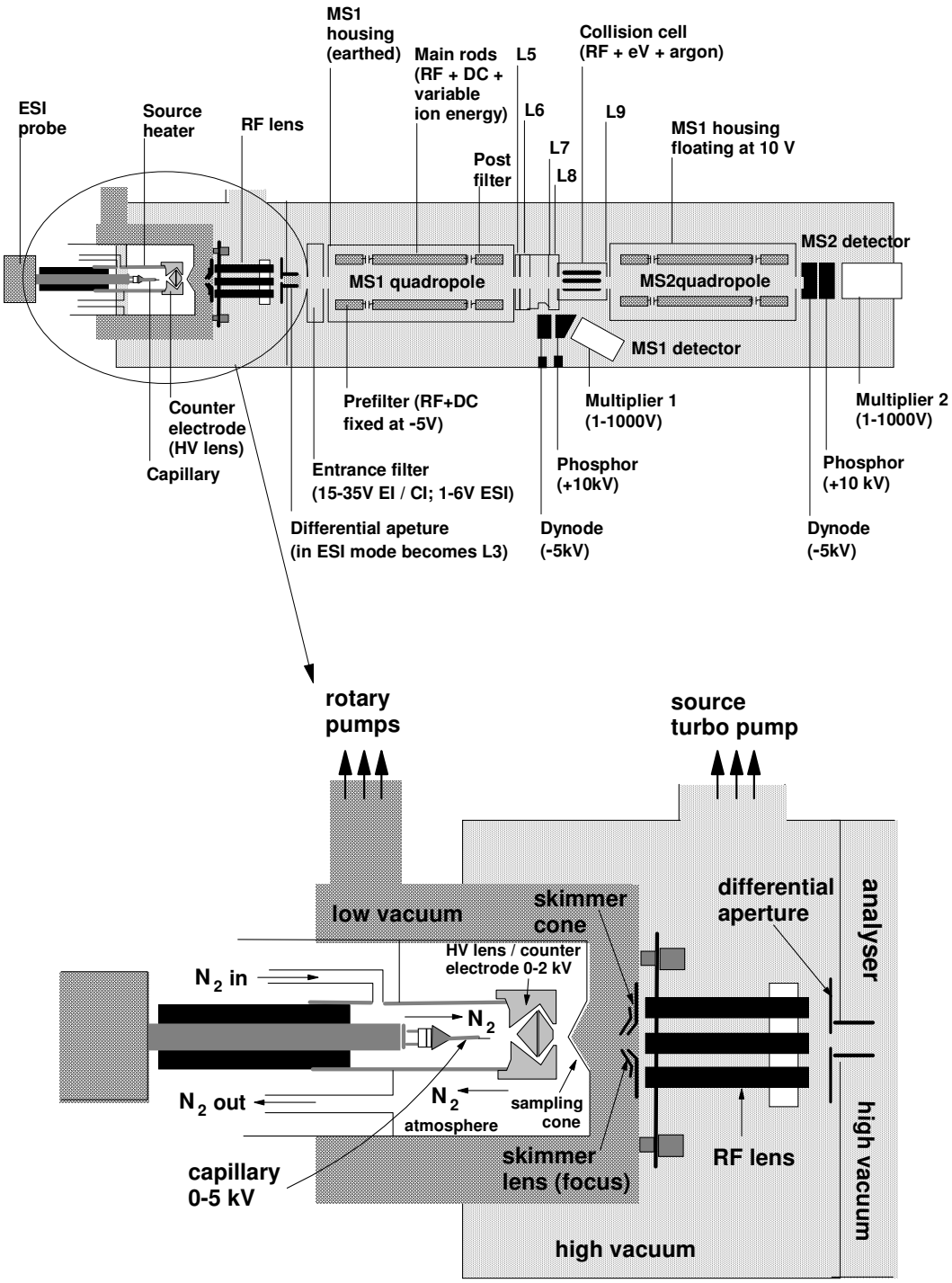

Figure 5.4 Diagrammatic representation of the Micromass Quattro Triple Quadrupole electrospray ionisation mass spectrometer [adapted from diagrams provided by Micromass].

As with ESI-MS, FAB-MS permits the study of peptide-ion interactions in the gas-phase, but because of the nature of ionisation, these studies may exclude some interactions that depend on the prior aqueous conformation of the peptide. Electrospray ionisation makes it possible to also observe weak non-covalent interactions that depend on native conformation [21, 22]. Solution and ESI-MS instrument parameters can be optimised to balance the processes occurring in solution as well as in the gas-phase. Assessment of peptide interactions is facilitated by the disassembling or fragmentation of the peptide complexes into discernible units. Regardless the mode of ionisation (EI, FAB, MALDI or ESI), fragmentation is dependent on the lability of the chemical bonds and therefore energy input in the mass analyser.

Fragmentation of peptides in FAB-MS, MALDI-MS and ESI-MS generally occurs at the peptide (amide) bonds (b and y product ions), but some other types of product ions from backbone fragmentation are also observed. The nomenclature of Roepstorff and Fohlmann [23], as revised by Biemann [24], was used to denote the product ions from fragmentation of peptide molecular ions described in this chapter (Fig. 5.5).

In an instrument with a triple quadrupole mass analyser the fragments are generally generated in the collision cell after selection of the parent ion in MS_1 (Fig. 5.4). The fragments are then detected in MS_2.The fragment or product ions (also called daughter ions) can be separated into two classes: (i) a_n, b_n and c_n and d_n product ions from the N-terminal, and (ii) x_n, y_n, z_n, v_n and w_n product ions from the C-terminal (Fig. 5.5). The subscript n indicates the number of amino acid residues in the positively charged fragment. The fragmentation pattern depends on the location of protons (and other associated cations) within the peptide and possibly also the conformation of the peptide. The characteristic N-terminal b_n and its complimentary C-terminal y_n product ion series is commonly observed for peptides, especially in low-energy collision induced decomposition/dissociation (CID) [25]. This fragmentation pattern occurs because of charge separation processes [26] and points to protonation at various positions along the peptide backbone. The y_n ions are more predominant in spectra, because b_n ions are susceptible to further degradation to e.g. the a_n ions formed by the loss of CO [27]. Sequence related fragmentation is observed for peptides containing proline and or basic amino acid residues such as arginine, lysine and histidine [25]. The peptide bonds flanking a Pro residue are particularly susceptible to cleavage [28]. This is possibly the result of the combination of conformational constraints induced by proline on the peptide backbone and favourable

protonation of the secondary amine group of proline [25]. Bonds in the vicinity of a protonated amino acid or a basic site are very labile and likely to be broken, but protonation and subsequent cleavage close to an already protonated site will be unlikely due to Coulomb repulsion [29]. A strongly basic amino acid residue, such as arginine, will thus influence the fragmentation pattern.

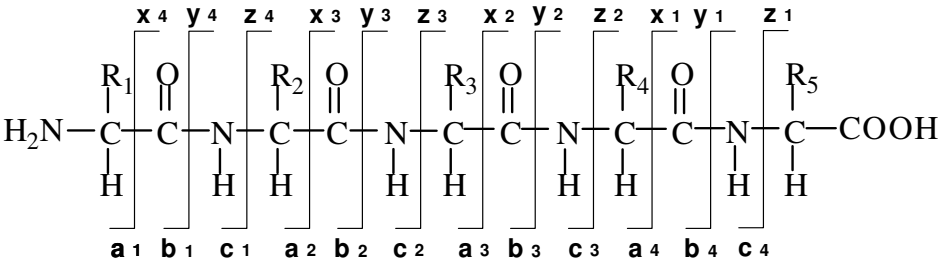

Peptide backbone product ions

a 1 $H_2\overset{+}{N}{=}CHR_1$

b 1 $H_2N{-}CHR_1{-}C{\equiv}O^+$

c" 1 $H_2N{-}CHR_1{-}\underset{\underset{O}{\|}}{C}{-}NH_3^+$

a 2 $H_2N{-}CHR_1{-}\underset{\underset{O}{\|}}{C}{-}\underset{H}{\overset{+}{N}}{=}CHR_2$

z 1 $R_5HC{=}\overset{+}{C}OOH$

y" 1 $H_3\overset{+}{N}{-}CHR_5{-}COOH$

x 1 $\overset{+}{O}{\equiv}C{-}\underset{H}{N}{-}CHR_5{-}COOH$

z 2 $R_4HC{-}\underset{\underset{O}{\|}}{C}{-}\underset{H}{N}{-}CHR_5{=}\overset{+}{C}OOH$

Side-chain ions

d-ions

$a_2 + H \xrightarrow{-R_{2a} \text{ or } R_{2b}} d_2$

v-ions

$y_2 + 2H \xrightarrow{-R_4H} v_2$

immonium ions (i-ions)

mass of residue - (CO + H)

w-ions

$z_2 + H \xrightarrow{-R_{4a} \text{ or } R_{4b}} w_2$

Figure 5.5 Fragmentation patterns of a peptide during mass spectrometry and nomenclature according to Roepstorff and Fohlmann [23], as revised by Biemann and Martin [24].

The fragmentation pattern changes dramatically if cationisation of a peptide by metal ions, such as the alkali metal cations, occurs. The long range Coulomb interaction of the cation with the peptide influences the chemistry of distant sites on the peptide [30]. This effect is more pronounced in the gas-phase where the shielding effects of surrounding solvent are absent [31-39]. The differences in fragmentation patterns reveal the nature of the interaction of the

metal ion with the peptide on the molecular and even atomic level. Teesch *et al.* [31, 32], used FAB-MS to study the interaction of various peptides with alkali metal ions. They concluded that alkali metal ions tend to complex to sites with basic carbonyl groups, such as the amide oxygen in Asn and Gln side-chains, and to the amide oxygen in the peptide bond. Other investigators, using FAB-MS [33-35], proposed that the alkali metal ion is complexed to the deprotonated carboxylate terminus. Mallis and Russel [36] suggested complexation to amide nitrogen, and were the first to note that the fragmentation of peptide-ion adducts also revealed additional information on the primary sequence. In an ESI-MS study of peptaibols, Kanai *et al.* [37] were able to deduce complete sequence information by fragmentation of sodium containing peptide complexes. Their study showed that fragmentation of the sodium adducts produced mainly N-terminal (b_n-type) product ions, a common phenomenon observed for peptide-alkali metal adduct decomposition. The C-terminal fragments contained sodium, but it was generated by the same bond cleavages found in CID of the non-complexed peptide. They did not investigate specific interaction between sodium and the peptides. Wang *et al*. [38] studied the association between sodium and nine different glycine containing tripeptides with the aid of ESI-MS. They proposed that the metal ion was complexed to one of the carboxy terminal oxygens (including the possibility of a salt-bridge between the carboxylate and sodium) and the nitrogens in the two amide bonds and amino terminal. Giogi *et al.* [39] again illustrated that cations tend to associate with the basic groups in peptides in their ESI-MS study of the complexation properties of (histidyl-glycyl)$_2$ with alkali metal ions. They concluded that the metal ion interacted with either the carboxylate anion or with the amide bonds. Consequently it is clear that many different types of gas-phase interactions between a peptide and an alkali metal ion are possible; some interactions are due to “non-specific” ionic interaction, while others depend on peptide length, specific amino acids or a specific sequence. Those interactions between biologically active peptides and alkali metal ions such as Na^+ and K^+, that are highly sequence specific and probably dependent on peptide conformation, may be biologically significant.

Many parameters affect ion formation during electrospray ionisation [40-46], and in our study the ESI-MS instrument settings and solvent composition had to be carefully optimised. When dissolved analyte is introduced into the mass spectrometer it is accompanied by solvent molecules and electrolytes. The characteristics of the solution are firstly important in the ionisation of the analyte and secondly in the electrospray process. The ionisation of the analyte is highly dependent on the pK_a values of its dissociating groups and therefore also on the pH

of the solution [40, 41]. It is also known that the actual pH in the ionisation chamber of the mass spectrometer can differ markedly from the pH in bulk solution [41, 42]. Not only is the pH of the analyte solution of great importance in ionisation, but also the concentration of electrolytes. Strong acids and salts in the analyte solution may lead to diminished sensitivity due to ion-pairing and "masking" of the ions (ion suppression) [40, 43-45]. The formation of the droplets during the electrospray process is also influenced by solution properties, such as surface activity of analytes and electrolytes, surface tension, dielectric constant and volatility of the solvent [40, 46]. Instrument settings such as the source temperature in the ionisation chamber and parameters relating to acceleration of ions in the mass spectrometer (thus energy charge) will also influence the ion current and the non-covalent complex.

The linear analogue of iturin A_2, 8-Beta with the β-aminotetradecanoic acid (β-NC_{14}) as N-terminal residue and L-Ser_8 as C-terminal residue, was used as model peptide and Na^+ as model ion to determine the maximum ion current (signal intensity) conditions and influence on ion current and cationisation. Parameters such as cone voltage (ΔV between sample cone and skimmer lens, refer to Fig. 5.3), carrier solvent composition, sodium concentration in the sample, pH (including the influence of different acids and bases), solvent composition in the sample and pre-incubation time of the lipopeptide with sodium were investigated. ESI-MS was also used to investigate the interaction between alkali metal ions, Na^+, K^+ and Rb^+, and a series of iturin A_2 analogues in which one of the β-turns was sequentially eliminated. The structure of iturin A, discussed in Chapter 4, includes a type II β-type turn in each of the tetrapeptide moieties: β-NC_n-L-Asn_2-D-Tyr_3-D-Asn_4 and L-Gln_5-L-Pro_6-D-Asn_7-L-Ser_8. In 7-Beta and cyclic 7-Beta the L-Asn_2 residue was omitted, in 6-Beta the L-Asn_2-D-Tyr_3 dipeptide unit, and in 5-Beta the L-Asn_2-D-Tyr_3-D-Asn_4 tetrapeptide unit (structures are given in Chapter 2, Table 2.1). 8-Beta was again used as model peptide for stability and structural investigations, because it includes the two intact sequences containing the β-turns. This linear analogue of iturin A_2 was investigated, because cyclic peptides give a much more complex fragmentation pattern than linear peptides.

5.2. Materials

HPLC grade trifluoroacetic acid (TFA, 99.5%), NaCl (99.9%), KCl (99.9%), HCl and NaOH were from by Merck (Darmstadt, Germany). Acetonitrile (HPLC-grade, UV cut-off 190 nm) and methanol (HPLC-grade, UV cut-off 205 nm) were from Romil LTD (Cambridge, UK). Triethylamine (TEA) and RbCl were from Sigma Chemical Co. (St. Louis, USA). Analytical quality water was prepared by filtering glass distilled water through a Millipore Milli Q® water purification system. Synthetic gramicidin S was donated by Dr. R. Levitt, previously from Fine Chemicals, South Africa. The synthetic iturin A_2 analogues were synthesised with the Fmoc-polyamide peptide synthesis protocol and purified by RP-HPLC and characterised as described in Chapters 2 and 3.

5.3 Methods

5.3.1 Sample preparation for ESI-MS

Lyophilised HPLC purified 8-Beta (a racemic mixture of 8-Beta I (D) and II (L)) was dissolved in a mixture of 50% acetonitrile in analytical quality water (glass-distilled, de-ionised) to a concentration of 5.0 mg/mL. This stock solution was diluted to 0.2 mg/mL (±0.2 µmole/mL) with 50% acetonitrile modified with 0.05% TFA in water, except when stated otherwise. To determine the influence of sodium concentration, a NaCl concentration range from 0.1 µM to 80 mM was used. Samples in the remaining investigations contained 10 mM NaCl. The influence of TFA and TEA was determined by varying their concentration from 0.01% to 0.5% in the sample solutions. To investigate the influence of the pH of the sample solution, the 0.2 mg/mL of 8-Beta was dissolved in analytical grade water and the pH adjusted with standardised HCl (pH 0, 1.0, 2.0, 3.0 and 4.0), TFA (pH 5.1), TEA (pH 7.0 and 8.9) and standardised NaOH (pH 10.0, 11.0 and 12.0). The sodium concentration was kept constant at 10 mM in all these samples. To determine the influence of the solvent polarity, different solvent compositions (25%, 50% and 80% acetonitrile in water) were used in the sample and carrier solvent. All samples were freshly prepared before analysis, except in the one case when the influence of cold storage on cationisation of the peptide was examined. To investigate the structures of the cationised 8-Beta and the effect of cationisation with sodium on its stability,

0.2 mg/mL peptide in 50% acetonitrile/water modified with 0.05% TFA and 10 mM of NaCl was used (this optimum solvent composition was determined as reported below).

To investigate the influence of primary structure on cationisation, the purified diastereomers of 8-Beta, 7-Beta, cyclic 8-Beta and cyclic 7-Beta and the isomeric mixtures of 6-Beta and 5-Beta were analysed in the presence of different alkali metal ions (Na^+, K^+ and Rb^+). As in the other analyses 0.2 mg/mL HPLC purified peptide in 50% acetonitrile, modified with 0.05% TFA in water, was incubated with NaCl, KCl and RbCl. In this competition assay all three of the alkali metal ions (10 mM of each chloride salt) were used.

5.3.2 Electrospray ionisation mass spectrometry

ESI-MS was performed using a Micromass triple quadrupole mass spectrometer fitted with an electrospray ionisation source (refer to Fig. 5.4). The carrier solvent was 50% acetonitrile in water, except in the investigation of solvent influence where 25% and 80% acetonitrile were also used. The solvent was delivered at a flow rate of 20 µL/minute during each analysis using a Pharmacia LKB 2249 gradient pump. Ten µL of the sample solution (2 nmole peptide) was introduced into the ESI-MS using a Rheodyne injector valve. A capillary voltage of 3.5 kV was applied and the source temperature was set at 80^0C. The skimmer lens offset was 5 V and the cone voltage was set at 70 V, except during the investigation of cone voltage influence when it was changed in increments from 20 V to 150 V. Triplicate analyses were done at each cone voltage value, using 10 µL 8-Beta sample solution per analysis. Analyses of other peptides were done at 70 V using 2 nmole peptide per analysis.

Data acquisition was in the positive mode, scanning the first analyser (MS_1), through *m/z* = 300 to1300 or 1500) at a scan rate of 100 atomic mass units/second. Representative scans were produced by combining the scans across the elution peak and subtracting the background. Signal intensity of each of the ions under investigation was determined by integrating the ion specific chromatographic peaks detected during analysis.

5.3.3 CID of peptides and product ions

The stability of each of the molecular species of 8-Beta was determined using collision induced decomposition/dissociation (CID) with multiple reaction monitoring (MRM; static

selection of specific ion in MS_1 and static monitoring of product ions in MS_2). These experiments were conducted using the same ionisation parameters as before, except that the solvent flow was increased to 50 µL/min and argon was introduced into the collision cell at $(2.5 \pm 0.3) \times 10^{-3}$ millibar. Collision energy settings ranging from 10 to 100 eV were used, with an injection of 2 nmole peptide at each value. The resulting chromatographic peaks were integrated to obtain the intensity of the measured ion at the set collision energy.

To determine the influence of cationisation on 8-Beta fragmentation patterns, each of the 8-Beta molecular species was selected in MS_1 and subjected to identical CID conditions to obtain product ion scans. The same ionisation parameters as before were used, but with continuous infusion at 5 µL/min using a Harvard Apparatus syringe pump. The argon pressure in the collision cell was as for the MRM experiments, and the collision energy was set at 30 eV. Data was acquired in continuum mode scanning MS_2 from *m/z* = 100 to 1200 at 100 atomic mass units/second for precisely six minutes.

Verification of the fragment identity was afforded by multiple injections of 10 µL sample or continuous flow injection at 5 µL/min and subjecting the peptide to cone voltage decomposition between 90 V and 110 V. The selected fragment ion was further fragmented by CID in MS_2 ("MS_3"). Data was acquired in the so-called MCA mode (cumulative acquisitions) through an *m/z* range of 10 to 50 atomic mass units above the mass of the selected ion.

5.4 Results and discussion

5.4.1 Optimisation of solvent composition for ESI-MS analysis

5.4.1.1 Incubation of the lipopeptide with NaCl

The influence of incubation of 8-Beta with 10 mM NaCl on the ESI-MS spectra is shown in Fig. 5.6. Cationised species containing one sodium ($[M+Na]^+$) and two sodiums ($[M+2Na-H]^+$), with signal intensities between 60% and 90% of that of the free peptide ($[M+H]^+$), were observed in fresh samples (compare Fig. 5.6 A and B). Molecular species associated with three sodiums ($[M+3Na-2H]^+$; $[M+3Na-H]^{2+}$) were also observed at very low signal intensities.

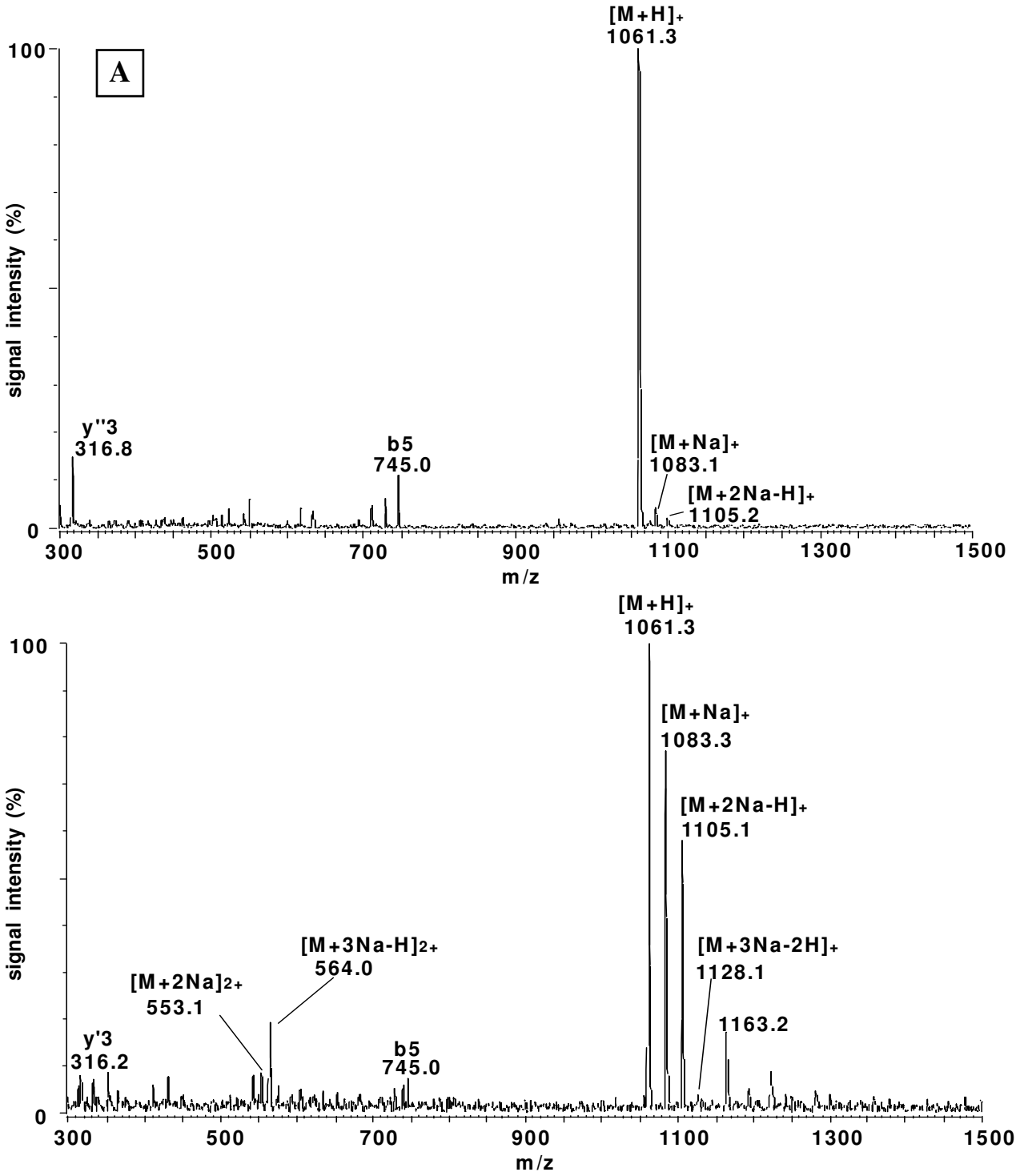

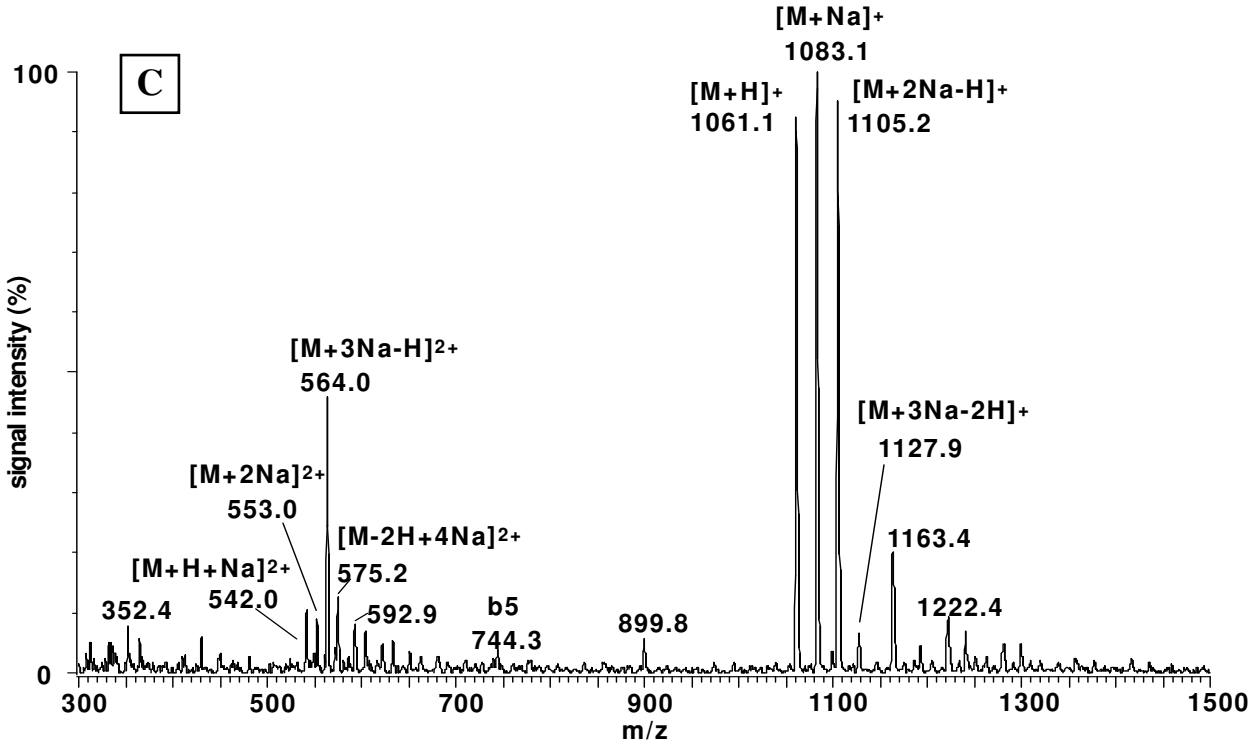

Figure 5.6 ESI-MS spectra of 8-Beta before (**A**) and after incubation with NaCl where (**B**) is the spectrum obtained with freshly prepared sample and (**C**) after 3 months cold storage. Spectra were obtained at 70 V cone voltage using 50% acetonitrile in water as carrier solvent. The sample consisted of 0.2 mg/mL peptide (without (A) or with 10 mM NaCl (B and C)) dissolved in 50% acetonitrile containing 0.05% TFA. The spectra were obtained using optimised conditions described in this study.

The singly charged specie $[M+3Na-2H]^+$ was absent in some of the spectra. After a long sample incubation (three months of storage at -10^oC), a substantial increase in the signals of the cationised species was observed (compare Fig. 5.6 B and C). A large increase in the signal of $[M+3Na-H]^{2+}$, to about 50% of the free peptide signal, and a specie associated with 4 sodiums $[M+4Na-2H]^{2+}$ (*m/z*=575) were observed. This change in spectrum is an indication that time-dependent cationisation of 8-Beta occurs in solution. 8-Beta also has a tendency to aggregate in solution with time and that this may influence solution equilibrium between sodium and the lipopeptide.

5.4.1.2 Influence of salt concentration in sample solvent

As in any type of ligand binding study it was also important to investigate the influence of ligand concentration on complex formation. At a NaCl concentration of 10 mM, background interference in the ESI-MS analyses was negligible (Fig. 5.7; also refer to Fig. 5.6 B). The binding curves depicted in Fig. 5.7 show that the peptide is almost saturated with sodium at

10 mM NaCl. Analyses done at 40 mM and 80 mM NaCl exhibited very high background interference due to ion clustering [47] and signal suppression as a consequence of the counter anion effect [43-45] (results not shown). Signal suppression by 10 mM NaCl was also observed, with the total signal amounting to only 74% of the signal obtained without added NaCl. These results indicated that the optimum NaCl concentration to study the interaction of 8-Beta with either one or two sodium ions was10 mM.

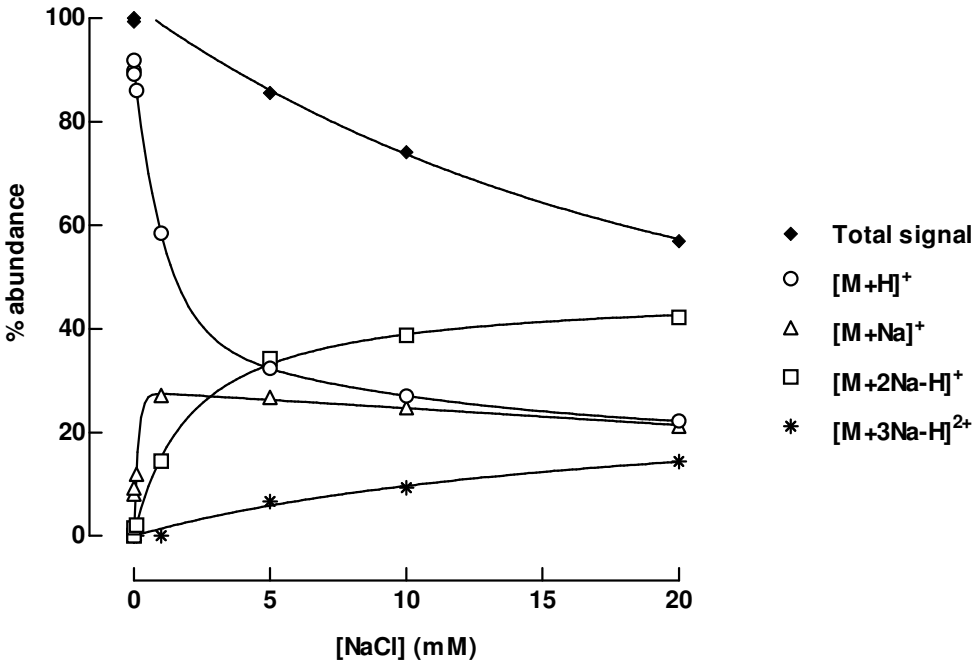

Figure 5.7 Influence of NaCl concentration on cationisation of 8-Beta with sodium as observed by ESI-MS at a cone voltage of 70 V. Results were calculated as a percentage of the sum of the signals of the four species under consideration. The signal values of $[M+2Na-H]^+$ was corrected with a factor of 1.7 for comparison. The influence of NaCl concentration on total signal is also depicted with the 100% signal taken as the total ion current of the spectra obtained with no added NaCl.

5.4.1.3 Influence of TFA and TEA concentration in sample solvent

To ensure the ionisation and positive ion detection of 8-Beta and its cationised species, TFA was used as solvent modifier. The optimum percentage TFA in 50% acetonitrile was determined as 0.05% (indicated with an arrow in Fig. 5.8 A). The decrease in signal intensity at 0.5% TFA was probably a result of the counter anion effect [43-45]. As expected, TEA in the sample solvent eradicated the positive ion signal of 8-Beta and its cationised species and no improvement of cationisation or adduct formation because of ionic interaction was seen (Fig. 5.8 B).

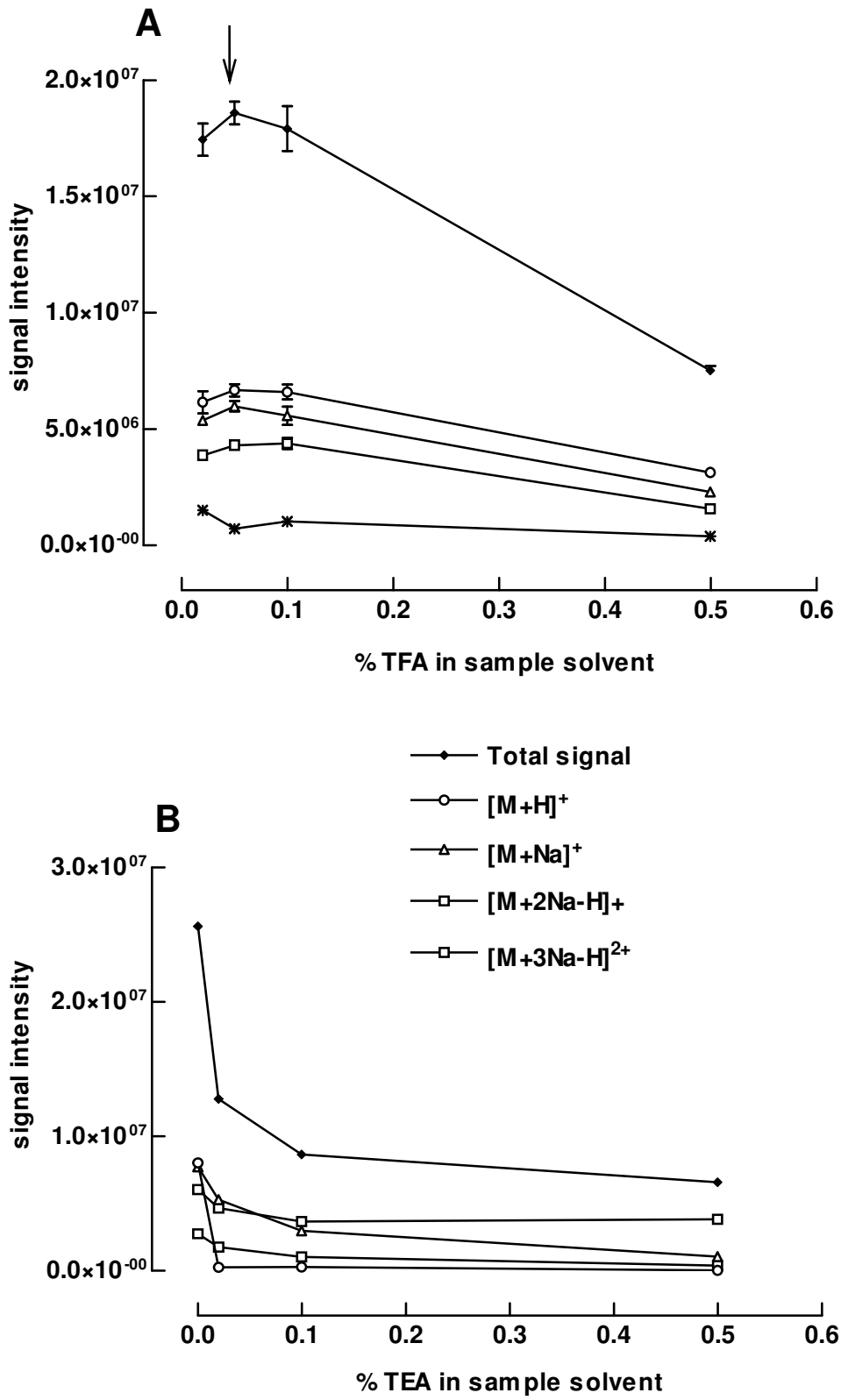

Figure 5.8 Influence of percentage TFA (**A**) and percentage TEA (**B**) in the sample solvent on cationisation of 8-Beta with sodium as observed by ESI-MS at a cone voltage of 70 V. Duplicate samples were analysed and SEM (standard error of mean) is shown for each value.

5.4.1.4 Influence of sample solvent pH

It is known that the use of solvent modifiers in high concentrations, in this case to adjust the pH, complicates the interpretation of the results [43-45]. In this study it was found that varying the sample solvent pH from 0 to 4 had a significant influence on the signal intensities of the major molecular species (Fig. 5.9 A). Signal depression at the lower pH values was due to the high counter anion concentration in the sample, eradicating the improved ionisation at lower pH values. Depression of the signal by the high chloride ion concentration is the consequence of ion-paring whereby masking of the positive ions takes place. The effect of chloride concentration is illustrated in Fig. 5.9 B. Low signal intensity at the high pH values was also the result of high counter anion concentration. The deprotonation of the peptide, however, is a major factor in the loss of signal (Fig. 5.9 A).

All species showed a maximum signal at pH 4. A negligible influence on the signal intensity of the sodium adducts of 8-Beta was observed in varying the sample solvent pH from 4 to 11, whereas the signal for the free peptide decreased substantially over this range (Fig. 5.9 A). The relatively constant signal intensity observed for the sodiated 8-Beta species over this range indicated contribution of the associated sodium ions to the overall positive charge of these species (Fig. 5.9 A). The eradication of the free peptide signal was expected at a much lower solvent pH due to the deprotonation of the free peptide. To explain this, the influence of the instrumentation must be considered. The metal capillary used to introduce the electrospray carries a 3.5 kV charge, thus redox reactions taking place in the capillary will result in a change of the initial solution composition entering the spray-capillary. Van Berkel *et al.* [41] showed that oxidation of water in the ESI-MS capillary actually lowered the pH of the solution with up to two units under certain conditions. This is therefore an explanation for the detection of the free peptide over an apparently broad pH-range (Fig. 5.9 A).

An 8-Beta molecular specie containing four sodiums ($[M+4Na-3H]^+$) was detected at pH 12 albeit at very low signal intensity (results not shown). The detection of this specie was probably because of the contribution of the extra sodium ion to the overall positive charge of the molecular species, illustrating the role of cationisation in detection of positive ions at high pH. From this data it could be deduced that there are at least four binding sites on the peptide of which only two, the C-terminal carboxylate group and the tyrosyl residue side-chain (phenolate group), can take part in ionic association with sodium. The specific interaction between sodium and 8-Beta will be addressed later on in this chapter. The strong influence of

counter ions in the sample solvent on detection was again confirmed. These results also supported the decision to use 0.05% TFA, which gave an apparent sample pH between 3 and 4, as modifier in the sample solvent.

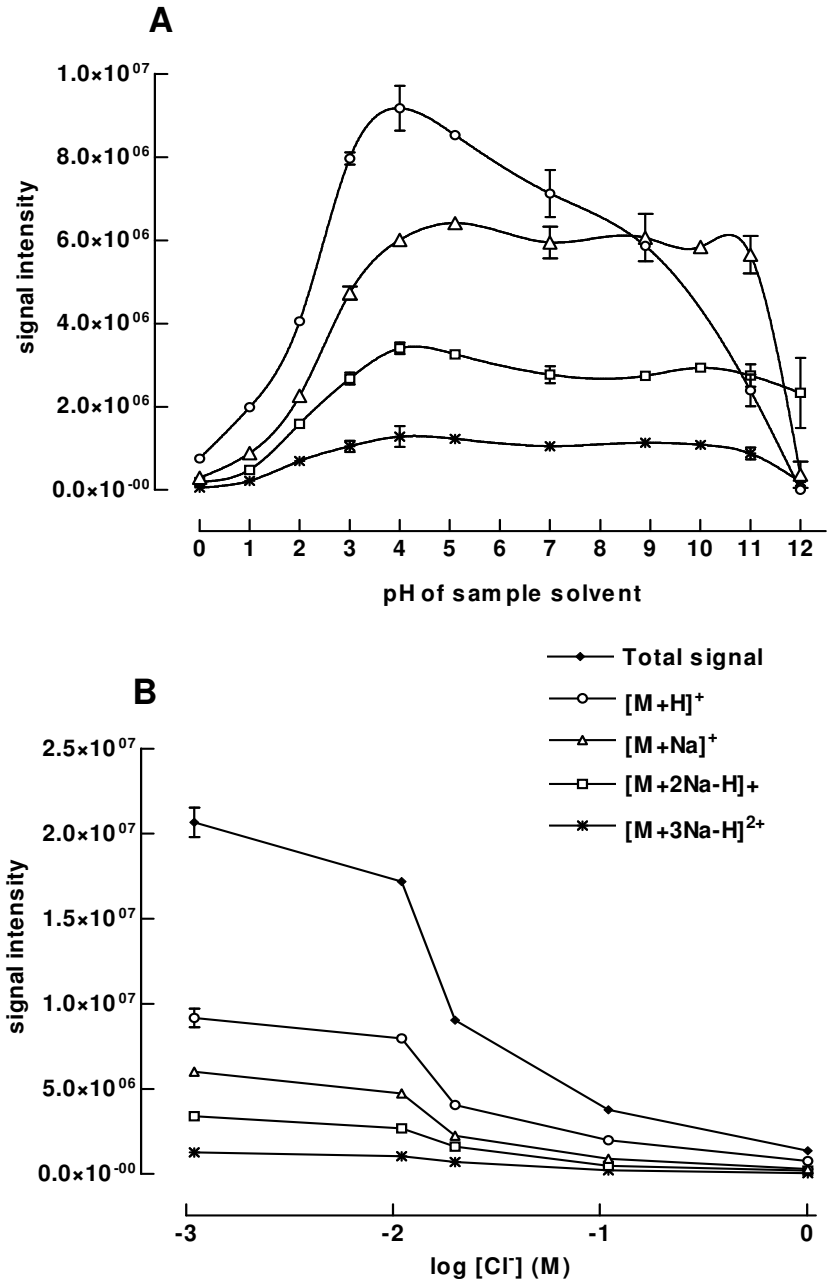

Figure 5.9 **A.** Influence of pH of the sample solvent on detection and cationisation of 8-Beta with sodium using ESI-MS at 70 V cone voltage. All samples contained 10 mM sodium. Duplicate samples were analysed and SEM is shown for each value. **B.** The influence of chloride ion concentration on ion current (deduced from the data in graph A (pH 0-4))

5.4.1.5 Influence of carrier solvent composition

To determine the influence of sample and carrier solvent on ion current and cationisation, 8-Beta and its cationised species were analysed using different percentages of acetonitrile in the solvent system. Acetonitrile was chosen as carrier solvent because of its high volatility and low background interference in the ESI-MS. A mixture of acetonitrile and water was also suitable for dissolving the lipopeptide, 8-Beta, which is insoluble in most organic solvents including methanol. It was found that the influence of acetonitrile concentration, and therefore also solvent polarity, on the signal intensity and cationisation was negligible (Fig. 5.10). The slight suppression of the signal intensities using 80% acetonitrile was probably due to solubility factors or weaker ionisation.

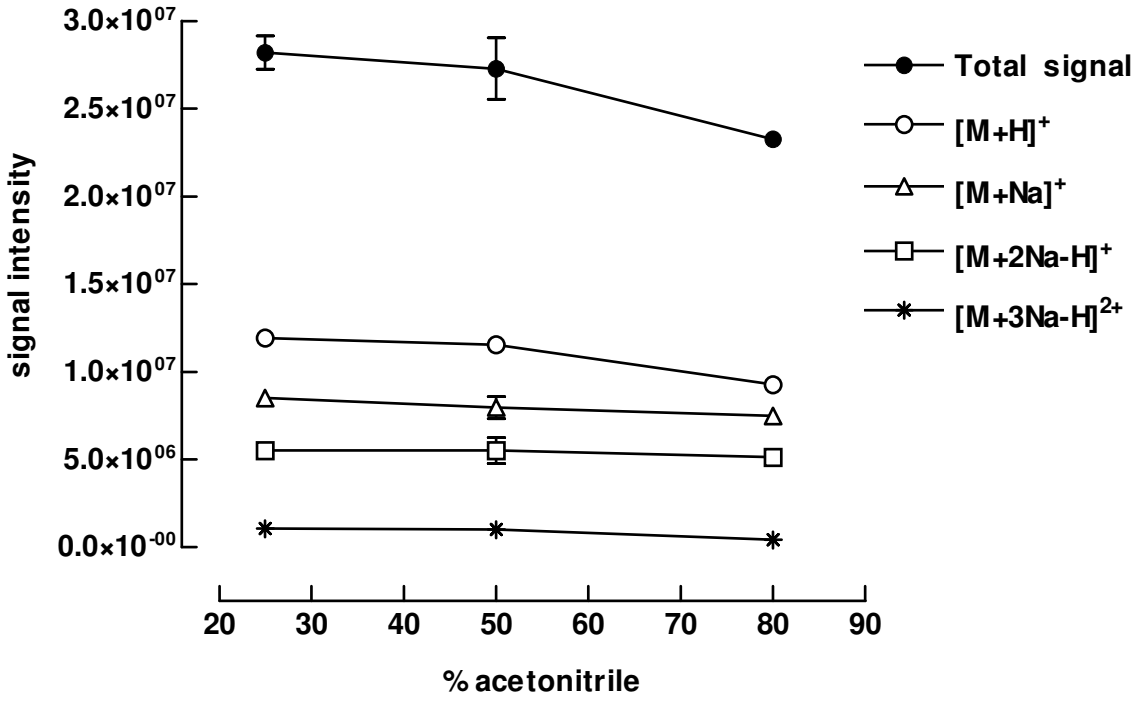

Figure 5.10 Influence of percentage acetonitrile in the carrier solvent and sample solvent on cationisation of 8-Beta by sodium as observed by ESI-MS at a cone voltage of 70 V. Duplicate samples were prepared using the same solvent composition as in carrier solvent, but including 0.05% TFA and 10 mM NaCl. SEM is shown for each value.

5.4.2 ESI-MS signal intensity and stability of the lipopeptides

5.4.2.1 Influence of cone voltage on 8-Beta and its cationised species

A concern in the study of the interaction of synthetic iturin A_2 analogues with alkali metal ions is the differences in signal intensity and therefore also the difference in stability between the different molecular species. If there were significant differences in the signal intensities of the different molecular species at a certain instrument setting, quantitative comparisons would be complicated. Cone voltage in the ESI-MS is one of the parameters that determines the acceleration of the sample particles in the ionisation source and has a large influence on detection and fragmentation of sample molecules. To select the best cone voltage for sensitivity and minimum fragmentation, 8-Beta and its cationised species (refer to Fig. 5.6) were analysed at different cone voltages.

For 8-Beta and its cationised species, spectra obtained at higher cone voltages (setting >50 V) produced less background noise and fewer multiple charged species, thereby facilitating interpretation. As expected in ESI-MS analyses, the doubly charged species were detected at the lower cone voltages, albeit at very low signal intensities, whereas the singly charged species were detected at the higher cone voltages. A bell-shaped relationship was found between signal intensity of any of the molecular species of 8-Beta and cone voltage over the 20 V to 150 V range (Fig. 5.11). The weaker signal at lower cone voltages was probably due to impairment of detection of the peptide ions. The sharp decrease in signal intensities at cone voltages higher than the "optimum cone voltage" were the result of peptide ion fragmentation.

The highest signal for free 8-Beta ($[M+H]^+$) was found at 70 V, while the peptide fragmented extensively at higher cone voltages causing a rapid decrease of its signal (Fig. 5.11 A). The 8-Beta molecular specie(s) containing one sodium ($[M+Na]^+$) was detected at maximum intensity over a broad cone voltage range, showing two maxima, namely at 70 V and at 100 V (Fig. 5.11 B). This may be explained by the existence of two or more different complexes of 8-Beta with one sodium, differing in their detection and stability. The maximum signal intensity of $[M+2Na-H]^+$ at 100 V was in the order of 1.7 times higher than the intensity of $[M+H]^+$ at 70 V, and $[M+Na]^+$ at both 70 V and 100 V (Fig. 5.11 A-C). Complexes of 8-Beta to three sodium ions were also observed at 10 to 17 times lower signal intensities than that of the other sodiated species. The signal for $[M+3Na-H]^{2+}$ was detected with maximum intensity at 70 V and at a comparable intensity to the $[M+3Na-2H]^+$ signal with its maximum at 100 V

(Fig. 5.11 D). It was concluded that 70 V is the optimum cone voltage to do comparative studies of $[M+H]^+$, $[M+Na]^+$ and $[M+3Na-H]^{2+}$, but in the case of $[M+2Na-H]^+$ and $[M+3Na-2H]^+$ values must be adjusted in comparative analyses. At 100 V all the singly charged sodiated species of 8-Beta could be compared, but at this cone voltage no or very little free peptide was observed.

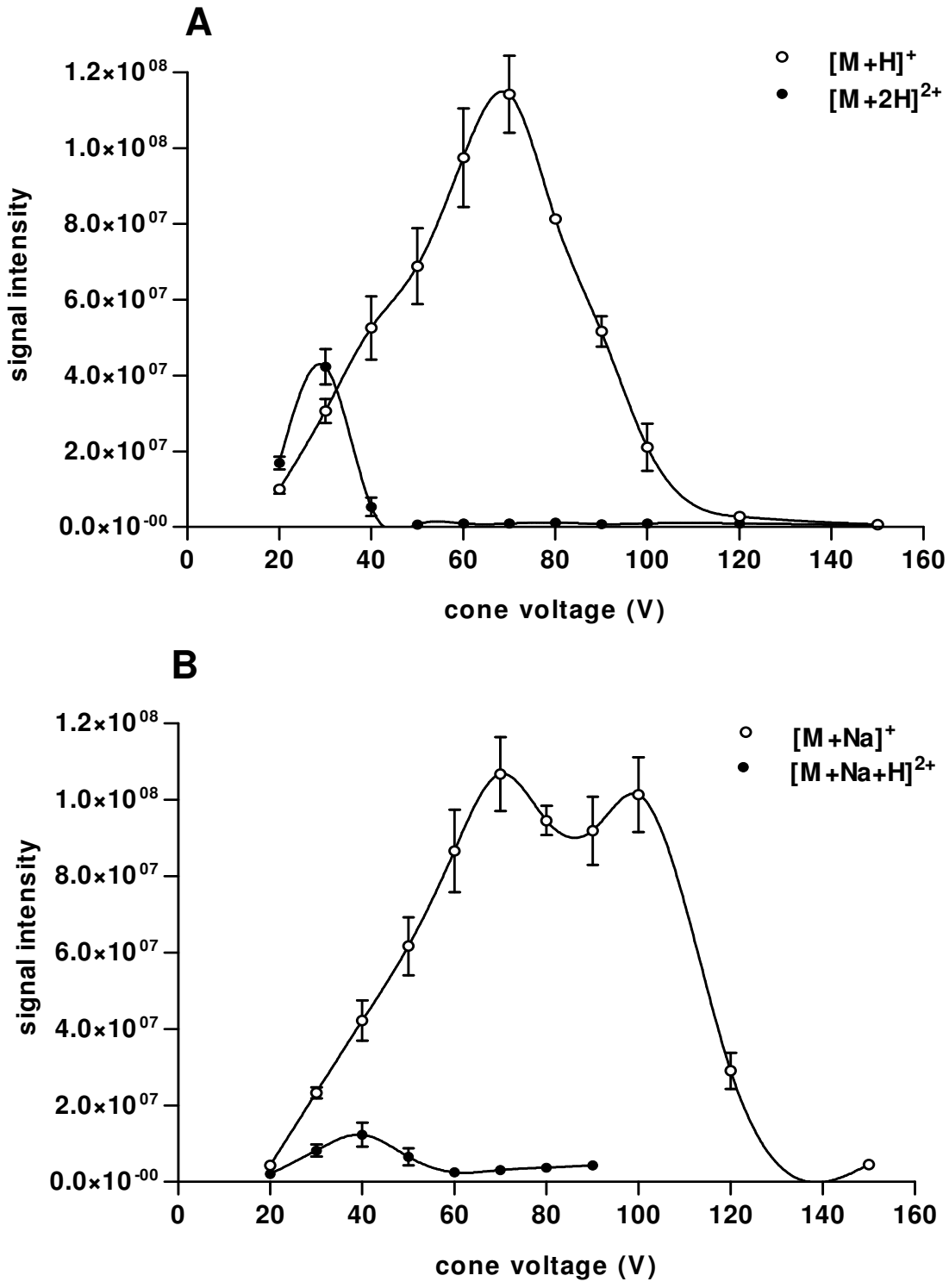

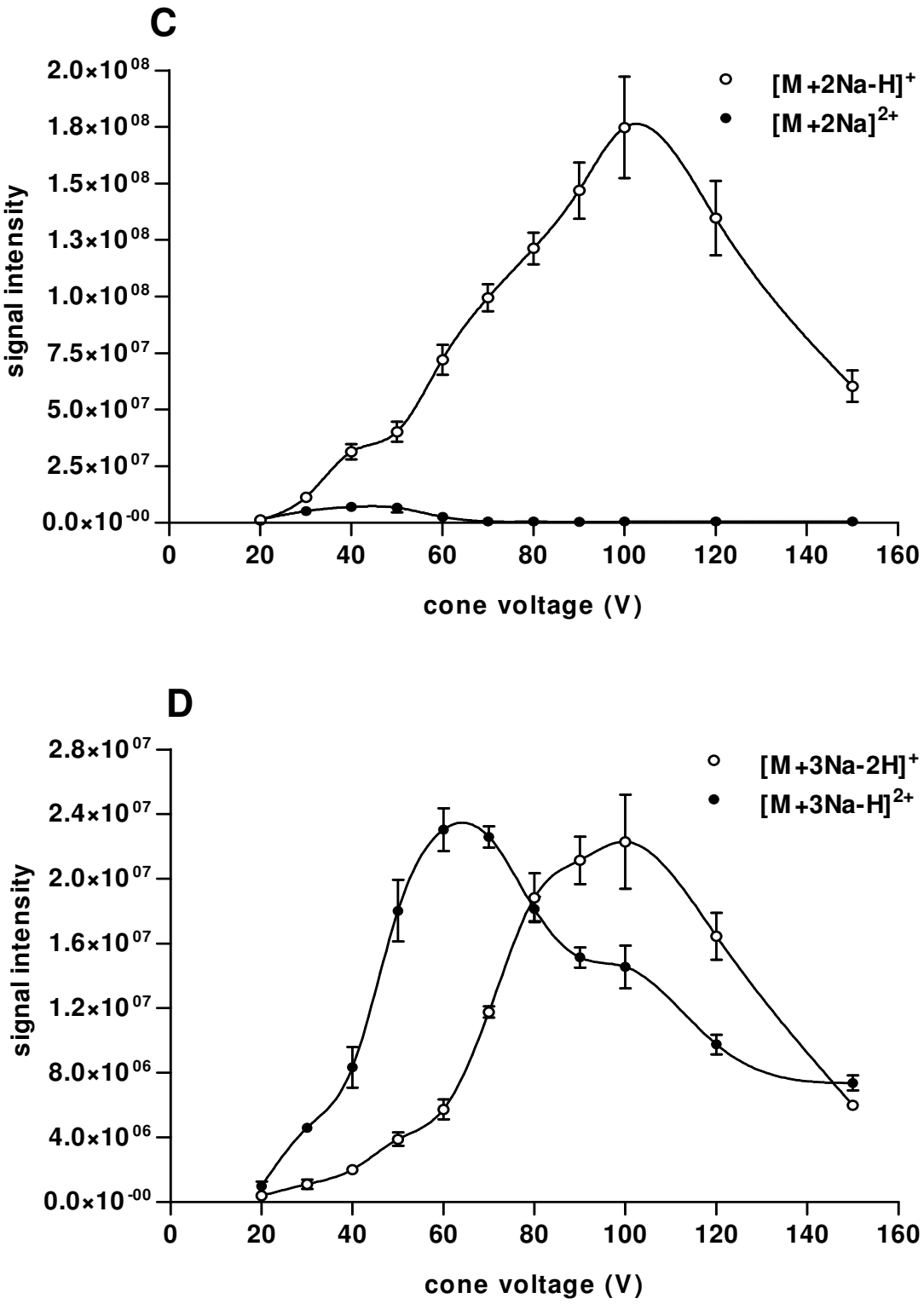

Figure 5.11 Correlation between cone voltage and the signal intensity of the 8-Beta molecular species. The values were calculated from data obtained in triplicate analyses and SEM is shown for each value. **A.** $[M+H]^+$ and $[M+2H]^{2+}$; **B.** $[M+Na]^+$ and $[M+Na+H]^{2+}$ (Data for $[M+Na+H]^{2+}$ are only shown to 90 V due to the interference of a peptide fragment with the same *m/z* at the higher cone voltages.); **C.** $[M+2Na-H]^+$ and $[M+2Na]^{2+}$; **D.** $[M+3Na-2H]^+$ and $[M+3Na-H]^{2+}$. (Note: Cone voltage = setting of instrument ± 2V)

5.4.2.2 Signal intensity and stability of the lipopeptides and their cationised species

The optimum solvent composition for 8-Beta, namely 50% acetonitrile in water containing 0.05% TFA and 10 mM NaCl, was used for the other peptides, because this composition minimised the counter anion effect.

Very little fragmentation of 8-Beta,7-Beta and their cyclic analogues (with and without 10 mM NaCl) was observed at 70 V cone voltage. The shorter peptides were much more sensitive to fragmentation at 70 V. Some stabilisation of the shorter peptides by sodium was, however, observed with 20% less fragmentation (35% vs. 53%) of 5-Beta and 5% less fragmentation (5% vs. 10%) of 6-Beta in the presence of 10 mM NaCl. The peptide backbone in the sodiated species was therefore protected from cone voltage dissociation. These observations substantiated the "cone voltage profiles" found for 8-Beta and its cationised species. The specific stabilisation and protection of the peptide backbone by sodium were studied in detail with 8-Beta as model peptide and will be discussed later in this chapter. Comparative analyses of all the lipopeptides were possible at 70 V, if the fragmentation of the two shorter peptides is also considered in the calculations.

These results suggested that the possible existence of specific interaction between iturin A_2 analogues and alkali metal ions at binding cavities or sites. Peptide size and the N-terminal sequence would be important for this interaction.

5.4.3 Interaction of the iturin A_2 analogues with alkali metal ions

In this part of the study the influence of increased hydrophobicity of the peptides, resulting from the elimination of one of the type II β-turns, was considered in the analysis of interaction with alkali metal ions. The influence of the peptide ring size and blocking of the N- and specifically the C-terminal on peptide-ion interaction were investigated using the cyclic analogues of the peptides 7-beta and 8-Beta. To probe the specificity and interaction cavity size, the alkali metal ions, Na^+, K^+ and Rb^+ which increase in radius, were incubated with the different peptides. The antimicrobial cyclic decapeptide, gramicidin S, was used as control peptide in some of these studies.

5.4.3.1 Cationisation of iturin A_2 analogues by sodium

Stable sodiated molecular ions (cationised species) in all the peptide samples, modified with 10 mM NaCl, were detected using positive mode ESI-MS (Figs. 5.6, 5.12, 5.13). The ESI-MS signal of the sodiated species of the linear lipopeptides ranged between 55% and 70% and that of the cyclic lipopeptides between 90% and 95% of the total peptide signal (Figs. 5.12, 5.13).

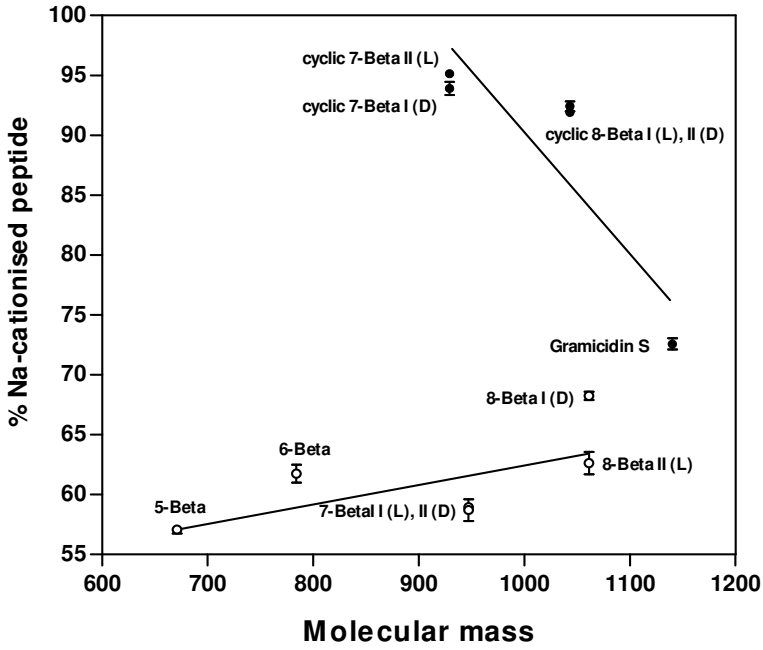

Figure 5.12 Relationship between molecular mass of the linear (o) or cyclic peptides (•) and percentage sodiated molecular specie detected in ESI-MS. The average of quadruplicate values with SEM is shown for each peptide.

It was generally found that association with sodium increased with length (molecular mass) of the linear lipopeptides, although a linear relationship was not demonstrated (Fig. 5.12). Specifically, a greater association with sodium for 6-Beta and less association for 7-Beta than expected was observed. The latter observation may be the result of steric interference by the Tyr residue side-chain on association of sodium with the basic carbonyl groups (e.g. in peptide bonds, Asn and Gln acid amide side-chains) in 7-Beta. Because the Tyr residue is not present in 6-Beta, more carbonyl groups are possibly exposed. It was also observed that the deletion of an N-terminal Asn residue from 8-Beta and from 6-Beta, resulting respectively in 7-Beta and 5-Beta, impaired the sodium interaction of these latter two peptides. Very little difference in sodium association between the two diastereomers of 7-Beta was found, but the differences between the diastereomers of 8-Beta were substantial (4%) and may be due to greater influence of the β-NC_{14} residue on the longer peptide's conformation or to two distinct

backbone conformations, as was indicated by molecular modelling and NMR (refer to Chapter 4).

The four cyclic peptides, derived from 7-Beta and 8-Beta, differed very little from each other in their tendency to associate with sodium. An inverse relationship between peptide molecular mass and sodium association was found, with the sodium association of cyclic decapeptide gramicidin S, used as control, the lowest of the cyclic peptides and more in line with that of the linear peptides (Fig. 5.12). It seems as if the shorter cyclic peptides, cyclic 7-Beta I (L) and II (D) bind sodium with higher affinity than the longer peptides, suggesting that the sodium ion binds within the cyclic peptide's cavity ("tighter" binding in a smaller cavity). The cyclic peptide, valinomycin, is such an example, with a non-solvated alkali metal ion (especially potassium) co-ordinated to the carbonyl oxygens in the cyclic cavity [1].

All the linear peptides, with almost equal distribution, associated with either one or two sodium ions as detected at a cone voltage of 70 V (Fig. 5.13). The longest linear peptides, 8-Beta I and II, also formed substantial complexes with a third sodium ion. Higher abundance of the mono-sodiated species was detected in the longer peptides, whereas the di-sodiated species of the shorter peptides predominated. This is attributed to differences in signal intensity and/or the stability of the different sodiated species under ESI-MS conditions.

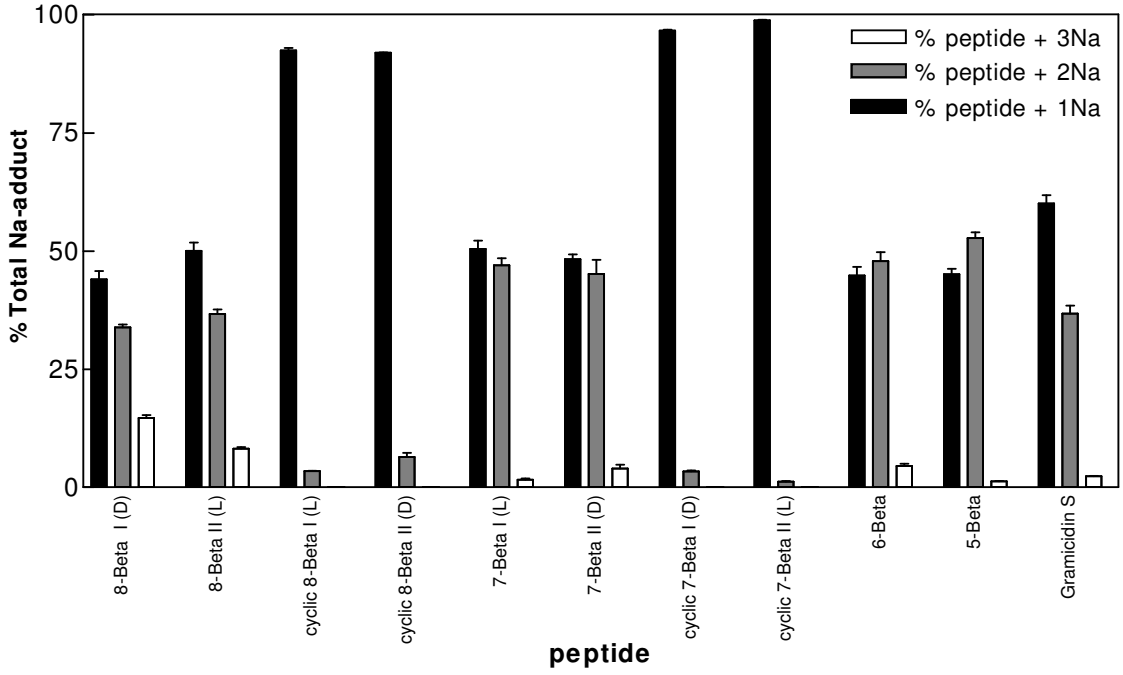

Figure 5.13 Preference of each of the iturin A_2 analogues and gramicidin S to either associate with one, two or three sodium ions as observed under ESI-MS conditions. Quadruplicate values and SEM for each of the detected molecular peptide species are shown.

The ESI-MS detection of the neutral free cyclic peptides was improved by the cationisation by sodium and the singly sodiated species of the four cyclic peptides was predominated (>90% of total signal) in spectra (Figs. 5.13, 5.14 B). The low abundance or absence of di-cationised complexes suggests possible association of the cation in the interior of the peptide ring. Electrostatic repulsion would restrict the inclusion of a second cation. The spectra of cyclic 8-Beta II (D) with and without 10 mM NaCl are given in Fig. 5.14 as example. The longer cyclic gramicidin S, used as control, bound to either one or two sodium ions resembling the sodium association pattern of the linear lipopeptides (Fig. 5.13). A previous study [48] of the alkali metal association of gramicidin S indicated that the alkali metal ion is bound to the exterior of peptide ring, therefore avoiding the charge repulsion of two cations in the interior of the peptide ring.

Because of the polar nature of the interaction between sodium and peptides it was predicted that sodium would preferentially associate with the more polar peptides. The polarity of each of the lipopeptides is influenced by their conformation in solution and the differences in polarity can be equated to retention by the hydrophobic matrix during HPLC, with the apparently less polar peptides eluting later than the polar peptides.

The dependence on polarity is illustrated by the relationship between HPLC retention time (refer to Chapter 2) and percentage sodiated species detected (Fig. 5.15). This is not a linear dependence, indicating that not only polarity, but primary structure (also refer to Fig. 5.13) and the specific solution conformation contributed to the interaction with sodium. The shorter less polar linear peptides tended to associate less with sodium. The difference of sodium association between the diastereomers of 8-Beta was substantial, when compared to the other diastereomers. Two low energy conformations, the so-called S- and W-structure were predicted using HyperChem®4.5 (refer to Chapter 4). It is proposed that the S-structure may be the more favourable structure in sodium association. If this S-structure is predominant in the 8-Beta II (D) preparation this may explain its better complexation to sodium.

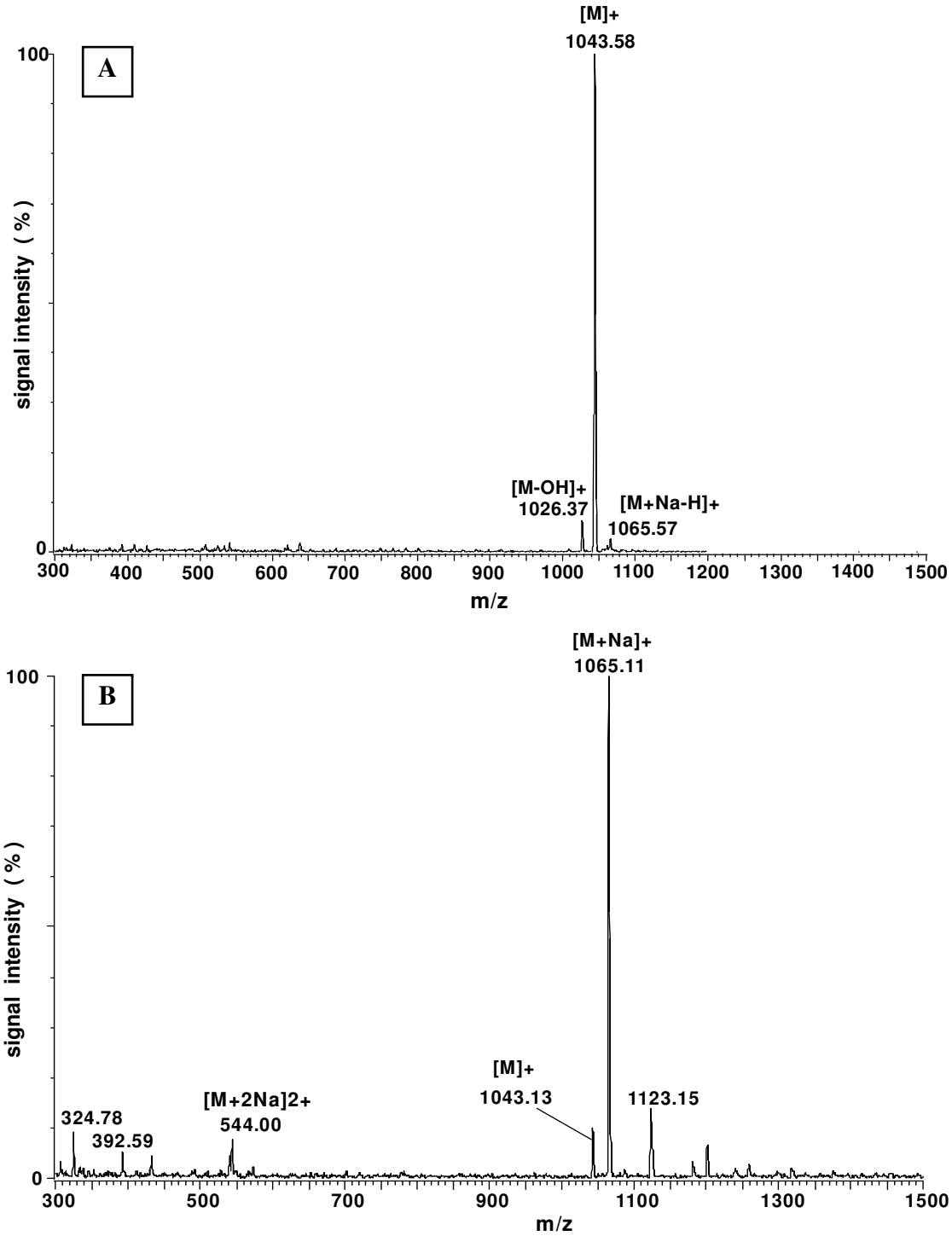

Figure 5.14 Positive ESI-MS spectra of cyclic 8-Beta II (D) before (**A**) and after incubation with NaCl (**B**). The sample consisted of 0.2 mg/mL peptide (without (A) or with 10 mM NaCl and 0.05 % TFA (B)) dissolved in 50% acetonitrile/water. The spectra were obtained using optimised conditions described in this study.

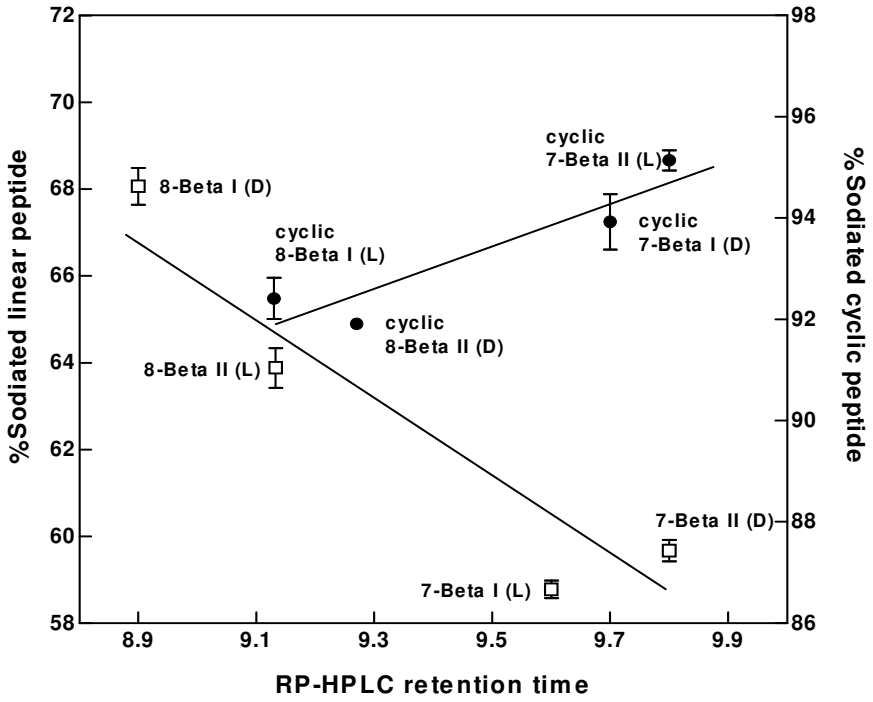

Figure 5.15 Relationship between RP-HPLC retention time of the iturin A_2 analogues and percentage sodiated molecular specie detected in ESI-MS. Average of triplicate values with SEM is shown. (All the HPLC analyses were done under identical conditions.)

5.4.3.2 Alkali metal ion selectivity

It has been observed that natural iturin A has a tendency to associate with cations, such as the alkali metal ions sodium and potassium [4]. The different lipopeptides were incubated with the chloride salts of sodium, potassium and rubidium in a competition assay. Difference in abundance of complexes between iturin A_2 analogues and the alkali metal ions Na^+, K^+ and Rb^+ can be related to the accessibility of the interaction sites. A range of cationised peptide species associated with either one or two alkali metal ions was found for all the linear peptides, but only mono-cationised species were detected for the cyclic peptides. Spectra of 7-Beta and cyclic 7-Beta, in Fig. 5.16, illustrate these observations.

The dominant species detected for all the lipopeptides, linear and cyclic, was the mono-sodiated species. Abundance of the mono-cationised species decreased with increase in size of the cation for all the peptides, indicating at least a size limitation in the “interaction cavity” (Fig. 5.17). This was further demonstrated by the fact that only mono-cationised species were detected for all the cyclic lipopeptides and also gramicidin S (Fig. 5.17). In the case of the cyclic peptides it was clear that only one alkali metal ion “interaction cavity” is accessible. All

the lipopeptides showed an identical gas-phase selectivity for the alkali metals namely: $Na^+ > K^+ > Rb^+$, which is the inverse of that observed for the longer valinomycin in methanol [49].

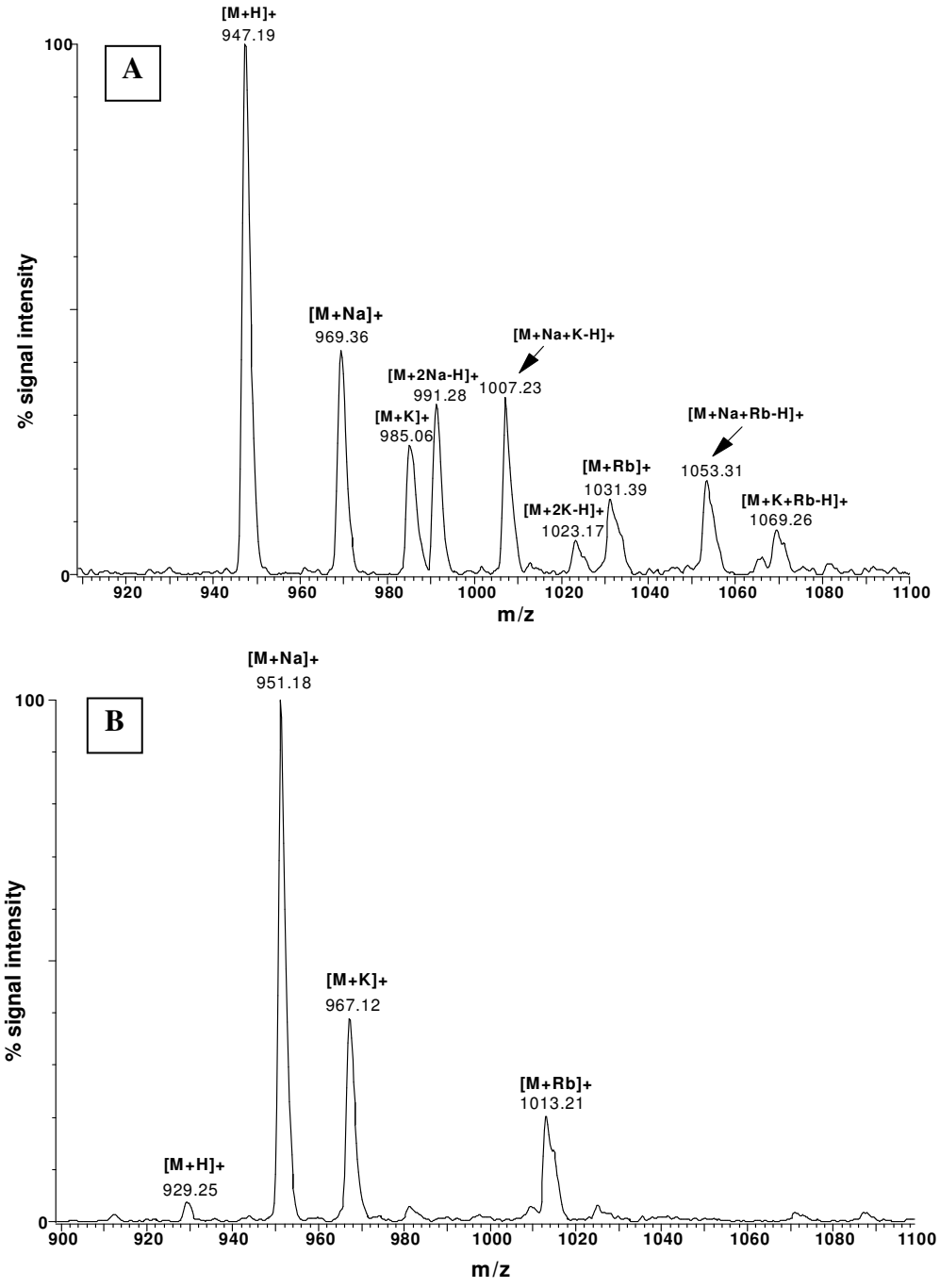

Figure 5.16 ESI-MS spectra of 7-Beta (**A**) and cyclic 7-Beta (**B**) incubated in the presence of NaCl, KCl and RbCl. The sample consisted of 0.2 mg/mL peptide dissolved in 50% acetonitrile/water modified with 0.05% TFA and 10 mM of each of the salts. The spectra were obtained using optimised conditions described in this study.

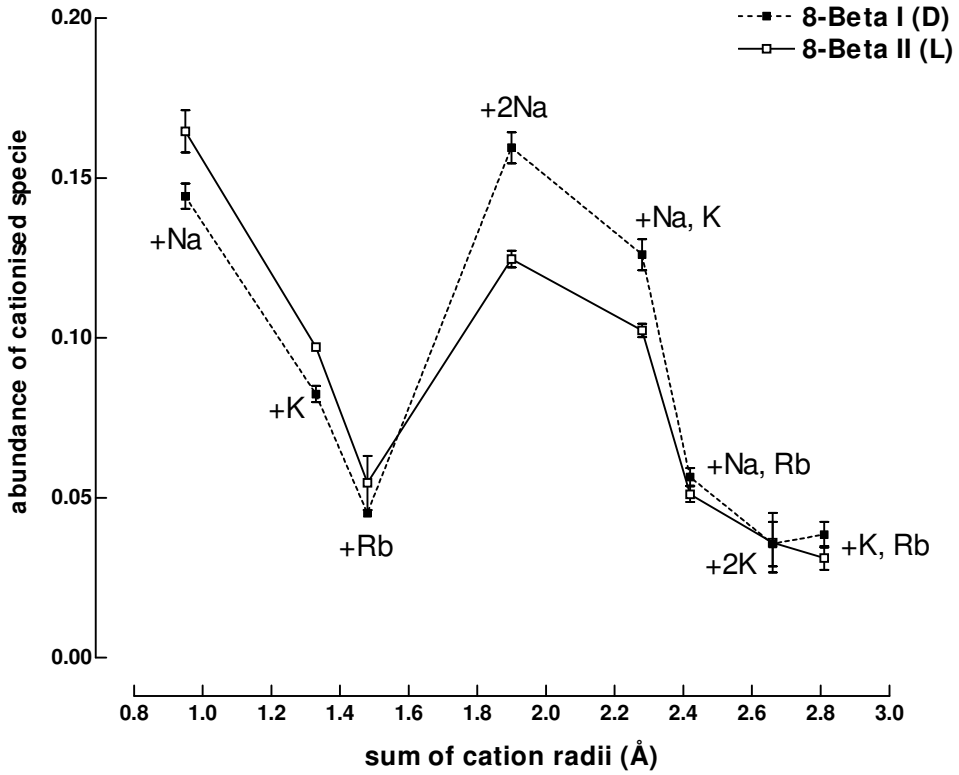

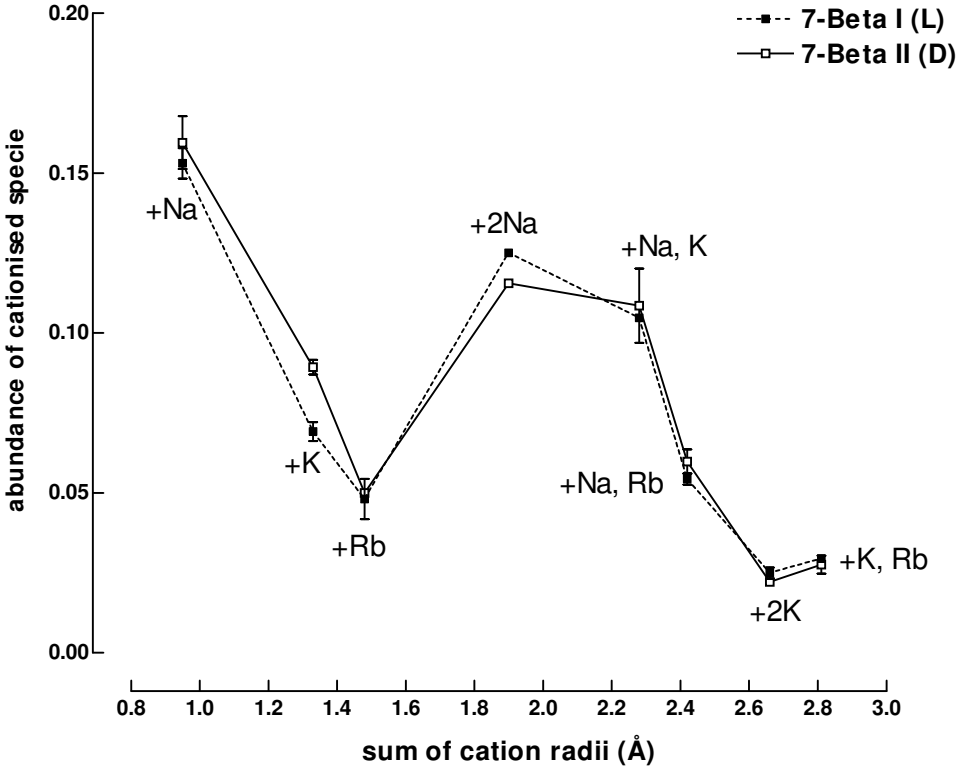

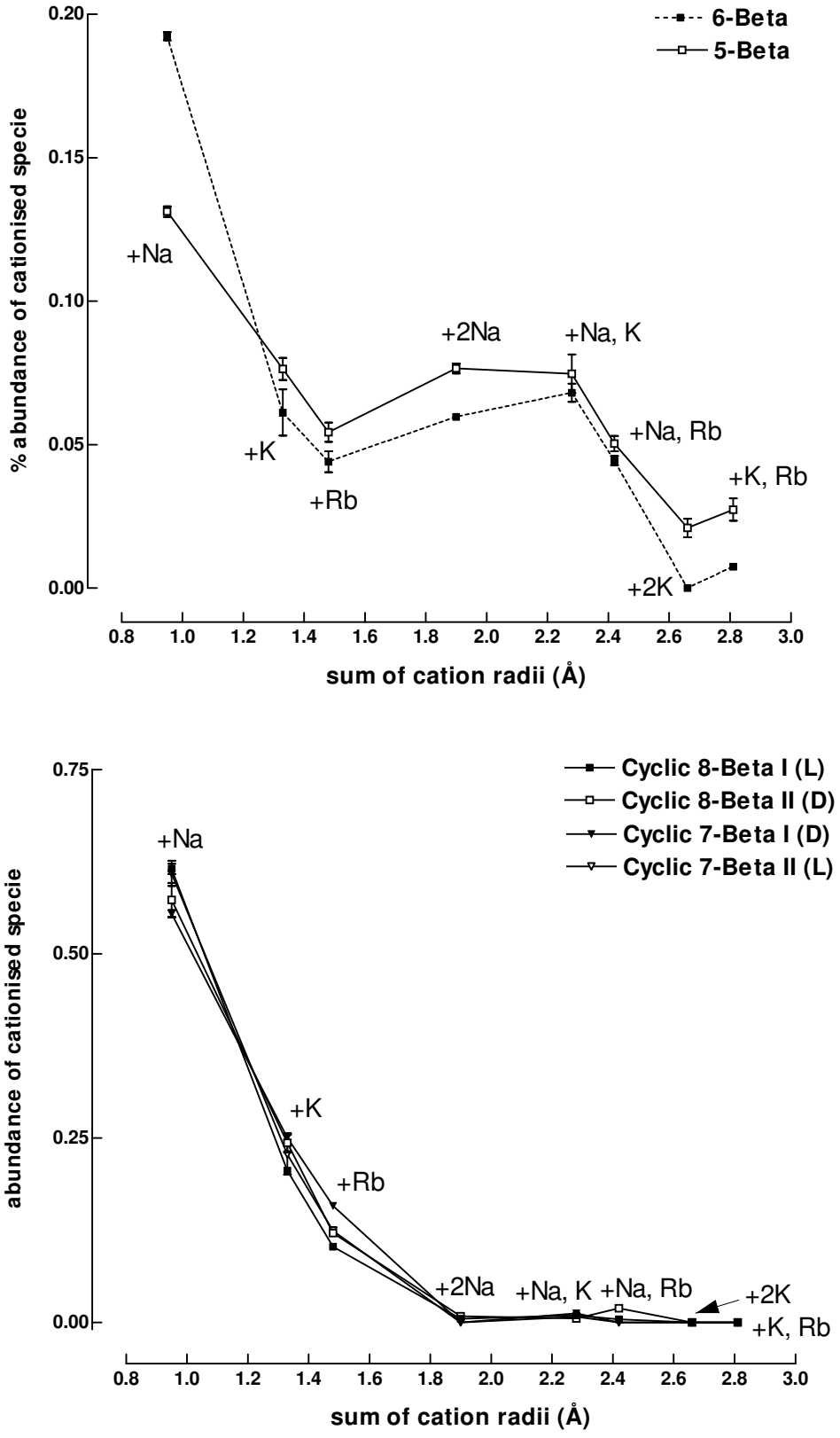

Figure 5.17 Relationship between the abundance of cationised peptide species and cation radii. The data points are the average of duplicate sample analyses. (Cation radii were taken from [50]; Na^+ = 0.95 C; K^+ = 1.33 C; Rb^+ =1.48C)

A substantial amount of di-cationised species, containing either two Na^+ or Na^+ and K^+, were detected for the longer linear peptide pairs of 8-Beta and 7-Beta (Figs. 5.16 A, 5.17). These results indicated that at least two "interaction cavities" are present in the linear hepta- and octalipopeptides. Di-cationisation of the shorter 5-Beta and 6-Beta was greatly impaired (Fig. 5.17), whereas di-cationised species of the cyclic peptides were virtually absent (Figs. 5.16 B, 5.17). The residues NY were omitted in 6-Beta and NYN in 5-Beta indicating that one of the cavities is probably situated in the C-terminal tetrapeptide moiety, QPNS. It can therefore be hypothesised that a second cavity is situated in the N-terminal tetrapeptide moiety, β-NC_{14}-NYN.

5.4.4 Investigation of specific interaction with alkali metal ions

ESI-MS-MS was also employed in the detailed investigation of the specific interaction between sodium, as model cation, and peptide moiety of iturin A. The peptide preparation used in this study was a diastereomeric mixture of 8-Beta I (D) and 8-Beta II (L). A difference in total sodium adduct signal intensity was observed between the diastereomers, but no distinctive difference in fragmentation patterns was observed (refer to Chapter 3). Using this preparation was still feasible because both diastereomers contain exactly the same α-amino acid peptide chain with similar backbone conformation as determined by *in vacuo* structure modelling (refer to Chapter 4).

5.4.4.1 CID Stability of 8-Beta and its sodium cationised species

To select the best condition for fragmentation by CID, the effect of increasing collision energy on the stability of 8-Beta and sodium cationised species was investigated (Fig. 5.18) The order of stability was found to be 8-Beta+1Na > 8-Beta+2Na > 8-Beta+3Na > 8-Beta. Under the specific experimental conditions used to obtain data in Fig. 5.18, the collision energy needed to reduce the signal by 50% (defined as I_{50}) increased in the order of 10 eV when one sodium was complexed to 8-Beta, whereas the I_{50} collision energy requirement decreased in the order of

2 eV for each further sodium complexed to the peptide after the first sodium. These results corroborated the cone voltage stability data (refer to Fig. 5.11) which showed that fragmentation of the 8-Beta occurred at cone voltages higher than 70 V, whereas sodiated species only fragmented at cone voltages higher than 100 V. Results from both CID and cone

voltage decomposition of 8-Beta and its cationised species indicated that complexation of sodium to 8-Beta afforded protection against fragmentation.

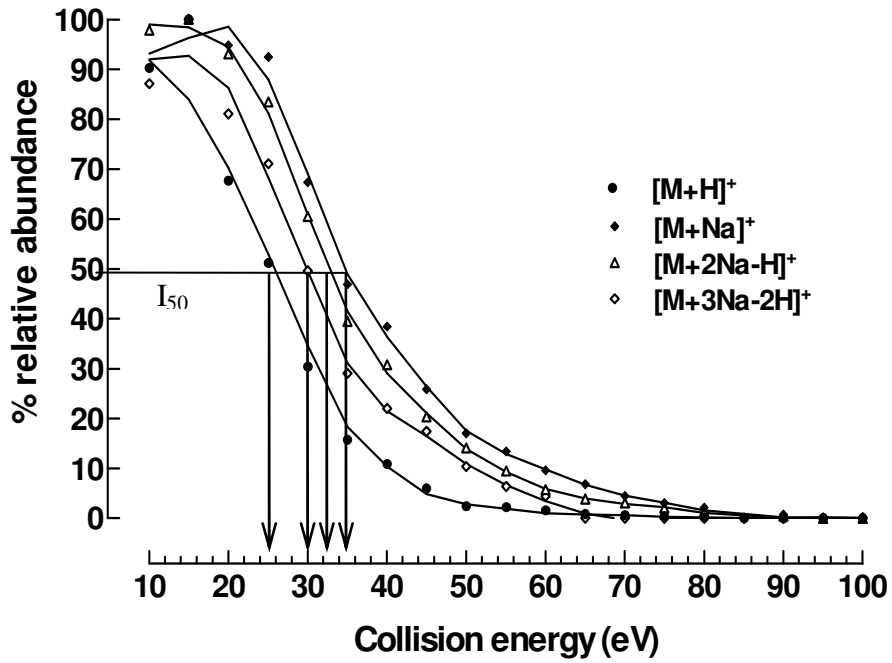

Figure 5.18 Correlation between signal intensity of the four different singly charged 8-Beta molecular species and collision energy at cone voltage of 70 V. The values were normalised using the signal obtained at 10 eV as 100%. The arrows indicate the collision energy at which the signal intensity of each of the species decreased by 50% defined as I_{50}. Data were collected using MRM with both MS_1 and MS_2 static at the parent ion *m/z*. The results of one of four similar experiments are shown.

The current hypothesis is that fragmentation reactions are induced by a protonated site; the location of these sites has therefore a considerable influence on the fragmentation of the peptide [25, 29, 52]. It is possible that the association of the sodium with basic sites in the peptide might lead to protection of bonds in its neighbourhood. In this study it was, however, shown with CID that cationised peptides containing more than one sodium were more inclined to fragment. This complicated the picture, indicating that binding of each additional sodium after the first increased the lability of some of the bonds in the peptide. This may be due to conformational changes in the peptide structure exposing new basic sites or as a direct result of Na^+ attachment. If the Na^+ is attached to carbonyl oxygens in peptides, as suggested by some authors [31-35, 52], it could have opposing effects. Tang *et al.* [52] proposed that the sodium attachment increases the double bond character of the peptide bond stabilising it, but conversely activates the carbonyl carbon making it more electrophilic and a target for nucleophilic attack. The overall stability of alkali metal cationised peptides in the mass

spectrometer has not specifically been addressed by other investigators. The subsequent study, was focused on the sequence specific protection afforded by the association of the model lipopeptide, 8-Beta, with sodium.

5.4.4.2 Fragmentation of 8-Beta and its cationised species

Fragmentation of each of the sodium cationised molecular species was greatly impaired under identical CID conditions used for the free peptide (Fig. 5.19), confirming the results obtained in the collision energy stability experiments. In this study it was also found, as in others [31-39, 51], that the fragmentation patterns were markedly different from that of the free peptide and that the sodium is retained in most of the product ions (Figs. 5.20, 5.22, Tables 5.2, 5.3). A neutral loss of 1 mass unit, from parent ions and some product ions, was also observed in spectra generated by CID. This could be explained by one or more of the following: rearrangement in the N-terminal β-aminotetradecanoic acid residue, neutral loss of a proton from the Tyr_3 side-chain or another acidic group, and the inherent low resolution of electrospray ionisation mass spectrometry at low signal intensity (imprecise centroid determination because of poor counting statistics). For these reasons we relied primarily on secondary product ion fragmentation ("MS_3") and previous interpretations in literature to assist us in product ion assignment. The nomenclature of Roepstorff and Fohlmann [23], as revised by Biemann [24], used in the product ions assignment was described earlier in this chapter (refer to Fig. 5.5).

Fragmentation of free 8-Beta (expected *m/z* 1062.2, observed MS_2 *m/z* 1061.3) occurred at all the peptide bonds, producing most of the expected b- and y-type product ions and y_nb_m-internal fragments (Figs. 5.6 A, 5.19, Table 5.1). Product ions b_5 (*m/z* 744.4; 728.1) and y_3 (*m/z* 317.5), from L-Gln_5-L-Pro_6 bond cleavages, were the major fragments of 8-Beta. It is known that the N-terminal peptide bond in which Pro participates is highly susceptible towards low energy fission [28]. A high abundance of internal fragments (*m/z* 212.3; 284.6) corresponding to L-Pro_6-D-Asn_7 indicated the lability of the L-Gln_5-L-Pro_6 bond, as well as that of the D-Asn_7-L-Ser_8 amide bond. A w_{a4} product ion (*m/z* 371.2), formed as a result of the loss of the Gln-side-chain from y_4, and the immonium ion of L-Gln_5 were also observed. This further indicated the lability of bonds in the neighbourhood of the L-Gln_5 residue. The low abundance product ion *m/z* 634.5 was attributed to b_4+OH (according to Teesch *et al.* [31, 32]) although this is relatively uncommon for non-cationised peptides. Internal fragments (*m/z* 278.5; 249.8) corresponding to D-Tyr_3-D-Asn_4 or L-Asn_2-D-Tyr_3 and the immonium ion of

D-Tyr$_3$ (*m/z* 136.5) were observed at relatively high abundance indicating the lability of the amide bonds in the neighbourhood of D-Tyr$_3$.

Table 5.1 Summary of the observed product ions generated by CID of the free peptide specie of 8-Beta. Only product ions detected at signal intensities equal to or above 45000 were taken into account. (* = loss of side-chain; f_i = internal fragment; ? = inconclusive results from product ion fragmentation; C-terminal product ions are indicated in italics)

***m/z* observed**	**intensity**	**relative intensity (%)**	**proposed fragment type**	***m/z* calculated**	**sequence**
1061.3	727488	100.0	$[M]^+$	1061.2	β-NC$_{14}$NYNQPNS
744.4	52712	7.2	b_5	744.9	β-NC$_{14}$NYNQ
728.1	59016	8.1	b_5-NH_3	727.9	β-NC$_{14}$NYNQ
711.5	47224	6.5	b_5-$2NH_3$	710.9	β-NC$_{14}$NYNQ
634.5	54584	7.5	b_4+OH	633.8	β-NC$_{14}$NYN
561.8	61788	8.5	a_4-CO	561.6	β-NC$_{14}$NYN
544.2	56504	7.8	a_4-$CONH_2$	543.5	β-NC$_{14}$NYN*
503.3	56628	7.8	b_3	502.7	β-NC$_{14}$NY
450.8	62092	8.5	2(b_1) ?	450.8	β-NC$_{14}$?
433.4	83136	11.4	(b_1-NH_3; b_1) ?	433.8	β-NC$_{14}$?
426.4	70372	9.7	f_i-CO	426.5	NQPN
416.4	81472	11.2	2(b_1-NH_3) ?	416.8	β-NC$_{14}$?
405.0	45424	6.2	f_i-H	405.6	YNQ
371.2	45708	6.3	w_{4a}	371.4	QPNS
323.3	55256	7.6	f_i-NH_3	323.3	NQP/QPN
320.2	75228	10.3	?		?
317.5	*245472*	*33.7*	*y''$_3$*	*317.3*	*PNS*
278.5	81868	11.3	f_i	278.3	YN/NY
249.8	57768	7.9	f_i-CO	250.3	YN/NY
220.6	*55164*	*7.6*	*y''$_2$*	*220.2*	*NS*
212.3	80636	11.1	f_i	212.2	PN
184.6	192752	26.5	f_i-CO	184.2	PN
136.5	93876	12.9	i_3	136.2	Y
101.4	50948	7.0	i_5	101.1	Q

The N-terminal β-NC_{14} residue complicated the interpretation of the fragmentation results, as it has a tendency to form adducts with itself (see b_1-product ion assignments in Table 5.1). CID produced mostly smaller product ions and internal fragments from the 8-Beta molecular ion, whereas larger product ions and very little internal fragments were produced from the cationised parent ions. The product ion with *m/z* 320.2 was not assigned after inconclusive product ion fragmentation results.

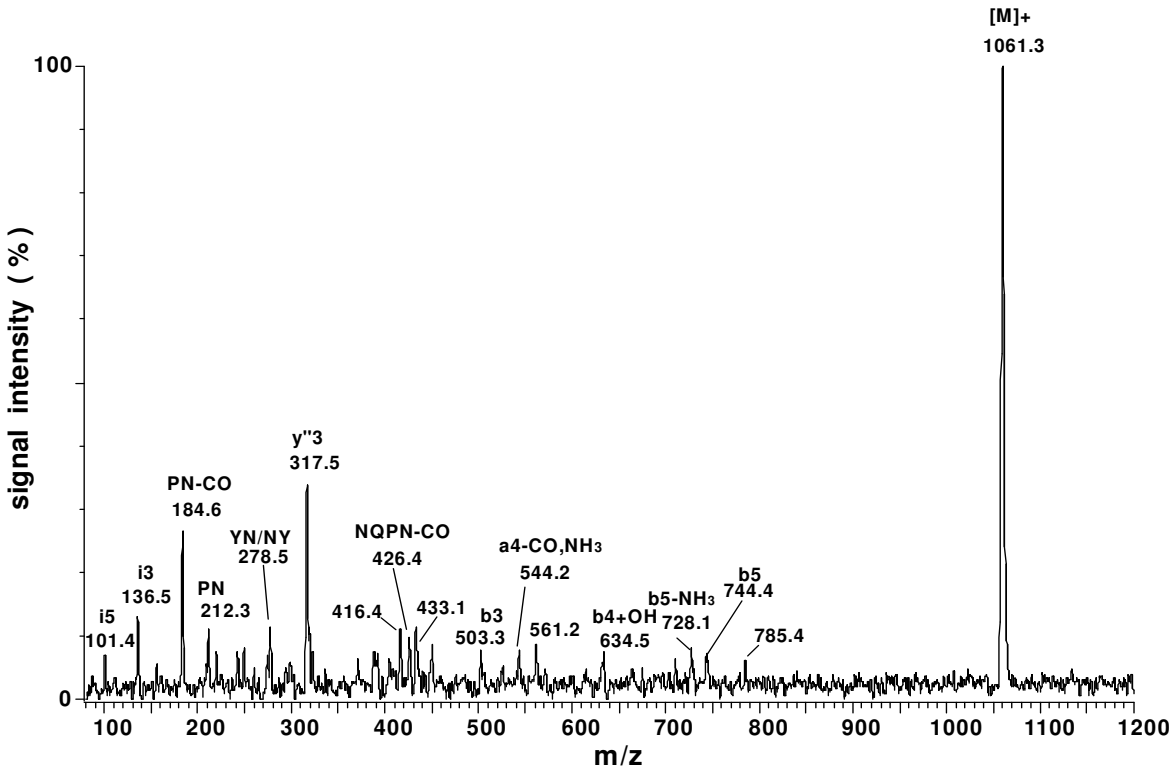

Figure 5.19 CID spectrum of $[M+H]^+$ at a collision energy of 30 eV and cone voltage of 70 V. Selection of the parent ion took place in MS_1 and fragmentation data was acquired by continuum mode scanning MS_2 from *m/z*=100 to 1200 at 100 atomic mass units/second for precisely six minutes.

Close inspection of fragments generated by CID revealed the specific interaction between 8-Beta and sodium. The major product ions from sodium cationised molecular species were N-terminal a_{n-m}, b_{n-m} and b_{n-m}+OH ions (n=7, m=0...6). Refer to Figs. 5.20 and 5.22, and Tables 5.2 and 5.3, for detailed product ion assignment. The pattern of predominantly N-terminal product ions from sodium adducts was also found by Teesch *et al.* [31, 32], in FAB-MS studies of alkali metal adducts of various peptides, and by Kanai *et al.* [36] in ESI-MS studies. Assignment of b_{n-m}+OH, rather than c_{n-m}, to some of the observed ions was favoured due to convincing evidence in literature describing the formation of this type of ion as a result of alkali metal cationisation [31-35, 52, 53]. Tang *et al.* [52] was the first to suggest that alkali metal cationisation leads to hydroxyl transfer from the C-terminal carboxyl to form

b_{n-m}+OH+Na product ions and not c-type ions as previously reported [36] (Fig. 5.21 A). Some a_{n-m}+Na−H product ions in the CID spectra of the cationised 8-Beta, as well as in the spectra from the b_{n-m}+OH+Na precursor ions, were also observed. Teesch *et al.* [31, 32] proposed the formation of a_{n-m}+Na-H product ions from precursors with the alkali metal ion complexed towards the N-terminal of the peptide with no involvement in an ionic bond with the C-terminal carboxylate.

Fragmentation of 8-Beta+1Na (*m/z* 1084.1, *m/z* expected 1084.2), under the CID conditions used, produced mostly only very low abundance product ions with relative intensity of 1-2% of the parent ion (Table 5.2, Fig. 5.20). The three major product ions were a dehydrated parent ion (*m/z* 1065.9) at 6.5% relative intensity, b_7+OH+Na−H (*m/z* 996.7) at 3.2% and b_7+Na−H (*m/z* 978.5) at 2.2%. The formation of b_7+Na−H product ion (probably via 1,2 elimination of OH from b_7+OH+Na [10]) indicated that the binding site of Na^+ is to the N-terminal side of the cleavage site. We also observed a_{n-m}+Na−H product ions in the CID spectra of *m/z*=996.7 product ion, in accordance with the evidence presented by Teesch *et al.* [31, 32]. This again indicates that the alkali metal ion is bound to the N-terminal side of the cationised 8-Beta.

Table 5.2 Summary of the observed product ions generated by CID of the singly cationised specie(s) of 8-Beta, namely 8-Beta + 1Na. Only product ions detected at signal intensities equal to or above 40000 were taken into account. (* = loss of side-chain to form *m*-ion; # = assignment confirmed by selection and fragmentation of product ion; C-terminal product ions indicated in italics)

***m/z* observed**	**intensity**	**relative intensity (%)**	**proposed fragment type**	***m/z* calculated**	**sequence**
1084.1	2853376	100.0	$[M+Na-H]^+$	1084.2	β-NC_{14}NYNQPNS
1065.8	185056	6.49	$[M+Na-H_2O-H]^+$	1065.2	β-NC_{14}NYNQPNS
1022.7	43200	1.51	m_8+Na-CO-3H	1023.2	β-NC_{14}NYNQPNS*
996.7	97188	3.41	b_7+OH+Na-H #	996.1	β-NC_{14}NYNQPN
978.5	63724	2.23	b_7+Na-H	979.1	β-NC_{14}NYNQPN
898.8	41684	1.46	a_7-CO-2H	899.1	β-NC_{14}NYNQPN*
880.8	40516	1.42	b_6+OH+Na-H #	881.0	β-NC_{14}NYNQP
739.6	50740	1.78	a_5+Na-H #	739.9	β-NC_{14}NYNQ
639.0	52448	1.84	b_4+Na-H #	639.8	β-NC_{14}NYN
580.5	*<40000*	*<1.4*	*y"$_5$+Na-#*	*580.5*	*NQPNS*
187.8	*41908*	*1.47*	*z'$_2$-NH_3*	*187.1*	*NS*

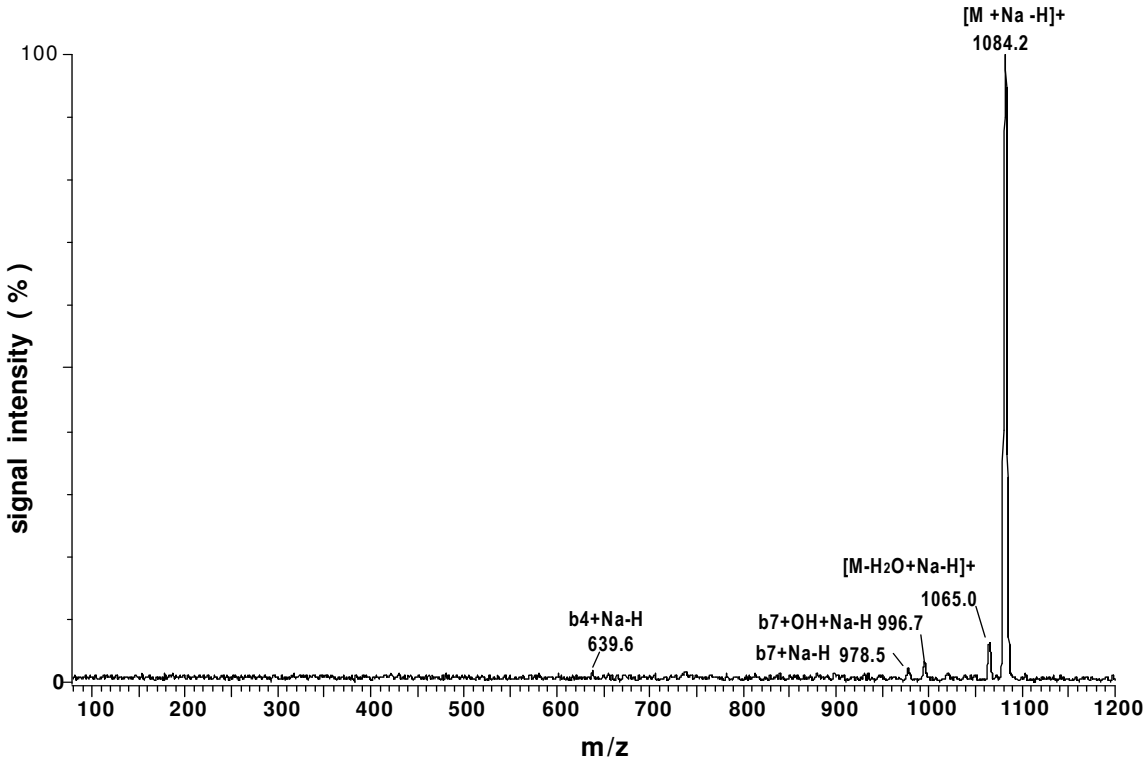

Figure 5.20 CID spectrum of $[M+Na]^+$ at a collision energy of 30 eV and cone voltage of 70 V. Selection of the parent ion took place in MS_1 and fragmentation data was acquired by continuum mode scanning MS_2 from *m/z*=100 to 1200 at 100 atomic mass units/second for precisely six minutes.

According to the mechanism depicted in Fig. 5.21 A, the C-terminal carboxyl (that of L-Ser_8 in 8-Beta) does not partake in an ionic interaction of the precursor ion with sodium, that is if no migration of the sodium took place. It is, however, possible that the formation of b_7+OH+Na−H was because of interaction with the C-terminal carboxyl group and the adjacent carbonyl oxygen of the peptide bond. Such a reaction mechanism, describing the loss of the C-terminal residues from alkali metal cationised peptides to form a "new peptide", was originally described by Renner and Spiteller [33] and endorsed by Thorne *et al*. [52] and Grese *et al*. [34, 35] (Fig. 5.21 B). In our studies the participation of C-terminal Ser_8 was indicated by a low abundance sodium adduct of x_1-type (*m/z* 154.1) observed in some of the CID spectra.

In contrast with the free peptide only very low abundance product ion from L-Gln_5-L-Pro_6 bond cleavages were detected, namely a_5+Na-H (*m/z* 739.6), indicating that the amide bond in this dipeptide unit is highly protected. This is of particular significance due to the well-characterised MS lability of the N-terminal peptide bond in which Pro residues participate [25, 28]. In an ESI-MS study of the fragmentation of alkali metal cationised peptaibols

(containing sub-sequences of α-aminoisobutyryl-prolyl) by Kanai *et al*. [37] such a protection of the N-terminal peptide bond of Pro by cationisation was not reported. We propose that the L-Gln_5 carbonyl oxygen in the peptide bond and the side-chain of L-Gln_5 participate in cationisation of 8-Beta. The participation of L-Gln_5 is also indicated by the absence (or very low abundance) of the w_{4a} product ion and the Gln immonium ion observed in the CID spectra of free 8-Beta.

The interpretation of these results is in accordance with that of Teesch *et al.* [31, 32] who used high resolution FAB-MS to study the interaction of various peptides with alkali metal ions. They concluded that alkali metal ions tended to complex to sites with basic carbonyl groups, such as the amide oxygen in Asn and Gln side-chains, and to the amide oxygen in the peptide bond. Further evidence of the association of sodium towards the N-terminal of 8-Beta is the observation of b_6+OH+Na−2H (*m/z* 880.8) and a_5+Na-H (*m/z* 739.6) and very low abundance b_4+OH+Na−H (*m/z* 656.9).

If the C-terminal carboxyl group participates in the reaction to form a b_n+OH product ion, it is important that the particular electrophilic carbonyl-carbons must be in close proximity to the nucleophilic group, which is either the hydroxyl group as in the Tang mechanism (Fig. 5.21 A) or carboxylate oxygen as in the Thorne mechanism (Fig. 5.21 B). In the case of 8-Beta, proximity of the peptide bond carbonyl of the dipeptide moiety, D-Asn_4-L-Gln_5, to the C-terminal carboxyl group, such as in a β-turn, would explain the observation of b_4+OH in the spectra of free and mono-sodiated 8-Beta. The structure of natural iturin A (as determined with NMR) includes a type II β-turn in each β-NC_{14}NYN and QPNS [4]. Molecular modelling studies on 8-Beta using HyperChem®4.5 (refer to Chapter 4), suggested two turns in the so-called S-structure, approximating β-turns, with a turn each in the N-terminal tetrapeptide (β-NC_{14}NYN) and C-terminal tetrapeptide (QPNS). These turn conformations place some of the peptide bond atoms in close proximity to the C-terminal carboxyl group and will also be conducive to multidentate and intrinsic binding of the alkali metal ions. The smallest fragments from the 8-Beta+1Na parent ion still associated with sodium were b_4 (*m/z* 639.0) and low abundance y''_5 (*m/z* 580.5) product ions corresponding to β-NC_{14}NYN and NQPNS respectively (Fig. 5.20, Table 5.2). The presence of sodiated N- and C-terminal product ions may be explained by the presence of two intrinsic binding sites (possibly two β-turns) for sodium in 8-Beta and at least two types of singly cationised parent ions. The existence of two

such cationised species may also explain the two “cone voltage maxima” observed for mono-sodiated 8-Beta (Fig. 5.11).

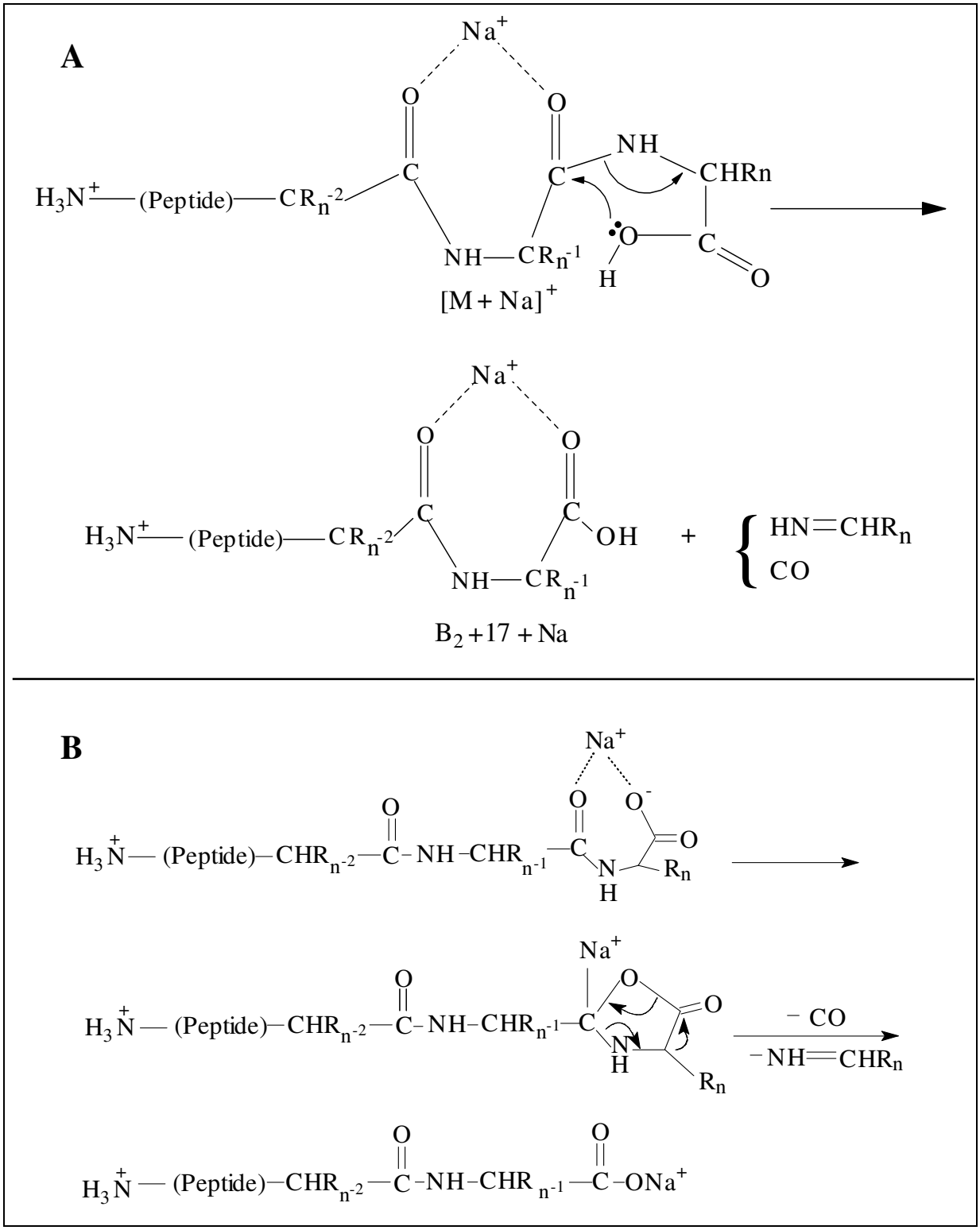

Figure 5.21 Mechanisms describing the b_n+OH+Na−H product ion formation: (A) Tang mechanism [51] (B) Thorne mechanism [52].

The multi-sodiated 8-Beta species were more inclined to fragment than the mono-sodiated 8-Beta. The CID of di-sodiated 8-Beta (expected *m/z* 1106.2, observed MS_2 *m/z* 1105.4) again produced sodiated b_{n-m}+OH, and a_{n-m} type product ions, a deaminated parent ion (*m/z* 1088.1) and a high abundance (17.5%) of m_8+2Na-2H product ion (*m/z* 1075.4, produced by the loss of the Ser-side-chain) (Fig. 5.22, Table 5.3). The smallest fragment, still associated to two sodiums, was b_7+OH+2Na−2H (*m/z* 1017.8) at 2.7% intensity. The corresponding low abundance a_7 product ion (*m/z* 949.8) contained only one sodium, which is an indication that at least one sodium is bound towards the N-terminal side of the peptide. Other N-terminal product ions, identical to that found for mono-sodiated 8-Beta, namely b_6+OH+Na-2H (*m/z* 881.7) at 3.6% intensity and a_5+Na-2H (*m/z* 739.1) at 2.1% intensity were observed. No product ions corresponding b_4+OH+Na were observed, which could possibly be the result of a subtle conformational change. A product ion with *m/z* 384.1, observed at 7.9% intensity, was assigned to $[x_6+Na-H]^{2+}$ after exhaustive secondary product ion CID. This assignment was also substantiated by the observation of other C-terminal product ions of sodiated x_6-type (*m/z* 769.6; 735.7) and the a_2 (*m/z* 313.3) N-terminal product ion. The formation x_6-type ions would require increased lability and/or exposure of the bond between the C_α of D-Asn_2 and the amide bond carbonyl carbon. The participation of the D-Asn_2 amide oxygen in interaction of the C-terminal side of the peptide with sodium may increase the stability (by increased double bond character) of the amide bond and/or expose the neighbouring bond. The participation of other amide bond atoms (amide bond oxygens of L-Gln_5, D-Asn_4 and D-Tyr_3) and basic groups (L-Gln_5 side-chain) with sodium are indicated by the absence (or very low abundance) of certain product ions, such as L-Gln_5 and D-Tyr_3 immonium ions, w_{a4} and sodiated b_4-type product ions. The smallest fragments bound to one sodium, from CID of di-sodiated 8-Beta, were a_5+Na-H (β-NC_{14}NYNQ; *m/z* 739.1) and y''_5 +Na−NH_3−H (NQPNS; *m/z* 566.1) (Fig. 5.22, Table 5.3). These results indicated that the major binding sites for sodium in di-sodiated 8-Beta are similar to those proposed for the mono-sodiated 8-Beta, and probably multidentate in both cases.

Table 5.3 Summary of the observed product ions generated by CID of the di-cationised specie(s) of 8-Beta, namely 8-Beta + 2Na. Only product ions detected at signal intensities equal or above 40000 were taken into account. (* = loss of side-chain to form *m*-ion; # = assignment confirmed by selection and fragmentation of product ion; ? = inconclusive results from product ion fragmentation; C-terminal product ions are indicated in italics)

***m/z* observed**	**intensity**	**relative intensity (%)**	**proposed fragment type**	***m/z* calculated**	**sequence**
1105.4	2270464	100.0	$[M+2Na-3H]^+$	1105.2	β-NC_{14}NYNQPNS
1088.1	58940	2.60	$[M+2Na-NH_2-2H]^+$	1088.2	β-NC_{14}NYNQPNS
1075.4	397632	17.51	m_8+2Na-2H	1075.2	β-NC_{14}NYNQPNS*
1017.8	60808	2.68	b_7+OH+2Na-2H #	1018.1	β-NC_{14}NYNQPN
949.8	<40000	<1.8	a_7+Na-H #	950.2	β-NC_{14}NYNQPN
881.7	81256	3.58	b_6+OH+Na-H #	881.0	β-NC_{14}NYNQP
739.1	46580	2.05	a_5+Na-H #	738.9	β-NC_{14}NYNQ
735.7	*40820*	*1.80*	*x_6+Na-2NH_3-H #*	*735.7*	*YNQPNS*
563.9	*< 40000*	*<1.8*	*y''_5+Na-H-NH_3 #*	*563.5*	*NQPNS*
555.4	68656	3.02	$[M+2Na+2H]^{2+}$ #	554.6	β-NC_{14}NYNQPNS
458.3	44000	1.94	a_3-NH_2	457.6	β-NC_{14}NY
384.1	179008	7.88	$(x_6+Na-H)^{2+}$ #	385.4	β-NC_{14}NYNQ
362.3	40636	1.79	b_2+Na-H ?	362.5	β-NC_{14}N ?
322.4	74964	3.30	b_2-H_2O ?	322.5	β-NC_{14}N ?
313.3	55312	2.44	a'_2	313.5	β-NC_{14}N

The fragmentation pattern of 8-Beta+3Na changed with pre-incubation time (age of sample) and because of this unpredictability and its very low abundance it was decided not to study this cationised specie in detail. It is, however, possible to predict from the data presented that the third binding site is probably due to ionic interaction between the carboxyl group of L-Ser_8 and sodium. This explains the low abundance of the 8-Beta+3Na molecular specie. Under the experimental conditions used in this study, it was not possible to show interaction between D-Tyr_3 and sodium, a putative binding site of the fourth sodium that was observed in aged samples and at high pH. The fragmentation patterns obtained with 8-Beta as model peptide and sodium as cation substantiated previous results (Figs. 5.13, 5.18).

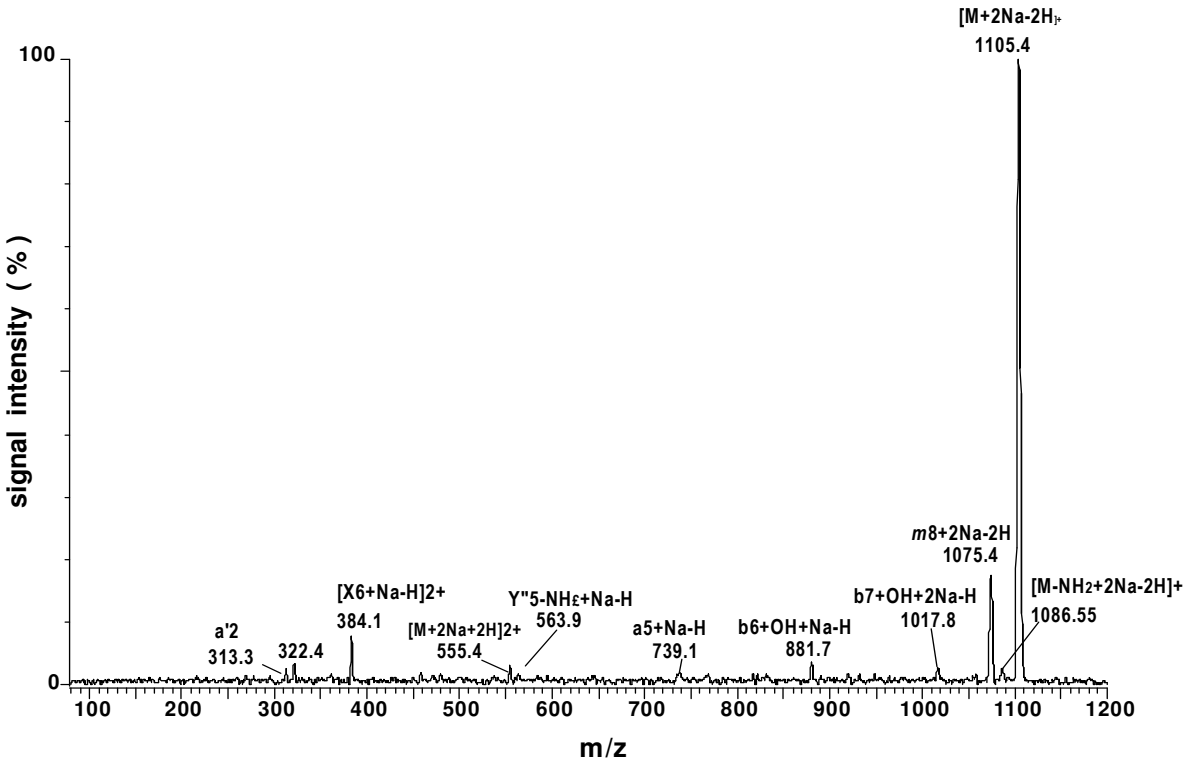

Figure 5.22 CID spectrum of $[M+2Na-H]^+$ at a collision energy of 30 eV and cone voltage of 70 V. Selection of the parent ion took place in MS_1 and fragmentation data was acquired by continuum mode scanning MS_2 from m/z=100 to 1200 at 100 atomic mass units/second for precisely six minutes.

5.5 Conclusions

The stable nature and ease of detection of 8-Beta and its cationised species allows the use of ESI-MS to study the specific interactions of 8-Beta and alkali metals. The cationisation of 8-Beta with sodium takes place in the solution and the complexation equilibrium is slow. Furthermore, under ESI-MS conditions, the lipopeptide-sodium interaction is not influenced by solvent polarity and is also independent of pH over a broad range. From the pH study it was further deduced that there are at least four binding sites for sodium to 8-Beta of which two, the C-terminal carboxylate and the side-chain of tyrosine, can take part in ionic interaction with sodium. Results from the pH study also showed that the pH is not as important as the concentration of the counter anions in the sample solvent. We also found, as did other investigators [43-45], that the influence of solvent counter ions on ionisation during the electrospray process must not be underestimated.

The optimum ionisation conditions for this study was determined with 8-Beta as model peptide and Na^+ as model ion. It was decided to conduct future studies with cone voltage set at 70 V, the apparent optimum from "cone voltage profiles" for comparative studies of the singly charged molecular species $[M+H]^+$ and $[M+Na]^+$. At this cone voltage, however, the signals of $[M+2Na–H]^+$ and $[M+3Na-2H]^+$ are somewhat underestimated. A carrier solvent of 50% acetonitrile in water was found to be suitable for dissolving the lipopeptide and for the ESI-MS analyses of the peptide sodium complexes. The same sample solvent composition, modified with 0.05% TFA and 10 mM NaCl, was chosen as the reference sample solvent for subsequent studies in which the stability and structures of the sodiated 8-Beta species were determined.

The interaction with sodium was influenced by the primary structure of the linear peptides, as a higher abundance of sodiated species of the longer peptides was observed. This is probably the result of the sequential elimination of the N-terminal β-turn in the shorter peptides. The cyclic peptides only bound to one sodium with a slightly higher abundance observed for sodiated cyclic 7-Beta, having a smaller cyclic cavity, than the sodiated cyclic 8-Beta. This is an indication of a cation binding site inside the peptide ring.

Very little fragmentation of 8-Beta and 7-Beta and the cyclic lipopeptides (with and without 10 mM NaCl) was observed at 70 V cone voltage. The shorter peptides fragmented substantially at 70 V, but some stabilisation by sodium was observed with 20% less fragmentation of 5-Beta and 5% less fragmentation of 6-Beta in the presence of 10 mM NaCl. This complexation to sodium therefore protected some of the very labile peptide bonds from cone voltage induced dissociation. Stability was specifically conferred by protection of the very labile L-Gln-L-Pro peptide bond in the sodiated peptide species. The difference in lability between the mono-sodiated and di-sodiated species in 8-Beta is possibly the result of better stabilisation of the labile D-Tyr_3-D-Asn_4 bond in the mono-sodiated specie. The fragmentation patterns observed for each of the sodiated species of 8-Beta were in accordance with the findings of Teesch *et al.* [31, 32], although these results did indicate limited interaction between the C-terminal carboxylate and sodium. Fragmentation of 8-Beta and its cationised species revealed two intrinsic binding sites for non-solvated sodium ions situated in the N-terminal peptide moiety, β-NC_{14}NYN(Q) and C-terminal peptide moiety, NQPNS (Fig. 5.23). The structure of natural iturin A includes a type II β-turn in each β-NC_nNYN and QPNS [50]. This type of turn conformation in the linear peptides could position the peptide chain in such a

way that multidentate binding of ions and the formation of b_{n-m}+OH ions are facilitated. The interaction of alkali metal ions with the two peptide moieties was also confirmed by the observed association between alkali metal ions and the shorter lipopeptides. The alkali metal ion selectivity sequence of all the lipopeptides was $Na^+ > K^+ > Rb^+$, indicating a size limitation in the interaction cavity or cavities. It is proposed that interaction of non-solvated sodium with most of the amide bond oxygens in the predicted turns, specifically that of β-NC_{14}, Asn_2 and Tyr_3 in turn A (β-NC_{14}NYN) and that of Gln_5 and Pro_6 in turn B (QPNS), and with the Gln_5 side-chain, provide the protection against low energy fragmentation of sodiated 8-Beta species during ESI-MS (Fig. 5.23).

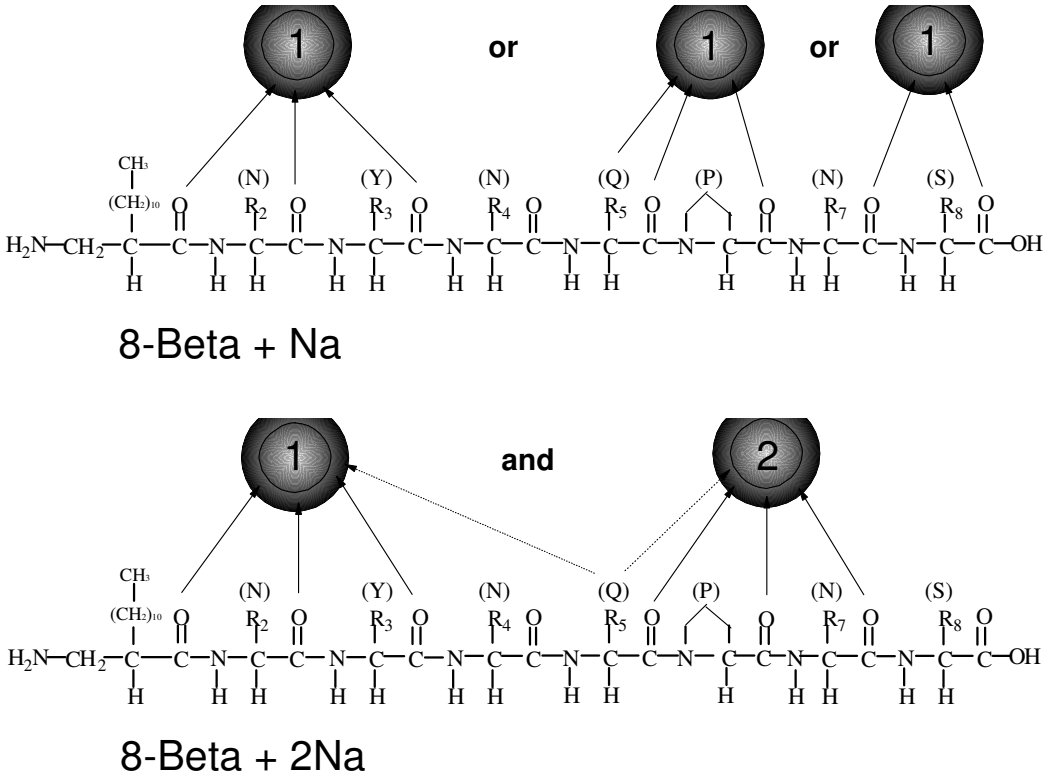

Figure 5.23 Proposed association between 8-Beta and sodium. All the interaction possibilities with 8-Beta predicted from CID fragmentation patterns of the mono-sodiated and di-sodiated 8-Beta.

One of the low energy structures of 8-Beta*D (*indicates the substitution of β-NC_{14} residue with a β-NC_5 residue for modelling purposes) predicted by HyperChem®4.5 is a backbone structure in the shape of a twisted S (S-structure) which includes two turns approximating β-turns (refer to Chapter 4). A model of this structure complexed to two sodium ions is depicted in Fig. 5.24. The proposed interaction is between one sodium and the carbonyl oxygens of β-NC_{14}, Asn_2 and Tyr_3 in turn A and between the second sodium and the carbonyl oxygens of

Gln_5 and Pro_6 in turn B. The atomic distance between the turn B carbonyl oxygens of Gln_5 and Pro_6 in the model is 3.56 . The triangular distances in turn A is 2.94 between the carbonyl oxygens of β-NC_{14} and Tyr_3, 4.15 between carbonyl oxygens of β-NC_{14} and Asn_2, and 3.36 between chain carbonyl oxygens of Asn_2 and Tyr_3. These gaps are adequate to allow the interaction of two or more of the oxygens with a alkali metal ion in the turn cavities.

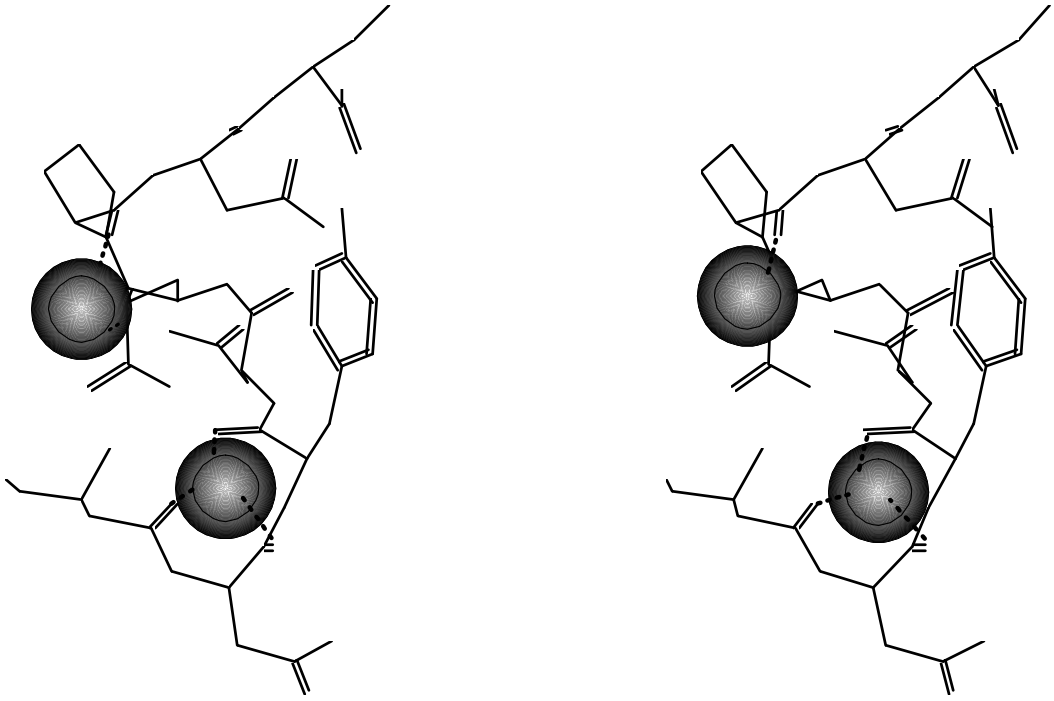

Figure 5.24 Stereotypgraphs of the predicted S-structure of 8-Beta*D showing the one of the possible structures including two sodium ions.

It is clear that each of the predicted turns in the so-called S-structure may serve as interaction cavities. The omission of amino acid residues in these cavities, as in 5-Beta an 6-Beta, leads to a diminished capacity to bind a second larger cation. Association of the cation in the interior of the peptide ring of the cyclic peptides is proposed from the absence of or observation of only low abundance di-cationised complexes, and the slightly better association of the cyclic heptalipopeptides. The inclusion of a second cation may be unfavourable because of electrostatic repulsion. This resembles valinomycin accommodating a single cation in its cyclic cavity [49] and not gramicidin S which binds the alkali metal cations on its exterior [48]. It is therefore hypothesised that alkali metal ions can bind in either one of the two β-turns in the peptide ring of natural iturin A molecule, with the carbonyl oxygens as chelating atoms. The specific interaction of the iturin A_2 analogues with alkali metal cations may point

to some role of this interaction with its biological activity which will be addressed in Chapters 6 and 7.

5.6 References

1. Franklin T. J., Snow G. A. (1981) Biochemistry of antimicrobial action 3rd Ed., Chapmann and Hall, London, pp. 67-72

2. Wang K., Gokel G. W. (1996) *Pure Appl. Chem.* **68**, 1267-1272

3. Battersby A. B., Craig L. C. (1951) *J. Am. Chem. Soc.* **73**, 1887-1888;
Hodgkin D. C., Oughton B. M. (1957) *Biochem. J.* **65**, 752-756

4. Marion D. Genest, M., Caille A., Peypoux, F., Michel G., Ptak M. (1986) *Biopolymers*, **25**, 153-170

5. Besson F., Peypoux F., Quentin M. J., Michel G. (1984) *J. Antibiotics* **37**, 172-177;
Latoud C., Peypoux F., Michel G., Genet R., Morgat J. L. (1986) *Biochim. Biophys. Acta* **856**, 526-535;
Latoud C., Peypoux F., Michel G. (1987) *J. Antibiot*ics **40**, 1588-1595

6. Maget-Dana R., Peypoux F. (1994) *Toxicology* **87**, 151-174

7. Besson F., Michel G. (1991) *Microbios.* **65**, 15-21

8. Wooley G. A., Wallace B. A. (1992) *J. Membr. Biol.* **129**, 109-136

9. Bevins C. L., Zasloff M. (1990) *Annu. Rev. Biochem.* **59**, 395-414

10. Ganz T., Oren A., Lehrer R. I. (1992) *Med. Microbiol. Immunol.* **181**, 99-105

11. Boman H. G., Faye I., Gudmundson G. H., Lee J.-Y., Lidholm D.-A (1991) *Eur. J. Biochem.* **201**, 23-31

12. Nakamura T., Hagiwara K., Miyata T., Tokunaga F., Muta T., Iwanaga S. (1988*) J. Biol. Chem.* **263**, 16709-16713

13. Marshall G. R., Beusen D. D. (1994) The structural basis of peptide channel formation, In: Advances in Chemistry Series, Volume 235 (Eds. Blank M., Vodynoy I.) American Chemical Society, pp. 259-314

14. Rao A. G. (1995) *MPMI* **8**, 6-13

15. Frensdorff H. K. (1971) *J. Am. Chem. Soc.* **93**, 600-606;
Pederson C. J., Frensdorff H. K. (1972) *Angew. Chem. Int. Ed. Engl.* **11**, 16-25

16. Barber M., Bordoli R. S., Garner D. B., Gordon, R. D., Sedgwick, R. D., Tyler A. N. (1981) *Biochem. J.* **197**, 401-404

17. Hillenkamp F., Karas M., Beavis R. C., Chait B. T. (1991) *Anal. Chem.* **63**, 1193-1202

18. Dole M., Hines R. L., Mack R. C., Mobley R. C., Ferguson L. D., Alice M. B. (1968) *J. Chem. Phys.* **49**, 2240-2249;
Fenn J. B. (1993) *J. Am. Chem. Soc. Mass Spectrom.* **4**, 524-535

19. Gaskell S. J. (1997) *J. Mass Spectrom.* **32**, 677-688

20. Mann M. (1990) *Org. Mass Spectrom.* **25**, 575-587;
Fenn J. B., Mann M., Meng C. K., Wong S. F., Whitehouse C. M. (1990) *Mass Spectrom. Rev.* **9**, 37-70;
Smith R. D., Loo J. A., Loo R. R. O., Bussman M., Udseth H. R. (1991) *Mass Spectrom. Rev.* **10**, 359-451

21. Sinzdak G. (1996) Mass spectrometry for Biotechnology, Academic Press, San Diego

22. Przybylski M., Glocker M. (1996) *Angw. Chem. Int. Ed. Engl.* **35**, 806-826;
Miranker A., Robinson C.V., Radford S. E., Dobson C. M. (1996) *FASEB J.* **10**, 93-101

23. Roepstorff P., Fohlman J. J. (1984) *Biomed. Env. Mass Spectrom.* **11**, 601

24. Biemann K. (1988) *Biomed. Env. Mass Spectrom.* **16**, 99-111

25. Vékey K. (1995) *Mass Spectrom. Rev.* **14**, 195-225

26. Vékey K., Candido M., Traldi P. (1990) *Rap. Commun. Mass Spectrom.* **4**, 74-76;

27. Tang X., Boyd R. K. (1992) *Rap. Commun. Mass Spectrom.* **6**, 651-657

28. Schwartz B. L., Bursey M. M. (1992) *Biol. Mass Spectrom*. **21**, 92-96;
Loo J. A., Edmonds C. C., Smith R. D. (1993) *Anal. Chem.* **65**, 425-438

29. Burlet O., Orkiszewski R. S. Ballard K. D., Gaskell S. J. (1992) *Rap. Commun. Mass Spectrom.* **6**, 658-662

30. Honig B., Nochols A. (1995) *Science* **268**, 1144-1149

31. Teesch, L. M., Orlando, R. C., Adams, J. (1991) *J. Am. Chem. Soc*. **113**, 3668-3675,

32. Teesch L. M., Adams J. (1991) *J. Am. Chem. Soc.* **113**, 812-820

33. Renner D., Spiteller G. (1988) *Biomed. Env. Mass Spectrom.* **15**, 75-77

34. Grese R. P., Cerny R. L., Gross, M. L. (1989) *J. Am. Chem. Soc.* **111**, 2835-2842

35. Grese R. P., Gross M. L. (1990) *J. Am. Chem. Soc.***112**, 5098-5104

36. Mallis L. M., Russel D. H. (1986) *Anal. Chem*. **58**, 1079-1080

37. Kanai M., Iida A., Nagoaka Y., Wada S., Fuijita, T. (1996) *J. Mass Spectrom*. **31**, 177-183.

38. Wang J., Ke F., Sui K.W.M., Guevremont, R. (1996) *J. Mass Spectrom*. **31**, 159-168

39. Giogi G., Ginanneschi M., Chelli M., Papini M., Laschi F., Boghi E. (1996) *Rapid Commun. Mass Spectrom.* **10**, 1266-1272

40. Mann M. (1990) *Org. Mass Spectrom.* **25**, 575-587

41. Van Berkel G. J., Zhou F., Aronson, J. T. (1996) Proceedings: The 44th ASMS conference on mass spectrometry and allied topics, Portland, Oregon, USA, p. 1088

42. Yen T.-Y., Charles M. J., Voyksner R. D. (1996) *J. Am. Chem. Soc.* **7**, 1106-1108

43. Wang G., Cole R. B. (1996) *J. Am. Soc. Mass Spectrom.* **7**, 1050-1058

44. Mirza U. A., Chait B. T. (1994) *Anal. Chem.* **66**, 2898-2904

45. Wang G., Cole R. B. (1994) *Anal. Chem.* **66**, 3702-3708

46. Zhou S., Hamburger M. (1995) *Rapid Commun. Mass Spectrom.* **9**, 1516-1521

47. Zhou S., Hamburger M. (1996) *Rapid Commun. Mass Spectrom.* **10**, 797-800
Wang G., Cole R. B. (1997) Proceedings: The 45th ASMS conference on mass spectrometry and allied topics, Palm Springs, California, USA, p. 373

48. Gross D. S., Williams E. R. (1996) *J. Am. Chem. Soc*. **118**, 202-204

49. Marrone T. J., Kenneth M. M. Jr. (1995) *J. Am. Chem. Soc*. **117**, 779-791

50. Masterton W. L., Slowinski E. J. (1977) Chemical Principles, Fourth Edition SI Version,W. B. Saunders Company, Philadelphia, pp. A8, A9

51. Tang X., Ens W., Standing K. G., Westmore J. B. (1988) *Anal. Chem*. **60**, 1791-1799

52. Thorne G. C., Ballard K. D., Gaskell S. J. (1990) *J. Am. Chem. Soc*. **1**, 249-257

Chapter 6

Hydrophobic properties and biological activity of iturin A_2 analogues

6.1 Introduction

The interaction of antimicrobial peptides with membranes and hydrophobic environments is crucial for their biological activity. Knowledge about the hydrophobicity of an antimicrobial peptide would be of great help in an understanding of their interaction with membranes. The retention of peptides by the hydrophobic octadecanoylsilane matrix (ODS or C_{18}), commonly used as packing material in HPLC, can be used as a measure of the peptides' solution-phase hydrophobicity—the more hydrophobic the peptide, the longer it will be retained. In assessing the purity of the synthetic iturin A_2 analogues (Chapter 2) it was observed that primary structure influenced HPLC behaviour. This chapter describes the analysis of the HPLC behaviour of the iturin A_2 analogues in terms of their hydrophobic nature and interaction with membranes.

Peptides that are membrane-active are amphipathic because interaction occurs at the interface between the hydrophobic aliphatic chains and the hydrated polar head groups of the membrane lipids. Accordingly, most antimicrobial peptides are amphipathic, for example, when interacting with membranes, the cationic magainins adopt an amphipathic α-helical conformation [1] and the cationic defensins an amphipathic β-sheet conformation [2]. Iturin A_2 is amphipathic because of the inclusion of the hydrophobic β-aminotetradecanoic acid (β-NC_{14}) in its otherwise polar structure [3]. The omission of the aliphatic chain destroys all biological activity [4].

After interaction with the membrane, many antimicrobial peptides form characteristic ion channels [5, 6] by self-aggregation and self-assembly in the membrane [7]. Aggregation of the iturin A_2 analogues was observed during purification and general handling (Chapter 2). In this chapter the aggregation of some of the linear iturin A_2 analogues will be discussed. Induction of secondary structures, possibly β-pleated sheet structures, caused by self-assembly of the

synthetic iturin A_2, was observed upon interaction with dimiristoylphosphatidylcholine (DMPC) liposomes (Chapter 4). The natural iturin A also tends to aggregate in membranes [8, 9], forming complexes with an ion-pore character [10-12]. The precise structure and composition of ion-conducting pores are as yet unknown. It was previously found that the iturin A aggregates or complexes in DMPC membranes consisted of only iturin A molecules [13], but in the presence of membrane sterols these complexes included cholesterol (1:1) or ergosterol (2:3) [13] (also refer to Chapter 1 and [3]). Maget-Dana and Peypoux [3] proposed the binding of cations in the iturin A ion-pores to explain their weak anion selectivity. In this study the synthetic iturin A_2 and the other analogues showed sequence specific interaction with alkali metal ions with higher selectivity for Na^+ than for K^+ (Chapter 5).

The target cell specificity of antimicrobial peptides depends on recognition of the target membrane. Some antimicrobial peptides can recognise specific lipids; for example, the cyclic antibiotic peptide, Ro09-0198, recognises phosphatidylethanolamine (PE) [14]. Magainins preferentially interact with bacterial membranes that contain lipopolysaccharides and mainly neutral PE and acidic phosphatidylglycerol in the outer monolayer of the membrane [15]. Melittin on the other hand has an affinity for erythrocyte membranes containing cholesterol and zwitterionic (neutral) phospholipids such as phosphatidylcholine (PC) and sphingomyelin [15]. This peptide also possesses antibacterial activity. Iturin A interacts with membranes containing PC and membrane sterols, such as cholesterol or ergosterol [13, 16-18]. Consequently, iturin A possibly recognises cholesterol or ergosterol and PC in eukaryotic target cells such as erythrocytes [8, 18, 20] and fungi [16, 17, 19, 21]. The recognition mechanism of one of the few prokaryotic target cells of iturin A, *Micrococcus luteus* [22-24], is unknown because it does not contain PC or membrane sterols in its membrane [25]. The precise role of iturin A's primary structure in the recognition of target cell membranes is unclear. The influence of iturin A's peptide moiety on the interaction with DMPC liposomes will be discussed in this chapter.

Living organisms are usually selective with respect to the chiral configuration of compounds, but the recognition of their membranes by most antimicrobial peptides does not seem to be stereoselective. Wade *et al.* [26] found that D-enantiomers (exact mirror images) of cecropin A, magainin 2 amide, melittin and some cecropin-melittin hybrids retained their antimicrobial activity. These enantiomeric D-peptides retained their amphipathic structure, but as left handed amphipathic α-helixes. It was also observed by Merrifield *et al*. [27] that a mixture of

D-peptides and L-peptides did not influence membrane activity and channel formation. They also tested a peptide with the N-terminal end containing D-amino acids and the C-terminal end L-amino acids that retained all membrane activity. Chen *et al.* [28], however, observed that substitution of three L-Ala residues with D-Ala to form magainin H lead to reduced antibacterial activity. Dathe *et al.* [29] found that double D-amino acid replacements in a model amphipathic antimicrobial peptide either increased or decreased its bioactivity. This type of replacement of some amino acid residues with their enantiomers leads to the formation of diastereomers and bioactivity depended on the extent of conformational disruption of the model peptide's amphipathic α-helix. Enantiomeric amino acid substitution leads to the formation of diastereomers of which bioactivity depended on the extent of conformational disruption of the peptide's amphipathic α-helix. Merrifield [27] proposed that the general amphipathic conformation of the antimicrobial peptides must be retained for activity and that sequence composition and charge are important, but that peptide length, chirality and amide bond direction are not. It is apparent that these peptides are not involved in chiral interaction with a receptor molecule or membrane lipids. This may not be the case with iturin A, because the possibility of stereospecific interaction with target cell membranes has been suggested. Phospholipases in the target cell membrane may act as chiral receptors, as activation by iturin A of these enzymes in membrane vesicles of *Saccharomyces cerevisiae* was observed [30]. Furthermore, changes in the invariant tetrapeptide moiety, β-amino fatty acyl-L-Asn_2-D-Tyr_3-D-Asn_4, resulted in diminished activity. An inactive derivative of iturin A, iturin C, has a L-Asp_2 instead of the L-Asn_2 in this moiety [18, 31]. The O-methylation of the D-Tyr_3 residue in iturin A decreased antifungal and haemolytic activity [32] and also modified its interaction with membranes [12, 33]. Another explanation for the loss of bioactivity could be that the amino acid modifications change the conformation of the iturin, resulting in inactive membrane complexes (no ion-pore formation and membrane disruption). It was found that the configuration of the β-NC_{14} residue did not greatly influence conformation of synthetic iturin A_2 diastereomers in DMPC liposomes. Cyclisation on the other hand had a marked influence, resulting in a different conformation from that of the linear iturin A_2 analogues (Chapter 4). In this chapter we report on the influence of cyclisation, the configuration of the β-NC_{14} residue, and omission of L-Asn_2 on bioactivity. The lytic activity was investigated using *M. luteus* and rabbit erythrocytes as target cells. Antimicrobial activity was evaluated by growth inhibition of the gram-positive bacterium, *M. luteus,* and the fungus, *Botrytis cinerea*, one of the post-harvest pathogens of stone fruit and grapes.

6.2 Materials

Freezer stock cultures of *Micrococcus luteus* were donated by Dr. B. J. H. Janse, department of Microbiology, University of Stellenbosch. Spores from *Botrytis cinerea* were donated by Prof. G. Holz, department of Plant Pathology, University of Stellenbosch. Chloroform (99%), NaCl, Triton X100, NaCl, potassium dihydrogen phosphate, disodium hydrogen phosphate, formaldehyde, sucrose, glucose, sodium citrate and citric acid were from Merck (Darmstadt, Germany). Bacto® tryptone, Bacto® tryptone soy broth and Bacto® yeast-extract were from DIFCO Laboratories (Detroit, USA). Agar powder was form Saarchem (Krugersdorp, South Africa) and low electroendosmosis-type agarose (LE-D1) was from Whitehead Scientific (Brackenfell, South Africa). Lysozyme was from Serevac (Cape Town, South Africa), 2-amino-2-(hydroxymethyl)-1,3-propandiol-hydrochloride (Tris-HCl) was from Boehringer (Mannheim, Germany) and Sepharose 4B from Pharmacia (Uppsala, Sweden). Casein and Tween 20 were from Fluka Chemicals (Buchs, Switzerland). Microtitre plates (Nunc™-Immuno Maxisorp) were from Nalge NUNC International (Roskilde, Denmark), Falcon® tubes from Becton Dickinson Labware (Lincoln Park, USA) and microcentrifuge tubes and culture dishes from Quality Scientific Plastics, USA. Bee-venom melittin and dimyristoyl-L-α-phosphatidylcholine (DMPC) were from Sigma Chemical Co. (St. Louis, USA). Acetonitrile (HPLC-grade, UV cut-off 190 nm) and methanol (HPLC-grade, UV cut-off 205 nm) were from Romil LTD (Cambridge, UK). Nova-Pak analytical C_{18} HPLC columns and 0.45 mikron HV membrane filters were from Millipore-Waters (Milford, USA). Nitrogen gas was supplied by Afrox, South Africa. Analytical grade water was prepared by filtering glass distilled water through a Millipore Milli Q® water purification system. The linear lipopeptides (6-Beta, 7-Beta and 8-Beta) and some cyclic analogues (cyclic 8-Beta and cyclic 7-Beta) were synthesised using the Fmoc-polyamide peptide synthesis protocol and purified using semi-preparative HPLC (described in Chapter 2).

6.3 Methods

6.3.1 RP-HPLC of peptides

Analytical reverse phase HPLC was done on a C_{18} Nova-Pak column, as part of the purity assessment of the lipopeptide peptide preparations (reported in Chapter 2). Capacity factors (k') for the HPLC separations were calculated using the following relationship:

$$k' = (R_t - R_{to}) / R_{to}$$

with R_t the retention time of the peptide and R_{to} that of acetone or water

Concentration dependent and time dependent aggregation were also monitored using the HPLC analysis described in Chapter 2, section 2.3.6.2. Freshly prepared solutions, containing an 8-Beta diastereomeric mixture (concentration range from 0.5 to 5.0 mg/mL), were subjected to HPLC to assess concentration dependent aggregation. A freshly prepared solution of 7-Beta (1.0 mg/mL) was also subjected to HPLC. After long term storage (±30 days) of the peptide solution at −20°C and it was again subjected to analytical HPLC. Aggregation was calculated from the following relationship:

$$\text{Aggregation} = \frac{\text{HPLC peak area of aggregated peptide}}{\text{peak area of free peptide + peak area of aggregated peptide}}$$

6.3.2 Interaction with phospholipid vesicles

6.3.2.1 Preparation of DMPC-vesicles [adapted from 34]

Small unilamellar vesicles were prepared by dissolving 50 mg dimyristoyl-L-α-phosphatidylcholine (DMPC) in 2 mL chloroform in a detergent free thin-walled glass test tube. The chloroform was evaporated either under a stream of N_2 or under vacuum (rotary evaporator) to leave a thin film of lipid on the glass. The lipid was resuspended in 5 mL 50 mM Tris.HCl[a], pH 8.3 containing 150 mM NaCl and flushed with N_2. The lipid-buffer mixture was sonicated in a sonic bath, half filled with 0.1% (v/v) Triton X100[b], until the solution was translucent. The transition temperature of DMPC is 24°C and it was therefore necessary to prepare the liposomes at 35-37°C[c]. The duration of sonication was 60±10 minutes (the duration depended on lipid concentration, temperature and energy transfer). The preparation normally resulted in roughly uniform sized SUV's of about 25 nm in diameter. (Liposomes have been reviewed extensively in [34, 35].)

[a] Any buffer may be used. The osmotic balance of the vesicle must, however, be maintained to prevent swelling, lysis or dehydration. The inert N_2 atmosphere is important to stop oxidation of unsaturated fatty acids.

[b] The detergent in the sonic bath helps with the energy transfer. It is very important to obtain maximum agitation of the lipid by optimal positioning of the enclosed test tube in the sonic bath. Bath temperature must also be controlled to prevent overheating.

[c] Liposome formation under the transition temperature (gel state to fluid state) is thermodynamically unfavourable and best results are obtained at temperatures above the transition temperature.

6.3.2.2 Interaction with DMPC [13, 35]

The DMPC liposomes, prepared as described in 6.3.2.1, were "purified" by passing it through a Sepharose 4B column (±100 mL bed volume) equilibrated with 0.15 M NaCl (35°C). The peak fraction absorbing at 330 nm was collected and used directly in the peptide interaction study. The purified DMPC vesicles were mixed in a 125:10 ratio (m/m) with each of the HPLC purified linear lipopeptides (diastereomeric mixtures). The mixture was then loaded on a Sepharose 4B column (4.5 mL bed volume), saturated beforehand with phospholipid to reduce non-specific interaction, and eluted with 0.15 M NaCl at 35°C. Peptide concentration was determined by UV spectrophotometry using standard curves described under 6.3.2.3. Lipid concentration was determined by the Stewart assay described under 6.3.2.4.

6.3.2.3 Determination of peptide concentration

Standard curves were used to determine the peptide concentration in DMPC liposome interaction experiments. Peptides were dissolved in 0.15 M NaCl; a concentration series from 10 to 100 µg/mL was prepared in triplicate and measured at the appropriate wavelength. The absorbance of Tyr-containing peptides was measured at 264 nm[d] and that of 6-Beta at 224 nm.

The concentrations of the Tyr-containing peptides in the biological activity experiments were calculated from a standard curve of Tyr-concentration at 274 nm.

Three samples per Tyr standard concentration was analysed and the linear curve fit (r^2) was determined as 0.997 with the linear relationship:

mmol Tyr/mL = (Absorbance at 274 nm) / 320.3

6.3.2.4 Determination of phospholipid concentration by the Stewart assay

The Stewart assay [36] utilises the tendency of phospholipids to form complexes with ammonium ferrocyanate in organic solutions. A 0.1 M ammonium ferrothiocyanate solution was prepared by dissolving 27.03 g ferric chloride hexahydrate and 30.4 g ammonium thiocyanate in 1 L analytical grade water. The solution is stable at room temperature for up to 6 months. The determination of phospholipid concentration was done on a small volume of the stock DMPC (or sample) diluted to 2 mL with chloroform to which 4 mL of the 0.1 M ammonium ferrothiocyanate solution was added. The mixture was vortexed for 15 seconds

[d] The interference of the DMPC at 264 nm was less than at 274 nm, the wavelength of maximum absorption for the Tyr.

and then centrifuged for 5 minutes at 300-500 g to separate the two phases. The chloroform layer was removed with a Pasteur pipette and its absorbance determined at 485 nm. The concentration of the lipid was determined from a DMPC standard curve with a concentration range from 0-500 µg/mL. Six samples per DMPC standard concentration was analysed and the linear curve fit (r^2) was determined as 0.999 with the linear relationship:

µg DMPC = (Absorbance at 485 nm – 0.00384) / 7.35 x 10^{-4}

6.3.3 Lytic and antimicrobial activity

6.3.3.1 Assay for haemolytic activity [adapted from 18]

Alsevier's solution (2.05% (m/v) glucose, 0.42% (m/v) NaCl, 0.8% (m/v) sodium citrate, 0.055% (m/v) citric acid, pH 7.20) was mixed in equal volumes with freshly drawn rabbit blood and left at 4°C for at least 72 hours. Erythrocytes were harvested by centrifugation for 15 minutes at 800 g, after which the cells were washed three times with 0.9% NaCl in 0.15 M phosphate buffer (phosphate buffered saline, PBS) at pH 7.2. The erythrocytes were then resuspended in PBS in an equal volume to the original blood volume, counted and diluted to a final cell count of $2.5x10^8$ cells/mL. The peptide preparations, dissolved in 50% acetonitrile/water, were mixed with $2.5x10^7$ erythrocytes in PBS and incubated for 30 minutes at 37°C. The mixtures were then centrifuged for 5 minutes at 1000 g and 100 µL of each of the supernatants carefully drawn of and pipetted into a microtitre plate. Absorbance measurements at 540 nm of each determination were done on a Titretek Multiscan Plus microtitre plate reader. The negative control was 50% acetonitrile/water and 100% haemolysis was determined using 200 µg/mL bee-venom melittin. Curve fitting and HC_{50} (peptide concentration inducing 50% haemolysis) calculations were done with the aid of PRISM 2.01 from GraphPad Software Inc. Data were fitted to a sigmoidal dose response curve with variable slope with the equation:

$$Y = Bottom + (Top - Bottom) / (1 + 10^{(\log HC_{50} \times HillSlope)})$$ where

Bottom = Y–value at the bottom plateau; Top = Y value at the top plateau

$\log HC_{50}$ = X–value of response halfway between top and bottom

Hill slope = Hill coefficient or slope factor, controls slope of curve

6.3.3.2 Cultivation of organisms

A small aliquot (10 µL of a 100 times dilution) of freezer stock of *M. luteus* was streaked on L-Broth containing agar culture plates (1 g tryptone, 0.5 g yeast extract, 1g NaCl and 2 g agar in 100 mL) and grown for 48 hours at 37°C. Single colonies were harvested and grown at 37°C in L-Broth to mid-log phase (A_{600} of 0.6±0.2 for *M. luteus*).

6.3.3.3 Lysis of *M. luteus* protoplasts [adapted from 23, 24]

Protoplasts of *M. luteus* were prepared by incubation of the bacteria under membrane stabilising conditions with lysozyme. An aliquot (1 mL) of *M. luteus*, grown to log phase in L-Broth, was washed twice with 30 mL of 20 mM Tris-HCl (pH 8) by centrifugation (15 min. at 800 g). The washed cells were suspended in 20 mM Tris-HCl (pH 8) containing 20% sucrose and further diluted to yield an absorbance reading at 600 nm (A_{600}) between 0.4 and 0.6. The suspension, with 0.5 mg/mL lysozyme added, was incubated at 37°C for 30-90 minutes. The incubation time depended on the activity of the lysozyme. The protoplast formation was monitored by evaluating aliquots under a light microscope. Healthy *M. luteus* tends to form cell groups (2 to 4 or more cells), easily distinguished under a light microscope, while the protoplasts tend to be single cells. After incubation the protoplasts were washed by centrifugation in 20 mM Tris-HCl (pH 8) containing 20% sucrose by centrifugation (5 minutes at 800 g). The protoplasts were then resuspended in 20% sucrose solution and diluted to an A_{600} of 0.35 and used immediately. Peptides (200 µg in 20 µL 50% acetonitrile/water) were mixed in the cuvette with 480 µL protoplasts. The lysis of protoplasts was monitored spectrophotometrically over 5 minutes at 600 nm in a Beckman DU650 spectrophotometer. The positive control was 20 µL of 0.15 M NaCl and the negative control 20 µL of 50% acetonitrile/water.

6.3.3.4 Microbial growth inhibition

A gel-diffusion microassay for growth inhibition was developed in a microtitre plate [37] by adapting the ultra-sensitive radial diffusion assay [38] and a microtitre liquid broth assay [39].

M. luteus was grown to log phase in L-Broth. The cells were harvested and washed by centrifugation (15 min. at 800 g) in Dulbecco's PBS[e]. The washed cells were resuspended in PBS to an A_{600} of 0.60 ± 0.02. An 1% low endosmosis agarose gel, containing 1.0 g tryptone

[e] Dulbecco's PBS (pH 7.4) contained 8.00 g/L NaCl, 0.2 g/L KCl, 0.2 g/L KH_2PO_4 and 1.15 g/L Na_2HPO_4.

soy broth and 0.02 g Tween, was heated to 45 ± 0.5°C. An aliquot (1000 µL) of the gel, at 45±0.5°C, was then mixed thoroughly (vortexed for 20 seconds) with 100 µL of the diluted *M. luteus* in a microcentrifuge tube. This mixture was pipetted (70 µL/well) carefully into eight wells of a microtitre plate, coated beforehand with 0.5% casein in PBS to prevent non-specific peptide interaction [40]. In order to ensure an even spread of gel in each well, a "reversed pipetting" technique was adopted: 70 µL of the heated mixture was drawn up with a Gilson pipette by fully depressing the plunger and then pipetting into the centre of the well (without touching the well bottom or sides) by depressing the plunger to the first "click". The first row (or blank row) in the microtitre plate contained 70 µL gel and Dulbecco's PBS (10:1 ratio).The prepared microtitre plate was closed and left for 30 minutes to set at room temperature. The peptide solution (30 µL of 10 to 1000 µg/mL stock solution in a 50% acetonitrile/water mixture) was placed into the centre of the well (without touching the gel or well sides) using a Hamilton syringe. The lightly sealed plate was then incubated at 37°C and microbial growth was monitored after 7 to 8 hours by light dispersion readings on a Multiscan Titertek Plus microtitre plate reader at 620 nm (A_{620}). The microbial growth was again measured after 16 to 18 hours. Growth was terminated by addition of 20 µL 6% formaldehyde in methanol when A_{620} of control wells, containing 30 µL of 50% acetonitrile/water instead of the peptide preparation, reached 0.250±0.05.

6.3.3.5 Activity against post-harvest pathogen *Botrytis cinerea*

Different amounts (1, 2, 4 or 8 µg) of the peptide preparations, in 10 mL of a 50% acetonitrile/water mixture, were spotted on a TLC plate. Each spot (5 mm in diameter) was carefully marked with a pencil and the peptide was applied inside the circle using a micropipette. The plate with the adsorbed peptide was allowed to dry and then sterilised under a UV light (254 nm) for 24 hours. Dry spores (3 mg/500 mL) from *B. cinerea* were suspended in 2% sucrose and applied evenly onto the plate using an aerosol applicator. The plate was then incubated in a humid chamber at room temperature for 4 days after which 2% sucrose was sprayed on the plate. The incubation was allowed to continue for a further 26 days to allow visible growth to take place (brown-grey patches/areas on plate). Growth in each spot, containing peptides, was then visually evaluated.

6.4 Results and discussion

6.4.1 Hydrophobic interaction

The analytical C_{18} HPLC results of each of the longer lipopeptides were reported in Chapter 2. The shorter peptides 5-Beta and 6-Beta aggregated to such an extent at very low concentrations that HPLC was not a viable option for purification or analysis. This aggregation is attributed to their more pronounced hydrophobic nature derived from the higher molecular mass fraction of the β-NC_{14} residue in these peptides.

Concentration dependent aggregation was illustrated by using 8-Beta as model peptide. An inverse linear relationship was observed between initial 8-Beta concentration and the formation of an early eluting aggregate (R_t=4.5 minutes) during analytical C_{18} HPLC (Fig 6.1). This aggregate formation corresponded with the decrease of the major fractions eluting at 9.4 and 9.6 minutes (Fig. 6.1).

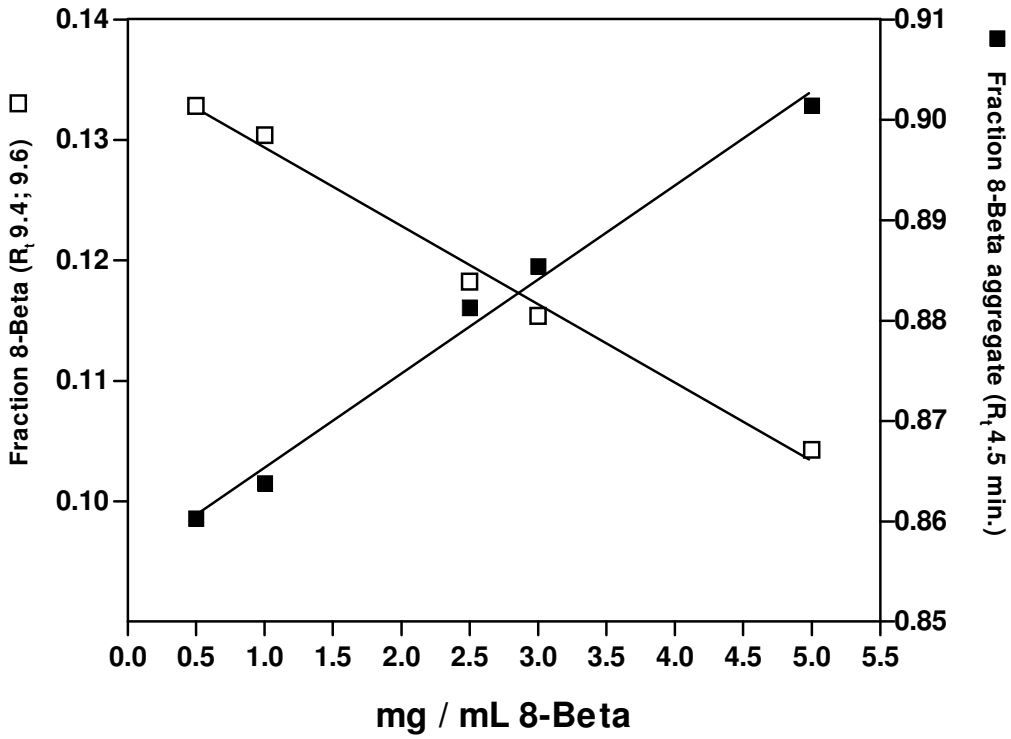

Figure 6.1 Concentration dependent aggregation of freshly prepared 8-Beta as evaluated using analytical C_{18} HPLC of peptide at different concentrations. The linear gradient was developed over 13 minutes with 0.1% TFA in water as solvent A and acetonitrile and 10% A as solvent B at a flow rate of 1mL/min; 20 µL of the sample was injected per analysis. The linear fit (r^2) of both lines is 0.99 and their slopes are identical except for its sign (+/−).

Analytical HPLC of the cold-stored 7-Beta showed the formation of stable aggregates that could be separated by HPLC (Fig. 6.2). Self-aggregation or micellisation, related to the hydrophobic/hydrophilic balance, depended on the length of the iturin A_2 analogue peptide chain. It was also found that aggregation in solution leads to loss of bioactivity, as will be discussed later on in this chapter.

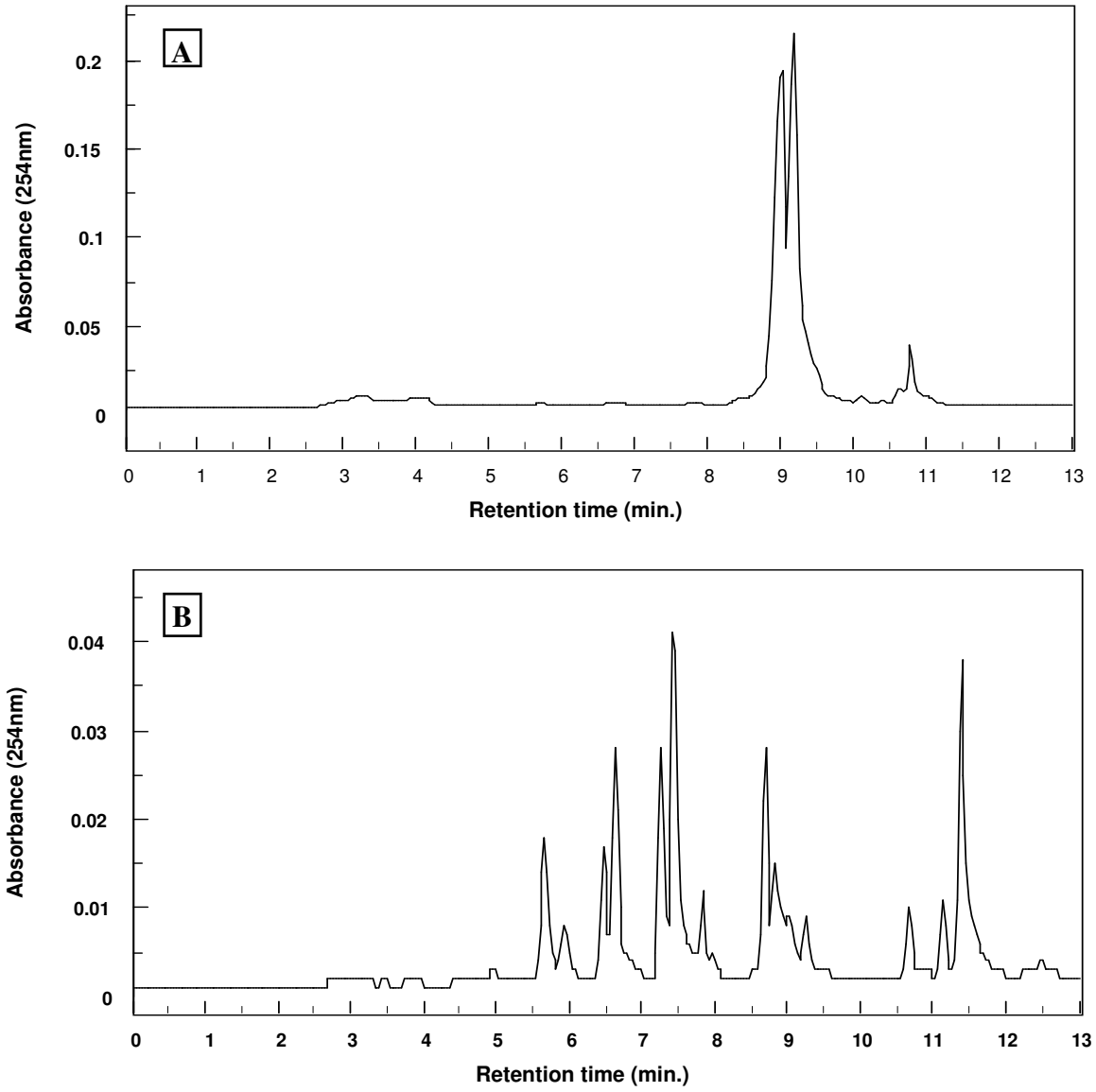

Figure 6.2 HPLC chromatograms of the purified 7-Beta diastereomeric preparation using a 150mm X 3.9mm C_{18} Nova-pak column with freshly prepared sample (**A**) and after long term storage at −20°C (**B**). A linear gradient was developed over 13 minutes with 0.1% TFA in water as solvent A and acetonitrile and10% A as solvent B at a flow rate of 1 mL/min. Approximately 25 µg peptide was injected per HPLC analysis.

The capacity factors (k') for each of the longer HPLC purified lipopeptides were calculated from retention times on a C_{18} analytical HPLC column and compared with the molecular mass fraction of β-NC_{14} residue in each peptide in Fig. 6.3 (capacity factors of the detected 5-Beta and 6-Beta aggregates ranged between 0 and 5 and were not taken into account). The molecular mass fraction of β-NC_{14} residue in each peptide (and possibly their hydrophobicity) correlated to some extent with their HPLC retention as the more polar octalipopeptides eluted earlier than the shorter heptalipopeptides in which the D-Asn_2 residue was omitted. Blocking of the N- and C- termini by cyclisation should, theoretically, lead to a more hydrophobic peptide, due to the removal of charged groups from the peptide structure. The cyclic lipopeptides, however, eluted earlier than the linear peptides from the ODS (C_{18}) column and therefore lower k' values were observed. The loss of retention is probably the result of weaker ion-pairing between the mobile phase trifluoroacetate and the peptide, and not because of decreased hydrophobicity. The formation of neutral, more hydrophobic species, because of ion-pairing with trifluoroacetate, or better interaction with the stationary phase coated with the ion-pairing agent, probably caused in the longer retention of the linear peptides. Although the diastereomeric peptide pairs are chemically identical, except for the β-carbon configuration of the β-NC_{14} residue, their HPLC retention were different (Fig. 6.3, also refer to Table 6.1). This is probably because of conformational differences between the peptide pairs leading to differences in retention and solution hydrophobicity.

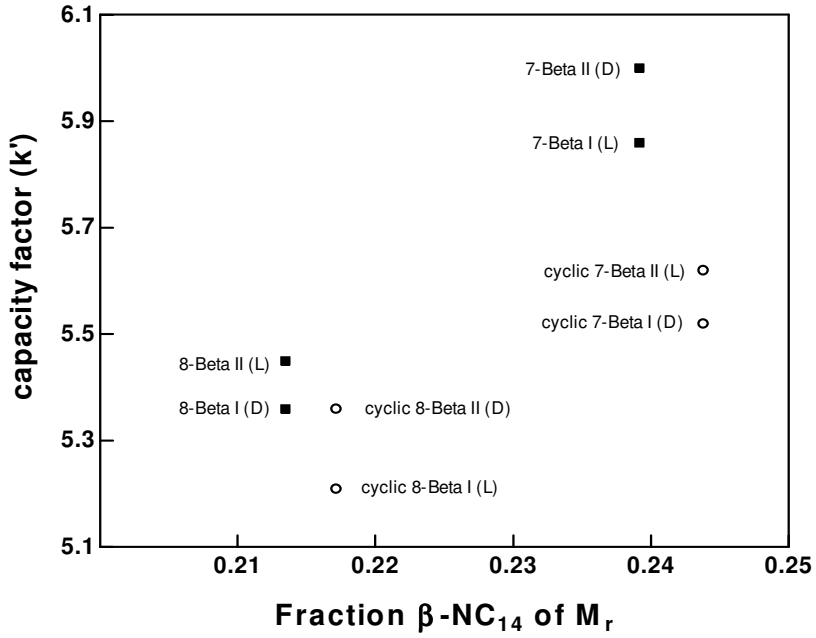

Figure 6.3 Comparison between HPLC capacity factors of eight iturin A_2 analogues and the molecular mass fraction of β-NC_{14} in each peptide.

The influence of peptide moiety of iturin A on the incorporation/association with membranes was investigated by using the three linear analogues (6-Beta, 7-Beta and 8-Beta) and liposomes consisting of DMPC. DMPC was chosen because phosphatidylcholine is one of the major phospholipids found in eukaryotic membranes and specific interaction by iturin A with this phospholipid has also been demonstrated by other investigators [13, 41]. A 125:10 lipid to peptide ratio was chosen, to promote interaction and limit liposome fusion and aggregation. The peptide-vesicle complexes were separated from the free peptide using gel-permeation chromatography (Fig. 6.4).

A positive correlation between k'-values and the incorporation of the linear peptides in lipid vesicles was observed—the higher the k'-value, the more peptide associated with lipid vesicles (Table 6.1). The peptide/lipid ratio, before vesicle collapse, was 2 to 3 times lower for 7-Beta and 8-Beta than the 0.1 ratio reported for iturin A with DMPC [13], probably because differences in peptide structure and the lower peptide concentration used. The tendency of 6-Beta to self-aggregate in solution (as discussed in Chapter 2) markedly decreased its capacity to interact with the vesicles (Fig. 6.4, Table 6.1). Minimal interaction between a control peptide containing the iturin heptapeptide moiety, Fmoc-GNYNQPNS, and the vesicles was observed (Table 6.1).

Table 6.1 Summary of the data from hydrophobic character investigation of the iturin A analogues using octadecanoylsilane matrices (C_{18}-HPLC) and DMPC liposomes.

Peptide	**C_{18} HPLC capacity factor (k')**	**mole peptide / mole DMPC**
6-Beta I, II	2.69 (aggregate)	0.019
7-Beta I (L), II (D)	5.86; 6.00	0.046
8-Beta I (D), II (L)	5.36; 5.45	0.037
cyclic 7-Beta I (D), II (L)	5.52; 5.62	not determined
cyclic 8-Beta I (L), II (D)	5.21; 5.36	not determined
Fmoc-GNYNQPNS	3.74	0.004

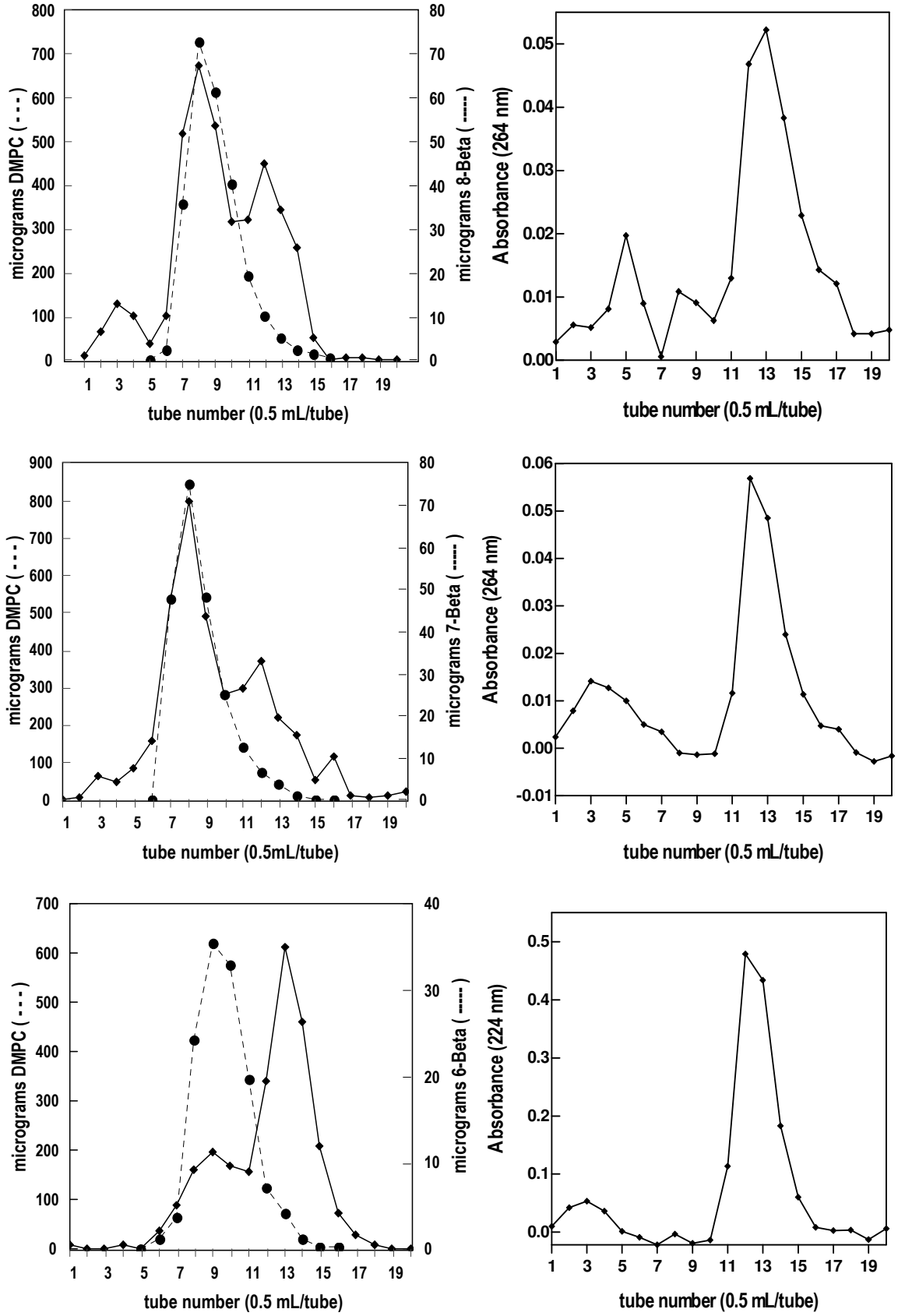

Figure 6.4 Example chromatograms of separation of the vesicle-peptide mixtures on a 4.5 mL Sepharose 4B column (left). The chromatograms on the right show the chromatography of the free peptides. Chromatography was done at 35ºC and fractions were eluted with 0.15 M NaCl.

6.4.2 Biological activity

6.4.2.1 Haemolytic and lytic activity

The haemolytic activity of antimicrobial peptides generally relates to their hydrophobicity as it was found that the more hydrophobic peptides tended to be more haemolytic [42]. This relationship between hydrophobicity and haemolysis was not observed for the iturin A_2 analogues (Fig. 6.5, also refer to Table 6.1).

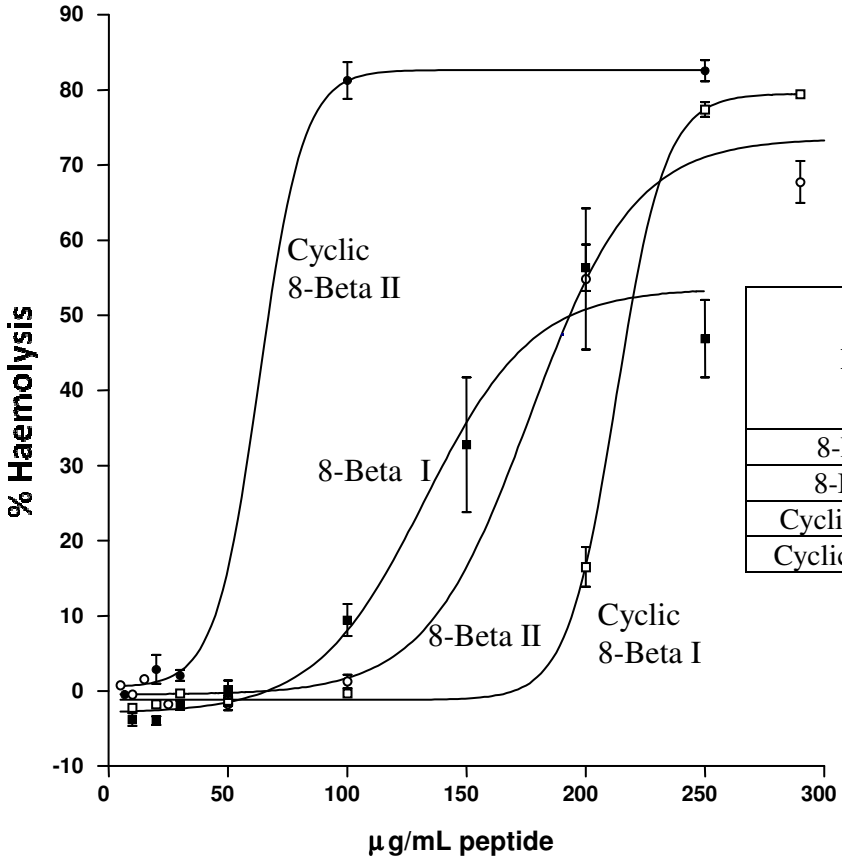

Peptide	Heamolysis of rabbit erythrocytes (HC_{50}, µM)
8-Beta I (D)	125±7
8-Beta II (L)	201±3
Cyclic8-Beta I (L)	169±8
Cyclic 8-Beta II(D)	61±9

Figure 6.5 Haemolysis of rabbit erythrocytes ($2.5x10^7$ cells/mL) by the octalipopeptide analogues. The mean of quadruplicate observations and standard error of the mean (SEM) are shown for each data point. The table shows the peptide concentration at 50% haemolysis (HC_{50}). Values were calculated from curve fitting using PRISM 2.01 sigmoidal curve with variable slope.

All the octalipopeptides showed haemolytic activity (Fig. 6.5). The haemolytic activity (50% haemolysis at 61 ± 9 µM) of synthetic iturin A_2 (cyclic 8-Beta II (D)) was comparable with results obtained in literature with natural iturin A [18]. All the shorter, more hydrophobic heptalipopeptides were not haemolytic in the concentration range used (HC_{50}>250 µg/mL). Cyclisation improved haemolytic activity, but omission of the L-Asn_2 residue in the heptalipopeptides markedly decreased haemolytic activity. From these results it could also be

deduced that the configuration of the β-NC_{14} residue has a strong influence, as cyclic 8-Beta II (D) and 8-Beta I (D), both containing the same β-NC_{14} enantiomer, were the most haemolytic octalipopeptides at low concentrations. The activity of the linear 8-Beta (I) decreased at higher concentration, probably because of self-aggregation in solution.

It is known that iturin A preferentially associates with membranes, such as erythrocyte membranes, containing neutral phospholipids such as phosphatidylcholine (PC) and cholesterol [13, 18]. It was, however, found that iturin A does interact with *M. luteus* protoplasts [23, 24], containing phosphatidylglycerol in its membrane [25]. The lytic activity of the diastereomeric peptide mixtures towards *M. luteus* protoplasts was initially used as an assay for bioactivity, as the lysis can be monitored spectrophotometrically by measuring light dispersion at 600 nm.

About a tenfold lower lytic activity for the cyclic 8-Beta mixture than that reported in literature [23, 24] was observed (Fig. 6.6). Some of this lower activity could be attributed to the contamination of the synthetic iturin A_2 with its diastereomer or aggregation of the peptide in the stock solution because of the high concentrations used in the assay. Other factors might be the inhibition of activity by contamination of divalent cations (Mg^{2+} and Ca^{2+}) and the omission of sodium in the form of sodium-EDTA from the reaction mixture [23, 24]. The higher activity reported in early literature [23, 24] may also be the consequence of synergism between iturin A and the co-produced surfactin, a biosurfactant [43] that could have contaminated their iturin A preparations. The total absence of lytic activity of 6-Beta preparation is probably because of its self-aggregation in solution and the omission of the invariant Tyr_3 (Fig. 6.6). This residue is important in the interaction with target cell membranes [9, 13, 32, 33]. Although this method had a low sensitivity, it could be deduced that peptide length is a crucial factor in lytic activity—this activity decreased with peptide length: 8-Beta>7-Beta>6-Beta (Fig. 6.6). A more reliable method was consequently developed to test antibacterial activity [37].

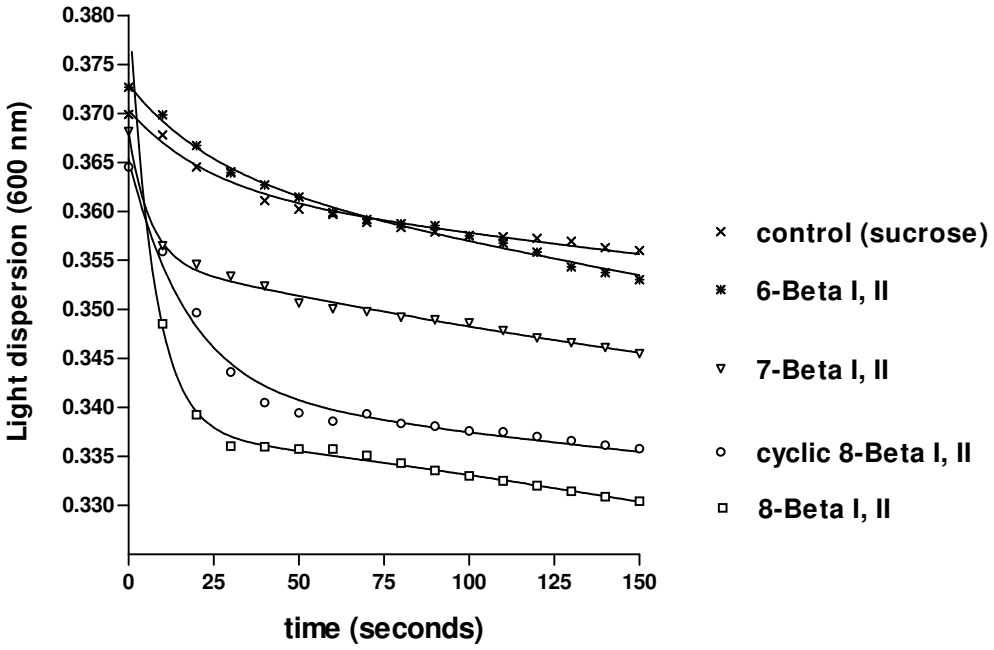

Figure 6.6 The lytic activity of iturin A_2 analogues (400 µg/mL) towards *M. luteus* protoplasts. The average of two determinations is shown.

6.4.2.2 Inhibition of microbial growth

The iturin A_2 analogues were tested against *M. luteus* as this is one of the bacterial species sensitive to iturin A. Growth inhibition of *M. luteus* was observed after 7.5 hours incubation at 37°C over a broad concentration range for all the Beta II lipopeptides, whereas the Beta I peptides showed only inhibition at very high concentrations (Figs. 6.7-6.9). The results for the Beta II peptides also corresponded with the initial results obtained from the lysis of *M. luteus* protoplasts, with the activity of 8-Beta, cyclic 8-Beta >7-Beta (refer to Fig 6.6). The highest activity at 30 µg/mL was observed for cyclic 8-Beta II (D), with 8-Beta II (L) the most active linear lipopeptide (Fig. 6.9). The *M. luteus* growth inhibition observed for cyclic 8-Beta II (D) (38 ± 3% by 20 µg/mL) was comparable to values reported in literature for iturin A [23]. Some growth inhibition was retained, but nearly all was alleviated after 17 hours of incubation at 37°C (Figs. 6.7-6.9). It is therefore highly probable that these iturin A_2 analogues have mostly bacteriostatic activity over the concentration range investigated (3-480 µg/mL). Overall the iturin A_2 analogues in this study were not strongly antibacterial if compared with gramicidin S. Gramicidin S was used as test peptide in the development of the gel-diffusion microassay and 50% growth inhibition of *M. luteus* was obtained with only 3-5 µg/mL peptide [37].

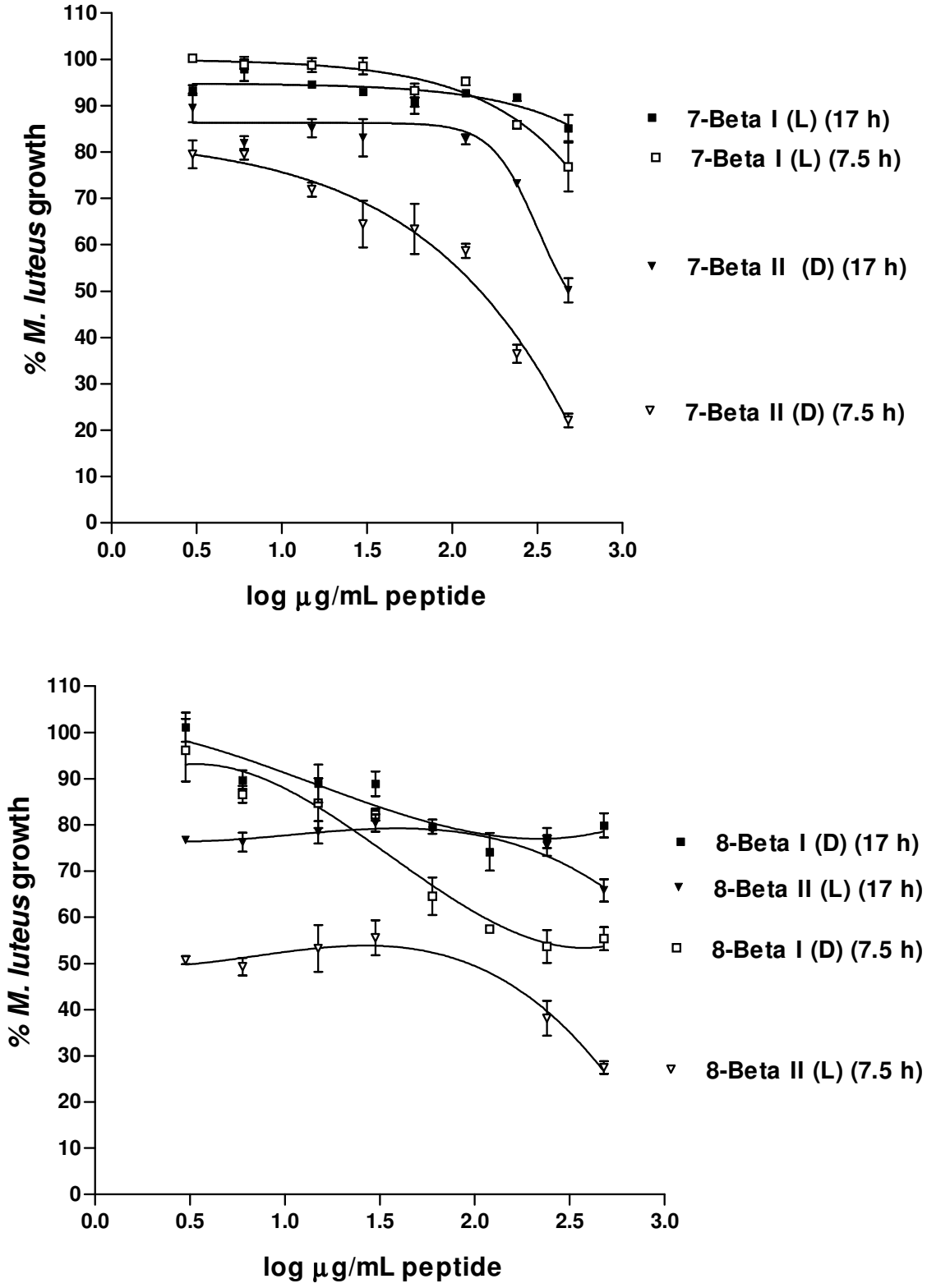

Figure 6.7 Percentage growth of *M. luteus* in the presence of the linear lipopeptides as observed over a period of 17 hours incubation at 37°C. The mean of quadruplicate observations and the SEM are shown for each data point. The 100% growth was taken as the light dispersion at 620 nm of the controls.

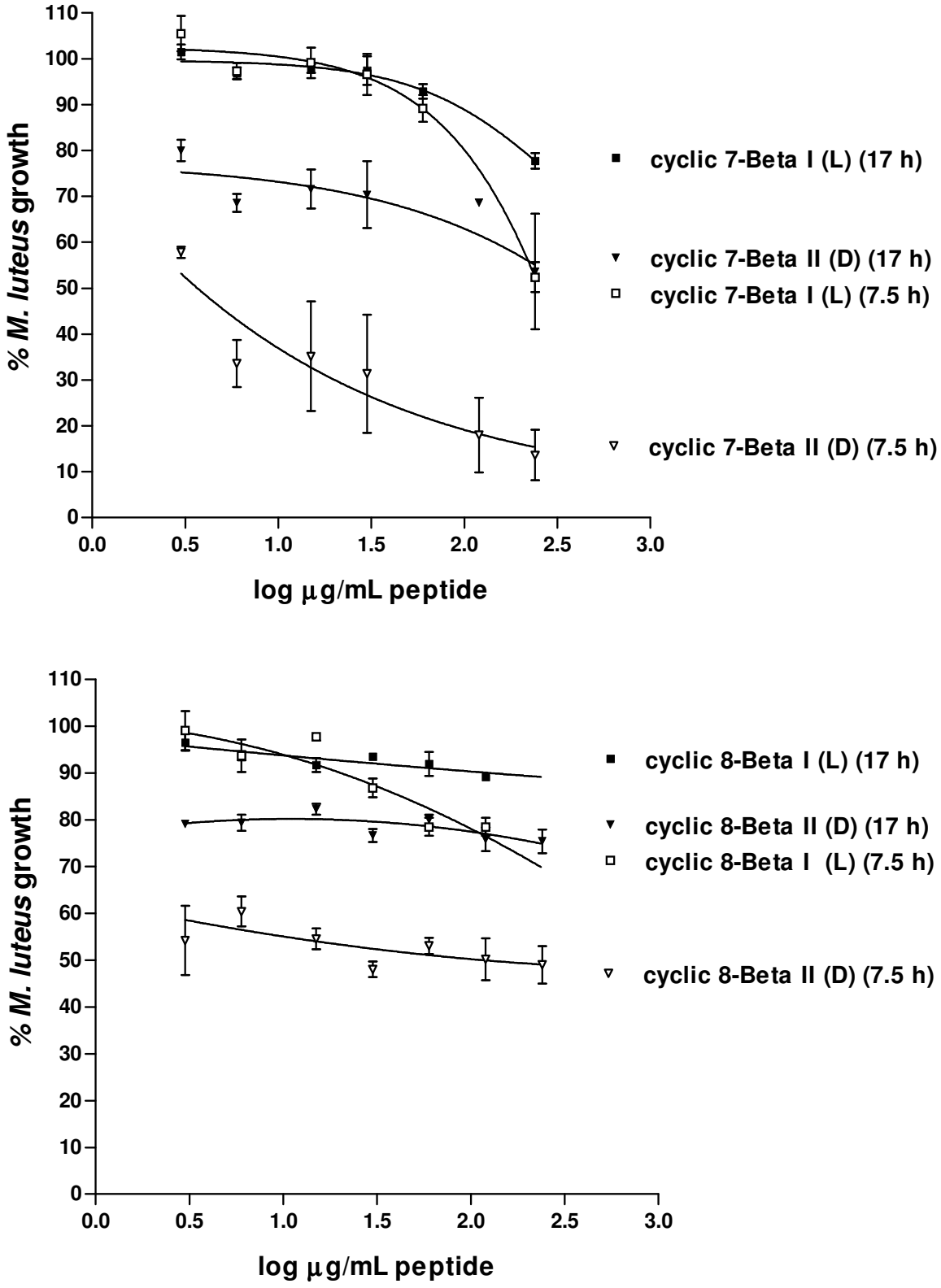

Figure 6.8 Percentage growth of *M. luteus* in the presence of the cyclic lipopeptides as observed over a period of 17 hours incubation at 37°C. The mean of quadruplicate observations and the SEM are shown for each data point. The 100% growth was taken as the light dispersion at 620 nm of the controls.

A 70-100% loss in activity against *M. luteus* was observed if the peptide solutions were stored at −20°C for a week (results not shown). This loss corresponded with the aggregation observed when the stored peptide solutions were subjected to analytical HPLC (Figs. 6.1, 6.2). It could therefore be deduced that the aggregation in solution leads to diminished activity and that the aggregates in solution are not the active form of the peptides.

Cyclisation did not necessarily improve the activity of the peptides as could be seen from results depicted in Fig. 6.9. In the case of 7-Beta I (L) and 8-Beta I (D) their cyclisation to form cyclic 7-Beta II (L) and cyclic 8-Beta II (D) improved activity. The reverse was true for the other four peptides. The most haemolytic peptide, the synthetic iturin A_2 (cyclic 8-Beta II (D)), also showed the highest activity at low concentration against *M. luteus*.

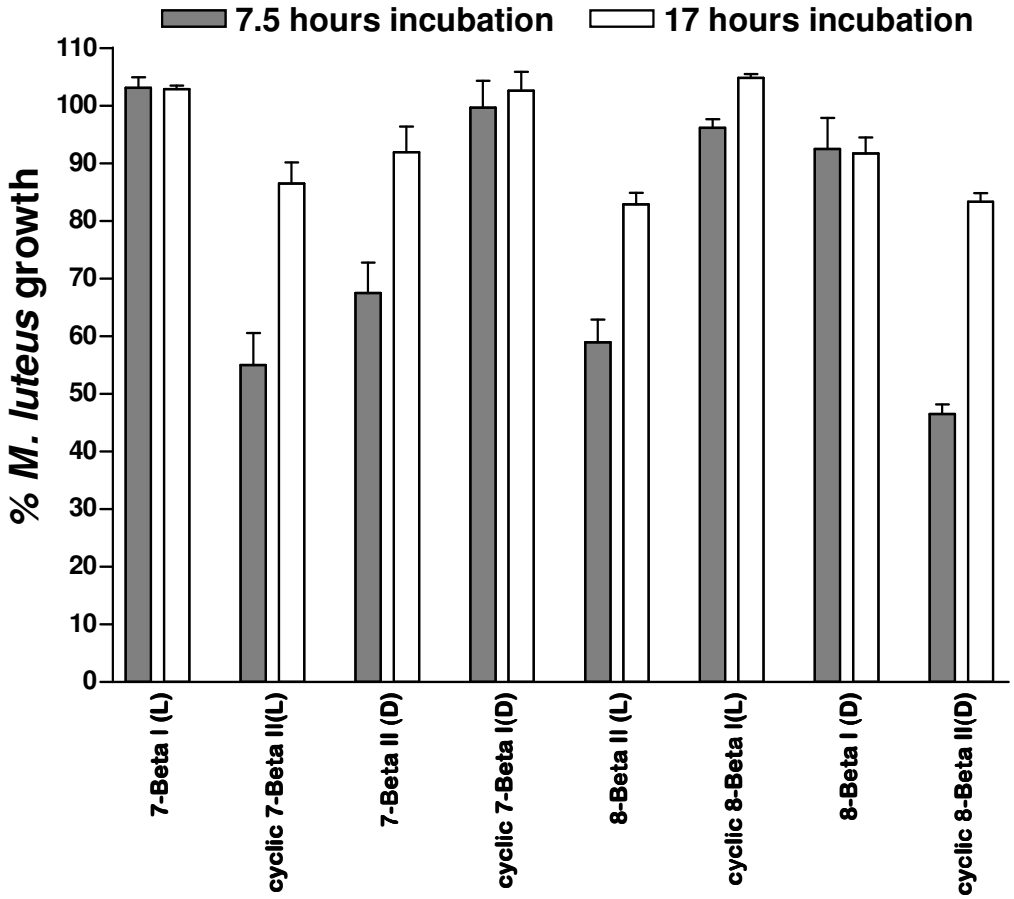

Figure 6.9 Percentage growth of *M. luteus* in the presence of the 30 µg/mL of each of the lipopeptides as observed over a period of 17 hours incubation at 37°C. The mean of duplicate observations for 7-Beta II (D) and cyclic 7-Beta II (L) and quadruplicate observations for the rest of the peptides and the SEM are shown for each data point. The 100% growth was taken as the light dispersion at 620 nm of the controls.

The inhibition of growth of *B. cinerea* in the presence of the lipopeptides was used to assay the antifungal activity. A mixture of the 8-Beta diastereomers, at a concentration of 200 µg/mL, did not inhibit the germination of *B. cinerea* spores as with witnessed with fluorescence microscopy [43]. In a previous study by Levitt [44], however, antifungal activity was observed for a diastereomeric mixture of a linear octalipopeptide analogue of iturin A_2 with L-Pro_6 as C-terminal and L-Gln_5 as N-terminal.

A TLC-based assay of the germination of spores and growth of *B. cinerea* over a 30 day period was used because of the advantage of multiple determinations under comparative conditions (Fig 6.10). The observed antifungal activity of these analogues may be highly influenced by the testing method, as is the case with many bioassays. This technique has some limitations such as uneven spore growth and possibility of inactivation of the peptide preparation by the SiO matrix. The limited amounts of high purity and fully characterised peptide preparations (refer to Chapters 2 and 3) prevented in depth investigation of antifungal activity. The results from this assay, however, confirmed results obtained by Holz [43] as three of the four linear peptides showed little or no antifungal activity. A surprising result was the activity of the linear 7-Beta I (L), which is currently under further investigation. All the cyclic peptides, except cyclic 8-Beta I (L) showed antifungal activity, with cyclic 8-Beta II (D) or synthetic iturin A_2 the most active.

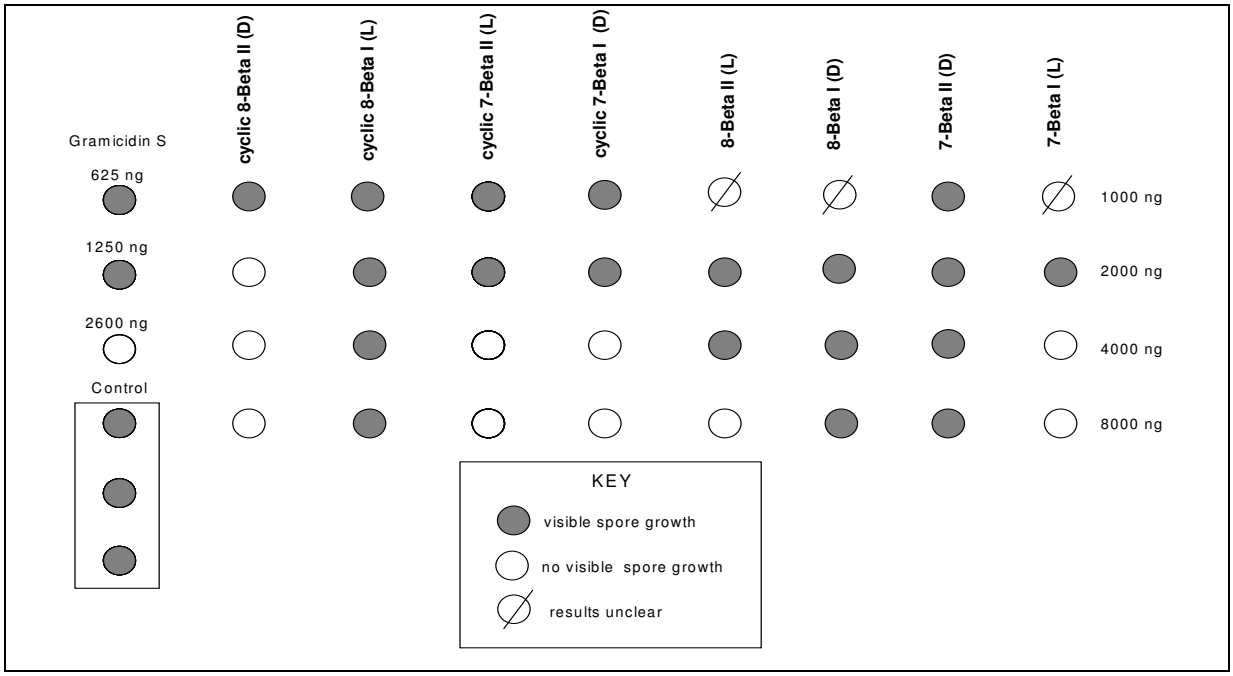

Figure 6.10 Germination and growth of *B. cinerea* over a 30 day period at room temperature on a TLC plate with different amounts of adsorbed lipopeptide.

6.5 Conclusions

Hydrophobic interaction is generally regarded as an important factor in evaluating the potential of amphipathic compounds to associate with cell membranes. However, as demonstrated in this study, hydrophobicity does not always correlate with the biological activity of these compounds. The interaction with lipid membranes is not only influenced by the hydrophobicity of the lipopeptides, but also their tendency to aggregate in solution. The linear lipopeptides with the lowest HPLC capacity factors (k') tended to associate less with DMPC. The longer lipopeptides had substantial interaction with lipid membranes.

Self-aggregation of the iturin A molecules occurs in the target cell membrane [8, 9]. It was also observed that the iturin A_2 analogues still have the ability to self-aggregate, but the peptide preparations that aggregated in solution lost most of their antibacterial activity. This observation corresponded to the low bioactivity observed for an O-methylated derivative of iturin A, MeTyr-iturin A, having a ten times higher tendency to aggregate than iturin A [9].

Cyclisation mostly improved activity and the longer octalipopeptides showed better overall bioactivity than the shorter heptalipopeptides. These results may be related to the conformation adopted in the membrane. It was shown in Chapter 4 that the structures of the octalipopeptide pair (8-Beta I (D), II (L)) differed largely from that of their cyclic analogues. One exception is cyclic 8-Beta I (L) which is almost totally inactive. There was little difference between the membrane bound structures of the cyclic 8-Beta pair, thus the inactivity of this peptide is probably related to the chirality of its β-NC_{14} residue.

No clear correlation between the association of the iturin analogues with sodium or the other alkali metal ions and bioactivity could be found. It was however observed that the less active linear peptides, 7-Beta and 8-Beta, associated with either one ion or two alkali metal ions, while the overall more active cyclic peptides associated only with one alkali metal ion (refer to Chapter 5).

For many antimicrobial peptides it is generally found that the more hydrophobic peptides tend to be more haemolytic [42], but this was not the case for iturin A and its analogues. A dramatic decrease of haemolytic activity was previously reported for a more hydrophobic iturin A derivative in which the D-Tyr_3 residue was methylated [23]. On the other hand it was found that O-acetylation of the L-Ser_8 residue, also producing a more hydrophobic iturin A derivative, had less influence on its activity [23]. In this study it was found that cyclisation,

the Asn_2 residue and the configuration of the β-NC_{14} are important in the lytic activity on rabbit erythrocytes. The synthetic iturin A_2 (cyclic 8-Beta II (D)) and its linear analogue (8-Beta I (D)) were the most haemolytic at low concentrations, therefore interaction with a chiral receptor, in which the β-NC_{14}-L-Asn_2-D-Tyr_3 tripeptide moiety is important, is possible. Candidates for this interaction may be phospholipases (refer to the discussion in the introduction).

The length of the peptide moiety seems to be important in the lytic activity against *M. luteus* protoplasts as the longest peptides were the most active. All the peptides Beta II peptide inhibited *M. luteus* growth, but it is unclear if inhibition was due to cytotoxic or cytostatic activity. This activity corresponded with interaction with ODS matrixes (HPLC retention) as the diastereomer in each pair with the highest k' and was the most active. Cyclisation did not necessarily improve the activity of the peptides and the configuration of the β-NC_{14} residue had little or no discernible influence on the growth inhibition of *M. luteus.* The mechanism of action against the gram-positive *M. luteus* is clearly different from that of haemolysis.

The activity against *B. cinerea* depended mainly on cyclisation as three of the four cyclic peptides showed some inhibition of this fungus. The exceptions were that 7-Beta I (L) also showed antifungal activity and that cyclic 8-Beta I (L) was inactive. This may be the result of the TLC based assay as hydrophobicity does have an influence on the "release" of the peptide from the polar SiO matrix for interaction with the fungal membrane. Cyclic 8-Beta I (L) had the lowest HPLC capacity factor of all the longer peptides and 7-Beta I (L) the second highest. The influence of the configuration of the β-NC_{14} on *B. cinerea* growth is not clear, but as with haemolytic activity and *M. luteus* growth inhibition, the most active peptide was synthetic iturin A_2.

6.6 References

1. Marion D., Zasloff M., Bax A. (1988) *FEBS Lett*. **227**, 21-26

2. Hill C. P., Yee J., Selsted M. E., Eisenberg D. (1992) *Science* **251**, 1481-1485

3. Maget-Dana R., Peypoux F. (1994) *Toxicology*, **87**, 151-174

4. Bland J. M., Lax A., Klich M. In: Peptides 1990: Proceedings of the Twenty-First European Peptide Symposium (Eds. Giralt E., Andreu D.) ESCOM, Leiden, IL, pp. 426-427

5. Huang H. W. (1994) Channel-forming peptides in uniformly aligned multilayers of membranes, In: Advances in Chemistry Series, Volume 235 (Eds. Blank M., Vodynoy I.) American Chemical Society, pp. 83-106

6. Marshall G. R., Beusen D. D. (1994) The structural basis of peptide channel formation, In: Advances in Chemistry Series, Volume 235 (Eds. Blank M., Vodynoy I.) American Chemical Society, pp. 259-314

7. Imanshi Y., Kimura S. (1992) *Proc. Japan. Acad*. **68**, 121-126

8. Latoud C., Peypoux F., Michel G., Genet R., Morgat J. L. (1986) *Biochim. Biophys. Acta.* **856**, 526-535

9. Harnois I., Maget-Dana R., Ptak M. (1988) *J. Colloid Interface Sci.* **123**, 85-91

10. Maget-Dana R., Heitz F., Ptak M., Peypoux F., Guinand M. (1985) *Biochem. Biophys. Res. Commun*. **129**, 965-971

11. Maget-Dana R., Ptak M., Peypoux F., Michel G. (1985) *Biochim. Biophys. Acta* **815**, 405-409

12. Maget-Dana R., Ptak M., Peypoux F., Michel G. (1987) *Biochim. Biophys. Acta* **898**, 1-5

13. Maget-Dana R., Harnois I., Ptak M. (1989) *Biochim. Biophys. Acta* **981**, 309-314

14. Aoki Y., Uenaka T., Aoki J., Umeda M., Inoue K. (1994) *Biochem. J.* **116**, 291-297

15. Matsuzaki K., Sugishita K., Fujii N., Miyajima K. (1995) *Biochemistry* **34**, 3423-3429

16. Latoud C., Peypoux F., Michel G. (1987) *J. Antibiotics* **40**, 1588-1595

17. Latoud C., Peypoux F., Michel G. (1990) *Can. J. Microbiol.* **36**, 384-389

18. Quentin M. J., Besson F., Peypoux F., Michel G. (1982) *Biochim. Biophys. Acta*. **684**, 207-211

19. Besson F., Peypoux F., Quentin M. J., Michel G. (1984) *J. Antibiotics* **37**, 172-177

20. Thimon L., Peypoux F., Exbrayat J. M., Michel G. (1994) *Cytobios* **79**, 69-83

21. Phae C. G., Shoda M., Kubota H. (1990) *J. Ferment. Bioeng*. **69**, 1-7

22. Besson F., Peypoux F., Michel G., Delcambe L. (1978) *Biochem. Biophys. Res. Commun.* **81**, 297-304

23. Peypoux F., Besson F., Michel G., Delcambe L. (1979) *J. Antibiot*ics **32**, 136-140

24. Besson F., Peypoux F., Michel G. (1979) *Biochim. Biophys. Acta*. **552**, 558-562

25. Op den Kamp J. A. F. (1979) *Ann. Rev. Biochem*. **48**, 47-71

26. Wade D., Boman, I. A., Wahlin B., Drain C. M., Andreu D., Boman H. G., Merrifield R. B. (1990) *Proc. Natl. Acad. Sci. USA* **87**, 4761-4765

27. Merrifield R. B., Merrifield E. L., Juvvadi P., Audreu D., Boman H. G. (1994) Antimicrobial Peptides, Ciba Foundation Symposium 186, John Wiley & Sons, New York pp. 5-20

28. Chen H., Brown J. H., Morell J. L., Huang C. M. (1988) *FEBS Lett.* **236**, 462-466

29. Dathe M., Schumann M., Wieprecht T., Winkler A., Beyermann M., Krause E., Matsuzaki K., Murase O., Bienert M. (1996) *Biochemistry* **35**, 12612-12622

30. Latoud C., Peypoux F., Michel G. (1988) *J. Antibiotics* **41**, 1699-1700

31. Peypoux F., Besson F., Michel G., Delcambe L., Das B. C. (1978) *Tetrahedron* **34**, 1147-1152

32. Besson F., Peypoux F., Michel G., Delcambe (1979) *J. Antibiotics* **32**, 828-833

33. Harnois I., Maget-Dana R., Ptak M. (1989) *Biochimie* **71**, 111-116

34. New R. R. C (Ed.) Liposomes, A practical approach (1990), Oxford University Press, pp. 33-48

35. Huang C. (1969) *Biochemistry*, **8**, 344-351

36. Stewart J. C. M. (1959) *Anal. Biochem*. **104**, 10

37. Du Toit E. A., Rautenbach M. (1998) Poster presented at 2nd FASMB and 15th South African Society of Biochemistry and Molecular Biology, Potchefstroom, RSA

38. Lehrer R. I., Rosenman M., Harwig S. S. S. L., Jackson R. (1991) *J. Immun. Meth.* **137**, 167-173

39. Hancock R. E., WWW home page: www.interchg.ubc.ca/bobh/peptides.htrr

40. Rautenbach M. (1989) The synthesis and characterisation of antigenic peptide determinants, M.Sc.-thesis (Biochemistry), University of Pretoria, pp. 127-128

41. Quentin M. J., Peypoux F., Michel G. (1983) *Biochem. Int*., **7**, 63-70

42. Bessalle R., Gorea A., Shalit I., Metzger J. W., Dass C. Desiderio D. M. (1993) *J. Med. Chem.* **36**, 1203-1209

43. Personal communication from G. Holz, Department of Plant Pathology, University of Stellenbosch

44. Levitt R. R. (1986) The synthesis of a novel octapeptidolipid antibiotic, Ph.D.-thesis (Biochemistry), University of Stellenbosch, pp. 130-139

Chapter 7

Conclusions

This is the first study where synthetic deletion analogues of iturin A_2 and synthetic iturin A_2 have been used to investigate the structure-function relationship of this cyclic antifungal lipopeptide, produced by strains of *Bacillus subtilis*. The aim of this study was the elucidation of iturin A's mechanism of action, known or/and hypothesised features of which can be summarised as follows [1, also see Chapter 1]:

- the recognition of the target cell membrane containing phosphatidylcholine and membrane sterols [2];
- interaction with the membrane lipids and the induction of aggregated structures [3, 4] of unknown size and conformation in the membrane in which the invariant Tyr plays a significant role [4, 5]);
- the activation of phospholipases [6], either directly and stereoselectively or indirectly by exposing of the phospholipid substrates to enzymatic action;
- the association with Na^+ and K^+ [7] with the possibility of ionophoric action [1] or the formation of active complexes including these ions;
- the formation of weakly anion selective ion-conducting pores [8];
- the ultimate leakage of cellular contents and release of vesicles (containing membrane lipids and iturin A) leading to cell death [9].

In this concluding chapter some of these above features will be related to the results obtained by synthesising and characterising eight analogues of iturin A_2. Before proceeding, just a short summation of the results from the initial synthesis and purification of these analogues. In the synthesis of four linear iturin A_2 analogues, in which the conserved tetrapeptide moiety, (L-Asn_2-D-Tyr_3-D-Asn_4) was sequentially omitted, high yields (92.5 ± 5%) and good coupling efficiencies per step (98.7 ± 0.9%) were obtained. Cyclisation of the heptalipopeptide (7-Beta) and octalipopeptide (8-Beta) was successful, although the yields of 33% and 30% respectively after purification, were somewhat lower than that of 46% reported by Bland [10] for the synthesis of iturin A_2. The low yields obtained during cyclisation could have been the result of 8-Beta being predominantly in the "S"-conformation, which would cyclise less readily than

the "W"-conformation (structures were predicted by HyperChem®4.5, Chapter 4). Protected precursors was not used in the cyclisation steps, which could also explain the lower yields that were obtained. Product losses occurred during the preparation and handling of the lipopeptides, because of aggregation and adsorption to plastic. This hydrophobic character of the peptides hampered both the purification of some of the shorter analogues and the bioactivity studies. The association of the peptides with sodium also influenced the ESI-MS experiments described in Chapter 5. The fraction of sodiated peptide in the peptide preparation increased with each sample drying procedure and therefore re-purification of samples was necessary on occasion. The synthetic products clearly retained some of the reported physical character of iturin A [1], namely the tendency to aggregate, adsorption to hydrophobic surfaces and affinity for alkali metal ions. It was also found that the biological activity (Table 7.1) of the iturin A_2 analogues was influenced by peptide length, configuration of the β-NC_{14} residue and cyclisation.

Table 7.1 Summary of the bioactivity of the iturin A analogues (refer to Chapter 6)

Peptide	**% *M. luteus* growth inhibition after 7.5 hours incubation by 30 µg/mL peptide**	**Activity against *Botrytis cinerea* (lowest inhibiting amount in TLC assay, µg)**	**Haemolysis of $2.5x10^7$ rabbit erythrocytes (HC_{50}, µM)**
8-Beta I (D)	8±5	>10	125±7
8-Beta II (L)	41±4	8	201±3
cyclic 8-Beta I (L)	4±2	>10	169±8
cyclic 8-Beta II (D)	54±2	2	61±9
7-Beta I (L)	0	4	> 250
7-Beta II (D)	33±5	>10	> 250
cyclic 7-Beta I (D)	0	4	> 250
cyclic 7-Beta II (L)	45±5	4	> 250

Enantiomerically pure β-D-aminotetradecanoic acid was not available at the time our synthesis, although this compound was synthesised recently using a protocol reported by Bland [11]. The racemic nature of the β-NC_{14}, incorporated into the peptides during the final coupling step, invariably led to the production of diastereomeric mixtures of the peptides. It

was, however, possible to purify eight of the lipopeptides to chiral purity of about 80% and higher (up to 100% for two of the cyclic peptides). The peptides were otherwise of high chemical purity as indicated by ESI-MS, HPLC and amino acid analysis. It was necessary to ascertain the absolute configuration of the β-NC_{14} residue in each of the hepta- and octalipopeptides and for this a method using chiral liquid chromatography linked to ESI-MS was developed (Chapter 3). The introduction of the racemic β-NC_{14} residue into the iturin A_2 analogues, however, added a new dimension of chirality to this investigation. The stereoselectivity of iturin A's biological action could subsequently be investigated. Evidence of stereoselectivity, was obtained from the activity of the iturin A_2 analogues on rabbit erythrocytes. The synthetic iturin A_2 (cyclic 8-Beta II (D)), and its linear analogue (8-Beta I (D)), were found to be the most haemolytic in these experiments (Chapter 6). Haemolytic activity depended on cyclisation, the inclusion of $Asn_{2\ residue}$ in the peptide chain and the configuration of the β-NC_{14}. The stereoselectivity is probably conferred by the β-D-NC_{14}-L-Asn_2-D-Tyr_3 tripeptide moiety, which may interact with a chiral receptor such as a phospholipase. A future investigation of the influence of the four octalipopeptides and possibly other octalipopeptide analogues on phospholipase activity may clarify the stereoselectivity aspect.

The tendencies of the peptides to aggregate and interact with hydrophobic matrices were exploited to evaluate the contribution of these factors to bioactivity (Chapter 6). The two longer linear lipopeptides, 8-Beta and 7-Beta, both associated with phosphatidylcholine (PC) vesicles, but the high tendency of 6-Beta to self-aggregate almost negated its membrane interaction and bioactivity. The length of the peptide moiety seems to be important in the lytic activity against *Micrococcus luteus* protoplasts as the longest peptides were the most active with the order of activity: 8-Beta>7-Beta>6-Beta. All the Beta II peptides showed growth inhibition of *M. luteus*, but are not regarded as strongly antibacterial (Table 7.1). This activity correlated with the interactions of these compounds with octadecanoylsilane matrices (HPLC retention) as the diastereomer in each lipopeptide pair with the longest retention was the most active. Although all the lipopeptides retained the ability to self-aggregate, aggregation in solution diminished activity against *M. luteus.* It is therefore feasible to propose that the aggregates formed in solution are not the active forms of these peptides, or iturin A. The activity against *M. luteus* is largely dependent on hydrophobic interaction and independent of

the chirality of the β-NC_{14} residue and cyclisation, therefore displaying a different mechanism of action than that responsible for haemolysis.

The structural investigation of the four octalipopeptides, reported in Chapter 4, revealed that the configuration of the β-NC_{14} residue had little effect on structure, whereas cyclisation had a pronounced influence. Two backbone conformations of 8-Beta, namely one with a distorted W-structure and the other with a twisted S-structure, were also predicted by structure modelling. NMR analyses of 8-Beta indicated a slow conversion between two conformations of 8-Beta, possibly a W↔S equilibrium, in which the Tyr residue side chain, and probably one or more of the Asn residues, are influenced. Circular dichroism (CD) spectra in buffer also revealed a large difference between the structures of the 8-Beta diastereomers. The structures of the 8-Beta pair did not differ much in phosphatidylcholine liposomes, therefore a single backbone conformation, that differs from that in buffer, possibly including a type II β-turn, was induced in the lipid environment. This backbone conformation is also different from that of the cyclic 8-Beta pair. The difference between the cyclic and linear octalipopeptides was also observed in the predicted structures. The induction of a secondary conformation in lipid membranes takes place in both the linear and cyclic octalipopeptides. Evidence of the ordering of the cyclic octalipopeptides in stacked aggregates to form antiparallel β-sheets in PC containing membranes was also obtained by CD. It is proposed that this formation of stacked antiparallel β-sheets in membranes that is one of the essential steps necessary for biological activity. The low haemolytic activity of the linear octalipopeptides is therefore probably related to their structures the membranes. The existence of the so-called "hydrophobic hub", formed by the invariable Tyr residue and the β-NC_{14} residue, is also a possible key to bioactivity, specifically antifungal activity [1, 4, 5]. This hydrophobic hub is absent in the predicted S-structure of the linear octalipopeptides and may be influenced in cyclic 8-Beta I (L) by the configuration of the β-NC_{14} residue, resulting in good overall bioactivity of only the synthetic iturin A_2 (cyclic 8-Beta II (D)) (Table 7.1, Chapter 6). The observed antifungal activity (Fig 7.1) of the cyclic heptalipopeptides (cyclic 7-Beta I (D) and II (L)) and the linear heptalipopeptide (7-Beta I (L)) is probably because of the close proximity of the Tyr residue to the β-NC_{14} residue diminishing the influence of the configuration of the latter. The absence of the invariant L-Asn_2 in the heptalipopeptides, however, led to lower activity in most cases. Future investigation into the structures of the heptalipopeptides, and improved antifungal assays, may help to explain some of these results.

The ability of iturin A to bind cations has been observed by several investigators [1, 6], but the precise role of this interaction is still unknown. This tendency of the iturin A_2 analogues to bind the residual sodium from glassware and in the solvents, prompted investigation of this interaction with alkali metal ions using ESI-MS (Chapter 5). The cationisation of the lipopeptides stabilised the peptide structure under ESI-MS conditions. This stabilisation is sequence specific in that the labile L-Gln-L-Pro and D-Tyr-D-Asn bonds are protected or shielded by the association with sodium and other alkali metal ions. Two intrinsic binding sites for non-solvated sodium ions, situated in the N-terminal peptide moiety, β-NC_{14}NYN(Q), and the C-terminal peptide moiety, NQPNS, were identified in 8-Beta. The structure of natural iturin A_2 includes a type II β-turn in each β-NC_{14}NYN and QPNS [12]. The predicted low energy S-structure of 8-Beta includes two turns approximating true β-turns (Chapter 4). The interaction of non-solvated sodium with most of the amide bond oxygens in the predicted turns, specifically that of β-NC_{14}, Asn_2, and Tyr_3 in the one turn and that of Gln_5 and Pro_6 in the other, and with the Gln_5 side chain, would provide the protection against low energy fragmentation of sodiated 8-Beta species. The omission of amino acid residues in the β-NC_{14}NYN tetrapeptide moiety in the shorter lipopeptides led to a reduced capacity to bind a second larger cation. The order of alkali metal ion selectivity of all the lipopeptides was $Na^+ > K^+ > Rb^+$, indicating a size limitation in the interaction cavity or cavities. The cyclic lipopeptides preferentially associated with only one cation, probably in the interior of the peptide ring of the cyclic peptides. Little or no di-cationised complexes were found, because the inclusion of a second cation may be unfavourable because of electrostatic repulsion. It is therefore proposed that alkali metal ions can bind in either one of the two β-turns in the peptide ring of natural iturin A molecule, with the carbonyl oxygens as chelating atoms.

In conclusion it is proposed that iturin A's mechanism of action on eukaryotic cells possesses the following features: (a) after interaction, iturin A molecules self-assemble in antiparallel β-sheets in the phospholipid membrane, (b) alkali metal ions are chelated by the peptide ring carboxyl oxygens to form of anion selective pores that cause the slow increase in membrane conductance, and (c) phospholipases are stereoselectively activated, in which the β-D-NC_{14}-L-Asn_2-D-Tyr_3 tripeptide moiety or hydrophobic hub of β-NC_{14} and D-Tyr is important. These actions result in total membrane disruption and leakage of the cellular contents and interference with any of the steps should influence iturin A's activity.

References

1. Maget-Dana R., Peypoux F. (1994) *Toxicology*, **87**, 151-174

2. Latoud C., Peypoux F., Michel G. (1987) *J. Antibiotics* **40**, 1588-1595

3. Maget-Dana R., Harnois I., Ptak M. (1989) *Biochim. Biophys. Acta* **815**, 309-314

4. Harnois I., Maget-Dana R., Ptak M. (1988) *J. Colloid Interface Sci.* **123**, 85-91

5. Besson F., Peypoux F., Michel G., Delcambe (1979) *J. Antibiotics* **32**, 828-833
   Maget-Dana R., Ptak M., Peypoux F., Michel G. (1987) *Biochim. Biophys. Acta* **898**, 1-5
   Harnois I., Maget-Dana R., Ptak M. (1989) *Biochimie* **71**, 111-116

6. Latoud C., Peypoux F., Michel G. (1988) *J. Antibiotics* **41**, 1699-1700

7. Maget-Dana R., Thimon L., Peypoux F., Ptak M. (1992) *J. Colloid Interface Sci.* **149**, 174-183

8. Maget-Dana R., Heitz F., Ptak M., Peypoux F., Guinand M. (1985) *Biochem. Biophys. Res. Commun*. **129**, 965-971
   Maget-Dana R., Ptak M., Peypoux F., Michel G. (1985) *Biochim. Biophys. Acta* **815**, 405-409

9. Thimon. L., Peypoux F., Wallach J., Michel G. (1995) *FEMS Microbiol. Lett*. **128**, 101-106
   Thimon. L., Peypoux F., Exbrayat J. M., Michel G. (1994) *Cytobios* **79**, 69-83

10. Bland J. M. (1996) *J. Org. Chem*. **61**, 5663-5664

11. Bland J. M. (1995) *Synt. Commun*. **25**, 467-477

12. Marion D., Genest, M., Caille A., Peypoux F., Michel G., Ptak, M. (1986) *Biopolymers* **25**, 153-170